Seismic Retrofit of Bridge Steel Truss Piers Using a Controlled Rocking Approach

by

Michael Pollino and Michel Bruneau
University at Buffalo, State University of New York
Department of Civil, Structural and Environmental Engineering
Ketter Hall
Buffalo, New York 14260

Technical Report MCEER-04-0011

December 20, 2004

NOTICE

Seismic Retrofit of Bridge Steel Truss Piers
Using a Controlled Rocking Approach

by

Michael Pollino[1] and Michel Bruneau[2]

1   Graduate Research Assistant, Department of Civil, Structural and Environmental
    Engineering, University at Buffalo, State University of New York
2   Professor, Department of Civil, Structural and Environmental Engineering, Univer-
    sity at Buffalo, State University of New York

Preface

The Multidisciplinary Center for Earthquake Engineering Research (MCEER) is a national center of excellence in advanced technology applications that is dedicated to the reduction of earthquake losses nationwide. Headquartered at the University at Buffalo, State University of New York, the Center was originally established by the National Science Foundation in 1986, as the National Center for Earthquake Engineering Research (NCEER).

Comprising a consortium of researchers from numerous disciplines and institutions throughout the United States, the Center's mission is to reduce earthquake losses through research and the application of advanced technologies that improve engineering, pre-earthquake planning and post-earthquake recovery strategies. Toward this end, the Center coordinates a nationwide program of multidisciplinary team research, education and outreach activities.

MCEER's research is conducted under the sponsorship of two major federal agencies, the National Science Foundation (NSF) and the Federal Highway Administration (FHWA), and the State of New York. Significant support is also derived from the Federal Emergency Management Agency (FEMA), other state governments, academic institutions, foreign governments and private industry.

The Center's Highway Project develops improved seismic design, evaluation, and retrofit methodologies and strategies for new and existing bridges and other highway structures, and for assessing the seismic performance of highway systems. The FHWA has sponsored three major contracts with MCEER under the Highway Project, two of which were initiated in 1992 and the third in 1998.

Of the two 1992 studies, one performed a series of tasks intended to improve seismic design practices for new highway bridges, tunnels, and retaining structures (MCEER Project 112). The other study focused on methodologies and approaches for assessing and improving the seismic performance of existing "typical" highway bridges and other highway system components including tunnels, retaining structures, slopes, culverts, and pavements (MCEER Project 106). These studies were conducted to:

- assess the seismic vulnerability of highway systems, structures, and components;
- develop concepts for retrofitting vulnerable highway structures and components;
- develop improved design and analysis methodologies for bridges, tunnels, and retaining structures, which include consideration of soil-structure interaction mechanisms and their influence on structural response; and
- develop, update, and recommend improved seismic design and performance criteria for new highway systems and structures.

The 1998 study, "Seismic Vulnerability of the Highway System" (FHWA Contract DTFH61-98-C-00094; known as MCEER Project 094), was initiated with the objective of performing studies to improve the seismic performance of bridge types not covered under Projects 106 or 112, and to provide extensions to system performance assessments for highway systems. Specific subjects covered under Project 094 include:

- development of formal loss estimation technologies and methodologies for highway systems;
- analysis, design, detailing, and retrofitting technologies for special bridges, including those with flexible superstructures (e.g., trusses), those supported by steel tower substructures, and cable-supported bridges (e.g., suspension and cable-stayed bridges);
- seismic response modification device technologies (e.g., hysteretic dampers, isolation bearings); and
- soil behavior, foundation behavior, and ground motion studies for large bridges.

In addition, Project 094 includes a series of special studies, addressing topics that range from non-destructive assessment of retrofitted bridge components to supporting studies intended to assist in educating the bridge engineering profession on the implementation of new seismic design and retrofitting strategies.

The research discussed in this report was performed within Project 094, Task C-3.3, "Steel Substructures." It investigates a seismic retrofit technique for steel truss bridge piers that allows pier rocking by using passive energy dissipation devices implemented at the anchorage locations to control the rocking response. Specially detailed hysteretic energy dissipating elements (buckling-restrained braces) are used to act as easily replaceable, ductile structural "fuses." The dynamic characteristics of the controlled rocking/energy dissipation system are investigated in order to formulate a capacity design procedure using simplified methods of analysis. Design constraints are established that attempt to satisfy performance objectives and nonlinear time history analyses are used to assess the seismic behavior of the bridge piers retrofitted per this strategy. The retrofit strategy is shown to be more applicable to slender piers. The methods of predicting key response values were found to be conservative in most cases and capacity protection of the existing pier (to the prescribed limits) was achieved in all cases considered.

ABSTRACT

In assessments of the seismic adequacy of existing steel truss bridges, the steel-to-concrete anchorage connections typically found at the base of steel truss piers can be potentially vulnerable, having little to no ductility and inadequate strength to resist seismic demands elastically. Many other non-ductile failure locations may also exist along the seismic load path. Failure would result in unacceptable performance, especially for bridges deemed critical for response and recovery efforts following an earthquake.

While strengthening is an option, this approach may only transfer damage to another location. An alternative solution could be to release the anchorage connection, allowing development of a rocking bridge pier system that can partially isolate the structure. An improvement on this approach, and the retrofit solution proposed here, allows this rocking mechanism to develop, but complements it by adding passive energy dissipation devices across the anchorage interface to control the rocking response. Specially detailed hysteretic energy dissipating elements (buckling-restrained braces) are used in this application to act as easily replaceable, ductile structural "fuses".

The dynamic characteristics of the controlled rocking/energy dissipation system are investigated in order to formulate a capacity design procedure using simplified methods of analysis. Design constraints are established that attempt to satisfy performance objectives and nonlinear time history analyses are used to assess the seismic behavior of the bridge piers retrofitted per this strategy.

The retrofit strategy is shown to be more applicable to slender piers as the required level of pier strength and stiffness increases significantly for less slender piers. The methods of predicting key response values were found to be conservative in most cases and capacity protection of the existing pier (to the prescribed limits) was achieved in all cases considered.

ACKNOWLEDGMENTS

TABLE OF CONTENTS

TABLE OF CONTENTS (cont'd)

TABLE OF CONTENTS (cont'd)

LIST OF FIGURES

LIST OF FIGURES (cont'd)

LIST OF FIGURES (cont'd)

LIST OF TABLES

NOTATIONS

A_d — cross-sectional area of pier diagonal

A_L — cross-sectional area of pier leg

A_{sc} — cross-sectional area of buckling-restrained brace, defined by SEAOC/AISC

A_{ub} — cross-sectional area of buckling-restrained brace

B_L — modification factor for damping in long period range

B_s — modification factor for damping in short period range

C_d — deflection amplification factor

d — pier width

E — modulus of elasticity

$f_{p,x}$ — stiffness factor for X-braced piers

$f_{p,v}$ — stiffness factor for V-braced piers

F_a — soil site factor for the short period range

F_v — soil site factor for the long period range

F_y — nominal yield stress of buckling-restrained brace core, defined by SEAOC/AISC

F_{yub} — yield stress of buckling-restrained brace core

FS — factor of safety against pier overturning

g — acceleration of gravity

h — pier height

k_b — buckling-restrained brace influence on rocking stiffness

k_{eff} — effective system stiffness

k_{eff2} effective system stiffness defined by Method 2

k_L axial stiffness of pier leg

k_o initial "fixed base" horizontal stiffness of pier

k_{py} post-yield system stiffness

k_r rocking stiffness

k_R required retrofitted stiffness to satisfy design constraints

k_{ub} elastic stiffness of buckling-restrained brace

k_v vertical shearing stiffness of pier

L_{ub} effective length of buckling-restrained brace

m tributary mass of pier

m_h horizontal tributary mass of pier

m_v vertical tributary mass of pier

M_r restoring moment

p_o maximum of applied step load

P_c horizontal load at the point of buckling-restrained brace compressive

        yielding

P_L maximum dynamic force developed in pier leg

P_{max} maximum spring force of elastic SDOF system under impulsive loading

P_r effective horizontal restoring force

P_{st} spring force of elastic SDOF system under static loading

P_u maximum base shear demand

P_{up1} horizontal base shear at point of uplift during 1st cycle response

P_{up2} horizontal base shear at point of uplift during 2nd cycle response

P_v load applied to pier leg caused by loads through pier diagonals

P_{vo}	load to pier leg caused by impact of tributary pier leg mass
P_{wL}	load to pier leg caused by tributary weight of pier leg
P_y	yield strength of controlled rocking system
PS_{ve}	pseudo-velocity for elastic response
PS_{vi}	pseudo-velocity considering inelastic response
R	response modification factor
R_d	dynamic amplification factor
R_{dL}	dynamic amplification factor for loading directly down pier leg during impact
R_{dv}	dynamic amplification factor for transfer of loads during uplift
S_1	1-second spectral acceleration value
S_a	spectral acceleration value at system's effective period
S_{D1}	design 1-second spectral acceleration
S_{DS}	design short-period spectral acceleration
S_s	short-period spectral acceleration value
t	time
t_r	rise time of step load
t_{r1}	rise time of first load transferred through pier vertically during rocking
t_{r2}	rise time of second load transferred through pier vertically during rocking
t_{rL}	rise time of loading directly down pier leg during impact
t_{rv}	effective rise time of loads transferred through pier vertically during rocking
T_e	effective period defined in FEMA 356
T_{eff}	effective period of controlled rocking system

T_n	period of vibration of elastic SDOF system
T_L	axial period of vibration of pier leg
T_s	characteristic spectral period
T_{sec}	secant period of controlled rocking system
T_v	period of vertical shearing mode of vibration
u_o	maximum displacement of elastic SDOF system under impulsive loading
$(u_{st})_o$	maximum displacement of elastic SDOF system under static loading
v_o	impact velocity
V	base shear strength from NCHRP 12-49
w	weight of pier
w_h	horizontal tributary weight of pier
w_v	vertical tributary weight of pier
#panels	number of pier panels
α_{ub}	post-yield stiffness ratio of buckling-restrained brace
β	modification factor for hysteretic behavior
β_L	modification factor for hysteretic behavior in long period range
β_s	modification factor for hysteretic behavior in short period range
Δ_c	horizontal displacement of pier at point of compressive yielding of buckling-restrained brace
Δ_G	global (deck-level) horizontal pier displacement
Δ_i	incremental horizontal displacement of pier
Δ_{st}	displacement of elastic SDOF system under static loading
Δ_t	maximum horizontal displacement of pier defined in FEMA 356

Δ_u	maximum horizontal pier displacement during rocking response
Δ_{ub}	maximum deformation of buckling-restrained brace
Δ_{up1}	horizontal pier displacement at point of uplift during 1st cycle response
Δ_{up2}	horizontal pier displacement at point of uplift during 2nd cycle response
Δ_{uplift}	maximum uplifting displacement ($=\Delta_{ub}$)
Δ_{y1}	horizontal pier displacement at point of yield during 1st cycle response
Δ_{y2}	horizontal pier displacement at point of yield during 2nd cycle response
Δ_{yub}	yield deformation of buckling-restrained brace
ε_{ub}	maximum strain of buckling-restrained brace
$(\varepsilon_{ub})_{allowable}$	maximum allowable strain of buckling-restrained brace
η_L	local strength ratio
η_o	initial, un-retrofitted lateral strength of pier
η_R	required retrofitted lateral strength of pier to satisfy design constraints
μ	displacement ductility ratio
μ_m	modified displacement ductility ratio
ω_L	axial circular frequency of pier leg
Ω_o	system overstrength factor

ABBREVIATIONS

AASHO	American Association of State Highway Officials
AASHTO	American Association of State Highway and Transportation Officials
ACI	American Concrete Institute
AISC	American Institute of Steel Construction
ASCE	American Society of Civil Engineers
ATC	Applied Technology Council
BRBF	buckling restrained braced frame
CALTRANS	California Department of Transportation
EBF	eccentrically braced frame
ESL	Engineering Seismology Laboratory
FEMA	Federal Emergency Management Agency
LRFD	load and resistance factor design
MCE	maximum considered earthquake
MCEER	Multi-disciplinary Center for Earthquake Engineering Research
MDOF	multi-degree of freedom
NCHRP	National Cooperative Highway Research Program
NEHRP	National Earthquake Hazards Reduction Program
NSP	nonlinear static procedure
OCBF	ordinary concentrically braced frame
OSHPD	Office of Statewide Health Planning and Development
SCBF	special concentrically braced frame
SDOF	single degree of freedom

SEAOC   Structural Engineers Association of California

SRSS   square-root-sum-of-squares

SUNY   State University of New York

TARSCTHS   Target Acceleration Spectra Compatible Time Histories

SECTION 1

INTRODUCTION

1.1 Statement of the Problem and Objectives

Many of the existing steel bridges in the U.S. were built at a time when seismic resistance was not considered in the design or construction of the bridge, or was considered at a level significantly less than adequate by today's standards. Recent earthquakes such as the 1989 Loma Prieta and 1994 Northridge in California, and the 1995 Kobe earthquake in Japan, as well as recent research, have exposed several deficiencies in the design and detailing of structural elements in steel bridges to resist earthquake excitation. Deficient elements in existing large steel bridges include the built-up members, their connections and the anchorage connections. Retrofit of these elements to resist seismic demands elastically is an option, but it can be very costly and gives no assurance of performance beyond the elastic limit. Cost effective retrofit techniques that are able to provide desirable seismic performance are needed.

Implementing a structural "fuse" (i.e. passive energy dissipation device) along the lateral load path can result in considerable savings by protecting existing vulnerable elements and forcing all damage into easily replaceable structural elements. This approach is especially attractive for retrofitting, as the "structural fuses" can be "calibrated" to protect existing non-ductile components. Although there has been extensive use of passive energy dissipation devices in the seismic design and retrofit of buildings in recent years, their use is relatively new for bridges. The number of implementations in bridges is foreseen to grow as more innovative retrofit techniques are formulated for this specific purpose. One such passive energy dissipation device foreseen to be successfully implemented in bridges is the buckling-restrained or unbonded brace.

The use of rocking structural systems for the seismic resistance of structures has received limited attention in research and thus implementations have been few. While certain aspects of rocking behavior have been studied in the past, systematic methods of predicting response and identification of key parameters for the design of rocking systems is needed.

1

The research presented in this report investigates a seismic retrofit technique for steel truss bridge piers that allows pier rocking with passive energy dissipation devices implemented at the anchorage locations, at the tower base, and act to control the rocking response.

1.2 Scope of Work

To investigate the controlled rocking response of truss towers, research has been conducted to:

- Determine the inelastic cyclic behavior of the controlled rocking system under static loading.

- Consider the dynamic response of the rocking truss pier with emphasis on the maximum developed forces in the pier members.

- Assess existing methods of analysis to predict the maximum displacements of the system and compare predictions with the results of nonlinear time history analyses.

- Determine relevant design constraints to ensure desirable behavior is achieved and examine the range of pier properties, representative of steel truss bridge piers, for which the controlled rocking system may be applicable.

- Compare the predictions of the key response quantities with results of time history analyses for ranges of pertinent system parameters.

As a result of the above work, parameters deemed relevant for providing desirable seismic performance are identified, and a design procedure is formulated.

1.3 Outline of Report

Section 2 provides a review of research related to vulnerable structural elements in typical existing bridges, to buckling-restrained braces, and to rocking structures. Also discussed are existing bridges that use a rocking approach to seismic resistance similar to the approach described here.

Section 3 investigates the static and dynamic response of the controlled rocking system and proposes a method of estimating the increased response due to dynamic effects. Also,

2

existing methods of analysis are considered for determining the maximum displacement response of the controlled rocking system and the predictions from the methods are compared with the results of time history analysis.

Section 4 proposes a design procedure for obtaining desirable, ductile performance of the controlled rocking system. Design constraints are established and methods to predict key response values are given. An example of the design procedure is given using a step-by-step approach and a graphical approach is introduced.

Section 5 provides results of a parametric study including design solutions for a range of key parameters and results of time history analyses to assess design predictions. Example response history results are also given for aspect ratios of 4, 3 and 2.

Conclusions on the work presented here are given in Section 6 along with recommendations for future research.

SECTION 2
LITERATURE REVIEW

2.1 General

The vulnerability of steel truss bridges subjected to earthquake shaking has been investigated through research and engineering evaluations and results suggest that these bridges may experience significant damage during a major earthquake. Vulnerable structural elements of steel truss bridges are reviewed in Section 2.2. This has triggered considerable research into the evaluation and retrofit of existing steel bridges.

The use of passive energy dissipation devices for the seismic resistance of bridges is relatively new, but the number of implementations is expected to grow as more innovative retrofit techniques are formulated. One such device is the buckling-restrained or unbonded brace and is discussed in Section 2.3.

Rocking of structures during past earthquakes has been observed and certain aspects of rocking behavior have been studied in past research. A review of some research investigating the behavior of rocking systems with particular focus on experimental and design studies is presented in Section 2.4 .

A few bridges have been designed or retrofitted using a rocking approach for seismic resistance in the past. It is also being considered or implemented as part of some on-going projects. Bridges for which a rocking approach has been used to provide seismic resistance are discussed in Section 2.5.

2.2 Vulnerable Structural Elements in Bridge Steel Truss Piers

Large U.S. steel truss bridges have not yet been subjected to severe earthquakes. However substantial evidence from research and engineering evaluations suggest that potential seismic vulnerabilities do exist. Particularly vulnerable details include built-up lattice members, that are typically found in older bridges, member connections and the steel/concrete anchorage connections.

2.2.1   Built-up, Lattice Bracing

The use of built-up sections for both gravity and lateral load resisting members has been used extensively in steel bridges. The built-up bracing members used in many older truss bridges typically used riveted lacing to increase the brace's moment of inertia thus increasing its global buckling capacity. The braces are typically in an x- or v-braced configuration. The load at the onset of buckling of these members can be predicted by the AISC LRFD Manual (1998) method of Chapter E for built-up members buckling in a direction parallel to lacing. For buckling in the direction perpendicular to lacing, an additional modification factor has been recommended by Caltrans (Dietrich and Itani, 1999) to reduce the effective moment of inertia of the member. However the cyclic, inelastic response of these members is not well known. The complex geometry and interaction of each built-up piece with its riveted (typically) connection does not allow use of existing theoretical models to predict its inelastic, cyclic response.

Until recently, a limited amount of information on the cyclic, post-buckling behavior of built-up members existed. Some research was initiated after the 1989 Loma Prieta earthquake as part of the seismic rehabilitation of the Golden Gate Bridge. Part of this work evaluated the compressive behavior, failure modes, and ductility of the main suspension truss chord and the column legs of the approach structure towers (Astaneh-Asl et. al., 1997). Two large size specimens were fabricated and tested. Resulting ductilities of the truss chord and tower legs were established as 1.5 and 2 respectively.

Some project-specific testing of built-up members for the rehabilitation of the San Francisco-Oakland Bay Bridge was performed to assess the expected performance of built-up pier diagonals (Dietrich and Itani, 1999). Static, cyclic testing of a half-scale member found that the lacing and rivets were not able to maintain the integrity of the laced member cross-section and the compressive capacity of the member should be predicted using Caltrans specifications.

Uang and Kleiser (1997) tested three half scale built-up members for the San Francisco-Oakland Bay Bridge with the objective of developing axial force-moment (P-M) interaction

relationships for these members. The members were subjected to axial loads with eccentricities of 0, 5, and 15 inches and their cyclic behavior and ultimate strength investigated. The testing showed that the compressive capacity could be predicted reliably by taking into account shearing effects on the lacing and effective length factors. The specimens exceeded the axial force-moment interaction surface predicted in the AISC LRFD Specifications.

However, this project specific testing does not provide enough data for the broad range of geometries of these members.

An experimental testing program has recently been completed, investigating the cyclic inelastic behavior of built-up members for a range of global and local slenderness parameters, namely kL/r and b/t (Lee and Bruneau, 2003). The definition of these parameters can be found in the LRFD Specification for Structural Steel Buildings (AISC, 1998). Members with small slenderness parameters provided ductile behavior for the initial post-buckling cycles. However the loss of stiffness, strength and thus energy dissipation in subsequent cycles was severe. The hysteretic behavior of type By specimens is shown in figure 2-1. The hysteretic life of the members was typically controlled by fracture from low cycle fatigue within hinging regions of the buckling brace. A picture of the buckled shape of member By 16-120 and the final fractured brace as a result of low
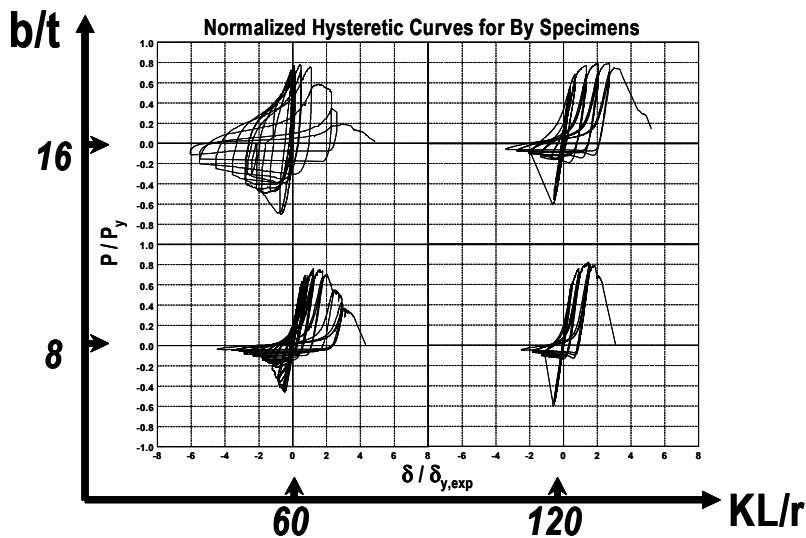
FIGURE 2-1 Hysteretic Behavior of Type By Specimens (adapted from Lee, 2003)

7

<center>(a)   (b)</center>

FIGURE 2-2   Specimen By16-120 (Lee, 2003). (a) Buckled Shape and (b) Final Fracture of Member

cycle fatigue is shown in figure 2-2a and figure 2-2b respectively. The testing revealed that the built-up members suffered global and local buckling causing significant member strength and stiffness degradation resulting in loss of pier lateral strength and major structural damage during an earthquake (Lee and Bruneau, 2003).

2.2.2   Member Connections

Most codes of practice today require that failure not occur in connections due to their inability to develop significant inelastic strains, resulting in sudden, brittle failure. Yielding of the members gross section is recognized to be a more ductile failure mode (although it may be possible in some instances to detail connections able to provide ductile failure modes).

While properly designed and constructed welded connections, to develop the full strength of members, can be very effective under cyclic earthquake loading, inadequate welded connections can also cause brittle failure as was evident in moment frame connections during the Northridge earthquake. However, this is not an issue here since the use of welded connections in bridge construction is uncommon due to the concerns of fatigue from day-to-day traffic loads.

Rivets were very prevalent in the construction of steel bridges in the past however high-strength bolts are the connector of choice in bridge construction today. While rivets tend to

<center>8</center>

have good ductility, the strength of riveted connections are typically inadequate to resist seismic loads. Connections continue to be vulnerable during earthquakes and can often be the weak link along the seismic load path (Ritchie et. al., 1999).

2.2.3   Anchorage Connections

Threaded steel bolts are the most common method to connect steel structures to concrete in bridge construction. A typical steel truss pier anchorage connection is shown in figure 2-3. They are typically either cast-in-place or adhesively bonded in drilled holes. The bolts are able to develop their full tensile and shear strength if proper embedment and edge distance is provided. Brittle fracture of bridge anchor bolts occurred during the 1994 Northridge earthquake (Astaneh-Asl et. al., 1994). Anchor bolts can be designed to act as the structural "fuse" during an earthquake or behave elastically, directing damage to another location. While the anchorage connection can be detailed to allow gross area yielding of the anchor bolts, they are likely unable to provide stable inelastic cyclic

hysteretic behavior. For instance, typical construction details do not transfer compressive loads to the bolts thus the bolts could yield in tension but these inelastic excursions could not be recovered by compressive yielding. Furthermore, the amount of hysteretic energy dissipated by anchor bolts is typically insufficient in the perspective of system response. A "typical" anchorage connection is analyzed to determine its pull-out capacity and the earthquake demand to cause its failure in Appendix A. Assuming yielding of the anchor bolts or concrete cone failure to be the possible failure mechanisms for this connection, it was found that gross area yielding of the anchor bolts was the governing failure mode. The corresponding pushover capacity of the representative bridge piers (discussed in

FIGURE 2-3   Typical Truss Pier Anchorage Connection

Appendix D) was then determined assuming the anchorage connection to be the weak link along the lateral load path. Finally, the pushover curves are shown on a spectral capacity-demand type format with demand curves defined by the NCHRP 12-49 (ATC/MCEER 2003) design spectrum with one-second spectral acceleration values of 0.125g and 0.25g (figure A-1). The system strength obtained indicated failure of the anchor bolts starting at a spectral acceleration of only 0.125g for each case considered. This provided some numerical evidence that anchorage connections are typically unable to resist even moderate seismic demands.

2.3 Buckling-restrained Braces (BRB)

2.3.1 General

Buckling-restrained braces, also known as unbonded braces (type of BRB made by Nippon Steel Corporation of Japan), are an emerging seismic device providing, in some cases, supplemental strength, stiffness and energy dissipation to structures. The concept of the buckling-restrained brace behavior contrasts from that of a conventional brace in a significant way. A conventional bracing member subjected to axial loads is able to yield in tension, but typically exhibits global and/or local buckling under compression at a load less than the tensile yield force. Under some circumstances, the buckling of these members within a structural system can provide satisfactory seismic performance (AISC, 2002), even though buckling is not an ideal form of energy dissipation. A buckling-restrained brace is designed to instead allow the brace to reach full yield in tension and compression. It consists of a ductile steel core, carrying axial load, surrounded by a restraining part that prevents global buckling of the core. An "unbonding" material is placed between the steel core and restraining part to limit the shear transfer between the two components, accommodate the lateral expansion of the brace in compression due to the poisson effect, and to ensure that the buckling prevention component will not carry axial load (i.e. will not significantly increase the strength of the brace). Figure 2-4 shows sketches of the primary components of a buckling-restrained brace.

2.3.2 Experimental Testing

Several different cross-sections of the steel core and restraining mechanisms have been
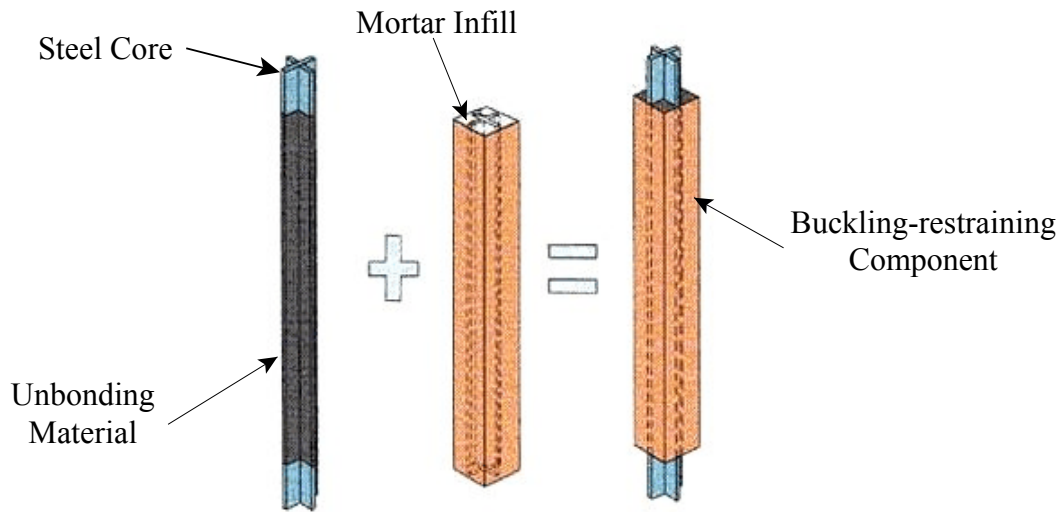
FIGURE 2-4 Primary Components of Buckling-restrained Brace

investigated. Use of a cruciform or rectangular plate as the yielding steel core, wrapped in an unbonding material, and inserted in a rectangular or square HSS steel tube filled with mortar has been a popular configuration that has shown to develop stable hysteretic behavior. Sample specimen dimensions considered in past experimental studies with this type of configuration are shown in figure 2-5. Results of some of the tests are discussed below.

Watanabe et. al. (1988), Wada et. al. (1989) and Watanabe et. al. (1992) investigated the effect of the outer tube configuration, in particular the outer tube flexural capacity, on the performance of the brace. As can be seen in the figure, identical inner steel cores were used in all tests. The outer steel tube's buckling strength, P_e, was varied such that the ratio P_e/P_y, where P_y is the steel core's yield strength, ranged from 3.5 to 0.55. It was found that a ratio of $P_e/P_y > 1.5$ resulted in stable and symmetric hysteretic brace behavior.

Hasegawa et. al. (1999) performed shake table testing of an unbonded brace subassemblage using the 1995 Kobe Marine Observatory Record and the 1940 El Centro record. The unbonded brace was subjected to a maximum axial strain of 7.2% in one of the tests. Stable hysteretic behavior was reported throughout the testing.

11

Iwata et. al. (2000) tested four braces with cross-sections shown in figure 2-6. Specimens 1 and 3 have a soft rubber sheet between the core and restraining part to act as the unbonding layer while specimens 2 and 4 only had a small clearance between the core and restraining part. Hysteretic behavior of the 4 specimens is shown in figure 2-7. It was found that each specimen behaved satisfactorily up to axial strains of 1% however at higher levels of strain the braces behaved differently. Rapid development of local buckling was observed in the specimens without the unbonding material, resulting in low cycle fatigue and eventual fracture.
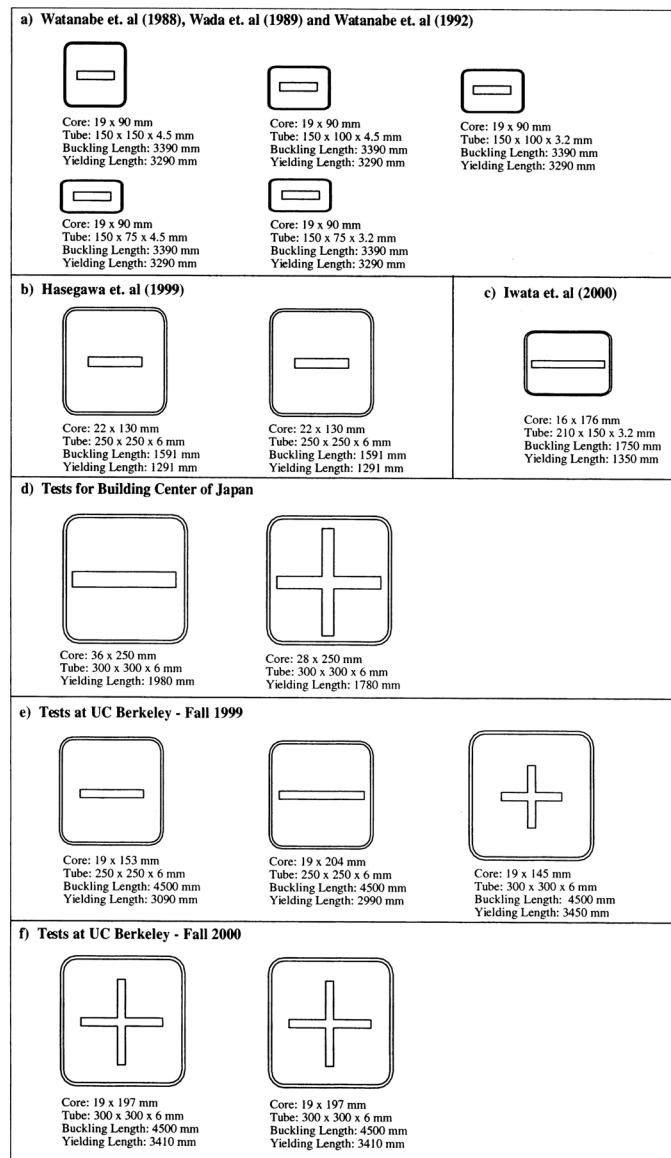
FIGURE 2-5 Experimentally Tested Cross-sections of Buckling-restrained Braces (Black et. al., 2002)
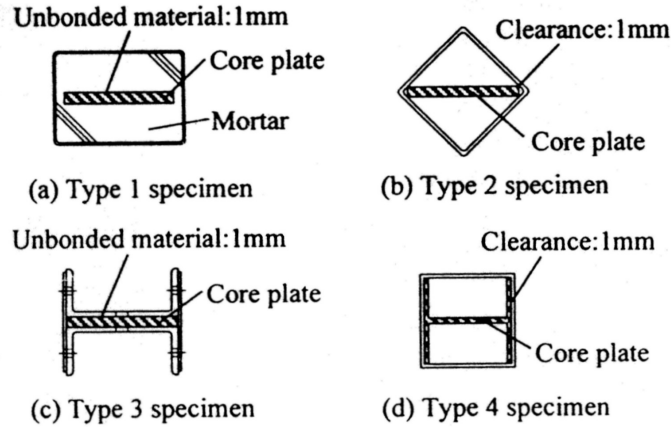
FIGURE 2-6   Cross-section of Experimentally Tested Unbonded Braces by Iwata et. al. (2000)
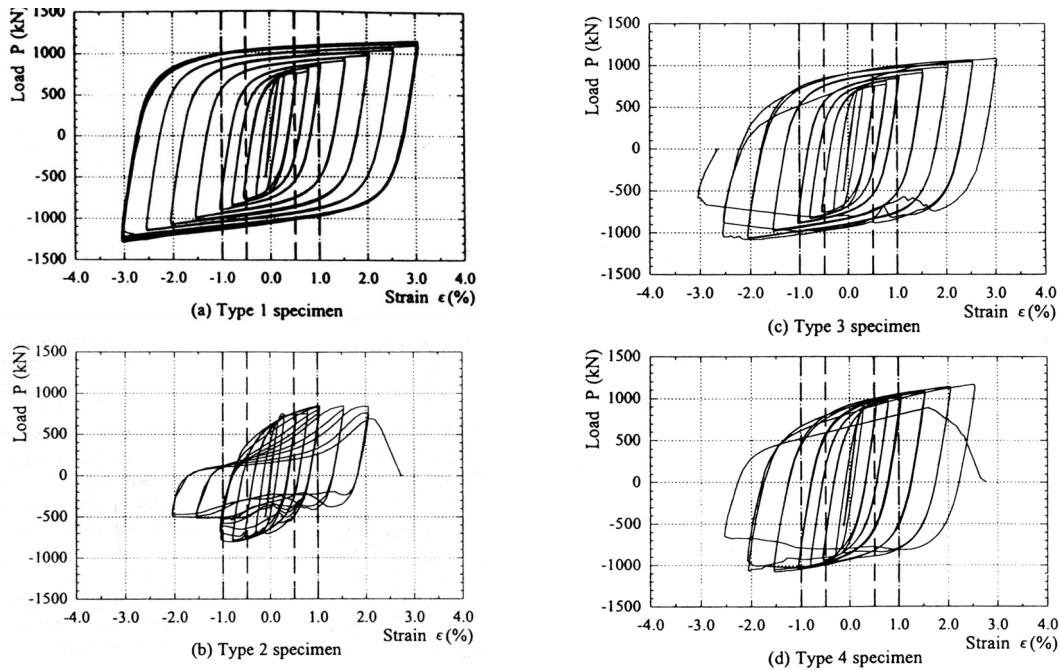
FIGURE 2-7   Hysteretic Response of Unbonded Braces Tested by Iwata et. al. (2000)

Black et. al. (2002) tested five specimens with properties representative of braces designed for implementation in two seismic retrofit projects in California. The specimens have the same configuration details as the braces discussed above. The specimen cross-sections are shown in figure 2-5. Each specimen had core lengths of approximately 3400mm and had yield strengths ranging from 1200kN to 2150kN. Loading protocols for the testing

13

included the SAC basic loading history, SAC near-field, OSHPD loading history, low-cycle fatigue tests, and displacement histories derived from predicted building response for specific earthquake records. The tested braces exhibited ductile, stable and repeatable hysteretic behavior. A Bouc-Wen analytical brace model (Wen, 1976) was found to model the behavior of the braces "with fidelity".

2.3.3 Product Availability

Buckling-restrained braces are patented products, with various manufacturers providing different implementations of the concept. The original developer and manufacturer of the buckling-restrained brace is Nippon Steel Corporation of Japan which named their version of the buckling-restrained brace the "unbonded brace". A few manufacturers in the U.S. are promoting alternative products based on the same idea (including Star Seismic, LLC.,Corebrace, LLC. and Associated Bracing Inc.).

Star Seismic produces a tube-in-tube design with a pin and collar connection to prevent the transfer of moment and shear forces to the yielding core. A picture of the Star Seismic buckling restrained brace is shown in figure 2-8a and typical experimentally obtained hysteretic behavior is shown in figure 2-8b (Merritt et. al., 2003a). The tests reveals good overall hysteretic behavior, with some slip of the pin and collar connection during each load reversal. The tube-in-tube design also allows for multiple yielding core tubes to be placed together to create a larger capacity brace still in a compact design. A multi-tube brace is shown in figure 2-8c.

The buckling restrained braces produced by Core Brace consists of a flat or cruciform steel core surrounded by a steel tube filled with mortar and a method of unbonding the yielding inner core from the buckling restraining outer core. A sketch of the brace is shown in figure 2-9. Component testing (Merritt et. al., 2003b) also shows hysteretic behavior typical of other similar implementations of the concept.

(a)   (b)

(c)
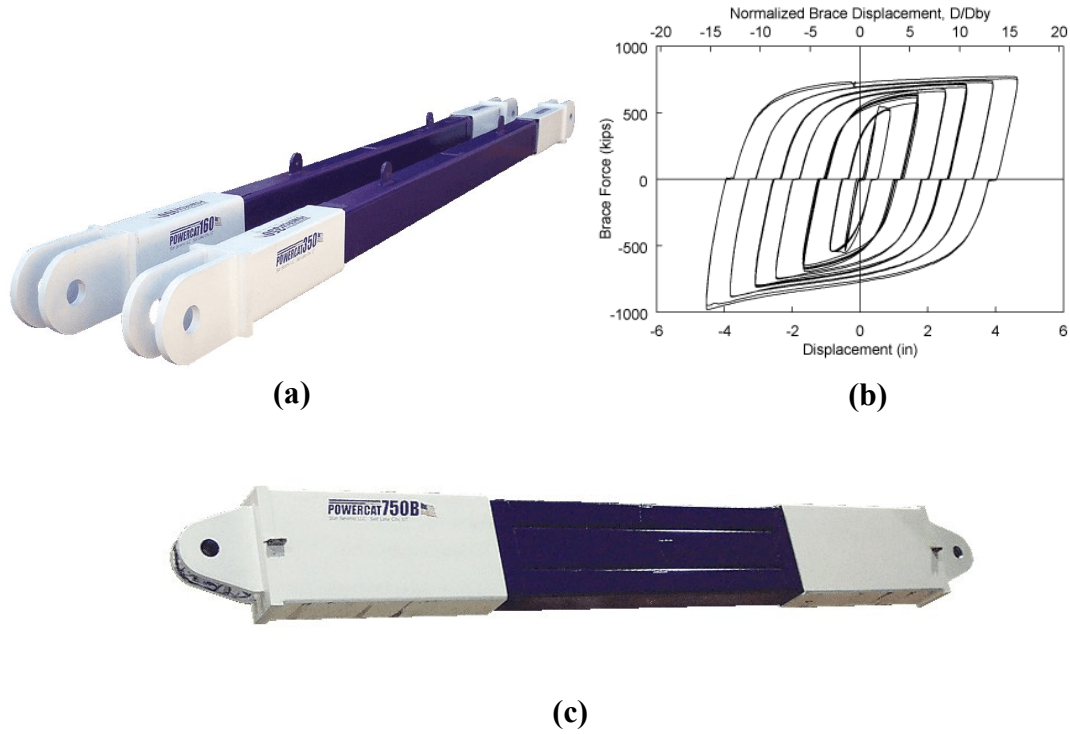
FIGURE 2-8   Buckling Restrained Braces produced by Star Seismic (Merritt et. al., 2003a). (a) Tube-in-Tube Design with Pin-Collar Connection, (b) Typical Hysteretic Response and (c) Multiple Tube Brace
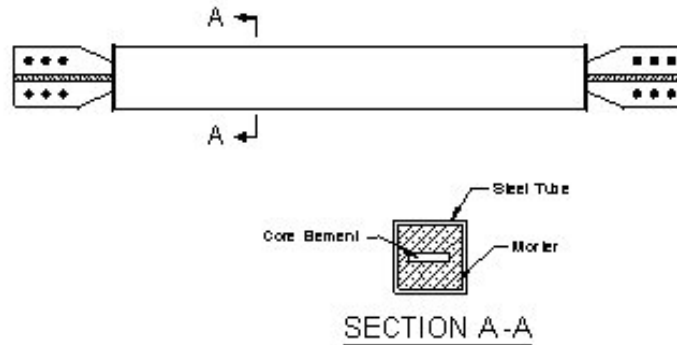
FIGURE 2-9   Buckling Restrained Brace produced by Core Brace (Merritt et. al., 2003b)

Buckling restrained braces manufactured by Associated Bracing use a steel core of constant cross-section along the entire length and welded stiffeners at the ends to accommodate bolted connections. End connection details and hysteretic response of the brace are shown in figure 2-10a and 2-10b respectively (Merritt et. al., 2003c).
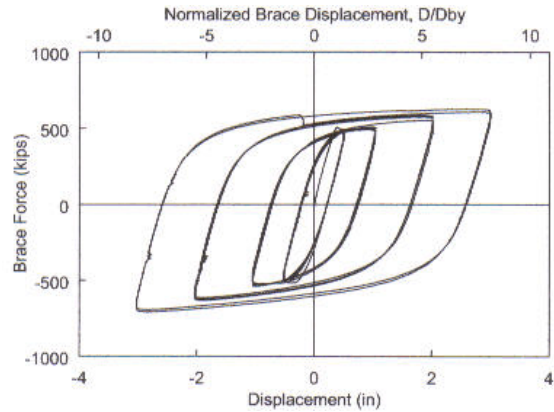
(a) End Connection   **(b)** Hysteretic Response

FIGURE 2-10   Buckling Restrained Brace produced by Associated Braces (Merritt et. al., 2003c). (a) Brace and End Connection and (b) Typical Hysteretic Response

2.3.4 Design Procedure

At the time of this writing, a joint SEAOC-AISC task group has developed recommended provisions for possible inclusion in the NEHRP Recommended Provisions for Seismic Regulations for New Buildings and Other Structures as well as the AISC Seismic Provisions for Structural Steel Buildings. These provisions (SEAONC-AISC, 2001) provide suggested values for seismic design coefficients, such as the response modification factor, R, the system overstrength factor, Ω_o, and deflection amplification factor, C_d. Table 2-1 shows these design coefficients for currently accepted seismic force-resisting systems along with those recommended for the design of buckling-restrained frame systems. For the existing systems, the response modification factor, R, and the deflection amplification factor, C_d, are taken from the Seismic Provisions for Structural Steel Buildings (AISC, 2002) and the overstrength factor, Ω_o, is taken from Minimum Design Loads for Buildings and Other Structures (ASCE, 2000).

Seismic Force Resisting System	R	Ω_o	C_d
Special Concentrically Brace Frame (SCBF)	6	2	5
Ordinary Concentrically Braced Frame (OCBF)	5	2	$4^1/_2$
Eccentrically Braced Frame (EBF): w/ moment connections away from link	8	2	4
EBF w/out moment connections away from link	7	2	4
Special Moment Frame	8	3	$5^1/_2$
Intermediate Moment Frame	$4^1/_2$	3	4
Ordinary Moment Frame	$3^1/_2$	3	3
Special Truss Moment Frame	7	3	$5^1/_2$
Buckling-Restrained Braced Frame (BRBF)	8	2	$5^1/_2$
Dual Systems w/ SMRF:			
SCBF	8	$2^1/_2$	$6^1/_2$
EBF w/ moment connections away from link	8	$2^1/_2$	4
EBF w/out moment connections away from link	7	$2^1/_2$	4
BRBF	9	$2^1/_2$	$5^1/_2$

TABLE 2-1   Seismic Design Coefficients for Existing Lateral Force Resisting Systems and Proposed Values for Buckling-Restrained Braced Frame System

The recommended provisions also require qualification testing of the braces unless experimental testing reported in research or documented tests have been performed that reasonably match project conditions. Relevant conditions may include beam and column member sizes, material strengths, brace-end connection details, and assembly and quality control processes. Individual brace testing is required to ensure that strength and inelastic deformation requirements are satisfied, and subassemblage testing is required to ensure that deformation and rotational demands can be accommodated and that brace behavior within the subassemblage is representative of that determined from uniaxial testing. Other specified factors proposed for the design of buckling restrained braces include a compression strength correction factor, to increase the brace compressive strength to approximately 1.3 times the nominal strength ($A_{sc}F_y$, where $A_{sc}F_y=A_{ub}F_{yub}$). A tension strength correction factor is also proposed to account for the increase in tension strength due to strain hardening (as determined by coupon testing of the prototype material). These strengths are used, per capacity design principles, to determine the minimum required strength of the brace connections and other surrounding members in the structural system. However, the nominal strength of the braces are considered for their design to resist the specified design loads.

2.4 Studies of Rocking Structures Subjected to Earthquake Excitation

Evidence of rocking of structures has been observed following major earthquakes and used to explain how very slender and relatively unstable structures may have been able to survive strong earthquakes (Housner, 1963). The study of rocking structures possibly started with investigation of the free-vibration response of rigid rocking blocks, and their response to some simple forms of dynamic loading (such as rectangular and sinusoidal impulses), as well as to earthquake excitations. An expression for an amplitude dependent period of vibration during rocking and a method to determine the amount of kinetic energy lost upon impact (occurring in each half-cycle) was developed assuming an inelastic collision to occur upon impact (Housner, 1963). Housner concluded that "the stability of a tall slender block subjected to earthquake motion is much greater than would be inferred from its stability against a constant horizontal force".

From that point some analytical and experimental work was done to predict the response of

rocking structures to earthquake motions. Many investigated the response of rigid blocks with emphasis on preventing overturning. Meek (1978) first introduced aspects of structural flexibility to the seismic response of single-degree-of-freedom rocking structures. Psycharis (1982) followed with an analytical study of the dynamic behavior of simplified multi-degree-of-freedom (MDOF) structures supported on flexible foundations free to uplift. Both two spring foundations and the Winkler foundation model were used to study the rocking of rigid blocks, and only the two spring foundation model was used to study MDOF flexible structures. Three different mechanisms were considered to introduce energy dissipation into the foundation attributed to soil radiation damping upon the assumed inelastic impact that occurs during each half-cycle. The energy dissipation mechanisms included spring-dashpot and elastic-plastic spring systems. It was noted that vertical oscillations were introduced to this uplifting system when subjected solely to horizontal excitation. Observations on the benefits of allowing uplifting to occur (opposed to a fixed-base structure) were not conclusive in terms of displacements and stresses, as response varied significantly depending on system parameters and the characteristics of the ground excitations.

Shake-table testing of a rocking frame with energy dissipating devices introduced at the uplift location was performed by Kelley and Tsztoo (1977). An approximately half-scale 3-story steel frame was designed (figure 2-11a), with restraints provided to prevent horizontal movement, and mild steel, torsionally yielding bars used as energy dissipating devices at the uplifting location (figure 2-11b). The test results indicated that the rocking concept with energy dissipating devices provided beneficial response, in terms of base shear, to the same frame with a fixed base, thus preventing uplift.

Priestley et. al. (1978) recognized that following the New Zealand seismic design requirements for buildings at the time would indirectly result in allowing rocking of part or all of some structures during an earthquake. However, rather than characterizing this as an unsafe condition, they recognized this could be advantageous in some instances. In
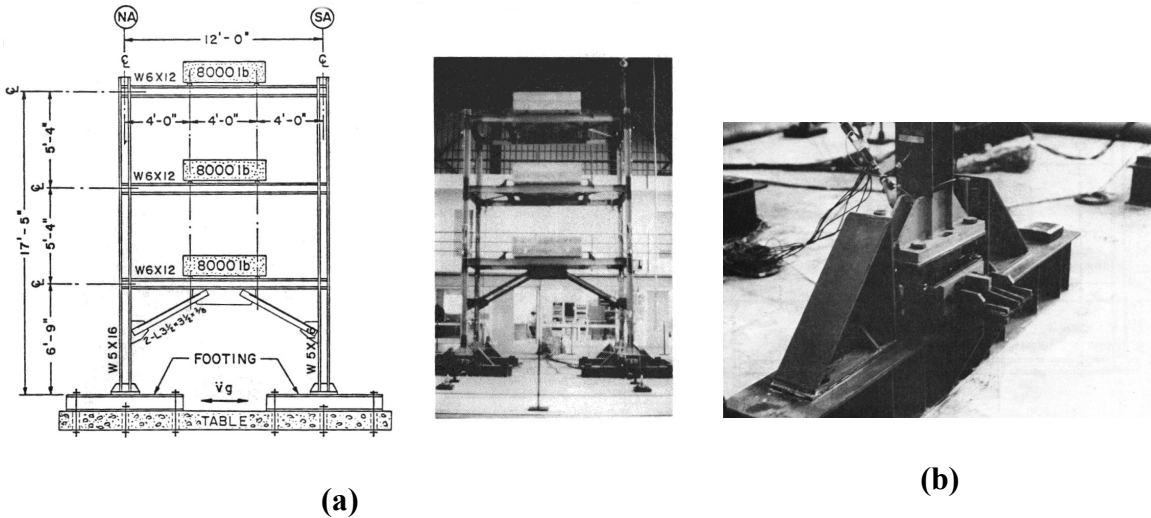
FIGURE 2-11   Uplifting Frame Tested by Kelley and Tsztoo (1977). (a) Elevation View of Steel Frame Specimen and (b) Steel Torsional Yielding Device Introduced at Base of Column

order to prevent excessive secondary structural damage caused by large rocking displacements, a simple method to predict the maximum displacement of the rocking response during earthquakes was developed. Using the work of Housner (1963), a response spectra design approach was used by transforming the rocking system into an equivalent SDOF linear viscous oscillator. The only energy dissipation in the structural system was assumed to be provided by the inelastic collisions occurring upon each impact. The simple SDOF model shown in figure 2-12, was tested, subjected to free-vibration response, sinusoidal excitations, and the 1940 –S El Centro record. Results verified Housner's theory on the amplitude dependent frequency assuming inelastic collisions, and the simple method developed by Priestley et. al. predicted the maximum displacements with reasonable accuracy, especially for design purposes. It was noted during testing that no significant rebound occurred after impact, that large vertical accelerations were induced during impact, and that placing rubber pads underneath the impacting legs to represent a flexible foundation decreased the vertical accelerations significantly.
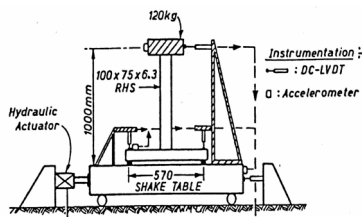
FIGURE 2-12   Simple SDOF Rocking Model Tested by Priestley et. al. (1978)

20

Mander and Cheng (1997) proposed rocking concrete bridge columns as a seismic resistant system consistent with a proposed design methodology called Damage Avoidance Design (DAD). In this concept, each bridge column was allowed to rock individually by making the rebar discontinuous at the column ends thus allowing rocking at the column/cap beam and column/foundation beam interfaces. The columns were subsequently designed as pre-cast elements, post-tensioned vertically to increase and control the lateral strength. A sketch of a deformed bridge pier with the rocking column concept is shown in figure 2-13a. The kinematics of the rocking behavior and force-displacement relationship were established for the rocking columns. The primary energy dissipating mechanism for the system is the lost energy upon impact. A method of converting the lost energy into equivalent viscous damping was established following the assumptions of Housner (1963). In some cases, yielding of the prestressing tendons was allowed for increased energy dissipation. A design procedure was proposed for the rocking column system similar to capacity-demand procedure presented in Constantinou et. al. (1996). Static testing was performed to verify the force-displacement behavior and the effect of the prestressing tendons. Shake table testing was also performed (for the specimen shown in figure 2-13b) to verify the concepts presented, along with the simplified design procedure.

| (a) | (b) |
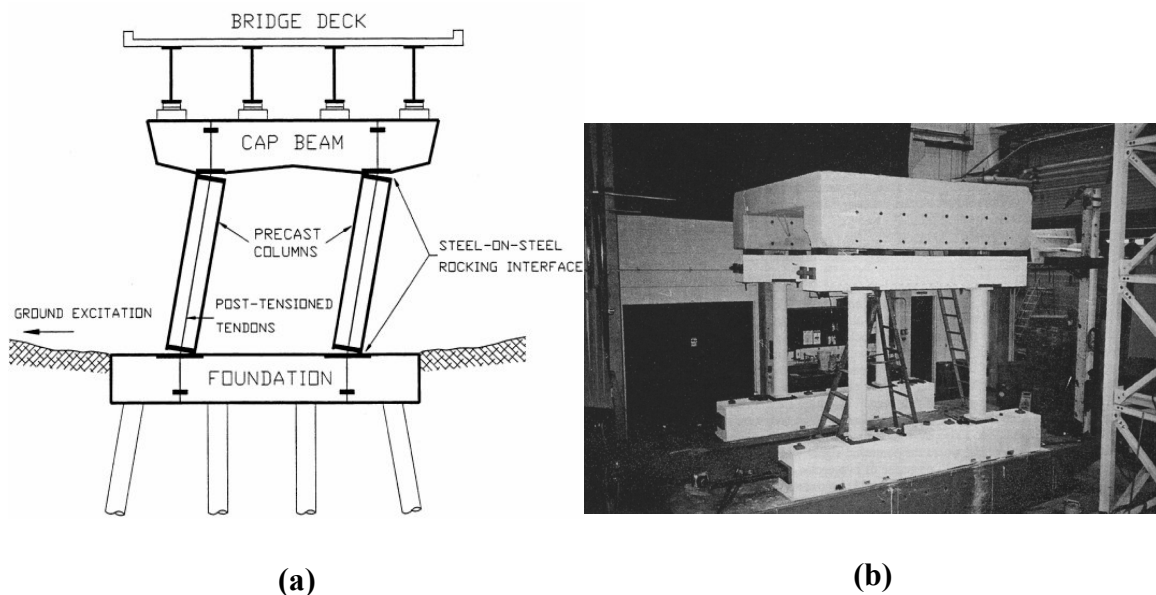
FIGURE 2-13   Rocking Column Concept of Mander and Cheng (1997). (a) Sketch and (b) Specimen Tested on Shake Table

Toranzo et. al. (2001) proposed a rocking wall system for buildings. Steel flexural yielding elements were placed at the uplifting locations to increase lateral strength and provide hysteretic energy dissipation. With the interest of providing a framework for design, a method for determining the maximum expected displacements was proposed based on the Direct Displacement Method (Priestley and Kowalsky, 2000). Also, maximum forces were determined by amplifying the static forces by a factor to account for the effect of impacting on the foundation. Testing of the rocking wall was performed using a uni-axial shake table. A picture of the rocking wall specimen tested, along with the hysteretic energy dissipating devices, is shown in figure 2-14. At the time of this writing, results of the rocking wall specimen were not available.

FIGURE 2-14   Rocking Wall Specimen with Flexural Steel Yielding Devices at Uplifting Location (Toranzo et. al., 2001)

Midorikawa et. al. (2003) experimentally examined the response of a steel braced frame (figure 2-15a) allowing uplift at the base of columns and yielding of specially designed base plates (figure 2-15b). A 3-story, 2-bay braced frame was subjected to shake table tests using

the 1940 El Centro motion, applied in a single horizontal direction. Tests were performed with plate details providing different levels of uplifting strength including a fixed-base case for comparison. It was found that the uplifting base plate yielding system effectively reduced the seismic response of building structures and that the base plates were able to provide reliable performance for the uplifting displacements while transferring shear forces. The axial forces observed in the columns during rocking may have been affected by the impacts caused during rocking.
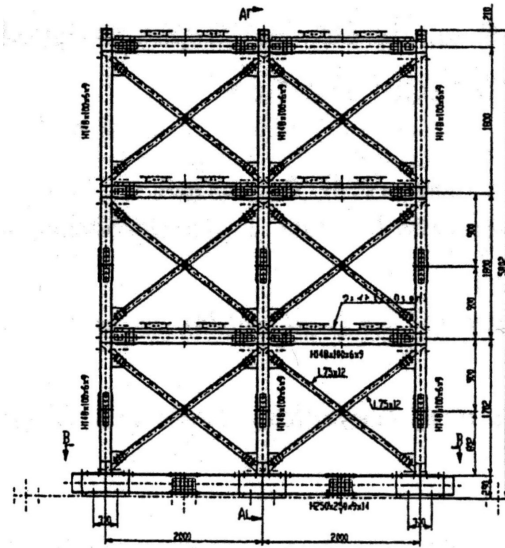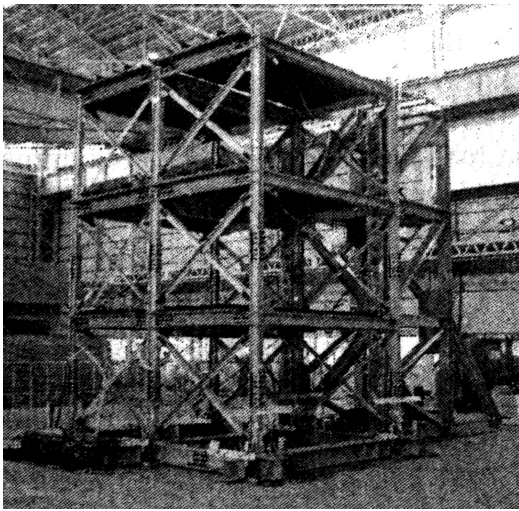
(a)
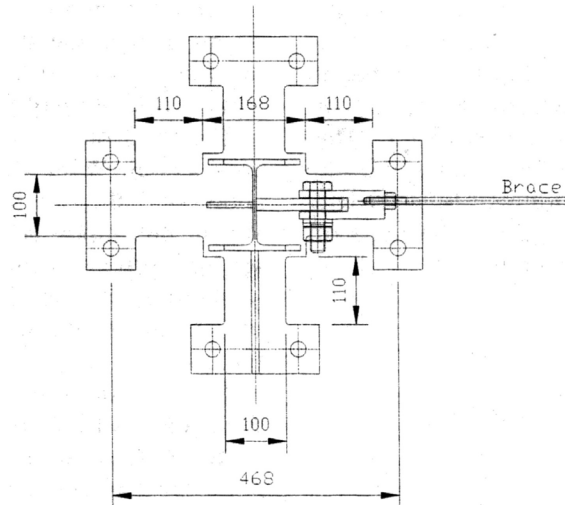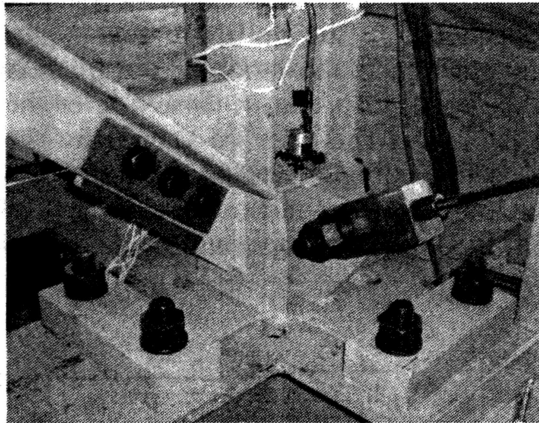
(b)

FIGURE 2-15   Uplifting Braced Frame Tested by Midorikawa et. al. (2003).
(a) Frame and (b) Specially Detailed Yielding Base Plate

Makris and Konstantinidis (2002) examined the fundamental differences between the response of a SDOF oscillator and the rocking response of a slender rigid block (inverted pendulum structure) and introduced the concept of a rocking spectrum. The rocking spectrum consists of rotation and angular velocity spectra as a function of a "period" defined by:

$$T = \frac{2\pi}{p} = \frac{2\pi}{\sqrt{\dfrac{3g}{4R}}} \tag{2-1}$$

where

$$R = \sqrt{b^2 + h^2} \tag{2-2}$$

where 2b and 2h are the block width and height respectively. The rocking spectrum is generated, assuming no sliding of the block such that only rocking response occurs, by solution of the following nonlinear equation of motion representing the rocking motion under a horizontal ground acceleration:

$$\ddot{\theta}(t) = -p^2 \left[\sin(\alpha \, sgn[\theta(t)]) - \theta(t) \right] + \frac{\ddot{u}_g}{g} \cos(\alpha \, sgn[\theta(t)] - \theta(t)) \right] \tag{2-3}$$

It was found that the rocking spectrum exhibits "noticeable order" until displacements that nearly cause overturning are reached. It was also reported that methods of predicting displacements of rocking blocks using typical response spectrum, such as the method used in Priestley et. al. (1978), may provide acceptable results in some cases, but that there are kinematic characteristics of the rocking system that cannot be reflected in the response spectrum.

2.5 Existing Rocking Bridge Piers

A limited number of bridges currently exist in which rocking of the piers during earthquakes has been allowed as part of their way to achieve satisfactory seismic resistance. The South Rangitikei Rail Bridge, located in Mangaweka, New Zealand (figure 2-16a) is such an example bridge, designed and constructed in the 1970's with pier legs allowed to uplift under seismic loads (Priestley et. al., 1996). With pier slenderness ratios of more than 5, large overturning moments develop at the base of the pier. Allowing pier rocking, significantly reduced moments that needed to be resisted.
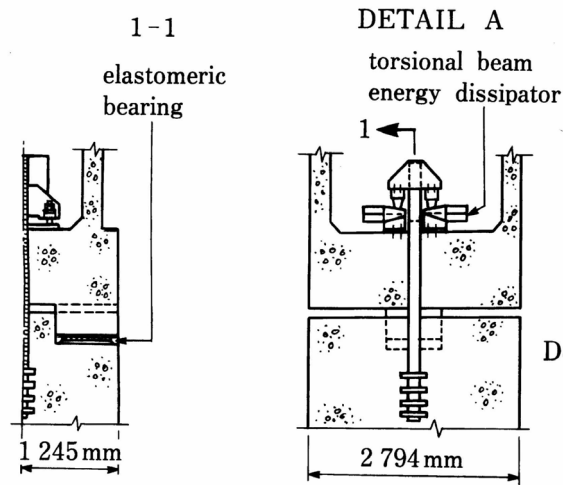
(a)   **(b)**

FIGURE 2-16   South Rangitikei Rail Bridge (Priestley et. al., 1996). (a) Pier and (b) Torsion Steel Yielding Device at Base of Pier Legs

Instead of allowing free uplift at the base of each pier leg, torsional steel yielding devices, shown in figure 2-16b, were added to control the amount of uplift while providing energy dissipation (damping). The amount of uplift was limited to 125mm by stopping mechanisms.

The North Approach of the Lions' Gate Bridge, located in Vancouver, British Columbia was seismically upgraded during the 1990's (Dowdell and Hamersley, 2000). The North Approach Viaduct consists of 25 composite plate girder spans with span lengths ranging from about 25-38 meters (figure 2-17a). Early investigations revealed that many piers would develop large uplifting forces at the foundation. Advantages of using a rocking

25

(a)   (b)

FIGURE 2-17 Lions' Gate Bridge North Approach Viaduct (Dowdell and Hamersley, 2000). (a) Steel, V-braced Piers and (b) Flexural Steel Yielding Devices Implemented at Uplifting Location

strategy for seismic retrofit provided a force limiting mechanism, while concentrating retrofit work at the tower bases (a more easily accessible location compared to other parts of the structure). Some concerns arose due to the effects of dynamic impacting of a pier leg with the foundation and coupling of vertical and horizontal modes during rocking. Implementation details for the rocking system included removing the nuts of the existing anchor bolts to allow uplift without damage, tying individual foundation pedestals together with tie beams to prevent differential settlement, driving piles through liquefiable soil layers, providing longitudinal and transverse restrainers at deck-level and installing lead core rubber bearings at the abutment. Also, the capacity of some pier diagonals and columns were increased by bolting additional material to the member to increase their elastic buckling capacity. Flexural yielding steel devices (figure 2-17b) were placed at the anchorage interface to provide hysteretic damping and limit the uplifting displacements.

The benefits of allowing partial uplift of the legs of bridge piers has been also recognized by other practicing engineers and the idea has been adopted for the retrofit of some major steel bridges in California. The seismic vulnerability of the Carquinez Bridge was assessed in 1994 and it was determined that the bridge would require retrofitting to meet current

26

seismic resistance standards. As part of this work, the displacement capacity of the A-frame piers (figure 2-18a), which are expected to carry a significant portion of the seismic loads, was evaluated using nonlinear pushover analysis (Jones et. al., 1997). It was determined that the existing pier was unable to provide the necessary seismic performance for this important transportation link. Three seismic retrofit strategies were investigated which included; rocking of the frames on the concrete foundations, base isolation with friction pendulum bearings, and using viscous dampers in the steel towers. Base isolation and viscous dampers provided a beneficial response, but member and connection retrofit would still have been necessary in both cases and the high costs associated with both of these systems was unattractive. The final retrofit solution was to allow limited rocking of the A-frame towers. A transfer girder, shear keys, restraining beams and elastomeric bearing pads were placed below the tower columns. A schematic of the base connection is shown in figure 2-18b. The restraining beams are allowed to yield during an earthquake, providing energy dissipation, while the elastomeric bearing pads are expected to partially absorb impacts during rocking.
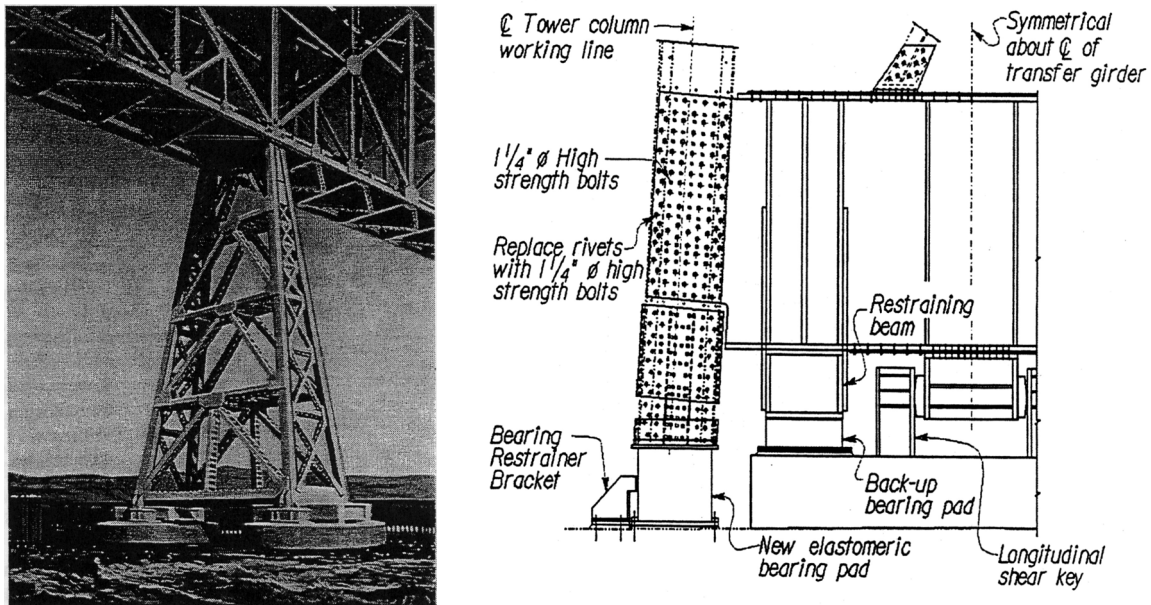
(a)   (b)
FIGURE 2-18 Carquinez Bridge, California (Jones et. al., 1997). (a) A-frame Pier and (b) Uplifting Restraining System Used

The Golden Gate Bridge, completed in 1937, began a seismic retrofit program in the 1990's following the 1989 Loma Prieta earthquake (Ingham et. al. 1997). While the Golden Gate Bridge was not damaged during the earthquake, the San Francisco Bay Bridge was closed for one month due to damage, causing huge economic losses thus prompting a seismic evaluation of all major crossings in California, including the Golden Gate Bridge. The retrofit solution for the bridge's main towers allowed each tower leg to uplift from the foundation by about 2.3 inches, which substantially reduced tower leg stresses compared to the fixed-base alternative. Finite element analysis was used to investigate the nonlinear deformation behavior of the tower leg's multi-cellular riveted steel construction. A picture of the model is shown in figure 2-19. The uplifting caused large axial compressive stresses to develop at the base of the tower legs upon impact requiring the significant stiffening within the multi-cellular construction of the tower leg. Also, the lack of edge distance from the compressive zone of the tower leg to the foundation pedestal's edge required the installation of post-tensioned, high-strength threaded bars through the concrete pedestals to provide confinement and increase the shear resistance near the pedestal edge.

Another major California toll bridge that underwent major rehabilitation following the Loma Prieta earthquake was the San Mateo-Hayward Bridge (Prucz et. al. 1997). The bridge is 7.1 miles long and has a 1.85 mile long main span supported on steel and concrete towers. The steel towers (shown in figure 2-20a) required an increase in overall ductility to satisfy performance objectives. To achieve the desired performance, modifications were made to the column base connections, the columns and the spandrel beams. The column base connections (shown in figure 2-20b) were modified to allow for each tower leg to rock and yield their anchor bolts during uplift. Steel sleeves were placed around the top of the anchor bolts that could resist compression following tensile yielding and was believed to improve cyclic behavior and reduce impact during the rocking motion. Modifications to the column base connections included adding anchor bolts between the existing anchor bolts to increase connection strength, ductility and redundancy. Also, steel pins were added at the column base to transfer the base shear and concrete was added inside the base of the column to increase the stability of its walls.
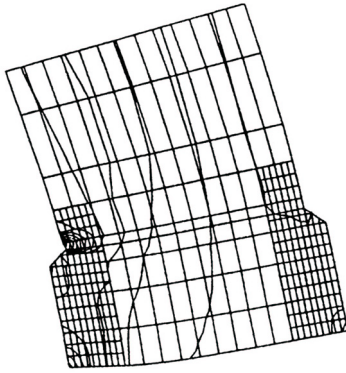
FIGURE 2-19 Uplifting at Base of Tower Leg of Golden Gate Bridge from Finite Element Model (Ingham et. al., 1997)
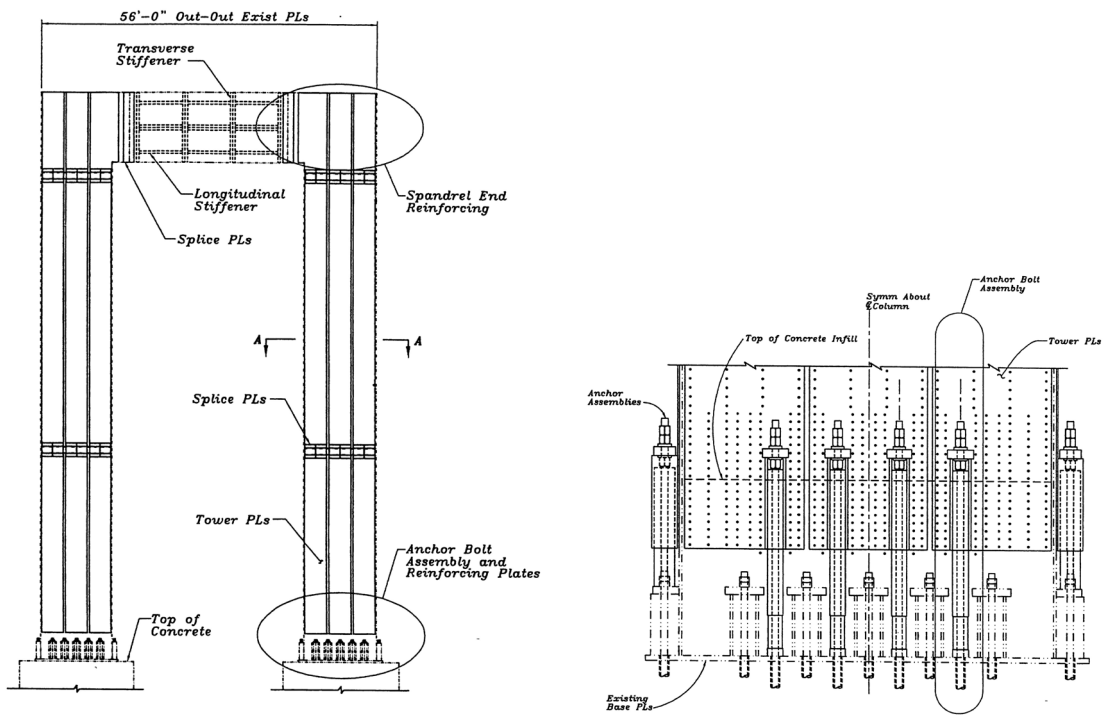
FIGURE 2-20 San Mateo-Hayward Bridge (a) Steel Tower and (b) Modified Anchorage Connection (Prucz et. al. 1997)

It is also worth noting that pier E17 of the San Francisco-Oakland Bay Bridge experienced rocking during the Loma Prieta earthquake (Housner 1990). Pier E17 serves as an anchor pier for the bridge superstructure from pier E11 to pier E17. The concrete bent was not intended to rock however damage following the earthquake provided evidence that rocking of the concrete columns had occurred.

Other projects are known to the authors, where the cost of retrofitting large truss towers was considerably reduced by allowing rocking, particularly since the fixed-base solution would have required significant strengthening of the unreinforced masonry foundations. However, due to security concerns in the post-September 11, 2001 environment, the owners do not allow the releasing of information on these projects.

SECTION 3
CONTROLLED ROCKING SYSTEM FOR SEISMIC RETROFIT OF STEEL TRUSS BRIDGE PIERS

3.1 Introduction

Recent earthquakes such as the 1989 Loma Prieta, 1994 Northridge and 1995 Kobe earthquake in Japan have demonstrated the need for improved methods for the design and construction of highway bridges to withstand seismic force and displacement demands. While collapse is rare, undesirable damage can leave the bridge unusable until repairs can be made. Highway bridges deemed critical in the response and recovery efforts following a major earthquake need to remain operational after an earthquake, requiring the bridge to respond in a mostly elastic manner with little to no residual displacements.

Many existing steel truss bridge piers consist of riveted construction with built-up, lattice type members supporting a slab-on-girder or truss bridge. Truss piers are typically in an x- or v-braced configuration. Steel truss bridges are found in nearly every region of the U.S. A typical steel truss bridge with this type of construction is shown in figure 3-1.
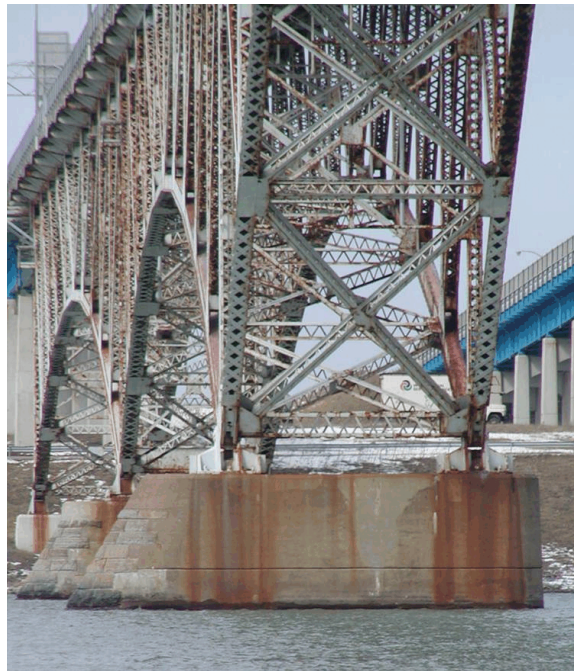
FIGURE 3-1   Typical Steel Truss Bridge

These built-up lattice type members and their connections can be the weak link in the seismic load path. Recent experimental testing of these members revealed that they suffer global and local buckling causing significant member strength and stiffness degradation resulting in loss of pier lateral strength and major structural damage during an earthquake (Lee & Bruneau 2003). Existing, riveted connections and deck diaphragm bracing members typically possess little to no ductility (Ritchie et. al. 1999). Another possible non-ductile failure location is the anchorage connection at the pier-to-foundation interface. Analyses of "typical" steel-concrete connections, discussed in Section 2.2.3 and Appendix A, suggests it may be unable to resist even moderate seismic demands.

While strengthening these existing, vulnerable elements to resist seismic demands elastically is an option, this method can be expensive and also gives no assurance of performance beyond the elastic limit. Therefore it is desirable to have structures able to deform inelastically, limiting damage to easily replaceable, ductile structural "fuses", able to produce stable hysteretic behavior while protecting existing non-ductile elements and to prevent residual deformations using a capacity-based design procedure.

Failure or releasing of the anchorage connection may allow a steel truss pier to rock on its foundation, partially isolating the pier. Addition of passive energy dissipation devices at the uplifting location complements the system otherwise free to uplift by restraining the uplift displacements while providing additional energy dissipation. This system also provides an inherent restoring force, capable of allowing for automatic re-centering of the tower, leaving the bridge with no residual displacements after an earthquake and limits the retrofit work to easily accessible locations. While many types of energy dissipation devices exist, the device used in this application is the buckling-restrained brace. A buckling-restrained brace consists of a steel core surrounded by a restraining part, allowing the brace to reach full yield in tension and compression. Details and results of experimental testing of buckling-restrained braces were discussed in Section 2.3. A sketch of a retrofitted bridge pier is shown in figure 3-2.
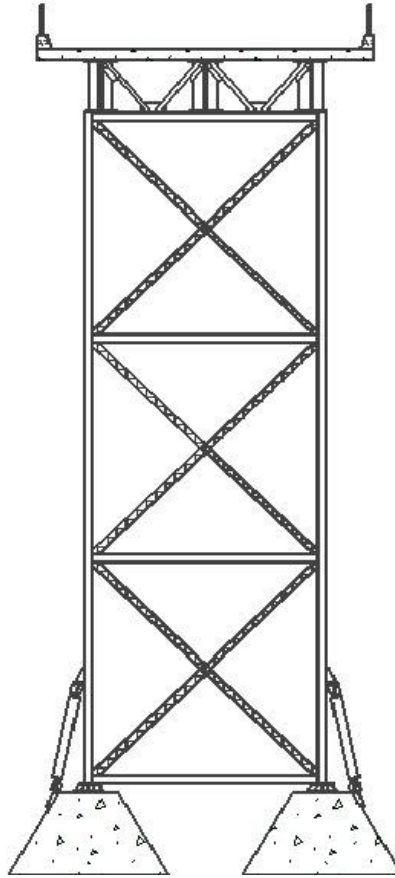
FIGURE 3-2   Retrofitted Steel Truss Bridge Pier using Controlled Rocking Approach

A rocking bridge pier concept has been implemented or considered for the design or retrofit of a few bridges, as discussed in Section 2.5. Rocking frames, walls and columns have been investigated through experimental testing as discussed in Section 2.4.

Static cyclic pushover calculations for a rocking pier with buckling-restrained braces implemented at the anchorage interface is presented in Section 3.2. Section 3.3 describes dynamic amplification of loads caused during impacting and uplift from the foundation. Due to the limited amount of research and proposed methods of characterizing the response of such a system, a parametric study was undertaken to better understand the response of simplified truss piers allowed to rock on rigid foundations. Section 3.4 describes the parametric study and Section 3.5 provides observations and results for the study.

3.2 Global Hysteretic Response of Rocking Bridge Pier System

Pushover curves are useful to determine the inelastic response of structures subjected to earthquake loading. Cyclic pushover response of a typical rocking bridge pier system under a static horizontal cyclic load applied at bridge deck level is shown in this section.

The key parameters for the hysteretic response of the rocking bridge pier system considered here include the fixed-base lateral stiffness of the existing steel truss pier (k_o), the aspect ratio of the pier (h/d) and the cross-sectional area, effective length and yield strength of the buckling-restrained brace (A_{ub}, L_{ub}, F_{yub}). Also, the weight excited by horizontally imposed accelerations (w_h) and the vertical gravity weight carried by a pier (w_v) are assumed equal here and expressed as w.

The simplified model used for static pushover analysis is shown in figure 3-3. The model considers motion of the pier in a direction orthogonal to the bridge deck and assumes there to be no interaction with other piers or abutments through the bridge deck. The
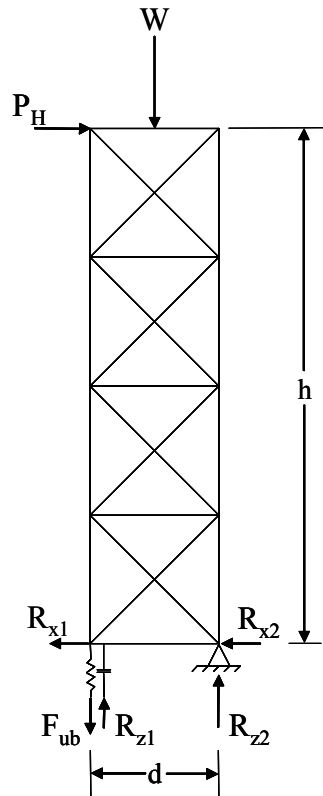
FIGURE 3-3 Model used for Static Pushover Analysis

34

various steps and physical behaviors that develop through a typical half-cycle are shown qualitatively in figure 3-4. By symmetry, the process repeats itself for movement in the other direction. Section 3.2.1 describes the pier response for the 1st cycle. Transition from 1st to 2nd cycle response occurs when the buckling-restrained braces yield in compression and the braces carry a portion of the weight after the system comes to rest upon completion of the cycle (a phenomena to be explained later). Section 3.2.2 describes how this response differs for the 2nd and subsequent cycles. Section 3.2.3 discusses some implications of the rocking response on the post-yield stiffness of the controlled rocking bridge pier system.
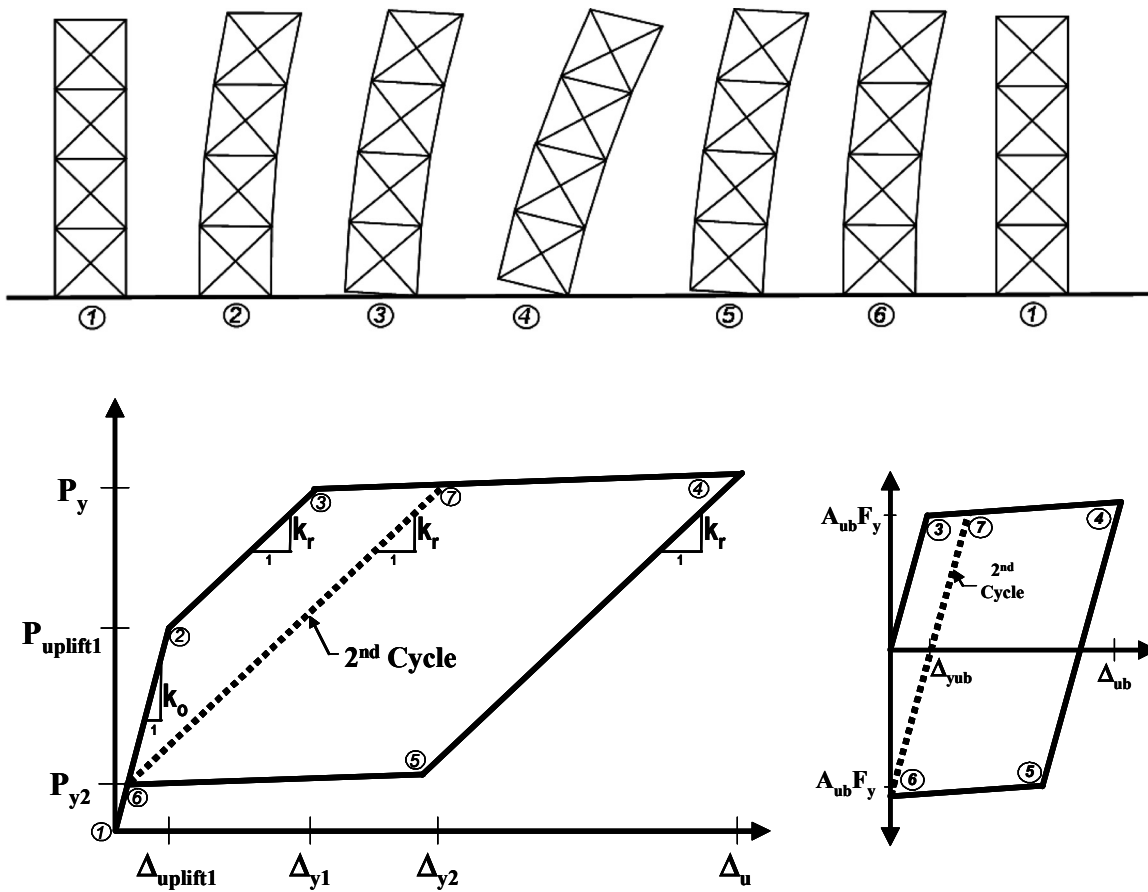
FIGURE 3-4   Cyclic Pushover Response of Rocking Bridge Pier. (a) Global Response and (b) Response of Buckling-restrained Brace

35

3.2.1 1st Cycle Response

As the horizontal load applied at the top of the pier is increased, the initial lateral displacement at that location is entirely due to elastic deformations of the pier's structural members. The stiffness of the pier, k_o, is a function of its bending and shear flexibility (step 1 to 2 in figure 3-4). The horizontal force-displacement response at the top of the pier, until uplift begins, is defined by:

$$P_H = k_o \Delta_G \tag{3-1}$$

where Δ_G is the "global" horizontal displacement at the top of the pier and k_o is defined above. Uplifting of a tower leg begins when the restoring moment created by the tributary vertical bridge weight is overcome by the applied moment (position 2 in figure 3-4). The horizontal force at the point of uplift is defined by:

$$P_{up1} = \frac{w}{2}\left(\frac{d}{h}\right) \tag{3-2}$$

where $^d/_h$ is the inverse of the aspect ratio and w was defined previously. The displacement at the point of uplift in the 1st cycle response is defined by:

$$\Delta_{up1} = \frac{P_{up1}}{k_o} \tag{3-3}$$

The global stiffness is reduced after uplift as the flexibility includes deformations of the pier and base rotations as a tower leg begins to uplift. The horizontal pier flexibility is given by k_o. The base rotational flexibility can be projected to give its effect on the total horizontal flexibility and is controlled by the brace stiffness and the pier aspect ratio as:

$$k_b = \frac{EA_{ub}}{L_{ub}}\left(\frac{d}{h}\right)^2 \tag{3-4}$$

These deforming mechanisms act as two springs in series as the horizontal load is increased. Thus, the structural stiffness from uplift to the yield point (step 2 to 3 in figure 3-4) is defined here as the elastic rocking stiffness and is expressed by:

$$k_r = \left(\frac{1}{k_o} + \frac{1}{k_b}\right)^{-1} = \left(\frac{1}{k_o} + \frac{1}{\frac{EA_{ub}}{L_{ub}}\left(\frac{d}{h}\right)^2}\right)^{-1} \tag{3-5}$$

The pier is then pushed until the buckling-restrained brace yields, which assumes the buckling-restrained brace to be the weak link along the lateral load path. The horizontal force at the onset of brace yielding, P_y, and thus the structural system yield strength is defined by:

$$P_y = \left(\frac{w}{2} + A_{ub} F_{yub} \right) \frac{d}{h}$$

(3-6)

The corresponding system yield displacement for the first cycle, Δ_{y1}, is defined as:

$$\Delta_{y1} = \left(\frac{w}{2k_o} + \frac{A_{ub} F_{yub}}{k_r} \right) \frac{d}{h}$$

(3-7)

Ignoring strain hardening in the brace and a second order effect to be discussed in Section 3.2.3, the system has zero post-elastic stiffness and is deformed to its ultimate displacement (Δ_u). The ultimate displacement is dependent on the seismic demand at the system's effective period of vibration (T_{eff}). Methods for determining the effective stiffness (k_{eff}) and thus the effective period are given in Section 3.4. For a system within the constant velocity region of the appropriate response spectrum, maximum displacements of elastic and inelastic systems can be assumed to be approximately the same (Newmark and Hall, 1982). Thus the ultimate displacement of the inelastic system can be defined by:

$$\Delta_u = \frac{F_v S_1 T_{eff}}{4 B_L \pi^2}$$

(3-8)

where S_1 and B_L are the 1-second spectral acceleration value and the long period damping coefficient respectively, as defined in NCHRP 12-49 (ATC/MCEER, 2003).

As the horizontal load is reduced, the pier first responds elastically with stiffness k_r, the tensile force in the buckling-restrained brace also reduces per its initial elastic properties. A deformation in the brace of $2\Delta_{yub}$, where Δ_{yub} is the yield displacement of the buckling-restrained brace equal to $\dfrac{F_{yub} L_{ub}}{E}$, is required for the brace to reach its yield strength in compression which requires a deck-level displacement of $\Delta_y + \Delta_{yub} \dfrac{h}{d}$ from the undeformed position. The applied lateral load at the top of the pier at the point of compressive yielding of the brace, (point 5 in figure 3-4), is defined by:

37

$$P_c = \left(\frac{w}{2} - A_{ub}F_{yub} \right)\left(\frac{d}{h} \right) \tag{3-9}$$

The corresponding displacement at this point is defined as:

$$\Delta_c = \Delta_u - \frac{2A_{ub}F_{yub}\dfrac{d}{h}}{k_o} - 2\frac{F_{yub}L_{ub}}{E}\frac{h}{d} \tag{3-10}$$

The buckling-restrained brace displaces plastically in compression and again is assumed to yield with no significant stiffness until the uplifted pier leg returns in contact to its support (step 5 to 6 in figure 3-4). At this point of contact, system stiffness is again defined by k_o. The slight difference in tensile and compressive in yield strength of buckling-restrained braces was discussed in Section 2.3 but is neglected here for simplicity.

It can be seen from (3-9) that if the brace yield strength ($A_{ub}F_{yub}$) is greater than half of the bridge deck weight tributary to the pier ($^w/_2$) then the horizontal force required at compressive yielding is negative. Thus the restoring moment provided by the vertical tributary weight is not enough to yield a buckling-restrained brace in compression upon unloading, leaving a tower leg slightly elevated above the foundation. By limiting the buckling-restrained brace strength to $^w/_2$, the plastic rotations accommodated at the pier base can be returned to the undeformed position leaving the pier with no residual deformations. A local strength ratio, η_L, is defined here as:

$$\eta_L = \frac{A_{ub}F_{yub}}{\dfrac{w}{2}} \tag{3-11}$$

Parameters that give η_L less than one allow for pier self-centering. The self-centering capability is a constraint in the capacity based design procedure discussed in Section 4.

3.2.2 2nd Cycle Response

As a buckling-restrained brace yields in compression and the pier settles back to its support, the buckling-restrained brace effectively carries a portion of the bridge weight equal to their compressive capacity (assumed to be $A_{ub}F_{yub}$). The corresponding free-body diagram of a pier in an undeformed shape after the 1st cycle is shown in figure 3-5. As a result of this transfer of the gravity load path, a smaller horizontal force is required to initiate uplift causing an earlier transition from stiffness k_o to the rocking stiffness k_r thus increasing the flexibility and system yield point from the 1st cycle response as can be seen by the 2nd cycle curve in figure 3-4.
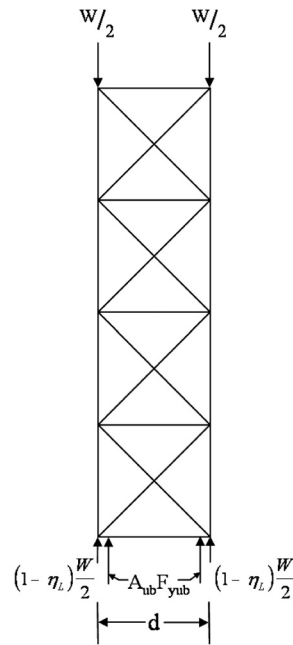
FIGURE 3-5   Free-Body Diagram of Pier, at Rest, after 1st Cycle

The horizontal force at the onset of uplift can be shown equal to P_c (defined by 3-9) and is defined for the 2nd and subsequent cycles as:

$$P_{up2} = P_c = (1 - \eta_L) \frac{w}{2} \frac{d}{h} < P_{up1} \tag{3-12}$$

The corresponding displacement at the point of uplift in the 2nd and subsequent cycles is equal to:

$$\Delta_{up2} = \frac{P_{up2}}{k_o} < \Delta_{up1} \tag{3-13}$$

The yield displacement can be expressed as:

$$\Delta_{y2} = \frac{(1-\eta_L)\frac{W}{2}\frac{d}{h}}{k_o} + \frac{2\,A_{ub}F_{yub}\frac{d}{h}}{k_r} > \Delta_{y1} \tag{3-14}$$

The yield strength of the system, P_y, is unchanged. The force in the buckling-restrained brace changes from its compressive strength ($A_{ub}F_{yub}$) to tension yielding ($A_{ub}F_{yub}$) for the 2nd and subsequent cycles that exceed deck level displacement of Δ_{y2}. Hysteretic behavior in the 1st and subsequent cycles, for a given magnitude of inelastic deformation in the buckling-restrained braces, are shown together on a single plot in figure 3-6. Note that the controlled rocking bridge pier system considered develops a flag-shaped hysteresis. This is due to the combination of pure rocking response from the restoring moment, provided by the bridge deck weight, and energy dissipation provided by yielding of the buckling-restrained braces.
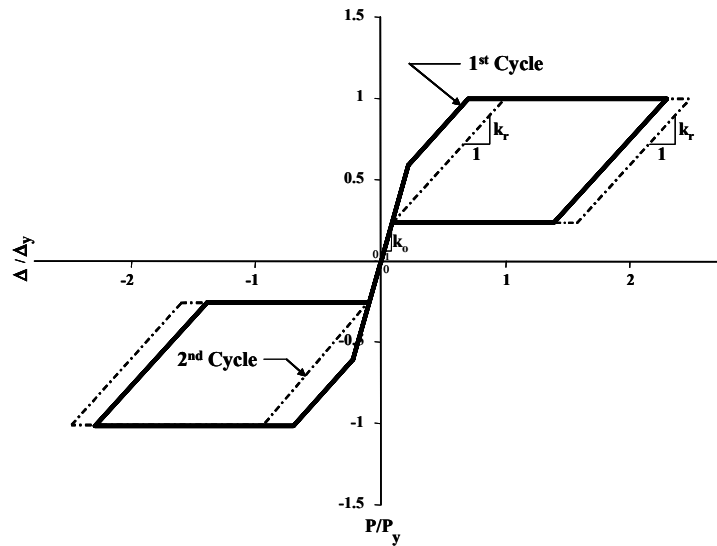
FIGURE 3-6   Hysteretic Behavior of 1st and 2nd Cycles

3.2.3 Influence of Second Order Effects on Hysteretic Response

The proposed rocking bridge pier system has characteristics of both a linear-elastic oscillator and a rigid rocking system. The restoring force for the pier flexibility is provided by elasticity while the restoring moment, M_r, for base rocking is provided by gravity and equal to:

$$M_r = w\frac{d}{2} \tag{3-15}$$

As the center of mass displaces, the restoring moment provided by gravity is reduced. The reduction of the restoring moment is dependent on the ratio of the horizontal seismically induced displacement of the bridge deck to pier width (d) such that the restoring moment can be defined in terms of the induced displacement as:

$$M_r\left(\Delta_i\right) = w\left(\frac{d}{2} - \Delta_i\right) \tag{3-16}$$

This loss in restoring moment can be written in terms of the loss in horizontal base shear as:

$$P_r\left(\Delta_i\right) = \frac{w}{h}\left(\frac{d}{2} - \Delta_i\right) = \frac{w}{2}\frac{d}{h} - \frac{w}{h}\Delta_i = P_{upl} - \frac{w}{h}\Delta_i \tag{3-17}$$

Thus from (3-17) it can be seen that there effectively exists a negative stiffness of $-\dfrac{w}{h}$ in the hysteretic response. The loss of restoring moment becomes more pronounced at larger displacements and is therefore examined further for the post-yield response. Considering this effect along with the strain hardening of the buckling-restrained brace, in the form of a post-yield stiffness ratio ($\alpha_{ub} = k_h/k_{ub}$), results in a global post-yield stiffness of:

$$k_{py} = \alpha_{ub}\, k_{ub}\left(\frac{d}{h}\right)^2 - \frac{w}{d}\left(\frac{d}{h}\right) \tag{3-18}$$

where k_{ub} is the initial, elastic stiffness of the buckling-restrained brace equal to:

$$k_{ub} = \frac{EA_{ub}}{L_{ub}} \tag{3-19}$$

Therefore, under some circumstances the strain hardening of the buckling-restrained brace can negate the effective negative stiffness due to the nonlinear geometric effect, thus resulting in a positive global post-yield stiffness, k_{py}.

For pier widths and aspect ratios considered herein (representing bridge piers), a modestly sized buckling-restrained brace can result in a positive global post-yield stiffness. However in some cases where the base width of a bridge pier is not of this magnitude, such as with an A-frame truss pier, this effect may be more critical.

Due to the fact that the restoring moment is lost with increasing displacement, the self-centering ability is also affected.

41

The methods of analysis proposed in Section 3.4, for determining the response of equivalent single-degree-of-freedom oscillators, and the design procedure presented in Section 4 do no reflect this effect thus assuming it to be negligible.

3.3   Excitation of Vertical Modes of Controlled Rocking System

If the bridge pier is designed to allow for pier rocking and self-centering, after a pier leg uplifts from the foundation, it eventually returns to its support with a certain velocity upon impact; this is followed by a transfer of gravitational and device forces vertically through the truss pier as the rocking motion continues.   The displacement-based passive energy dissipating devices (buckling-restrained braces) can be calibrated to control the rocking response to certain limits.

The impacting and uplift that occurs during the rocking motion is illustrated in figure 3-7. As the pier shifts its axis of rotation from the base of one leg to another, vertical modes of vibration of the truss pier are excited during the impact and uplift process, even when the structure is only subjected to horizontal ground motions. The impacting process increases demands in the pier legs without affecting the magnitude of the base overturning moment.

However excitation of a vertical mode during uplift causes an increase in the ultimate base overturning moment due to the excitation of the pier mass vertically. This results in an increase in the effective horizontal base shear, above that considering static push-over analysis as seen in figure 3-8, comparing static, cyclic pushover behavior with the dynamic behavior from an example time history analysis. Demands to members and connections along the lateral load path need to be increased for the above dynamic effects in order to capacity protect existing elements. The dynamic effects are investigated with particular emphasis on the role played by the impact and impulsive loads applied during pier rocking.
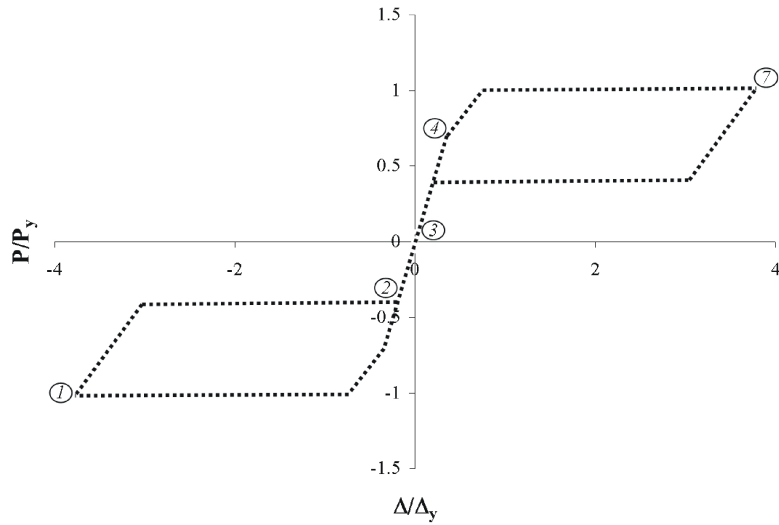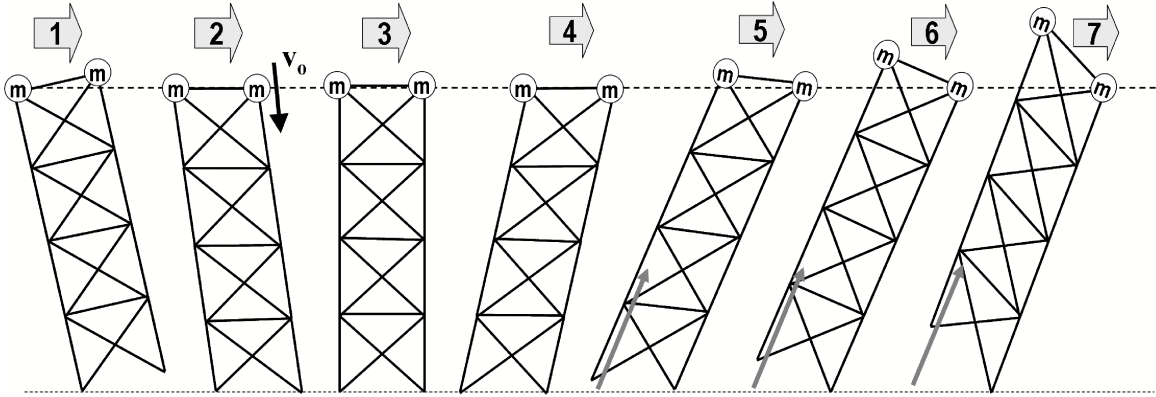
FIGURE 3-7   Critical Force Response During Rocking Motion due to Impact and
Uplift
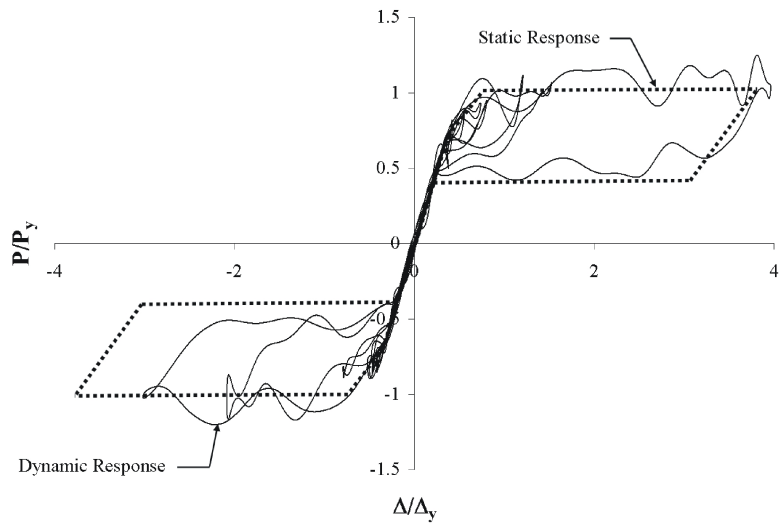
FIGURE 3-8   Dynamic and Static Hysteretic Response

3.3.1 Static and Dynamic Transfer of Vertical Loads

3.3.1.1 Static Transfer of Vertical Loads

For illustration of the concept presented here, rocking motion of the pier is taken starting from a displacement of - Δ_{y1}, a point at which one side of the pier has uplifted from the foundation by an amount equal to the yield displacement of the buckling-restrained brace, Δ_{yub}. At this point the buckling-restrained brace has reached its yield point in tension but does not yield in compression when the pier leg travels back to its support. The free body diagram of the pier in five different positions while rocking from left to right, considering static response, is shown in figure 3-9. As the pier travels from position 1 to 2, the force in the buckling-restrained brace is released and reaches zero at position 2. As seen in figure 3-9, half of the vertically acting gravitational force (i.e. the weight), $^W/_2$, is being transferred

Position 1:
$^W/_2$ $^W/_2$ $P=(^W/_2+A_{ub}F_{yub})^d/_h$
$R_{x1}=^P/_2$ $R_{x2}=^P/_2$
$R_{f1}=W+A_{ub}F_{yub}$ $A_{ub}F_{yub}$

Position 2:
$^W/_2$ $^W/_2$ $P=^W/_2(^d/_h)$
$R_{x1}=^P/_2$ $R_{x2}=^P/_2$
$R_{f1}=W$

Position 3:
$^W/_2$ $^W/_2$ $P=0$
$R_{f1}=^W/_2$ $R_{f2}=^W/_2$

Position 4:
$P=^W/_2(^d/_h)$ $^W/_2$ $^W/_2$
$R_{x1}=^P/_2$ $R_{x2}=^P/_2$
$R_{f1}=W$

Position 5:
$P=(^W/_2+A_{ub}F_{yub})^d/_h$ $^W/_2$ $^W/_2$
$R_{x1}=^P/_2$ $R_{x2}=^P/_2$
$A_{ub}F_{yub}$ $R_{f1}=W+A_{ub}F_{yub}$
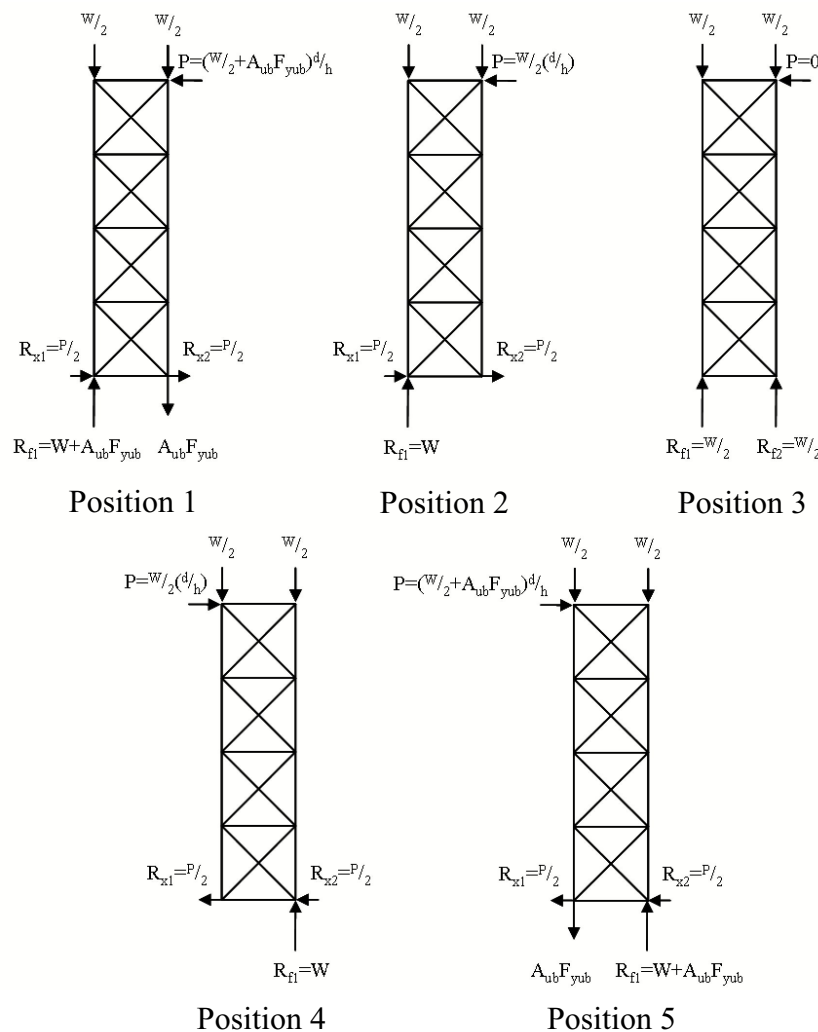
FIGURE 3-9   Free-Body Diagram of Each Critical Step

44

directly down a pier leg while the other half is transferred through the truss to the single support in position 2. From 2 to 3 the portion of the weight, $^w/_2$, that was transferred through the truss is progressively returned directly down its supporting leg as it impacts. From 3 to 4 the pier begins to move in the other direction and the other half of the weight, $^w/_2$, is transferred to the leg on the compressive side through the truss pier. At position 4, uplift is initiated, and from 4 to 5 the buckling-restrained brace is pulled until it reaches its yield force in tension (assumed to equal $A_{ub}F_{yub}$) at point 5. This force is also transferred through the truss to the support on the compressive side.

3.3.1.2   Review of SDOF Linear Mass-Spring Systems Subjected to Impulsive Load

The response of simplified linear mass-spring systems subjected to a step force with finite rise time is first reviewed to provide the relevant theory to determine the dynamic amplification during the rocking response.

A general solution for the displacement response of a linear dynamic system, based on an impulse-momentum formulation, known as the convolution integral, can be found in Clough and Penzien (1975) expressed as:

$$u(t) = \int_0^t p(\tau)\, h(t-\tau)\, d\tau \tag{3-20}$$

where p( )d   is the magnitude of the impulse at time   and h(t-) is defined as the unit impulse-response function. More specifically, the form of loading can be described as a step force with finite rise time (t_r) defined as:

$$p(t) = p_o \frac{t}{t_r} \quad \left(t \le t_r\right) \tag{3-22}$$

$$p(t) = p_o \quad \left(t \ge t_r\right)$$

The undamped displacement response for this type of loading (assuming zero initial conditions), for time greater than t_r, can be shown to equal:

$$u(t) = \left(u_{st}\right)_o \left(1 - \frac{1}{\omega_n t_r} \left[\sin \omega_n t - \sin \omega_n \left(t - t_r\right) \right] \right) \tag{3-20}$$

where ω_n is the natural frequency of the mass-spring system, $(u_{st})_o$ is the static displacement response of the system subjected to the same maximum force, p_o, and is defined as:

$$\left(u_{st}\right)_o = \frac{p_o}{k} \tag{3-23}$$

where k is the stiffness of the spring in the simple mass-spring system. A dynamic amplification factor, R_d, defined as the ratio of maximum displacement response over time, u_o (maximum of 3-22), to the static displacement response (3-23) can be shown to equal:

$$R_d = \frac{u_o}{(u_{st})_o} = 1 + \frac{\left| \sin\left(\frac{\pi t_r}{T_n}\right) \right|}{\frac{\pi t_r}{T_n}} \tag{3-24}$$

Therefore the dynamic amplification factor is dependent only on the rise time of the applied load (t_r) and natural period of the mass-spring system (T_n). These values will be determined in the next section. Since the system is linear, forces are directly proportional to deformation thus R_d also defines the ratio of maximum force response to the static force response. The maximum force can thus be determined by amplifying the static force by R_d.

3.3.1.3   Pier legs

As described above, as the pier steps from one leg to another a series of loads are transferred through the pier vertically. A number of behaviors above start when the pier leg impacts the foundation; an impulsive load, defined by (3-21) with magnitude $^w/_2$, is then being applied to the pier leg. The first simple mass-spring system investigated represents the axial vibration of a pier leg with mass and loading concentrated at the top of the pier leg as shown in figure 3-10(a). The stiffness of this system, assuming a rigid foundation, can be taken as:

$$k_L = \frac{EA_L}{h} \tag{3-25}$$

where A_L is the cross-sectional area of a pier leg and h is the total height of the pier. The system mass is assumed to only consist of a concentrated mass, $^m/_2$, at the top of the pier leg,
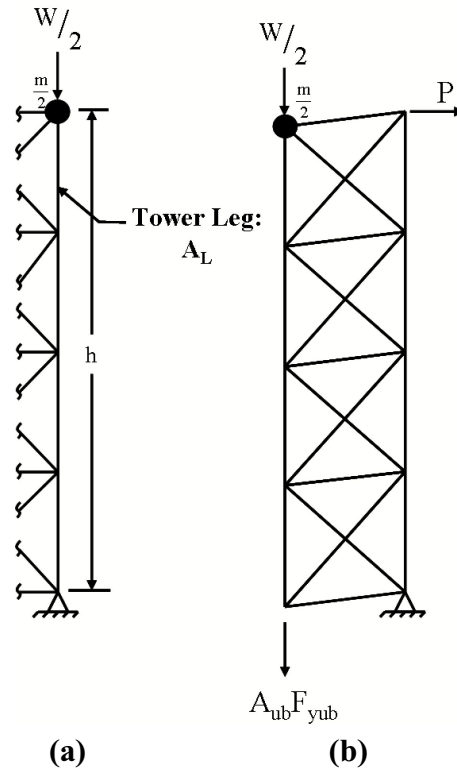
FIGURE 3-10   Vertical Modes of Vibration Excited During Rocking. (a) Axial Vibration of Pier Leg and (b) Vertical Shearing Mode of Pier Panels

therefore the period of vibration can be taken as:

$$T_L = 2\pi \sqrt{\frac{m}{2 k_L}} \tag{3-26}$$

The pier leg impacts the foundation with an initial velocity, v_o. The response of the pier leg, using the simplified system discussed above, to the initial velocity upon impact, v_o, can be defined as:

$$u(t) = \frac{v_o}{\omega_L} \sin \omega_L t \tag{3-27}$$

An approach to approximate the rise time of the impulsive loads during the rocking response is based on free-vibration response of the bridge pier assuming it to be a linear

elastic system as shown in figure 3-11. Thus the response with respect to time can be expressed as:

$$\Delta(t) = \Delta_u \sin\left(2\pi \frac{t}{T_{sec}}\right) \tag{3-28}$$

where $_u$ is the maximum global horizontal displacement of the bridge pier (methods for $_u$ will be discussed in Section 3.4) and T_{sec} is an effective linear elastic horizontal natural period of vibration of the bridge pier system taken to be:

$$T_{sec} = 2\pi \sqrt{\frac{m\Delta_u}{P_y}} \tag{3-29}$$

where P_y is the horizontal yield force of the controlled rocking system, defined by (3-6), and m is the effective horizontal mass. Therefore the time it takes the system to travel from step 2 to 3 is defined as the rise time for the load applied directly down a pier leg, t_{rL}, and can be approximated by the expression:

$$t_{rL} = \frac{T_{sec}}{2\pi} \sin^{-1}\left(\frac{\Delta_{up1}}{\Delta_u}\right) \tag{3-30}$$

where $_{up1}$ is defined by (3-3). Finally, the dynamic amplification factor for this load,
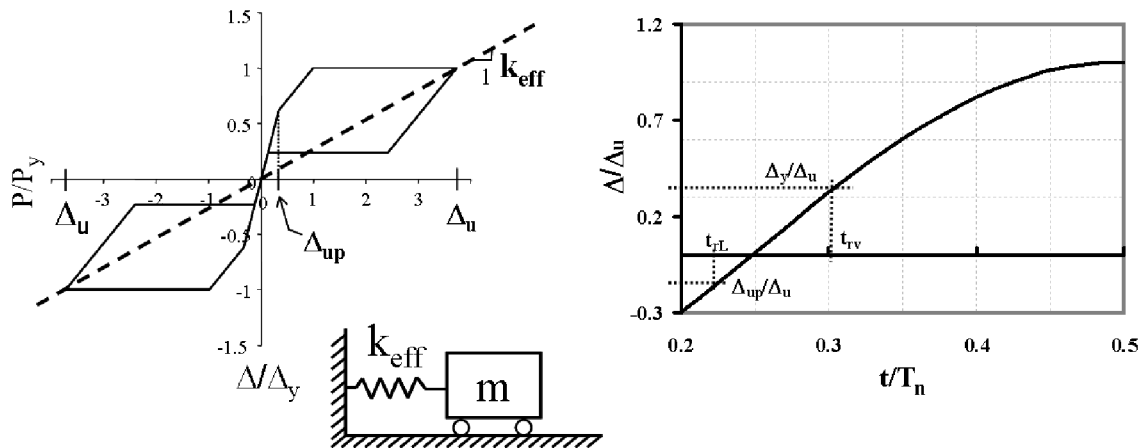
FIGURE 3-11   Illustration of Linear-Elastic System used for Determination of System Rise Times

R_{dL}, can be defined by:

$$R_{dL} = 1 + \frac{\left| \sin\left(\dfrac{\pi t_{rL}}{T_L} \right) \right|}{\dfrac{\pi t_{rL}}{T_L}}$$ (3-31)

Since this load acts through the new axis of rotation, it does not affect the base overturning moment. However, it will affect the maximum axial force developed in the leg.

3.3.1.4 Vertical shear mode of pier

As the rocking motion continues, vertical loads are transferred through the truss vertically to the other side as the pier uplifts. During uplift the simple mass-spring system, shown in figure 3-10b, is assumed to be subjected to zero initial conditions unlike during impact. Two loads are applied in series during uplifting (steps 3 to 5). First, a load of $^{w}/_{2}$ is transferred through the truss vertically as the gravitational restoring moment is overcome followed by the yield force of the buckling-restrained brace (assumed to equal $A_{ub}F_{yub}$).

The vertical stiffness in shear of the truss system for piers with panel heights equal to the pier width could be taken as:

$$k_v = f_p \frac{EA_d}{d} (\#panels)$$ (3-32)

where A_d is the cross-sectional area of the pier diagonals, d is the pier width and E is the modulus of elasticity for the existing bridge diagonals as can be seen in figure 3-12. The vertical shear stiffness is directly proportional to the number of panels due to each panel acting in parallel to resist the vertical shearing loads. The factor f_p can be shown to equal:

$$f_{p,X} = \frac{1}{\sqrt{2}} \quad (for\ X\text{-}braced\ piers)$$ (3-33)

$$f_{p,V} = \frac{1}{\sqrt{5}} \quad (for\ V\text{-}braced\ piers)$$ (3-34)
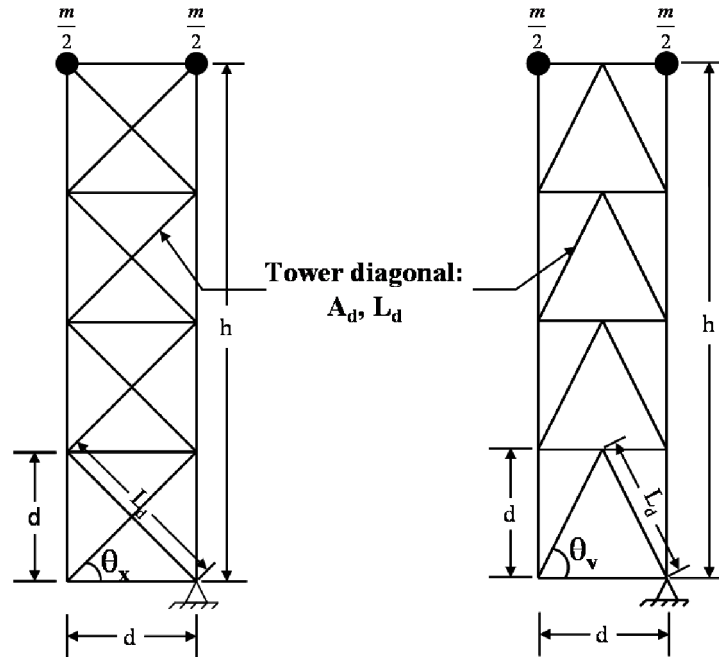
FIGURE 3-12   Representative Piers for Calculation of Vertical Stiffness of X- and V- braced Piers

For the vertical shearing mode of vibration, the effective mass for the vertical truss system is taken equal to $^m/_2$. The period of vibration of the vertical truss system is therefore:

$$T_v = 2\pi \sqrt{\frac{m}{2k_v}} \qquad (3\text{-}35)$$

As the pier moves from position 3 to 5, the two uplifting forces ($^W/_2$ and $A_{ub}F_{yub}$) are applied through the truss vertically with rise times t_{r1} and t_{r2} respectively. It can be shown that t_{r2} is greater than t_{r1}, assuming free-vibration response, while both forces vibrate at the same frequency. Looking at a sample response of figure 3-13, the motions tend to be somewhat out of phase. They will become in-phase as t_{r2} approaches T_v however the amplification factor approaches 1 as t_{r2} approaches T_v. Consideration of the two separate loads and superposition of their individual dynamic amplification considering phase differences can
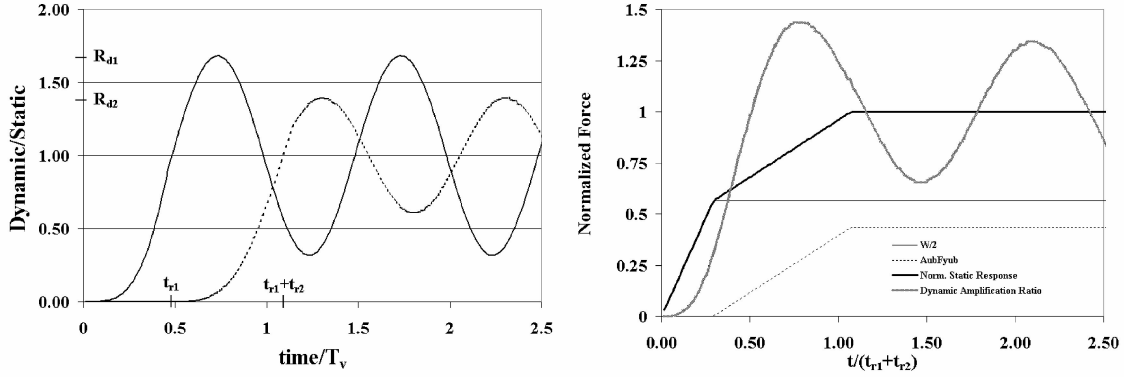
FIGURE 3-13   Dynamic and Static Response of Loads Through Truss Pier Vertically. (a) Dynamic Response of Each Load (w/2, $A_{ub}F_{yub}$) and (b) Normalized Total Dynamic and Static Response

become complex. Therefore a simpler approach is taken to obtain a single amplification factor for the two uplifting loads. Following that approach, a rise time, t_{rv}, is defined for the sum of the two loads during uplift as:

$$t_{rv} = \frac{T_{sec}}{2\pi} \sin^{-1}\left(\frac{\frac{1}{2}\Delta_{y1}}{\Delta_u}\right) \tag{3-36}$$

where Δ_{y1} is the pier displacement at the point of yield using 1st cycle properties. This is equivalent to taking the average rise time for the two forces during uplift. Therefore the dynamic amplification factor for the sum of these two loads is taken as:

$$R_{dv} = 1 + \frac{\left|\sin\left(\frac{\pi t_{rv}}{T_v}\right)\right|}{\frac{\pi t_{rv}}{T_v}} \tag{3-37}$$

Due to the dynamic nature of the structural response shown above, and close coupling of vertical dynamic modes and horizontal base shear, the increased response due to dynamic effects needs to be taken into account in order to adequately capacity protect existing structural elements. The dynamic amplification factors for the impulsive loads applied

51

during rocking were established in this section and will be used in the capacity based design procedure presented in Section 4.

3.4 Parametric Study to Provide Proof of Concept

A parametric study was undertaken in order to provide a preliminary understanding of system behavior and to assess some simple, existing methods of analysis in predicting maximum developed pier displacements. These methods are used to size the buckling-restrained braces (based on limiting device strains) and nonlinear time history analyses used for verification of predicted response. Results obtained are also used to assist in formulating a design procedure (presented in Section 4) that can reliably predict the system's ultimate seismic response.

3.4.1 Methods of Analysis

One of the objectives of this parametric study was to assess the accuracy of some approximate, simplified techniques in predicting seismic response of controlled rocking pier systems. Therefore, a number of such procedures were considered. A first method of analysis considered consists of characterizing system response in a manner similar to the nonlinear static procedure (NSP) described in FEMA 356 (FEMA 2000), while a second is similar to the nonlinear static procedure for passive energy dissipation systems found in FEMA 274 (FEMA 1997). An analysis procedure similar to the latter one can be found in the NCHRP 12-49 document (ATC/MCEER 2003) and the AASHTO Guide Specifications for Seismic Isolation Design (2000). For the purpose of this parametric study, the only constraint imposed using the above procedures was to limit axial strain on the buckling-restrained braces to an arbitrarily selected value of 1.5%. Examples for each method of analysis are given in Appendix C.

The first method attempts to characterize the controlled rocking system as an effective SDOF, bi-linear hysteretic system and determine its displacement response using a 2% damped response spectrum. A pushover curve is developed, incorporating the nonlinear load-deformation characteristics of individual elements. A lateral load profile representative of the dominant mode of vibration should be used. The load profile for the

rocking bridge pier system is taken as a single horizontal load applied at the level of the bridge deck and the only nonlinear behavior is attributed to the buckling-restrained brace. Due to the system's increased flexibility in the 2nd and subsequent cycles, 2nd cycle properties (discussed in Section 3.2.2) are used to develop the pushover curve. The displacement demand of the pier is then determined from:

$$\Delta_u = C_0\,C_1\,C_2\,C_3\,S_a\,\frac{T_{\text{eff}}^{\;2}}{4\pi^2}\,g \qquad (3\text{-}38)$$

where T_{eff} is an effective period of vibration, determined by:

$$T_{\text{eff}} = 2\pi\sqrt{\frac{m}{k_{\text{eff}}}} \qquad (3\text{-}39)$$

and methods to determine k_{eff} will be discussed below. Factor C_0 is used to relate displacements in an MDOF system to the displacement of an equivalent SDOF system calculated by (3-38). Factor C_2 is to account for stiffness and/or strength degradation and factor C_3 is to account for dynamic P- effects. All factors, except for C_1, are set equal to 1.0 since the controlled rocking system is assumed to be an SDOF system without stiffness nor strength degradation and has positive post-yield stiffness. Factor C_1 is used to account for the expected increase in displacement in the short period (or equal energy) range of the spectrum. C_1 is defined in the long period range ($T_{\text{eff}} \geq T_s$) as:

$$C_1 = 1.0 \qquad (3\text{-}40)$$

and in the short period range, is defined as:

$$C_1 = \frac{\left[1.0 + (R-1)\dfrac{T_s}{T_{\text{eff}}}\right]}{R} \qquad (3\text{-}41)$$

where T_s is the characteristic period, separating the long and short period ranges of the spectrum and is defined as:

$$T_s = \frac{S_{DS}}{S_{D1}} \qquad (3\text{-}42)$$

S_{DS} is the design short period spectral acceleration and S_{D1} is the design 1-second spectral acceleration. R, in (3-41), is the ratio of the elastic strength demand to the system yield strength and equal to:

$$R = \frac{S_a}{P_y/w} \cdot C_m \qquad (3\text{-}43)$$

where C_m is an effective mass factor for the mode of vibration considered. Since the controlled rocking system response is assumed to be dominated by a single mode, this factor is taken to be 1.0. Factor C_1 is used as described above where appropriate, however this factor was not necessarily established for such a hysteretic system.

A conservative estimate of the effective stiffness (k_{eff}) can be taken as the rocking stiffness (k_r), as defined by (3-5). This will be referred to as Method 1 in the parametric study. A rational expression for the effective stiffness can also be taken as:

$$k_{eff2} = k_o \left(\frac{\Delta_{up2}}{\Delta_{y2}} \right) + k_r \left(\frac{\Delta_{y2} - \Delta_{up2}}{\Delta_{y2}} \right) \qquad (3\text{-}44)$$

where all terms have been defined previously. This will be referred to as Method 2, and is a characterization of the effective stiffness similar to that in FEMA 356 (FEMA 2000) for systems that experience progressive yielding and do not have a definite yield point. As $_L$ approaches unity, $_{up2}$ approaches a value of zero and (3-44) approaches the rocking stiffness, thus Method 2 becomes equivalent to Method 1. This characterization of effective stiffness for Methods 1 and 2 is illustrated in figure 3-14a and 3-14b respectively.

The method proposed in the FEMA 274 document for the design of passive energy dissipation systems uses spectral capacity (pushover) and demand curves and can represent the response in a graphical format. Conversion of the demand and capacity (pushover) curve to spectral ordinates is based on modal analysis theory. The bridge piers are assumed here to behave as a single degree of freedom system representing the dominant horizontal mode of vibration. The added energy dissipation from the unbonded braces is converted to equivalent viscous damping and the seismic demand curve reduced from the 2% damped spectrum. For the flag-shaped hysteretic behavior of the controlled rocking system, the equivalent viscous damping can be determined by:

$$\xi_{eff} = \xi_o + \xi_{hys} \qquad (3\text{-}45)$$

where $_o$=inherent structural damping (assumed to be 2%) and $_{hys}$=hysteretic damping provided by unbonded braces during rocking response. The hysteretic damping can be

approximated by modifying the equivalent damping of a bi-linear system (with no strain hardening) by a factor q:

$$\xi_{hys} = q \cdot \xi_{bi} = \frac{\eta_L}{1+\eta_L} \cdot \frac{2}{\pi} \cdot \left(1 - \frac{1}{\mu_2}\right) \tag{3-46}$$

where μ_2=displacement ductility ratio considering 2nd cycle properties such that:

$$\mu_2 = \frac{\Delta_u}{\Delta_{y2}} \tag{3-47}$$

Factors for reducing the spectrum in the short (B_s) and long period ranges (B_1), for the effective damping (ξ_{eff}) from (3-45), are given in the FEMA 274 document. This will be referred to as Method 3 and is illustrated in figure 3-14c. Further discussion on simple methods for calculating the response of passive energy dissipation systems can be found in Ramirez et al. (2000).

Rocking structures also dissipate energy through the radiation of stress waves into the soil (or assumed as an inelastic impact) that occurs during each half-cycle. Conversion of this form of energy dissipation into equivalent viscous damping has been considered by Housner (1963), Priestley et. al. (1978) and Mander and Cheng (1997). The amount of energy dissipation, in the form of equivalent viscous damping, has been shown to be in the range of 2-6% and decreases with increasing aspect ratio of the rocking element. The energy dissipated by the yielding steel elements is much more significant and ignoring this effect is conservative.
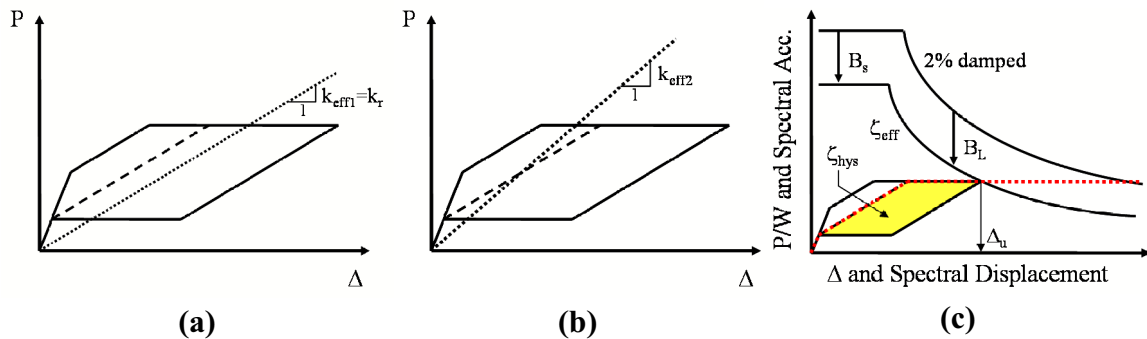
FIGURE 3-14   Methods of Analysis (a) NSP-FEMA 356 (k_{eff1}=k_r), (b) NSP-FEMA 356 (k_{eff2}), (c) Spectral Demand-Capacity, FEMA 274

3.4.2 Discussion of Pier Properties Used

A range of parameters assumed representative of steel truss bridge piers were established to investigate the response of self-centering, flag-shaped hysteretic systems. The parameters related to existing steel truss bridge piers are largely dependent on the pier aspect ratio ($^h/_d$). Inspection of drawings of a few existing steel truss bridges revealed some consistent details. They include:

- aspect ratios generally ranging from 1 to 4, although other values also exist
- pier diagonals of constant cross-section over pier height
- pier legs continuous over height
- pier diagonals and legs of similar sizes for different aspect ratios

These particular details reflect design practice at the time of construction. The piers carry their own tributary vertical gravity load. If vertical loads are assumed to be the same for all pier aspect ratios then pier legs would all be the same size. Similarly, if the design base shear is assumed identical for all piers (uniform design wind load) then the lateral load resisting elements may also be similar for all pier aspect ratios.

A set of pier properties, assumed to be representative, were adopted and some of their relevant dynamic properties for both horizontal and vertical vibrations are given in table 3-1 for rocking truss piers. More details of the piers used are given in Appendix D. Inclusion of the bridge deck flexibility would be required for a particular bridge application however this would only change the fixed-base horizontal stiffness (k_o) which already has somewhat arbitrary properties and will not significantly change the concepts presented here.

3.4.3. Description of Inelastic Computer Program

The structural analysis program SAP2000 version 7.40 is used for nonlinear static and dynamic analyses. Non-linear dynamic time history analyses are used for response verification of the simple design methods proposed in Section 3.4.1. This program uses

h/d	h (m)	d (m)	w (kN)	k_o (kN/mm)	T_o (sec)	k_L (kN/mm)	T_L (sec)	k_v (kN/mm)	T_v (sec)
4	29.26	7.32	1730	12.5	0.74	213	0.13	549	0.08
3	21.95	7.32	1730	23.1	0.55	283	0.11	411	0.09
2	14.63	7.32	1730	47.5	0.38	425	0.09	274	0.11
1	7.32	7.32	1730	123	0.24	850	0.06	137	0.16

TABLE 3-1   Relevant Horizontal and Vertical Dynamic Properties of Each Aspect Ratio

the Fast Nonlinear Analysis (FNA) method, presented in Wilson (2000) for solution of the nonlinear modal equations. Ritz vectors are used to take into account the spatial distribution of the dynamic loading. A force and energy convergence check are performed at the end of each time step. If the convergence criteria is not met, the time step is divided into smaller sub-steps until convergence is achieved. Inherent structural damping is approximated by assigning equivalent viscous damping to each mode.

3.4.4   Earthquake Loading

Spectra compatible ground acceleration time histories used for the dynamic analyses are generated using the Target Acceleration Spectra Compatible Time Histories (TARSCTHS) software developed by the Engineering Seismology Laboratory (ESL) at the State University of New York (SUNY) at Buffalo (http://civil.eng.buffalo.edu/users_ntwk/index.htm). Synthetic ground motions were generated by TARSCTHS matching the elastic response spectra defined by the NCHRP 12-49 (ATC/MCEER, 2003) spectrum for the specified 1-second spectral acceleration value (S_1). A range of seismic demands with values of S_1 ranging from 0.25g to 0.75g are used. The short period spectral acceleration value (S_s) is assumed equal to 2.5 times S_1. Values of T_0 and T_s can be determined using the NCHRP 12-49 document. Seven motions for each demand level were produced. The resulting SDOF oscillatory response spectrum for each motion is given in Appendix E.

3.4.5 Analytical Model

An analytical model was developed to study the behavior of the proposed rocking bridge pier system, more specifically the response of representative piers subjected to a horizontal excitation applied in a primary orthogonal direction. Each pier is assumed to carry an equal inertia mass both vertically and horizontally. Thus, each pier is assumed to carry an equal length of bridge deck and interaction between adjacent piers is assumed negligible. A 2-D model of each representative truss pier is used with half of the mass applied to each of the top two nodes of the truss. The pier itself is modeled with its elastic properties and all nonlinear action is modeled to occur at the foundation interface. A compression-only, "gap" element and a hysteretic element are placed in parallel across the anchorage interface, at the base of each tower leg, to model the rocking behavior. The "gap" elements represent the foundation with no tensile capacity and a linear force-displacement relationship in compression. The buckling-restrained brace is modeled using a bi-linear hysteretic model in the vertical (uplifting) direction. The model is defined by an initial, elastic stiffness (k_{ub}, (3-19)), yield force ($A_{ub}F_{yub}$), post-yield stiffness ratio ($_{ub}$) and a factor for the smoothness (or sharpness) of the yield transition. The post-yield stiffness ratio was set equal to 0.01 (1% hardening) and the yield transition factor was set to be representative of behavior of the braces discussed in Section 2.3. The element is based on the model proposed by Wen (1976). Restraints are provided at the anchorage level that prevent movement in the horizontal direction but provide no resistance to vertical movements. A sample SAP2000 input file is given in Appendix F.

3.4.6 Results and Observations

Results of the parametric study are presented to show the adequacy of the simple methods of analysis to predict the maximum displacement response of the controlled rocking system. With the only system design constraint of limiting axial strains of the buckling-restrained braces, the buckling-restrained brace lengths were designed by initially taking their length equal to 305cm and iterating upon the buckling-restrained brace area. In some cases however, the buckling-restrained brace length was also modified to satisfy the constraints. Thus systems with varying local strength ratios, $_L$, resulted somewhat arbitrarily from this process. For reference, the local strength ratios for all designs are given in table 3-2.

Results are presented in terms of the average strain on the buckling-restrained brace, from the inelastic time history analyses using seven synthetic motions, normalized by the target strain of 1.5%. Pier aspect ratios of 2, 3 and 4 were used with seismic demands characterized by 1-second spectral accelerations of 0.25, 0.5 and 0.75g. Results are presented in figure 3-15 for Methods 1, 2 and 3.

With the exception of Method 2, for the aspect ratio of 4, all designs were shown to be conservative. Method 1 was shown to be overly conservative when a relatively small brace (A_{ub} and L_{ub}) was used, as evident from figure 3-15a for a demand of S_1=0.25g and the values of $_L$ for these cases (table 3-2). Since Method 1 uses the rocking stiffness (k_r) to completely define the effective stiffness of the system, small values of A_{ub} and L_{ub} results in the rocking stiffness having limited participation in the elastic response, i.e. this stiffness occurs only over a small range of displacement for the entire hysteretic loop.

With this type of system (flag-shaped hysteretic), results in figure 3-15 shows that Method 3 can be more reliable for all possible designs. Yet, although Methods 1 and 2 use a design philosophy that was initially established for elasto-plastic systems, they appear to work reasonably well for systems with $_L$>0.6. Method 3 accounts for system strength, elastic stiffness, post-elastic stiffness and energy dissipation while Methods 1 and 2 are highly dependent on the system's initial elastic stiffness properties. Thus, the lack of hysteretic energy dissipation of the controlled rocking system (compared to a system exhibiting full hysteretic loops) can result in under-prediction of the maximum displacement using Methods 1 and 2.
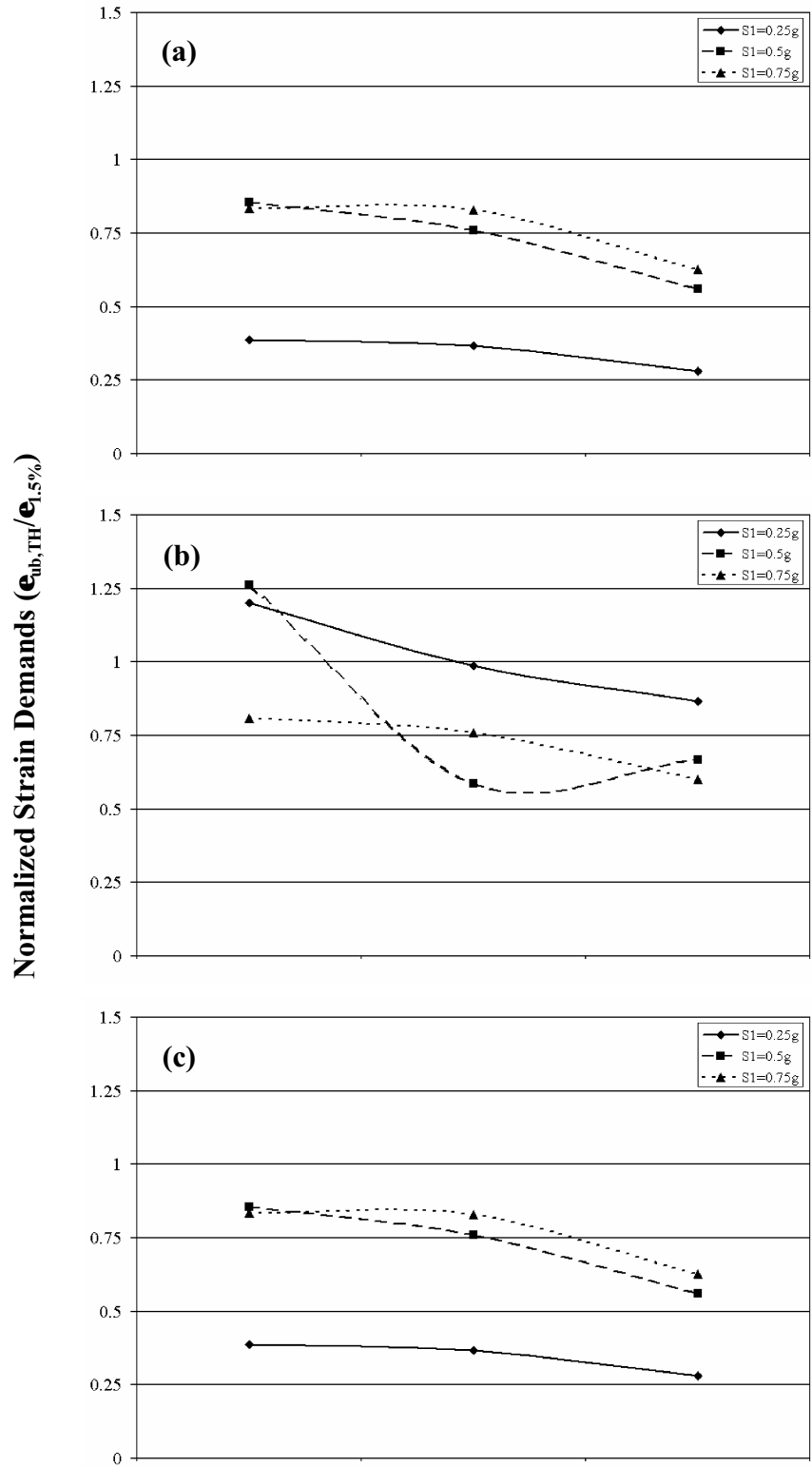
FIGURE 3-15   Results of Parametric Study for (a) Method 1, (b) Method 2 and (c) Method 3

Method 1	1-Second Spectral Acceleration		
h/d	0.25g	0.5g	0.75g
4	0.08	0.38	1.22
3	0.08	0.38	1.25
2	0.07	0.38	1.31

Method 2	1-Second Spectral Acceleration (S_1)		
h/d	0.25g	0.5g	0.75g
4	0.23	0	1.3
3	0.22	1.44	1.38
2	0.23	0.64	1.46

Method 3	1-Second Spectral Acceleration (S_1)		
h/d	0.25g	0.5g	0.75g
4	0	0.34	0.98
3	0.18	0.36	0.96
2	0.17	0.34	0.95

TABLE 3-2   Local Strength Ratios of Systems in Parametric Study

SECTION 4

PROPOSED DESIGN PROCEDURE FOR CONTROLLED ROCKING SYSTEM

4.1 Introduction

The retrofit strategy presented in Section 3 requires that a set of design constraints be established to ensure satisfactory seismic performance. A capacity based design procedure is proposed here to protect non-ductile elements while forcing all inelastic action into specially detailed steel yielding devices that are able to dissipate energy in a stable, predictable manner. A large number of constraints may be needed and thus a systematic design procedure to satisfy all constraints is desirable. A proposed design procedure, using a graphical approach in which the boundaries of compliance and non-compliance of the design constraints are plotted with respect to two key design parameters, is used along with a simpler step-by-step approach. The two design parameters used in the graphical procedure are the length and cross-sectional area of the buckling-restrained brace, L_{ub} and A_{ub} respectively.

The proposed design procedure enables designers to select buckling-restrained brace properties and modify existing elements to control the stiffness and strength parameters of the structural system in order to achieve desirable seismic performance. The pier is assumed to remain elastic and thus must be capacity protected by determining a conservative ultimate expected demand. Strength of existing bridge elements will vary from bridge-to-bridge and partial strengthening may be required in some cases.

Each design constraint is discussed in detail in Section 4.2 and methods to predict the key response quantities for design are discussed in Section 4.3. Section 4.4 compares the prediction of maximum dynamic forces during rocking, using methods presented in Section 4.2 and 4.3, with the "exact" response. The step-by-step procedure along with a design example is presented in Section 4.5 and a brief discussion of the graphical design procedure solution method is given in Section 4.6.

4.2 Design Constraints

Strength, drift, velocity and ductility demand limits need to be established such that ductile seismic performance can be achieved without undermining the gravity load carrying capacity of the pier. A set of design constraints are proposed here that attempt to satisfy these limits while limiting damage to the ductile structural fuses.

4.2.1 Deck-level Displacement

To the writer's knowledge, there exists no established maximum allowable deck level displacements for the serviceability limit state of bridges (although limits corresponding to various states of structural damage do exist). Although there are generally no non-structural components within bridge structures that would require limited drifts to prevent damage, there likely exists structural elements for which deformations must be limited to prevent their damage or damage of their connections. Either these elements need to be modified to be able to sustain the displacement without damage, or displacement demands must be kept within acceptable limits. These limits will vary from bridge to bridge.

Therefore, for the purpose of this study and to illustrate the design procedure, a displacement limit is set that attempts to prevent P-Δ effects from affecting the seismic behavior and another limit is imposed based on preventing overturning instability. The smaller of these two limits is used here. Additional limits can be added on a case-by-case basis as necessary.

A requirement shown to limit P-Δ effects based on the dynamic analysis of SDOF systems with various hysteretic relationships is taken from the NCHRP 12-49 document (ATC/MCEER, 2003). The limit is given by:

$$\Delta_u \le 0.25 \frac{V}{W} h \qquad (4\text{-}1)$$

where V is the lateral strength of the pier equal to P_y (defined by 3-6).

Another limit is set based on preventing displacement of the center of mass from exceeding half of the base width ($^d/_2$) with a large factor of safety since this is the point of overturning. This limit is defined by:

$$\Delta_u \leq \frac{d}{2FS}$$ (4-2)

A factor of safety (FS) of 5 is recommended.

4.2.2 Ductility Demands on Buckling-restrained Brace

Limits on the inelastic strain demands are set in order to ensure that the buckling-restrained brace behaves in a stable, predictable manner. These limits should be based on engineering judgement and experimental test data on the ultimate inelastic cyclic response of the brace. A strain of 1.5% has been selected here. This is a modest level of strain for most structural steels and some buckling-restrained braces have been shown, through experimental testing, to develop twice this strain level with very stable hysteretic behavior (Iwata, 2000). This constraint can be established in terms of brace elongation by:

$$\Delta_{ub} \leq 0.015 L_{ub}$$ (4-3)

4.2.3 Forces to Existing Members and Connections

The capacity of steel truss bridge piers in terms of maximum allowable forces can be limited by many mechanisms. Vulnerabilities were discussed in Section 2.2. Failure of connections or members can cause undesirable response by imposing ductility demands in regions that are unable to withstand these demands. Capacity design procedures are used to conservatively predict the maximum force demands such that these non-ductile elements can remain elastic thus forcing all inelastic action to the specially detailed, ductile structural elements.

A method is proposed here that creates an "effective" static shear that can be used to evaluate the adequacy of the pier's lateral load path followed by a method to determine the ultimate demands placed on the pier legs and foundation.

4.2.3.1 Effective Lateral Shear Demand

The "effective" base shear demand is determined by the static yield force from (3-6) amplified to account for the increased demand caused by dynamic effects as discussed in Section 3.3. Thus, the ultimate base shear demand can be expressed as:

$$P_u = \left(\frac{w}{2} + A_{ub} F_{yub} \right) \frac{d}{h} R_{dv} \tag{4-4}$$

where R_{dv} is defined by (3-37). Limiting the buckling-restrained brace strength, $A_{ub} F_{yub}$, to an acceptable level or strengthening of the weak elements along the lateral load path can satisfy this constraint.

4.2.3.2 Pier Leg Demands

Conservatively estimating the ultimate load on the pier legs is essential because they resist gravity loads of the bridge. The max base shear defined above imposes demands to the pier legs, however the pier legs must also resist additional demands. As was discussed in Section 3.3, demands to the impacting pier leg include a velocity upon impact followed by impulsive loads. The leg is assumed to be supported on a rigid foundation as was done for the amplification factors discussed in Section 3. Using (3-22) and (3-27), the maximum demands on a pier leg could be determined by superposition of each resulting response. However with the simplifications made in determining the rise times and period of vibration of the simplified systems and the sensitivity of the total response to these factors, an alternative approach is taken. In this approach, the maximum response of each action individually is summed to conservatively estimate demands.

Using such an approach, neither time nor damping is taken into account thus the response caused by the initial velocity and applied forces are assumed to be in-phase. The total force in the leg can be written as:

$$P_L = P_{vo} + P_{wL} + P_v \tag{4-5}$$

where P_{vo} is the force developed due to the initial velocity upon impact, v_o, and is defined by:

$$P_{vo} = v_o \sqrt{\frac{m \cdot k_L}{2}} \tag{4-6}$$

where v_o is the vertical velocity of the pier leg upon impact and methods to determine v_o will be discussed later. P_{wL} is the force developed in the leg, including dynamic amplification, caused by the tributary weight of the leg and is defined as:

$$P_{wL} = R_{dL} \cdot \frac{w}{2} \tag{4-7}$$

and P_v is the force developed in the leg due to the transfer of loads through the pier diagonals and is defined here as:

$$P_v = R_{dv} \cdot \left(\frac{w}{2} + A_{ub} F_{yub} \right) \tag{4-8}$$

Therefore, the total force developed in a pier leg using the approach discussed above is equal to:

$$P_L = v_o \sqrt{\frac{m \cdot k_L}{2}} + R_{dL} \cdot \frac{w}{2} + R_{dv} \cdot \left(\frac{w}{2} + A_{ub} F_{yub} \right) \tag{4-9}$$

In the perspective of seismic retrofit, the buckling-restrained brace strength, $A_{ub}F_{yub}$, and the impact velocity, v_o, are the primary parameters influencing demands to the pier legs.

4.2.3.3 Demands to General Foundation Element

Including the foundation flexibility in the response of the controlled rocking system would result in increased flexibility of the hysteretic behavior overall, however, the influence on other factors is not as clear. Also, in considering the influence of a flexible foundation, the ability to dissipate energy in the form of stress waves radiating into the foundation and supporting medium (radiation damping) should be considered. The influence of the foundation flexibility is beyond the scope of this report and thus the foundation will continue to be assumed rigid here.

With the assumption of a rigid foundation, the maximum force developed in a foundation element supporting a pier leg is identical to the maximum force developed in the pier leg. Therefore the maximum allowable force in the pier leg can also be controlled by the capacity

of the foundation. For the purpose of illustrating the design procedure, the foundation is assumed to be a trapezoidal concrete foundation pedestal and its capacity, in terms of an allowable force, can be determined based on equations from the American Concrete Institute (ACI) *Building Code Requirements for Structural Concrete* (ACI, 2000). The capacity of an arbitrary foundation pedestal is determined in Appendix G and used in later design examples.

4.2.4 Self-centering

The final constraint places an upper-bound on the buckling-restrained brace strength to ensure that the self-centering ability of the system is ensured. Assuming the buckling-restrained brace strength to simply equal $A_{ub}F_{yub}$ and ignoring the second order effects discussed in Section 3.2.3, this constraint can be defined as:

$$\eta_L \le 1 \qquad (4\text{-}10)$$

where η_L is the local strength ratio defined by (3-11).

4.3 Prediction of Key Response Values for Design

4.3.1 Maximum Deck-level Displacement

The maximum deck-level (global) displacement of the controlled rocking bridge pier system can be determined using methods presented in Section 3.4.

4.3.2 Prediction of Impact Velocity

The demand to the pier leg caused by the initial velocity of the pier leg prior to impact requires the prediction of this initial velocity. The velocity upon impact is predicted here using two approaches, a ductility reduction approach and another which uses a linear, viscous characterization of the controlled rocking system.

Yield strength reduction factors for each region of the spectrum, as a function of the displacement ductility ratio, have been proposed by researchers to relate the response of a linear-elastic system to an inelastic hysteretic system with identical initial stiffness. One set of factors based on the analysis of elasto-plastic SDOF systems was proposed by

Newmark and Hall (1982). Reduction of the elastic design spectrum to obtain inelastic, constant-ductility, design spectrum using the factors of Newmark and Hall is shown in figure 4-1.
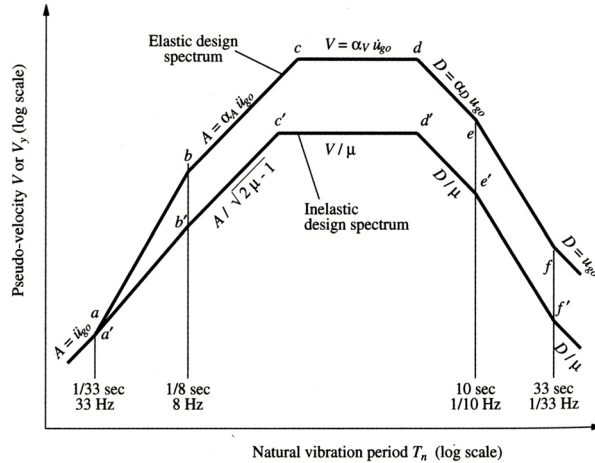
FIGURE 4-1   Inelastic Design Spectrum with Newmark and Hall Reduction Factors (adapted from Chopra, 2001)

It is important to note that these factors were developed based on the analysis of elasto-plastic systems developing full hysteretic loops. The controlled rocking mechanism proposed here develops flag-shaped hysteresis which dissipates less energy per cycle compared to an elasto-plastic system with the same yield force, yield displacement and ultimate displacement, as shown in figure 4-2. Although flag-shaped hysteresis is less effective at dissipating energy, its behavior is stable, without strength nor stiffness degradation, and is assumed to have zero post elastic stiffness.
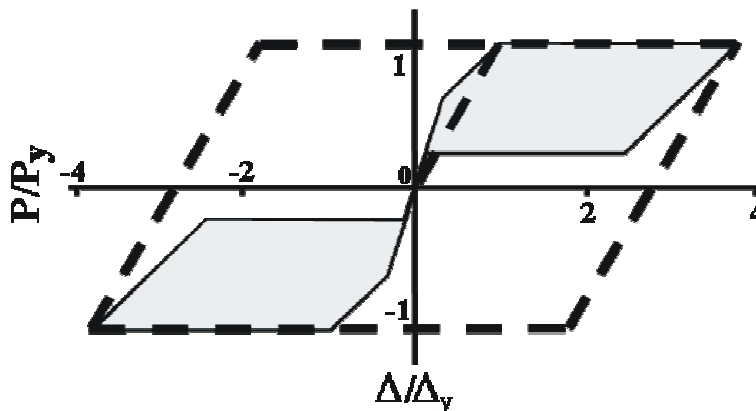
FIGURE 4-2   Flag-shaped and Elasto-plastic Hysteretic Behavior

69

Based on results of the parametric study of SDOF flag-shaped hysteretic systems performed by Christopoulos et. al. (2002), some qualitative conclusions can be drawn on the effectiveness of this nonlinear, hysteretic system to reducing demands from the elastic spectral response. When comparing the response of the flag-shaped hysteretic system to elasto-plastic systems, the ultimate displacement response was shown to be very similar for systems in the long period range and with energy dissipation coefficients (η_L) equal to unity. Energy dissipation coefficients less than unity leads to increased displacement response from that of the elasto-plastic system. Response of flag-shaped systems in the short period range can be significantly greater than that of an elasto-plastic system.

Thus a modified displacement ductility ratio is proposed to account for the deviation in behavior from that of an elasto-plastic system. The modified displacement ductility ratio is defined here by:

$$\mu_m = \beta\mu \qquad (4\text{-}11)$$

where μ is the well known displacement ductility ratio defined as:

$$\mu = \frac{\Delta_u}{\Delta_{y2}} \qquad (4\text{-}12)$$

where Δ_u is the ultimate global displacement and Δ_{y2} is the yield displacement in the 2nd and subsequent cycles defined by (3-14). The approach taken to determine the "modifying" factor, β, is based on the energy dissipated per cycle. Modifying factors are proposed for the short and long period range.

The modifying factor for the long period range (constant velocity region), β_L, is taken equal to:

$$\beta_L = \frac{2\eta_L}{1 + \eta_L} \qquad (4\text{-}13)$$

where η_L is the local strength ratio defined by (3-11). The modifying factor for the short period range (constant acceleration region), β_s, is defined as:

$$\beta_s = \frac{1}{2}\beta_L = \frac{\eta_L}{1 + \eta_L} \qquad (4\text{-}14)$$

70

These factors simply represent the ratio of area enclosed by the flag-shaped hysteresis to the baseline system which represents the "50% system" ($\eta_L=1$) and an elasto-plastic system in the long and short period ranges respectively. The expressions used to define this ratio of areas is a simplification but the difference compared to the "exact" areas is minimal.

The modified displacement ductility ratio, μ_m, can be used to reduce the elastic response spectrum in a similar manner to that shown in figure 4-2, replacing μ by μ_m. Using the response spectrum, the inelastic pseudo-spectral velocity, PS_{vi}, can be predicted for a system with an effective period, T_{eff}, determined using the effective stiffness defined by (3-39). Use of the pseudo-spectral velocity for the maximum relative velocity is an approximation and correction factors to relate the two have been proposed by Ramirez et. al. (2000), Pekcan et. al. (1999) and Sadek et. al. (1999).

Another method, which attempts to predict the relative velocity, by first predicting the pseudo-velocity from a linear, viscous characterization of the nonlinear hysteretic system (as is used by analysis Method 3). Thus the pseudo-velocity can be determined from:

$$PS_{vi} = \Delta_u \sqrt{\frac{P_u}{m\,\Delta_u}} = \Delta_u \sqrt{\frac{P_y + \left(\Delta_u - \Delta_{y2}\right)\left[\dfrac{1}{k_o} + \dfrac{1}{\alpha_{ub} k_{ub} \left(\dfrac{d}{h}\right)^2}\right]^{-1}}{m\,\Delta_u}} \tag{4-15}$$

where P_u/Δ_u is the effective linear (secant) stiffness taken at the ultimate system displacement (Δ_u) and α_{ub} is the post-yield stiffness ratio of the buckling-restrained brace. The pseudo-velocity is then multiplied by a correction factor, taken from Ramirez et. al. (2000), to relate relative and spectral velocity.

Using either of these approaches to determine the pseudo-spectral velocity, the resulting impact velocity is determined from:

$$v_o = PS_{vi} \cdot \frac{d}{h} \tag{4-16}$$

The prediction of the impact velocity using these two methods is compared to the results of time history analysis in Section 5.

4.4   Comparison of Dynamic Forces Developed in Representative Piers

To investigate the adequacy of the methods used to predict the maximum developed dynamic forces presented in Section 4.2.3, the response of each load over time and the superposition of loads is investigated using concepts presented in Section 3.3 assuming a rigid foundation. The response over time is determined from (3-22) for both the pier leg response and the vertical shearing response.   Damping 2% of critical is assumed, although maximum impulsive response occurs before damping can significantly change the response. Shown in figure 4-3 and 4-4 is the response of the pier leg and vertical shearing due to the impact and impulsive loads applied during the rocking motion with arbitrarily assumed buckling-restrained brace strength of w/4 (η_L=0.5) and impact velocity of 0.2 m/sec. Figure 4-3 shows results for piers of aspect ratios of 4 and 3 while figure 4-4 presents results for aspect ratios of 2 and 1. The response is normalized by the total static response for each simplified system (P/P_{st} or Δ/Δ_{st}). The time scale begins (t=0) at the point of impact of a pier leg (i.e. position 2 in figure 3-7). Loading for the vertical shearing begins after the first load $(w/2)_1$ is applied to the pier leg. The dynamic response of each individual load, the superimposed total dynamic load, the static load curve and horizontal lines for the predicted maximum response using (4-9) and (4-4), for the pier leg and vertical shearing respectively, are all shown in figures 4-3 and 4-4. A square-root-sum-of-squares (SRSS) combination of each maximum load is also shown in the figures.

Observations

Some observations can be made on the response of the piers to the dynamic loading. The displacement response of a SDOF system to the initial velocity is given by (3-27). As the

72
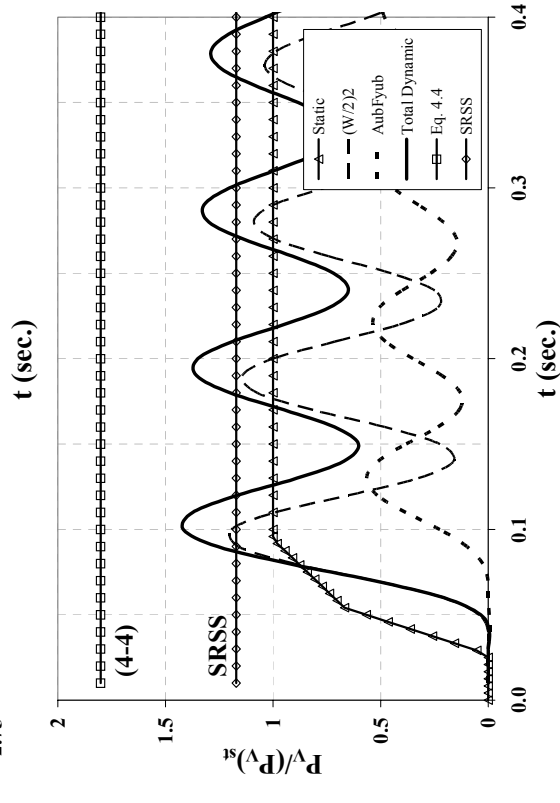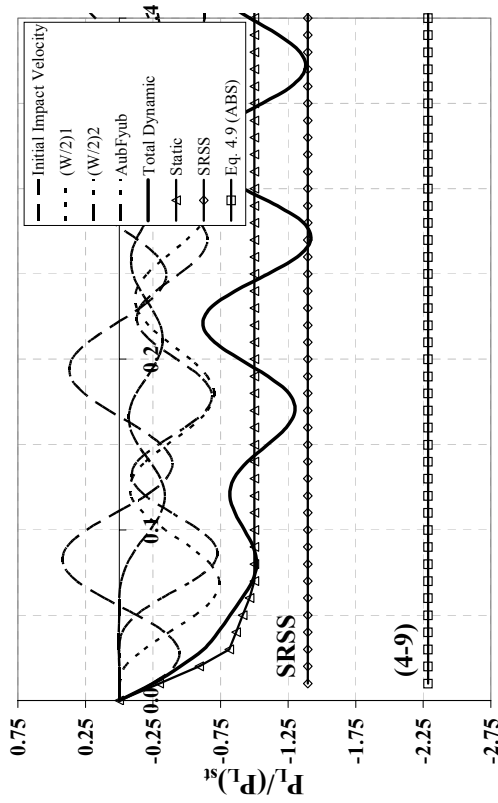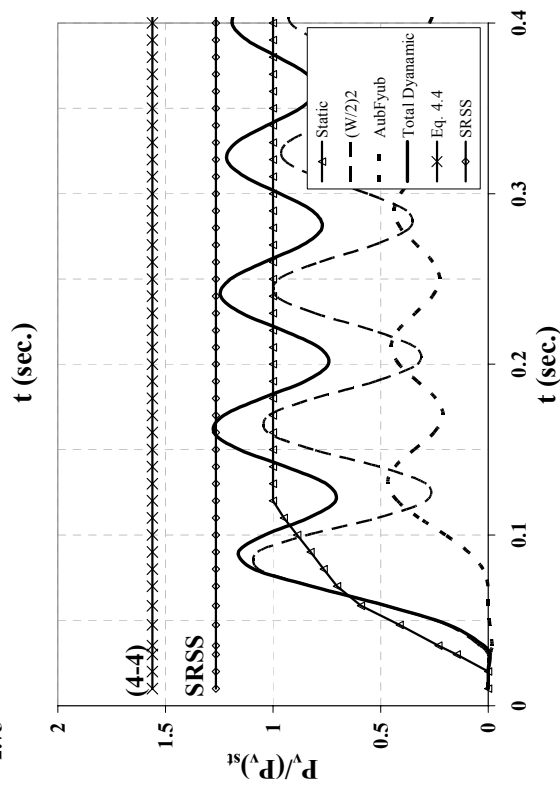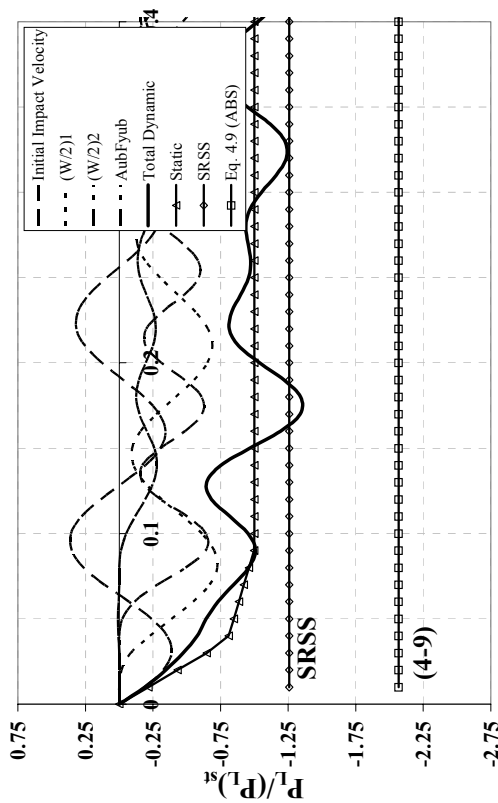
FIGURE 4-3 Normalized Dynamic Load to Total Static Load for (a) h/d=4 and (b) h/d=3
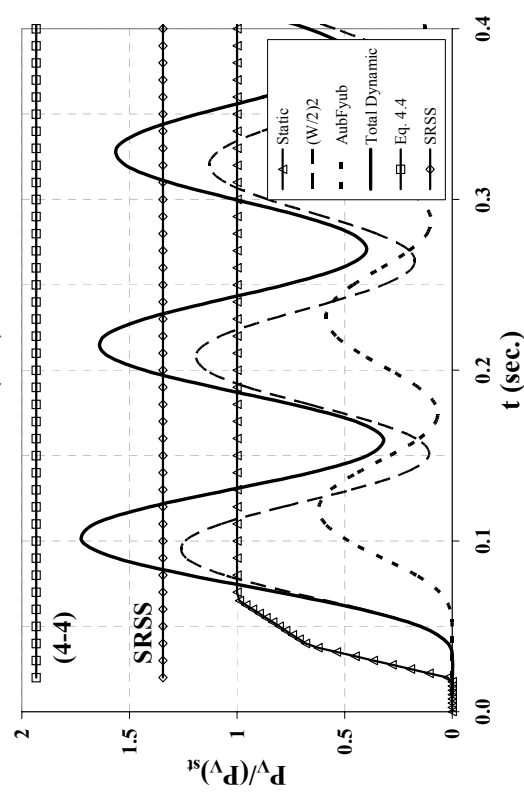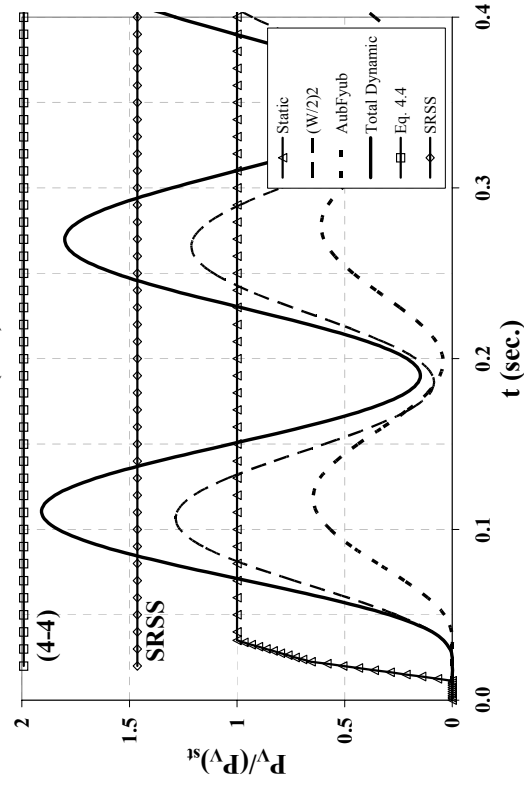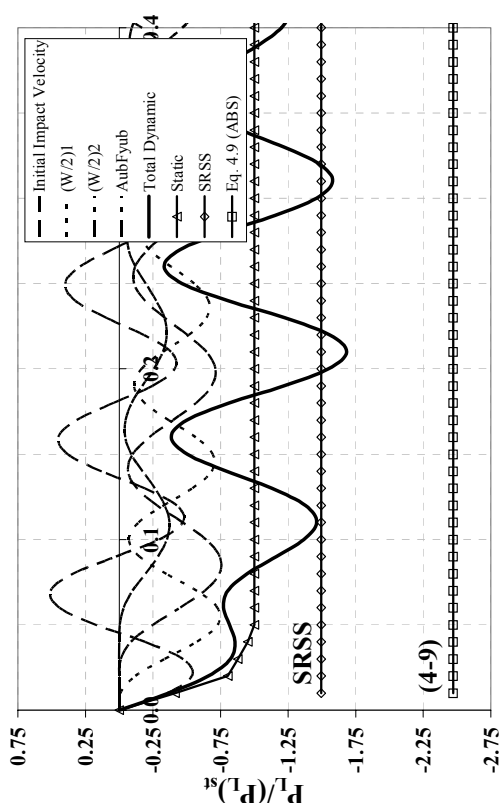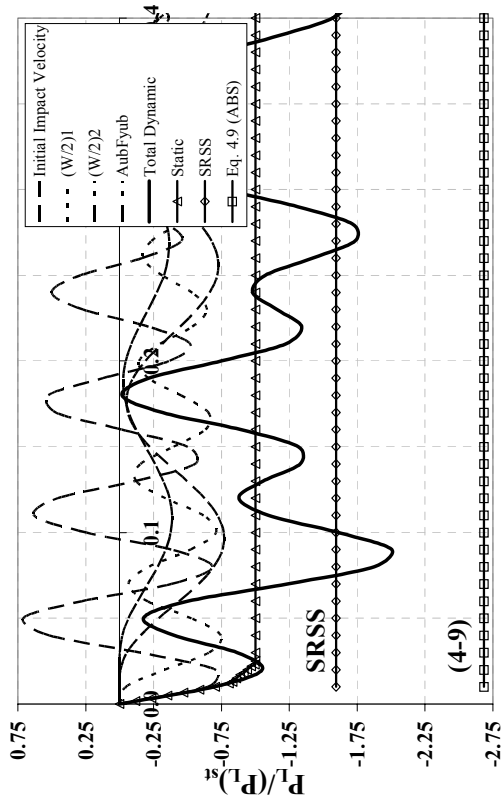
FIGURE 4-4 Normalized Dynamic Load to Total Static Load for (a) h/d=2 and (b) h/d=1

74

aspect ratio decreases, the leg stiffness increases resulting in smaller deformations however the force developed (from 4-6) increases as the aspect ratio decreases.

The amplification of the first impulsive load applied to the pier leg, $(w/2)_1$, remains essentially constant (~2) even as the stiffness of the pier leg changes by a factor of 4 from $h/d=4$ to $h/d=1$. The rise time also decreases with decreasing aspect ratio due to the effective, global period (defined by 3-29) decreasing. These two values do not necessarily change at the same rate.

The effect on the dynamic loads transferred through the pier during uplift as the aspect ratio changes is significant, as seen in figures 4-3 and 4-4 due to the ratio of rise time to the period of vibration (t_{rv}/T_{rv}) increasing with increasing aspect ratio.

The methods to predict the maximum, total dynamic response (4-9 and 4-4) are shown to be conservative for all cases examined here while the SRSS combination was shown to either accurately predict or under-predict the response in all cases.

4.5 Simple Design Procedure and Example

In order to achieve the desired ductile performance of steel truss bridge piers, buckling-restrained braces must be proportioned to meet the relevant design constraints. An example is presented here to show the key steps of the design procedure followed by a presentation of the automated graphical procedure developed to evaluate compliance and non-compliance of solutions with the design constraints.

In the perspective of seismic retrofit, the key steps of the design procedure are:

1. Establish seismic demand parameters to construct a design response spectrum. Following the NCHRP 12-49 (ATC/MCEER, 2003) document, the key parameters include the 0.2 second spectral acceleration (S_s) and 1 second spectral acceleration (S_1) which may be obtained from the U.S. Geological Survey. Spectral acceleration values are typically given for a 5% damped system. Factors to account for other

values of damping in the short and long period range, B_s and B_1 respectively, are given in the NCHRP 12-49 (ATC/MCEER, 2003) document. Selection of these factors depends on the analysis method used (Section 3.4.1) and the level of damping (ξ_{eff}). As discussed in that section, Methods 1 and 2 consider a 2% damped spectrum while Method 3 uses the effective damping, ξ_{eff}, given by (3-45). Also, site coefficients for the short (F_a) and long period range (F_v) need to be established and depend mainly on soil properties at the site. With these values the elastic spectral value may be determined in the long period range as:

$$S_a = \frac{F_v S_1}{B_1 T} \tag{4-17}$$

where T is an effective period of vibration.

2. Determine existing pier properties relevant for dynamic analysis. These values include the pier aspect ratio (h/d), the "fixed-base" lateral stiffness of the pier (k_o) and the horizontal and vertical tributary reactive weights for the given pier, w_h and w_v respectively. Determine the "fixed-base" period of vibration as:

$$T_o = 2\pi \sqrt{\frac{w_h}{g k_o}} \tag{4-18}$$

If T_o is greater than the characteristic period defined by NCHRP 12-49 as:

$$T_s = \frac{S_{D1} B_S}{S_{DS} B_1} \tag{4-19}$$

then the elastic spectral acceleration for all designs can be defined assuming a constant spectral velocity for all periods of vibration. This is because the retrofit technique proposed here elongates the existing "fixed-base" natural period of this dominant mode of vibration. The elastic spectral acceleration is thus defined by (4-17).

To ensure that uplifting will indeed occur, determine the spectral value for the "fixed-base" period of vibration and if the following statement is true then the rocking motion will be initiated:

76

$$\frac{S_a}{g} \geq \frac{1}{2} \frac{w_v}{w_h} \frac{d}{h}$$
(4-20)

3. Determine the design constraints defined by in Section 4.2.

(i) The limiting deck-level displacement does not generally govern the retrofit design given that the constraints used here are based on global instability, leading to fairly large allowable displacements. Serviceability requirements that could impose more stringent limiting displacement limits may exist and need to be determined on a case-by-case basis.

(ii) Based on the results presented in Section 2.3 and the discussion in Section 4.2, an allowable strain of 1.5% in the buckling-restrained brace is used here with a seismic demand representing a maximum credible earthquake (MCE) with 3% probability of exceedance in 75 years, as defined by the NCHRP 12-49 (ATC/MCEER, 2003) document.

(iii) Determine the ultimate horizontal base shear that can be developed by applying a lateral load profile representative of the dominant mode of vibration, which could be assumed to be a single point load applied at deck-level, and finding the weak-link along the seismic load path. The design intent is to keep all members (other than the buckling-restrained braces) and connections within the linear-elastic range. The capacity of the existing members and connections could be evaluated using the AASHTO LRFD Bridge Design Specifications (AASHTO, 1998). Limiting the buckling-restrained brace cross-sectional area (A_{ub}) is the most effective means of satisfying this constraint.

(iv) The limiting impact velocity needs to be determined to prevent damage to the foundation and pier leg during the rocking motion. Since protection of these elements depends on both A_{ub} and v_o, A_{ub} could initially be taken as the value that satisfies constraint (iii) or constraint (v). Taking $A_{ub}F_{yub}$ to satisfy constraint (v), the limiting impact velocity could be determined from:

$$v_{o,max} = \frac{P_{max} - \frac{w}{2} \cdot \left(R_{dL} + 2R_{dv} \right)}{\sqrt{\frac{m \cdot k_L}{2}}}$$

(4-21)

where P_{max} is the maximum allowable force, controlled by either the strength of the pier leg or foundation. Other limits may need to be defined to prevent foundation settlement and/or other serviceability requirements.

(v) In order to ensure re-centering of the bridge pier, η_L (defined by 3-11) should remain less than 1.

Constraints (i), (iii) and (iv) above can be satisfied by selecting appropriate buckling-restrained brace dimensions or by retrofitting existing pier structural elements. Constraint (ii) depends primarily on the buckling-restrained brace effective length (L_{ub}).

4. Begin sizing of buckling-restrained braces by assigning a yield force to the braces $(A_{ub}F_{yub})$ to limit P_y (3-6), reduced by a factor of $1.5R_{dv}$ (R_{dv} from 3-37), to satisfy constraint (iii). The dynamic amplification factor is increased by a factor of 1.5 for further conservatism to protect existing pier elements. If no buckling-restrained brace area can satisfy constraint (iii) with this level of safety, partial pier strengthening may be required.

5. The effective length of the buckling-restrained brace is now sized to satisfy constraint (ii). This is done by determining the ultimate deck-level displacement as:

$$\Delta_u = \frac{S_1 T_{eff}}{4\pi^2}$$

(4-22)

with the effective period of vibration initially set equal to $1.25T_o$, and the uplifting displacement as:

78

$$\Delta_{uplift} = \left[\Delta_u - \frac{\left(\frac{w}{2} + A_{ub} F_{yub} \right) \frac{d}{h}}{k_o} \right] \frac{d}{h}$$ (4-23)

where all terms have been defined previously. Based on this initial estimate of the uplifting displacement, the buckling-restrained brace effective length can be sized using constraint (ii) and taken here as:

$$L_{ub} = \frac{\Delta_{uplift}}{(\epsilon_{ub})_{allowable}} = \frac{\Delta_{uplift}}{0.015}$$ (4-24)

6. After the buckling-restrained brace has been initially sized, the ultimate displacement can be more accurately determined using a method discussed in Section 3.4.1. It is recommended that the method given in the FEMA 274 document for passive energy dissipation systems (Method 3) be used if η_L is less than 0.6, for reasons to be discussed in Section 5.

7. Verify that all constraints defined in step 3 are satisfied.

EXAMPLE

The following example is presented, to illustrate the proposed design procedure for a pier with an aspect ratio of 4. The pier is assumed to have an equal amount of horizontal and vertical reactive mass, and interaction between adjacent piers is assumed to be negligible. The braces are assumed to be implemented vertically and have a yield stress of 235MPa.

1. The seismic demand parameters are assumed for a given site with the 1-second spectral acceleration equal to 0.5g and the short period acceleration equal to 1.25g for a damping ratio of 5%. The bridge is assumed to be located on site class B (as defined in NCHRP 12-49), and the site coefficients F_a and F_v are equal to 1. The steel truss pier is assumed to have an inherent viscous damping of 2%, therefore the 5% damped spectrum needs to modified by factors B_1 and B_s. The characteristic period, T_s, can therefore be determined by:

$$T_s = \frac{S_{D1}}{S_{DS}} = 0.4\sec \tag{4-25}$$

by initially assuming $B_1 = B_s$.

2. Properties of the representative pier with an aspect ratio of 4 are found in Appendix D. The height and width of the pier is equal to 29.26m and 7.32m respectively. The "fixed-base" horizontal stiffness of the pier is 12.6 kN/mm, and the horizontal and vertical reactive weights are 1730kN. Therefore the "fixed-base" horizontal period of vibration is equal to:

$$T_o = 2\pi\sqrt{\frac{w_h}{gk_o}} = 0.74\sec \tag{4-26}$$

Since T_o is greater than T_s, all designs will have effective periods of vibration in the long period range ($>T_s$). Thus the elastic spectral acceleration can be defined as:

$$S_a = \frac{S_1}{B_1 T} = \frac{0.625g}{T} \tag{4-27}$$

With the horizontal and vertical reactive weights assumed equal, the statement of (4-20) indicates that uplift and rocking motion will occur.

3. The constraints defined in Section 4.2 can be defined as follows:

(i) Limiting deck-level displacement is the smaller of the following two equations:

$$\Delta_u \le 0.25\frac{P_y}{w_h}h = 914\,mm \tag{4-28}$$

where P_y is determined assuming no tensile strength in the anchorage connection, thus $A_{ub}=0$. The other limiting displacement relationship is taken as:

$$\Delta_u \le \frac{d}{2FS} = 732\,mm \tag{4-29}$$

which is the governing limiting deck-level displacement in this case.

(ii) The allowable axial strain demands on the buckling-restrained brace is taken as 1.5% for the MCE.

(iii) The limiting horizontal base shear strength is arbitrarily assumed to be equal to 0.5w_h. Therefore, the limiting horizontal base shear is taken equal to:

$$P_u \leq 865\,kN \qquad (4\text{-}30)$$

(iv) Using the representative properties defined in Appendix D, the dynamic amplification factors determined in Appendix B, and assuming the foundation to control the limiting strength (determined from Appendix G), the limiting impact velocity, as a result of (4-21), is found to be:

$$v_{o,\max} = 19\,cm/\sec \qquad (4\text{-}31)$$

and the limiting deck-level (global) velocity can be determined from:

$$PS_{vi,\max} = v_{o,\max} \cdot \frac{h}{d} \qquad (4\text{-}32)$$

This constraint can be defined as:

$$PS_{vi} \leq 75\,\frac{cm}{\sec} \qquad (4\text{-}33)$$

(v) Assuming a buckling-restrained brace yield stress of 235MPa, the limiting buckling-restrained brace area to allow for the re-centering capability is:

$$A_{ub} \leq \frac{w}{2F_{yub}} = 3684\,mm^2 \qquad (4\text{-}34)$$

4. An initial cross-sectional area of the buckling-restrained brace (A_{ub}) is determined using constraint (iii) where the limiting system yield force is defined as:

$$P_y \leq \frac{0.5 \cdot w}{1.5 \cdot R_{dv}} = \frac{865\,kN}{1.5 \cdot 1.56} = 370\,kN \qquad (4\text{-}35)$$

Buckling-restrained brace area can be determined, using (3-6), as:

$$A_{ub} \leq \frac{P_y \dfrac{h}{d} - \dfrac{w_v}{2}}{F_{yub}} = 2617\,mm^2 \qquad (4\text{-}36)$$

Therefore A_{ub} will initially be taken as 2400mm^2.

5. An initial estimate of the ultimate displacement demand is determined by:

81

$$\Delta_u = \frac{S_1\left(1.25T_o\right)\sec}{4\pi^2} = 115\,mm \tag{4-37}$$

resulting in an uplifting displacement (determined from 4-23) of:

$$\Delta_{uplift} = 21.4\,mm \tag{4-38}$$

Therefore the effective length of the buckling-restrained brace will initially be taken as:

$$L_{ub} = \frac{\Delta_{uplift}}{\epsilon_{allowable}} = \frac{21.4\,mm}{0.015} = 1427\,mm \tag{4-39}$$

6. The initial buckling-restrained brace area given by (4-36) leads to a local strength ratio ($_L$) of 0.65. Therefore Method 2 (Section 3.4.1, Appendix C) will be used to evaluate the ultimate displacement demands. Holding the buckling-restrained brace area constant at the value determined in Step 4, and initially taking the buckling-restrained brace effective length from Step 5, the ultimate displacement can be determined and the effective length of the buckling-restrained brace iterated to satisfy constraint (ii). Using this approach, the resulting ultimate displacement is 149mm, the uplifting displacement is 30.1mm and a buckling-restrained brace effective length of 2000mm.

7. Check all constraints to ensure they have been satisfied.

   (i) $$\Delta_u = 149\,mm < 732\,mm \quad OK \tag{4-40}$$

   (ii) $$\epsilon_{ub} = \frac{30.1\,mm}{2000\,mm} = 0.015 \le 0.015 \quad OK \tag{4-41}$$

   (iii) $$P_u = P_y\, R_{dv}\, FS = 357\,kN\,(1.56)\,(1.5) = 836\,kN \le 0.5\,W \quad OK \tag{4-42}$$

   (iv) In order to evaluate the inelastic pseudo-spectral velocity, a ductility reduction factor strategy (discussed in Section 4.3) is used. The elastic pseudo-spectral velocity is taken as:

$$PS_{ve} = \frac{S_1 \sec}{2\pi B_1} = 97.6 \frac{cm}{\sec}$$ (4-43)

The modified displacement ductility ratio is defined for the long period range (from 4-13) as:

$$\mu_m = \left(\frac{2\eta_L}{1+\eta_L}\right)\frac{\Delta_u}{\Delta_{y2}} = (0.79)\frac{149\,mm}{47.4\,mm} = 2.5$$ (4-44)

where η_L and Δ_{y2} were defined in Section 3. Therefore the inelastic pseudo-spectral velocity can be taken equal to:

$$PS_{vi} = \frac{PS_{ve}}{\mu_m} = 39\frac{cm}{\sec} < 75\frac{cm}{\sec} \quad OK$$ (4-45)

(iv) Finally the local strength ratio, η_L, is:

$$\eta_L = 0.65 < 1 \quad OK$$ (4-46)

ensuring the self-centering ability.

The final selected buckling-restrained braces have an effective length (L_{ub}) of 2000mm and a cross-sectional area (A_{ub}) of 2400mm^2.

4.6 Graphical Design Procedure

The design procedure and constraints discussed above were established to achieve the desired seismic performance of the controlled rocking bridge pier system. A graphical design approach can be used, similar to that proposed by Sarraf and Bruneau (1998), to define the range of admissible solutions. Each constraint is written in terms of A_{ub} and L_{ub} such that the boundaries of compliance and non-compliance with the design constraints are established. Many existing pier properties affect the response of the controlled rocking pier however these parameters would ideally not need to be modified to reduce the retrofit effort. An automated procedure was developed to evaluate many designs quickly. The ultimate system displacement response is determined using either Method 2 or 3, described in Section 3.4.1. An example of the procedure is given in Appendix H. Retrofit solutions for the representative bridge piers are provided in Section 5. For illustration purposes the graphical solution for the example given above is shown in figure 4-5 with the brace dimensions indicated in the solution space. As can be seen from this figure, it is possible to decrease A_{ub}

to allow for a greater factor of safety to protect existing structural elements while still satisfying all other constraints. Iteration of the step-by-step procedure by decreasing A_{ub} could further optimize response of the system.
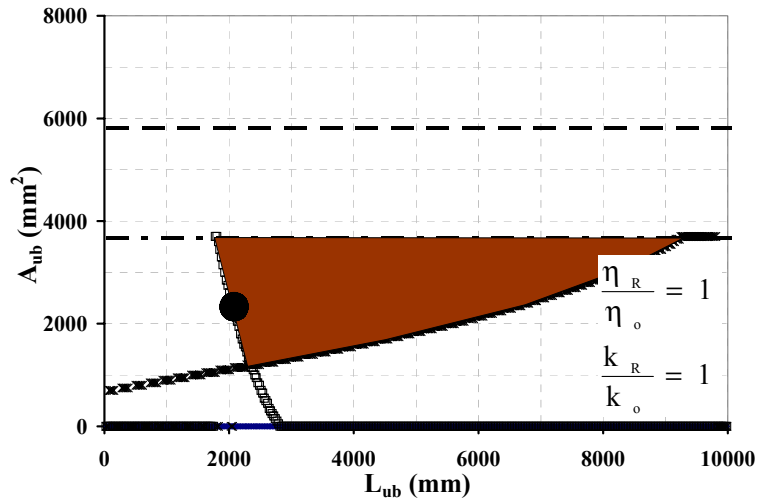
FIGURE 4-5   Graphical Design Procedure Plot

SECTION 5
GRAPHICAL DESIGN PROCEDURE SOLUTIONS AND RESULTS OF TIME HISTORY ANALYSES COMPARED TO DESIGN PREDICTIONS

5.1   General

This section provides results for the range of buckling-restrained brace sizes that satisfy the design constraints established in Section 4 for the representative piers in Appendix D. Results of nonlinear time history analyses are given, normalized to the predicted response quantity (displacements, forces, etc.), to show the adequacy of the design procedure to predict system response. Response history analysis examples are also provided for a few cases.

5.2   Graphical Design Procedure Solutions

The graphical procedure was developed to evaluate many designs quickly for a large range of buckling-restrained brace area (A_{ub}) and effective lengths (L_{ub}). The two key retrofit parameters were chosen because they control the post-uplift stiffness (k_r) and system strength (P_y). The procedure follows the same constraints as the step-by-step procedure established in Section 4 but provides a solution "space" of buckling-restrained brace dimensions that satisfy the constraints. The solution method creates solution "surfaces" for the response quantities (displacements, velocities, etc.) for the array of buckling-restrained brace areas and lengths. The boundary lines for the solution "space" are then determined by finding the intersection of the surface with the "critical response plane". This solution method is shown graphically in figures 5-1a and 5-1b for an example of limiting strains on the buckling-restrained brace for an aspect ratio of 4, a seismic demand characterized by S_1=0.5g and the ultimate global displacement determined using Method 3 (Section 3.4.1). Two "critical response planes" that bound the critical response value (figure 5-1b) are used due to the surface not being continuous but rather a finite number of values set for computational efficiency.

While parameters such as the existing pier stiffness and strength, among others, can be modified to provide the desired performance, ideally, these existing properties should remain

unchanged to limit the retrofit effort. However, in some cases, pier stiffening and/or strengthening may be required. For these instances, the required strength and stiffness of the retrofitted pier are expressed as a normalized quantity with respect to the existing pier strength (η_R/η_o) and stiffness (k_R/k_o). The existing pier stiffnesses (k_o) can be found in table 3-1 and the existing strength (η_o) is assumed equal to 0.5w for all pier aspect ratios.

Results obtained from the graphical design procedure are shown in figure 5-2 for an aspect ratio of 4, seismic demands characterized by a 1-second spectral acceleration (S_1) of 0.25g, 0.5g and 0.75g (with $S_s=2.5S_1$) and using Method 2 of Section 3.4.1. Similarly, the solutions for pier aspect ratios of 3 and 2 are shown in figures 5-3 and 5-4 respectively. Figures 5-5 and 5-6 provide solutions for the same parameters except Method 3 of Section 3.4.1 is used.

In some cases it was found that the stiffness and/or strength of the existing piers needed to be increased to satisfy the design constraints. Figures 5-2 through 5-6 also provide the normalized parameters (η_R/η_o) and (k_R/k_o) that were required such that a solution space exists (i.e. the design constraints are satisfied). As can be seen in figure 5-4, for larger seismic demands the applicability of the retrofit strategy for a pier with an aspect ratio of 2 begins to diminish due to the required level of strengthening and stiffening becoming excessive (η_R/η_o or $k_R/k_o>2$). Using Method 3, no realistic solution for an aspect ratio of 2 exists. Thus results are not given for piers with an aspect ratio of 1.

It becomes more clear that using the base overturning moment as the force limiting mechanism requires relatively slender piers in order to provide an efficient retrofit using this method. More squat piers require significant strength and stiffness to resist demands including dynamic effects and may experience only a few excursions beyond the point of uplift, forcing the pier to resist and dissipate seismic energy in a mostly elastic manner.

5.3 Results of Time History Analyses to Assess Design Predictions

In assessing the response of the controlled rocking system, a range of buckling-restrained brace dimensions were established to explore all practical possibilities given the representative piers established in Appendix D. The buckling-restrained brace area (A_{ub}) is varied from zero (elastic rocking) to the point at which the self-centering ability is lost ($\eta_L = 1$). It was determined that, based on the solution spaces presented previously, practical designs fell within 1-1.5 times the existing, pre-uplift period of vibration of the pier (T_o) using the Method 2 characterization of the effective period (k_{eff2} defined by 3-44). Results are presented for 3 effective periods of vibration (~$1.0T_o$, $1.25T_o$ and $1.5T_o$), aspect ratios of 4, 3 and 2, and for local strength ratios (η_L) of 0, 0.25, 0.5, 0.75 and 1. For each combination, seven synthetic ground motions (as discussed in Section 3.4.4) are used and the mean result of each case shown. For the case of $\eta_L = 0$, only the initial period of vibration of the pier is relevant since no buckling-restrained brace is used. Therefore a total of 39 cases and 273 analyses were performed. Results for time history analyses are presented normalized by their respective response parameter predicted by the design procedure established in Section 4 and are shown in figures 5-7 to 5-12.

5.3.1 Deck-level Displacement Results

It is important to be able to predict the ultimate response of structures in order to adequately design them to meet performance objectives. While the over-prediction of displacements will conservatively protect elements that are solely displacement dependent, this may result in inefficient designs that do not utilize the ductile, passive energy dissipating abilities of the system.

Results of the normalized deck-level displacements are shown in figure 5-7 for analysis Method 2 of predicting maximum displacements (Section 3.4.1). Results for Method 3 are shown in figure 5-8. As can be seen in the figures, Method 3 is able to more accurately predict displacements for all ranges of parameters considered here. Method 2 works well for systems with $\eta_L > 0.5$, however for smaller values of η_L the method under-predicts the maximum displacements.

87

Differences between the two methods can be seen on the surfaces of predicted displacements for an aspect ratio of 4 and a seismic demand of S_1=0.5g, as shown in figures 5-13 and 5-14. The primary difference is seen at small buckling-restrained brace areas where large increases in displacements are predicted by Method 3 due to the decrease in system strength and energy dissipation with small buckling-restrained brace areas. As a result, Method 2 under-predicts displacements, as seen in figure 5-7, especially for the case of the bilinear elastic rocking system (η_L=0). While Method 3 does not necessarily provide the exact solution, it captures trends in flag-shaped behavior that have significant influence on response. These trends include the system strength, initial stiffness, post-elastic stiffness and energy dissipating ability.

Method 2 is completely dependent on an effective initial, elastic stiffness with coefficients that do not apply for the system presented. While Method 2 uses a coefficient, C_2 (see Section 3.4.1), to account for differences in hysteretic models between an inelastic SDOF system with bilinear hysteretic systems, it only considers systems with pinched hysteresis causing stiffness and strength degradation and assigns values of C_2 for systems that typically exhibit this type of behavior. As was demonstrated on Section 3.2, the flag-shaped hysteretic system has stable hysteretic behavior without strength nor stiffness degradation but simply lacks in the amount of energy dissipation per cycle. For systems within the long period range and some amount of energy dissipation (say η_L=0.5), the lack of energy dissipation does not appear to increase the response from that of a bilinear system. For systems that are excited by motions with frequency response near the natural frequency of the structure (typically assumed in design as being the short period range), this lack of energy dissipation is expected to become more critical. However since the retrofit strategy presented tends to be more applicable to slender piers and the controlled rocking system increases the system's period of vibration from the fixed-base period, the retrofitted system will, for typical rock and firm soil sites, have a period of vibration in the long period range.

Other benefits of the self-centering, flag-shaped behavior also exist (not accounted for in any of the analysis procedures) that are believed to limit the increased displacement response due to the lack of energy dissipation. First, the highly non-linear behavior of the system helps to prevent resonant response by changing stiffness many times during each cycle. Also, the

restoring force is always acting during the excitation to bring the system back to the undeformed position such that inelastic excursions tend not to build off of past residual deformations.

Finally it is recommended that Method 3 be used in evaluating the displacement demands of the controlled rocking system. There is not a large increase in the analysis effort from using Method 2 to 3 from a designers standpoint since both methods require mathematical models, incorporating the nonlinear behavior of structural components, to develop the static pushover curves.

5.3.2 Impact Velocity Results

Results of the impact velocity normalized by the predicted impact velocity using methods of Section 4.3 is shown in figure 5-9 and 5-10. Results are presented for the modified displacement ductility ratio method with the maximum displacement, Δ_u, determined using Method 3 (Ductility Approach). Also, velocity results are presented using the linear, viscous characterization of the controlled rocking system with the pseudo-spectral velocity determined using (4-15) and Δ_u determined using Method 3 (Linear-Viscous Approach). Using either the ductility approach or the linear, viscous approach, unconservative predictions of velocity in many cases are evident. Using (4-15) appears to result in the best estimate of velocity for each method.

The prediction of the impact velocity is important for protection of the pier legs. Even with the under-prediction of velocity, the pier leg demands (presented in a following section) are still able to be conservatively predicted.

5.3.3 Maximum Developed Dynamic Forces

Prediction of the maximum developed dynamic forces (base shear and pier legs) requires evaluation of the dynamic amplification factors discussed in Section 3.3. Following the methods presented in Section 3.3, table 5-1 provides the resulting values of R_{dL} (3-31), R_{dv} (3-37), and the design secant period of vibration T_{sec} (3-29).

5.3.3.1 Base Shear Results

The normalized base shear results presented in figure 5-11 show that the prediction of the ultimate base shear including dynamic effects determined by multiplying the static system yield force, P_y (from 3-6), by the dynamic amplification factor during uplift, R_{dv} (from table 5-1), was shown to be conservative for $\eta_L \geq 0.25$ except for an aspect ratio of 2 with $\eta_L = 0.25$. It was also shown to be unconservative for the case of bilinear, elastic rocking. However exceeding the predicted base shear, due to dynamic amplification, for a limited number of excursions such that small ductility demands occur may not be very critical if the ductility demands occur in locations that can accept the demand however brittle failure of a connection (for example) should be avoided.

Also, it can be seen in figure 5-11 that the base shear response decreases with increasing values of η_L, especially for an aspect ratio of 2. This decrease may be a result of the buckling-restrained brace contributing to the vertical shearing stiffness, k_v (defined by 3-32) and thus decreasing the dynamic amplification during uplift. The buckling-restrained brace stiffness would be more effective at increasing k_v for h/d=2 since the smaller aspect ratios have the smallest value of k_v. Thus the relative increase of k_v, due to the buckling-restrained brace acting in parallel with the pier vertically, would be greater for h/d=2.

5.3.3.2 Pier Leg Force Demands

Results of the forces developed in the pier legs are shown in figure 5-12. Results from time history analyses are shown, normalized to the predicted demands determined by (4-9). Even with the under-prediction of velocity in some cases (from previous section), the conservative assumptions made in the derivation of (4-9) (in-phase response of the dynamic effects during impact and uplift), resulted in conservative estimates of the pier leg demands in all cases considered. As was discussed in Section 4, conservative predictions of the demands to the pier legs is essential due to the pier legs resisting the gravity loads of the pier.

5.4 Example Response History Analysis Results

Example responses of each aspect ratio with braces sized using the graphical design procedure and analysis Method 2 is given in figures 5-15 to 5-17. Each response parameter is shown over time and the global hysteretic response given for each example. The limiting values for each response parameter are shown by the solid horizontal lines. For an aspect ratio of 2, a limited amount of rocking is observed in the hysteretic response.

5.5 Summary

Solutions of the automated, graphical design procedure for the representative piers used in this study excited for a range of demands are presented. It became more evident that the retrofit strategy is more applicable to slender piers due to the use of the base overturning moment as the force limiting mechanism. Also, the seismic response of bridge steel truss piers allowed to rock on their foundation was observed for a range of key parameters and the response compared to that predicted by the design procedure developed in Section 4. Example response history analysis results are provided for a few cases with the limiting response values shown.

h/d		4			3			2		
η_L	T_{eff}[a]	1.0	1.25	1.5	1.0	1.25	1.5	1.0	1.25	1.5
1.0	T_{sec}	1.56	1.72	1.85	1.05	1.21	1.29	0.61	0.64	0.67
	R_{dv}	1.71	1.63	1.52	1.89	1.91	1.91	1.95	1.94	1.93
	R_{dL}	1.92	1.94	1.94	1.88	1.91	1.92	1.92	1.93	1.94
0.75	T_{sec}	1.47	1.56	1.66	1.12	1.33	1.43	0.67	0.72	0.74
	R_{dv}	1.68	1.56	1.43	1.91	1.93	1.93	1.96	1.95	1.95
	R_{dL}	1.89	1.90	1.91	1.87	1.91	1.92	1.92	1.93	1.94
0.5	T_{sec}	1.74	1.82	1.90	1.29	1.54	1.66	0.79	0.85	0.87
	R_{dv}	1.76	1.67	1.55	1.93	1.95	1.95	1.97	1.97	1.96
	R_{dL}	1.89	1.90	1.91	1.88	1.92	1.93	1.92	1.93	1.94
0.25	T_{sec}	2.30	2.39	2.45	1.57	1.95	2.10	1.04	1.13	1.16
	R_{dv}	1.86	1.80	1.7	1.95	1.97	1.97	1.98	1.98	1.98
	R_{dL}	1.91	1.92	1.92	1.90	1.94	1.95	1.94	1.95	1.95
0	T_{sec}	3.85			2.69			1.73		
	R_{dv}	1.97			1.98			1.99		
	R_{dL}	1.95			1.96			1.97		

a: Effective Period in units of $1/T_o$ (T_o for each aspect ratio given in TABLE 3-1)

TABLE 5-1   Design Secant Period (T_{sec}), Dynamic Amplification Factor During Uplift (R_{dv}) and During Impact (R_{dL}) for Each System Considered in Analytical Study
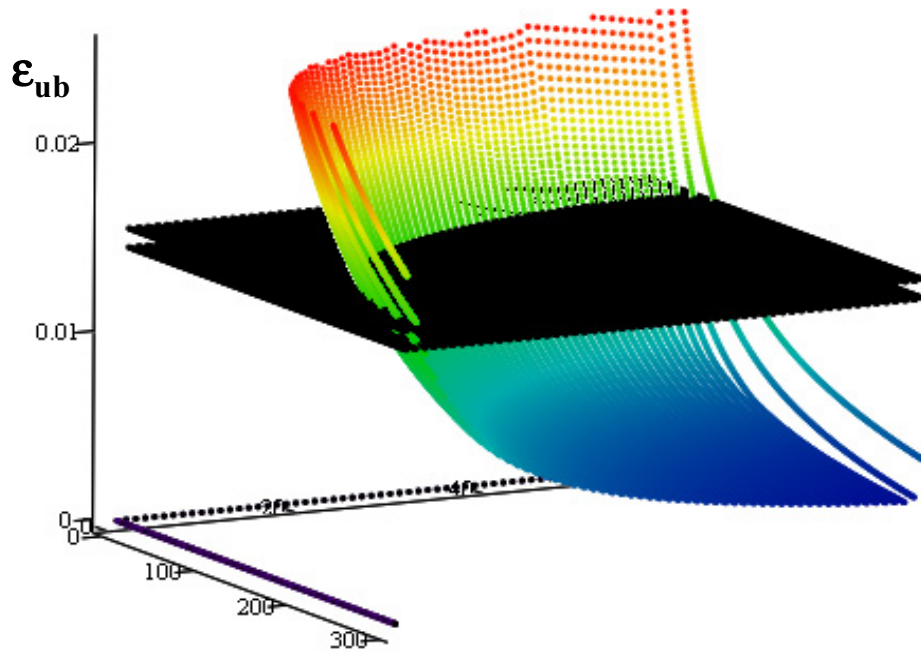
(a)
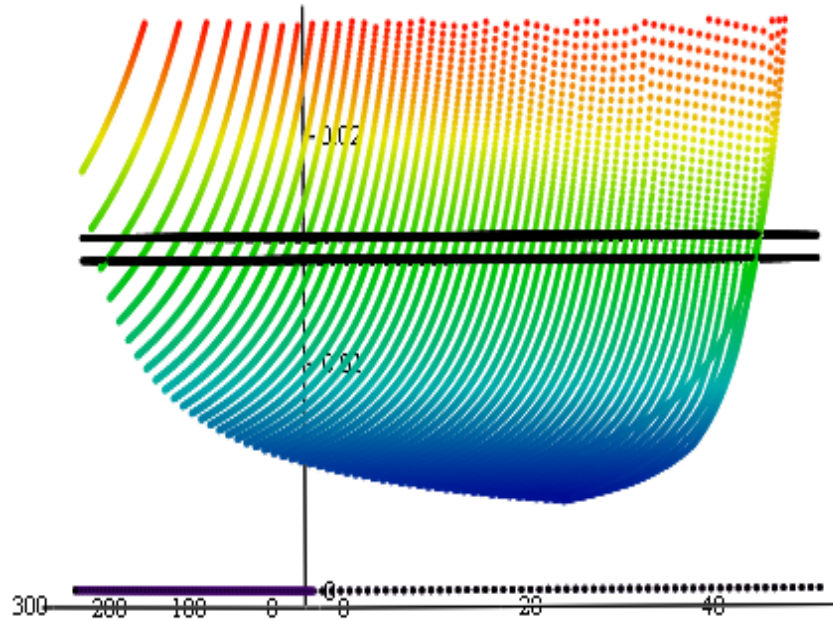
(b)

FIGURE 5-1   Graphical Design Procedure Solution Method. (a) Buckling-restrained Brace Strain Response "Surface" and (b) Upper and Lower Bounding Planes of Critical Response Value (ε_{max}=0.015)

93
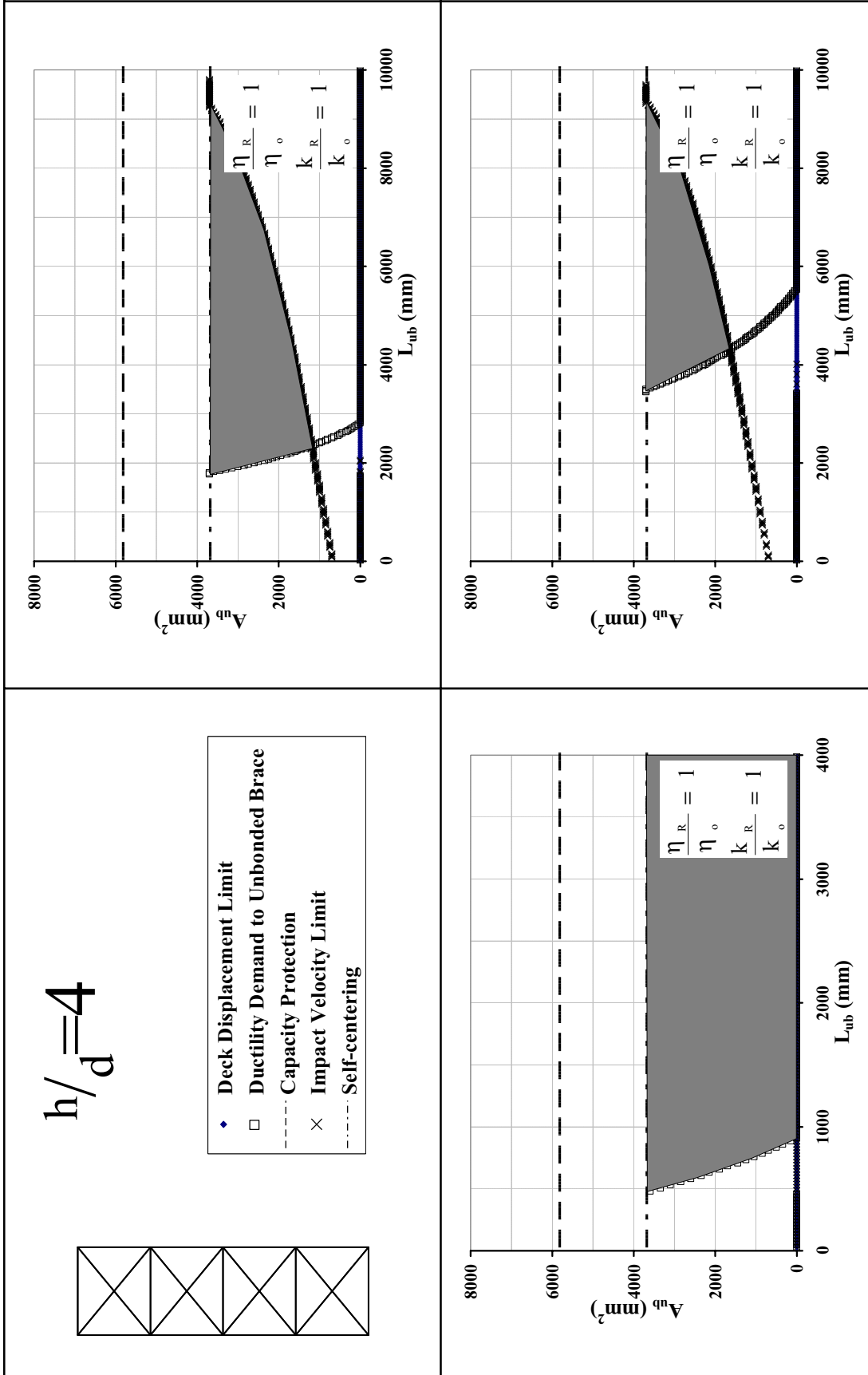
FIGURE 5-2 Graphical Design Procedure Plots (h/d=4, Method 2)
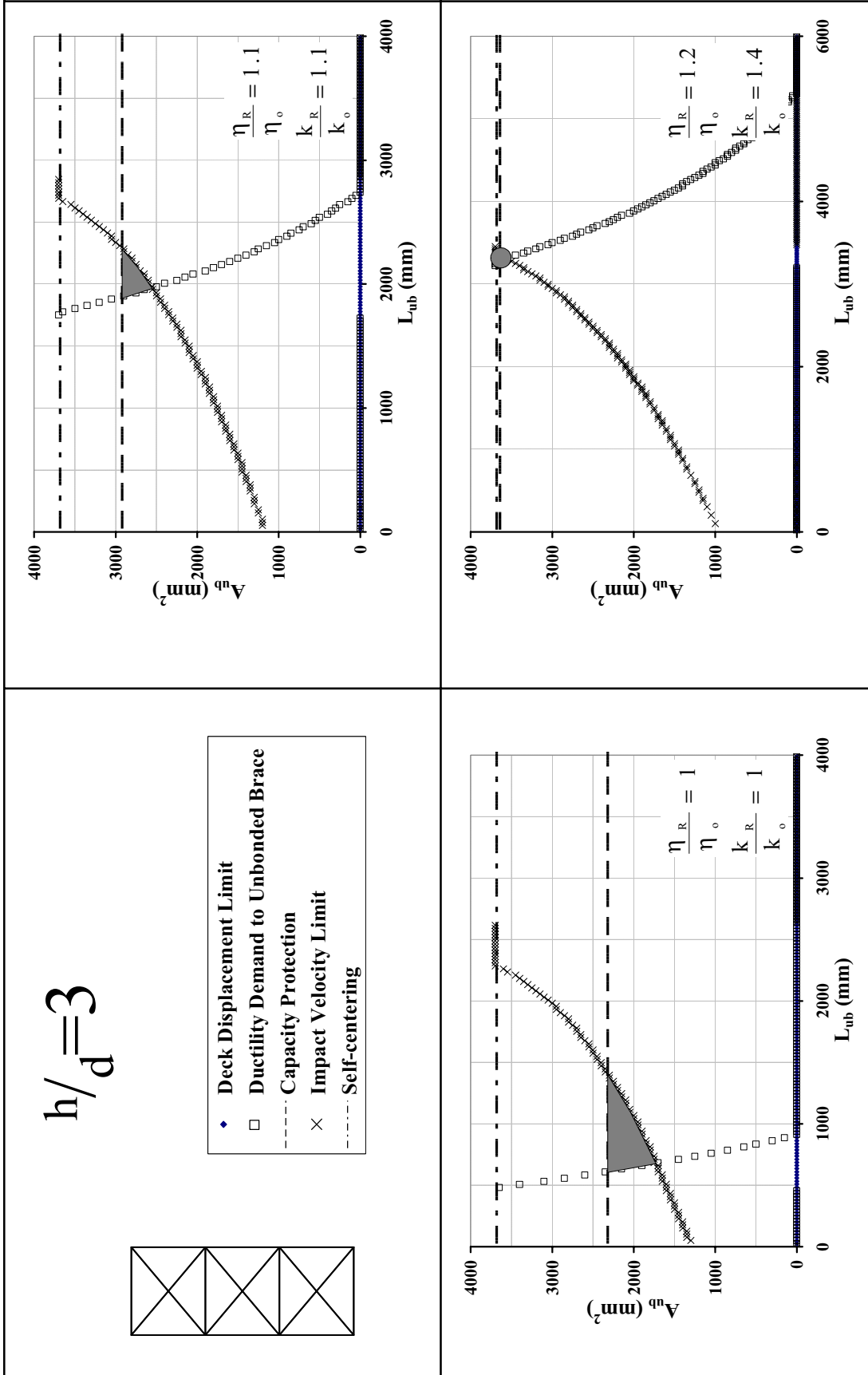
FIGURE 5-3 Graphical Design Procedure Plots (h/d=3, Method 2)
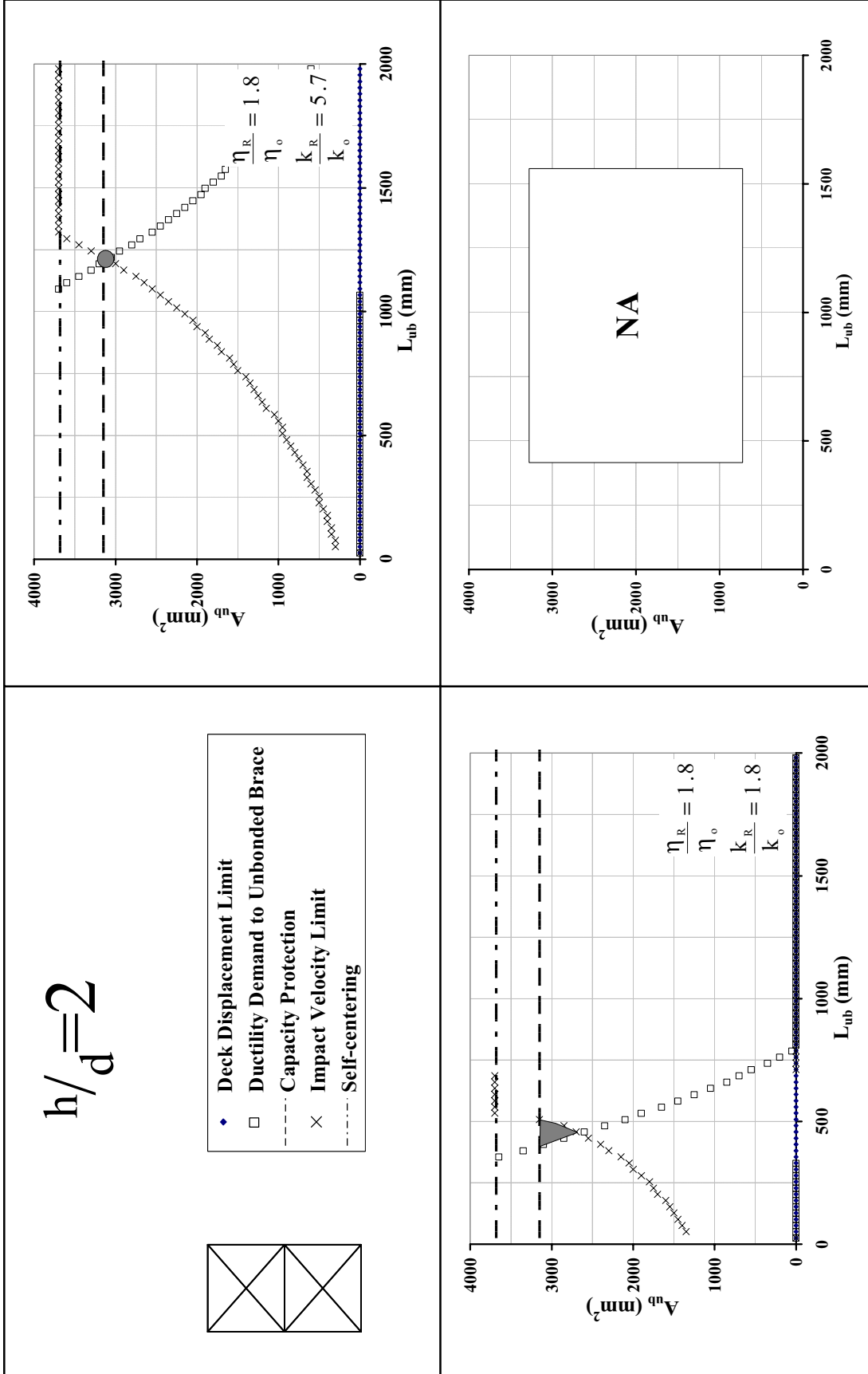
FIGURE 5-4 Graphical Design Procedure Plots (h/d=2, Method 2)
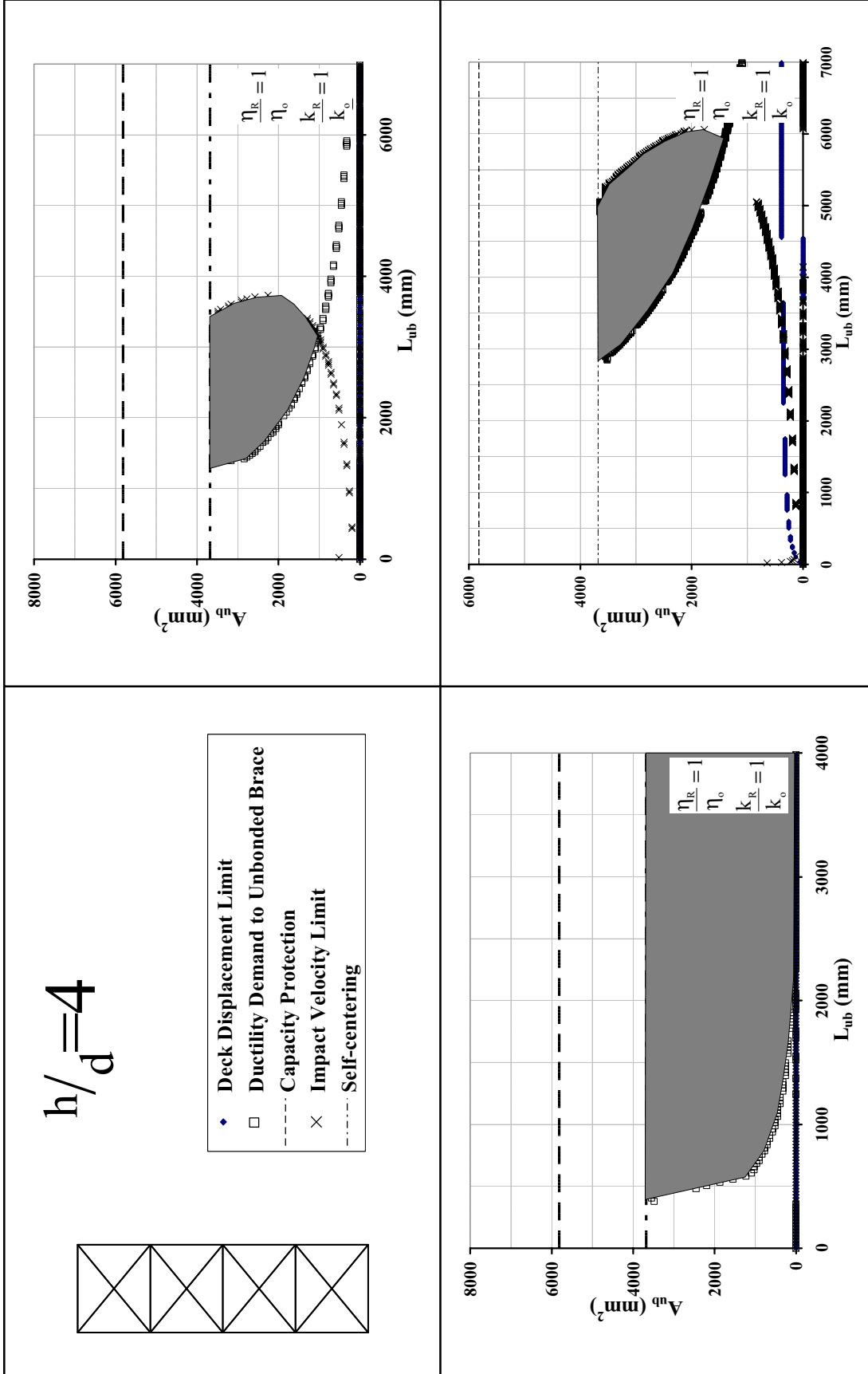
FIGURE 5-5 Graphical Design Procedure Plots (h/d=4, Method 3)
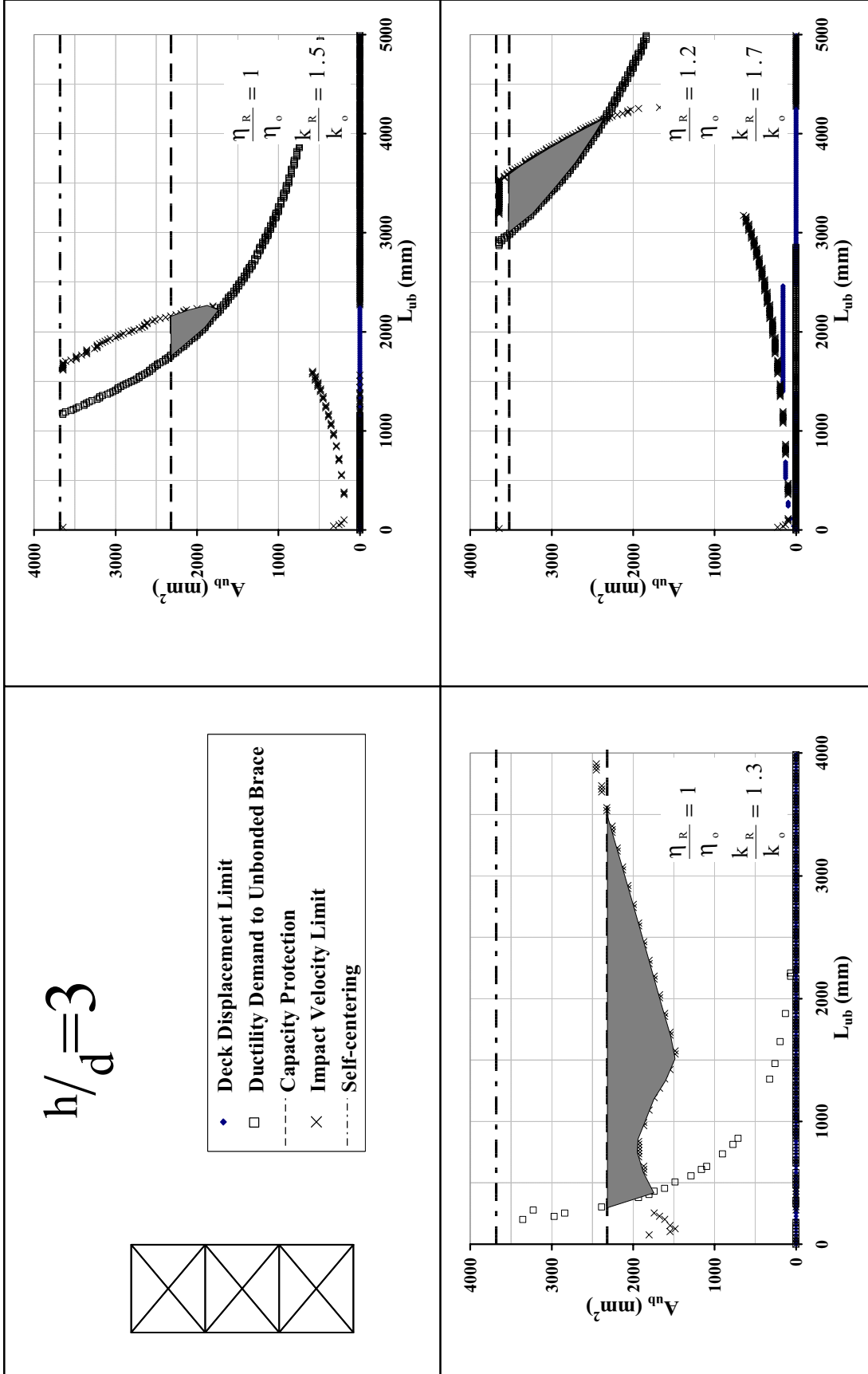
FIGURE 5-6 Graphical Design Procedure Plots (h/d=3, Method 3)
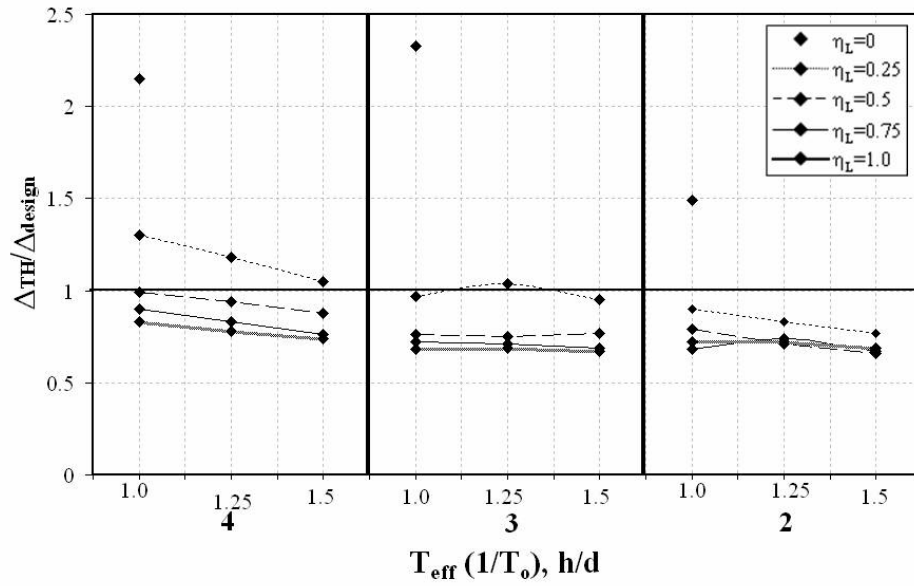
FIGURE 5-7   Normalized Global Displacement Demands (Method 2)
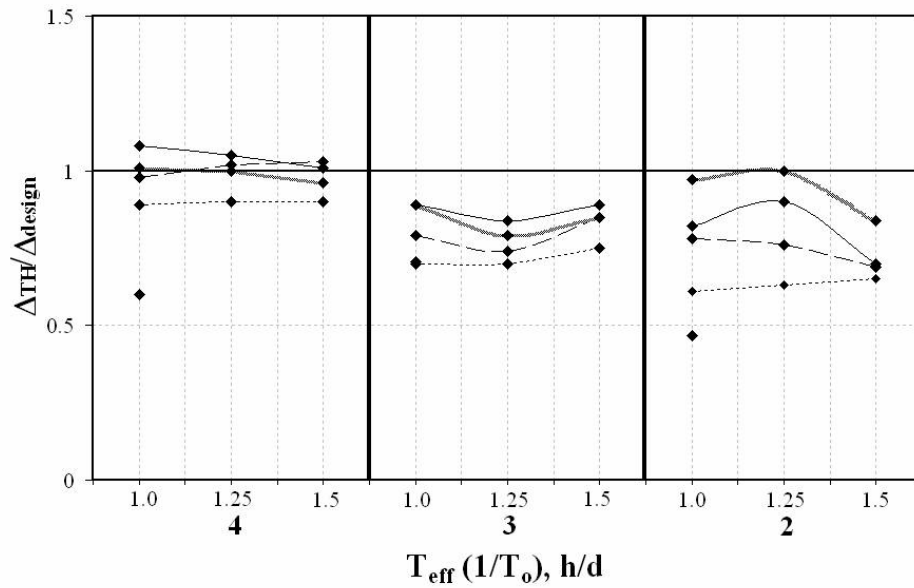
FIGURE 5-8   Normalized Global Displacement Results (Method 3)

99
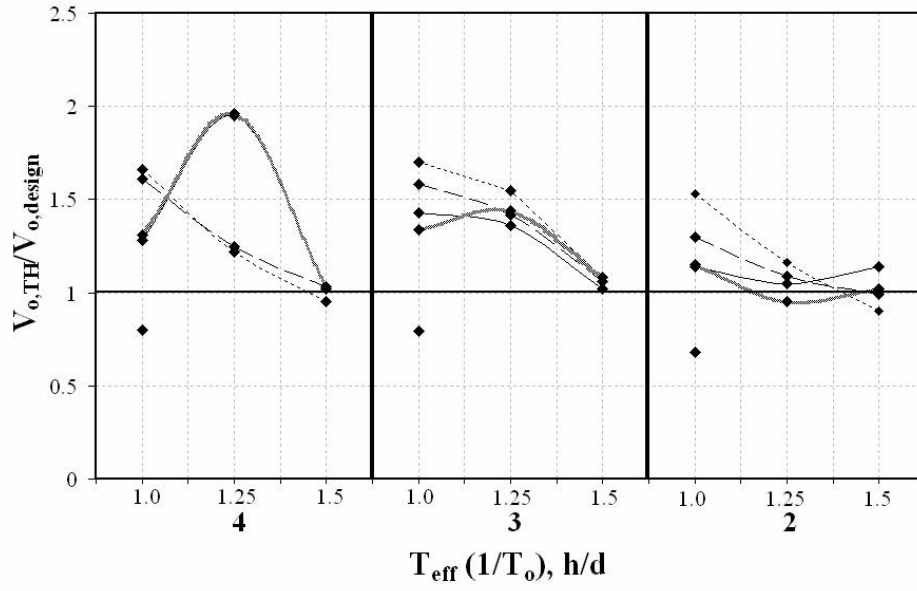
FIGURE 5-9   Normalized Impact Velocity Results (Ductility Method)
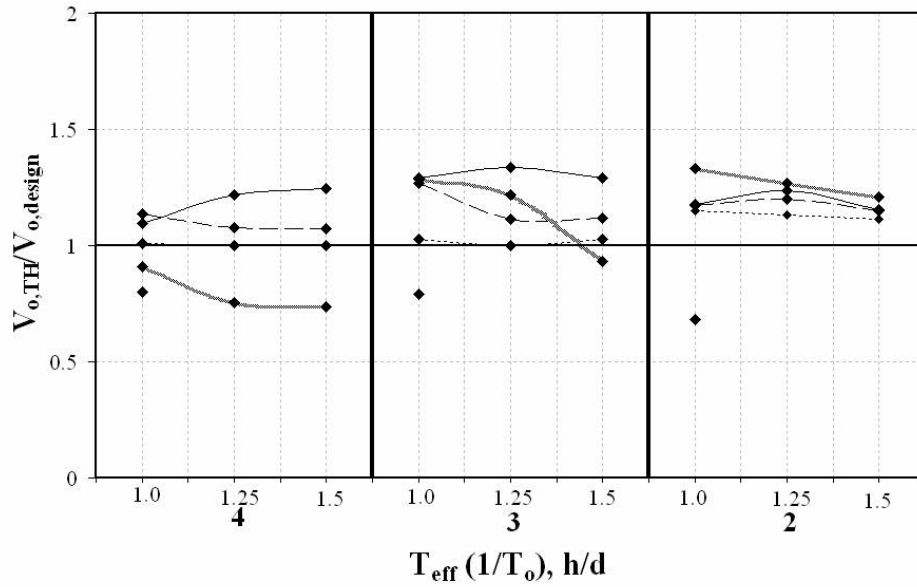
FIGURE 5-10   Normalized Impact Velocity Results (Linear-Viscous Approach)

100
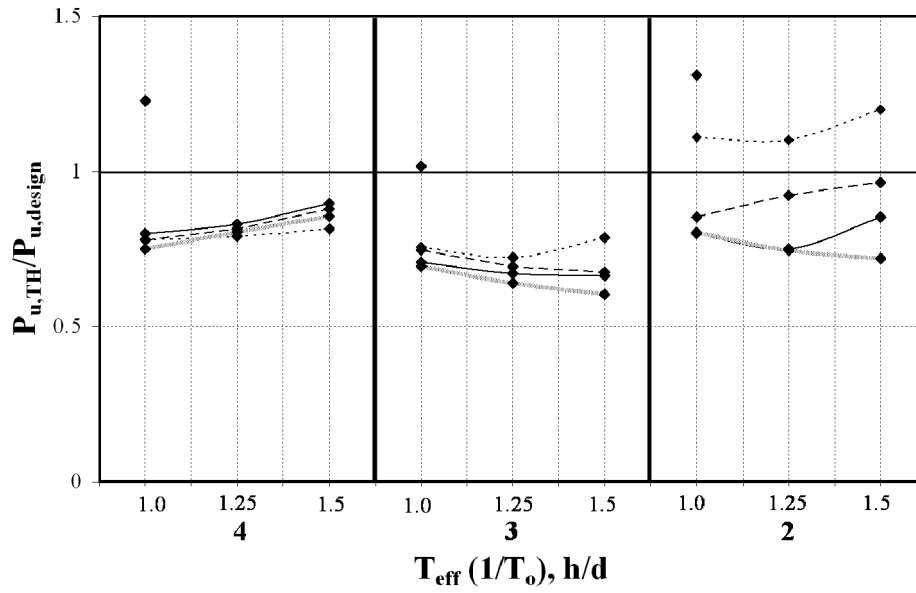
FIGURE 5-11   Normalized Base Shear Results
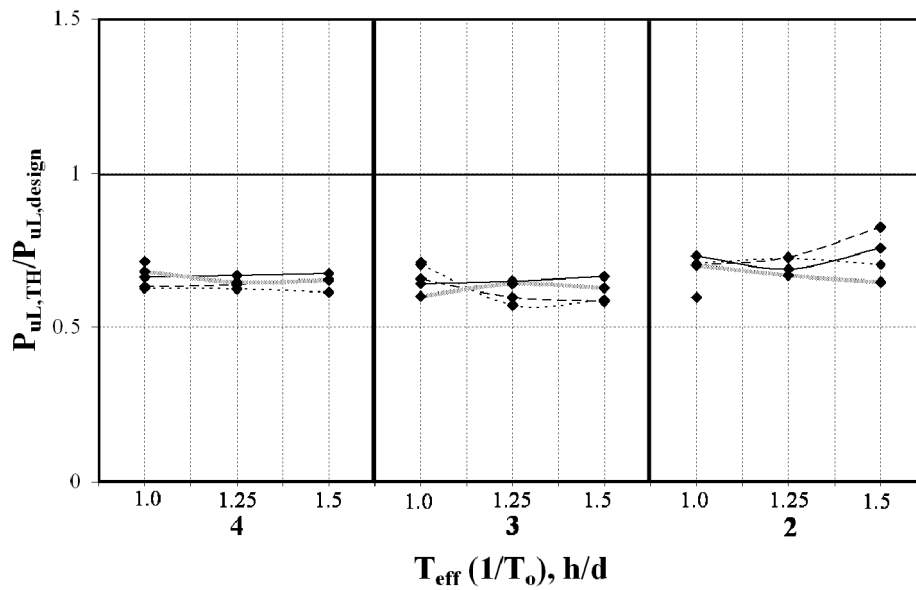
FIGURE 5-12   Normalized Pier Leg Force Results

101
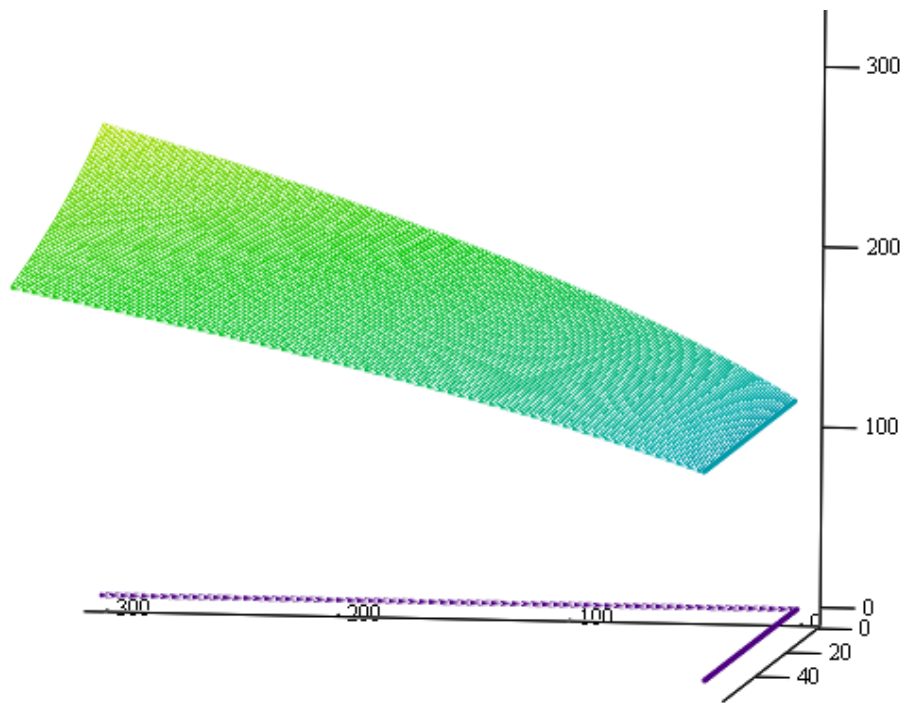
FIGURE 5-13   Displacement Response "Surface" for Aspect Ratio of 4, S_1=0.5g (Method 2)
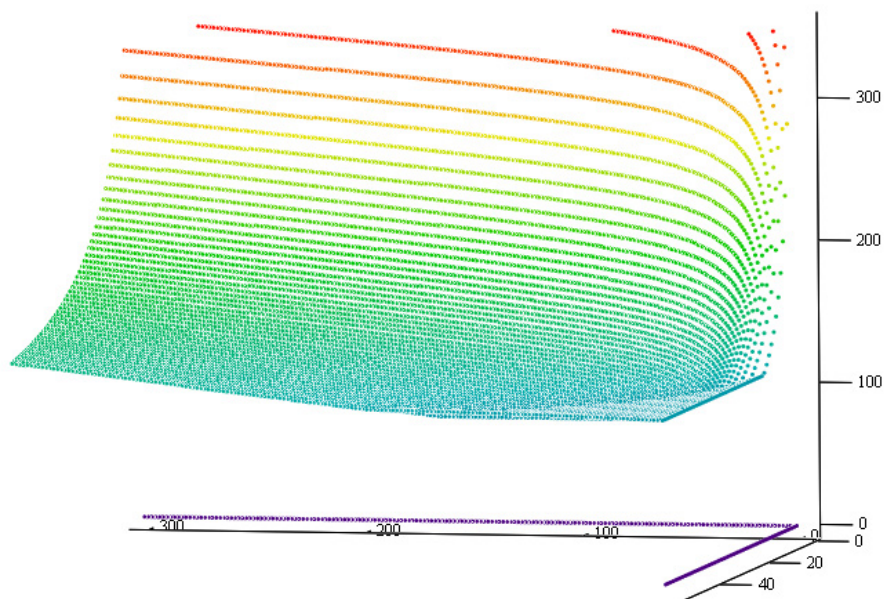
FIGURE 5-14   Displacement Response "Surface" for Aspect Ratio of 4, S_1=0.5g (Method 3)
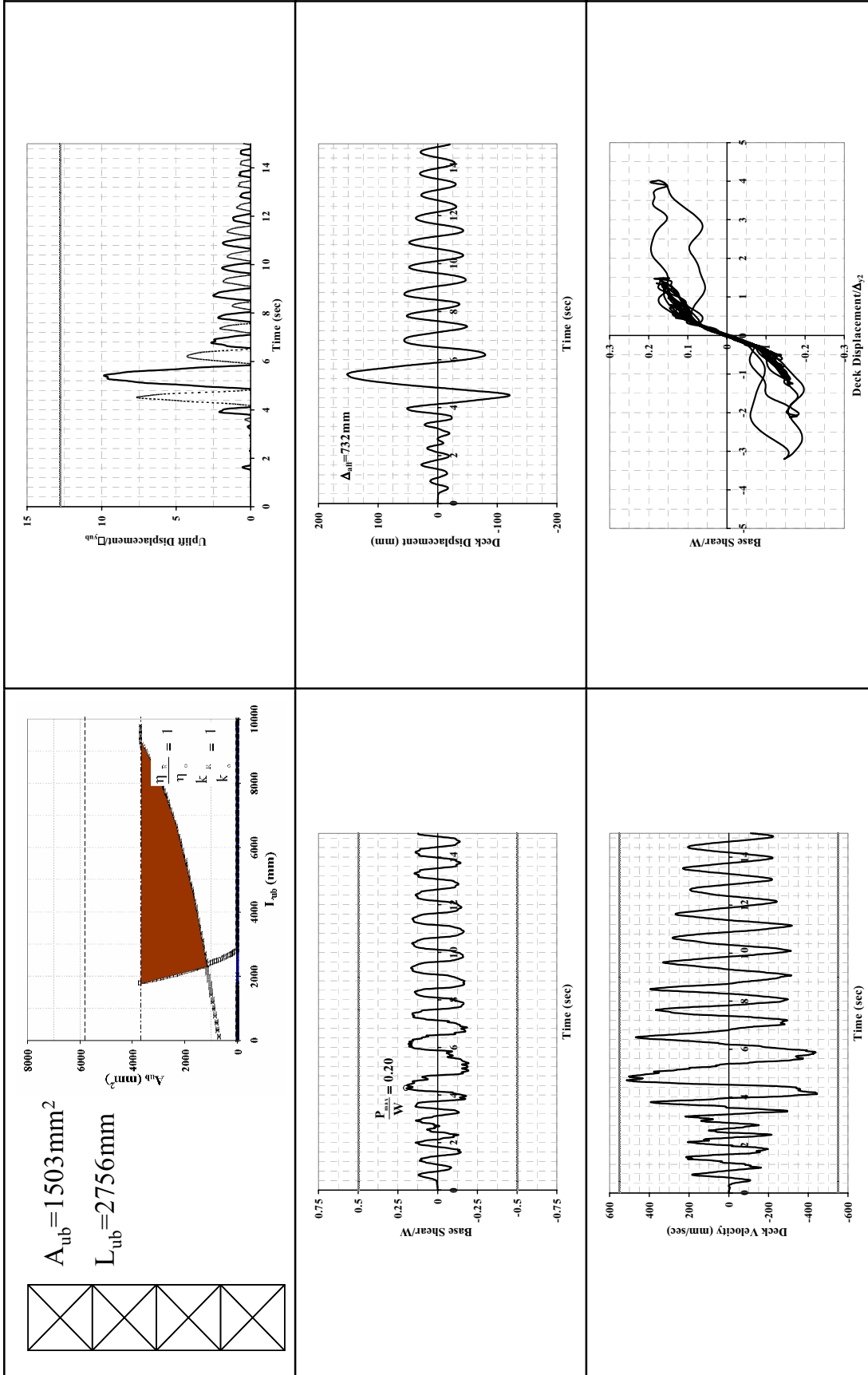
FIGURE 5-15 Example Response History Results for h/d=4
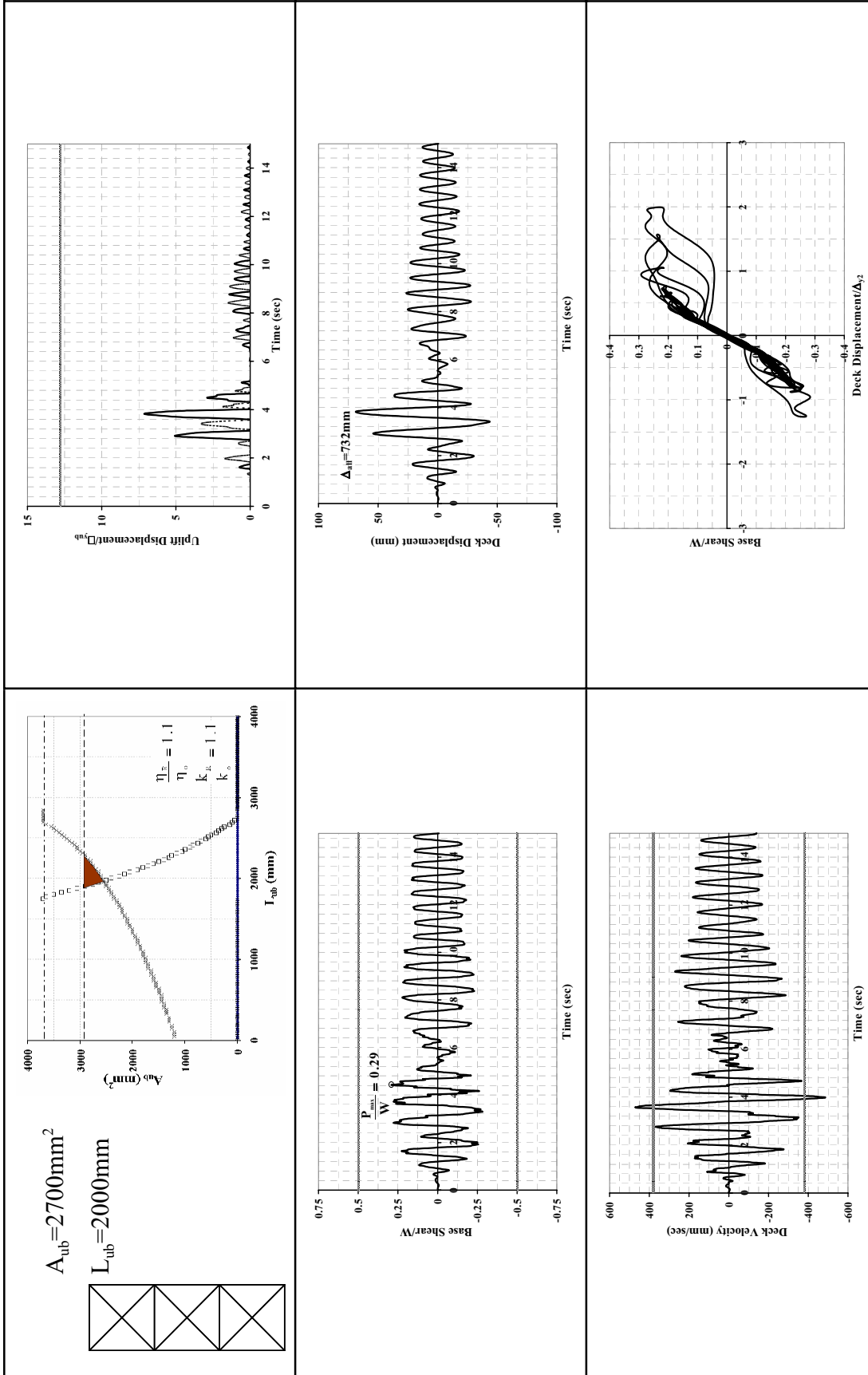
FIGURE 5-16 Example Response History Results for h/d=3
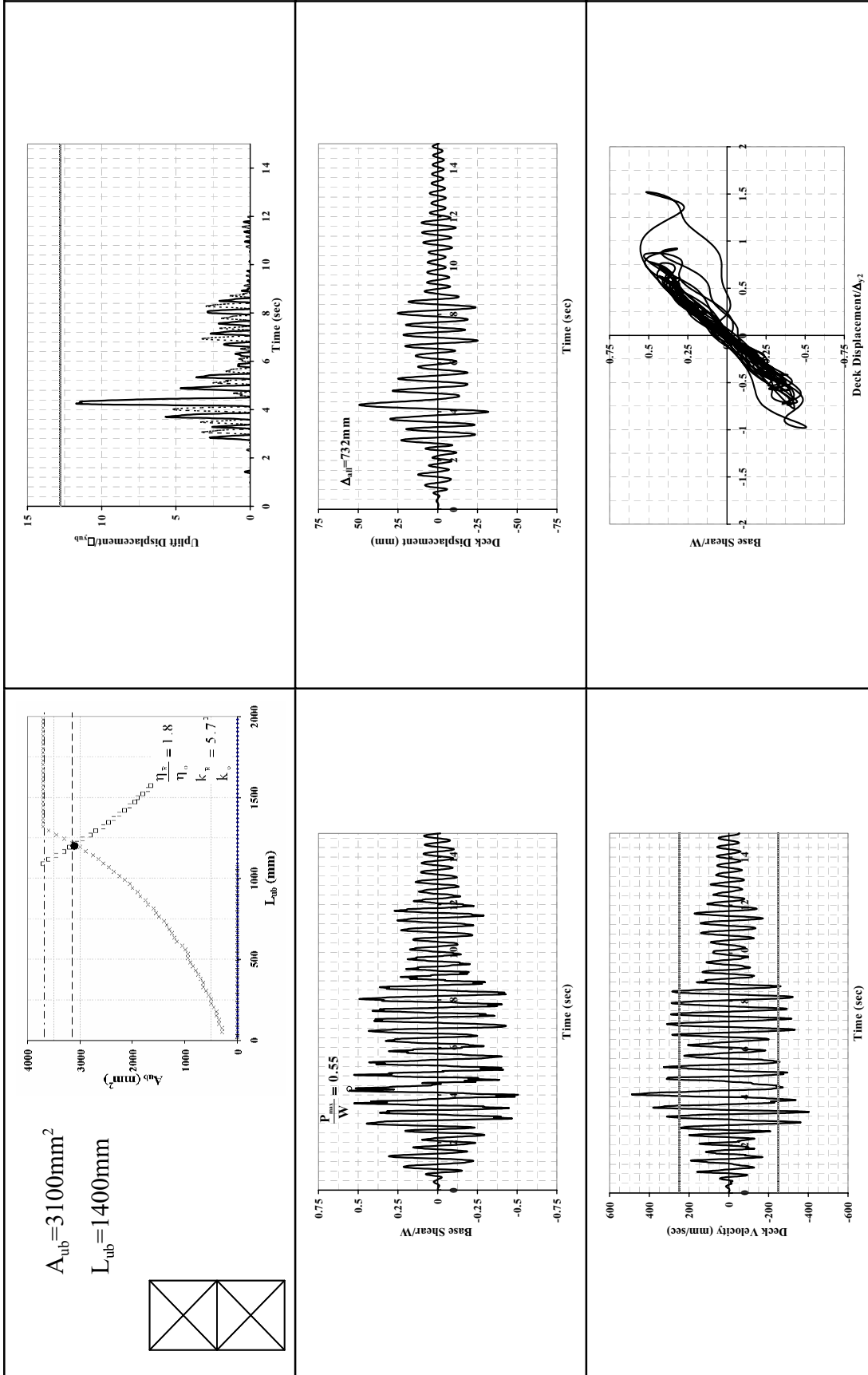
FIGURE 5-17   Example Response History Results for h/d=2

105

SECTION 6
CONCLUSIONS

6.1 General

This study investigated a seismic retrofit technique that allows bridge steel truss piers to uplift and rock on their foundation. To complement the benefits of allowing rocking, passive energy dissipation devices, in particular unbonded braces, are used to control the rocking response while providing additional energy dissipation. The unbonded braces also act as structural "fuses" in this application to limit the demands placed on vulnerable elements contained in existing bridge steel truss piers. The system has an inherent restoring force that can be designed to provide pier self-centering and leave the bridge with no residual displacements following an earthquake.

With emphasis on providing a framework for which the controlled rocking system can be implemented in practice, a set of design constraints is established that include maximum deck-level displacements, ductility demands to the unbonded brace, maximum allowable forces and impact velocity to the foundation. A step-by-step design procedure is proposed and illustrated using an example. A procedure is also used that provides graphical solution spaces, for a number of pier aspect ratios, to illustrate the range of unbonded brace dimensions that are able to satisfy the design constraints. Piers may require strengthening and/or stiffening in order to satisfy the design constraints.

Results of time history analyses are provided for pier aspect ratios of 4, 3 and 2 and local strength ratios, η_L, of 0, 0.25, 0.5, 0.75 and 1.0, to evaluate the performance of the controlled rocking system. It is found that in most cases the methods proposed to predict the dynamic system response are conservative. Unconservative estimates existed primarily for systems with a local strength ratio of zero ($\eta_L=0$) and in the prediction of the impact velocity in some cases. Even with the under-prediction of the impact velocity (which influence demands only to the pier legs), the method used to conservatively predict the maximum forces in the pier legs was indeed found to be always conservative. The retrofit technique is also found to be more effective for piers with larger slenderness ratios.

6.2 Recommendations for Further Research

Further research is needed to validate the proposed concept. In particular, studies should investigate the effect of vertical ground motions on the seismic performance of rocking systems, as well as the impact of soft soil and near field earthquake motions, in order to provide a more complete representation of the seismic demand. Also, the effects of bi-directional motions on the response of 4-legged piers, that resist both transverse and longitudinal demands in bridges, is also needed. Methods to predict the response of controlled rocking to include these effects (possibly by adapting the procedures presented here) are needed.

The use of other types of passive energy dissipation devices to provide more optimal response at the uplifting locations could be investigated. This may include velocity dependent devices and impact absorbing devices.

The assumption of a rigid foundation should be revisited and future analyses could include the foundation flexibility and the interaction of soil and foundation. The effects of the repeated pounding on the foundation and soil should also be investigated for the possibility of settlement.

The behavior of an entire rocking bridge pier system; that includes the interaction of rocking piers, non-rocking piers and abutments through the bridge deck, should be investigated.

Finally, dynamic experimental testing of a rocking frame with energy dissipation devices implemented at the base, should be performed, possibly using 3 components of excitation, to verify analytical results.

SECTION 7
REFERENCES

AASHO (1949). *Standard Specifications for Highway Bridges*, The American Association of State Highway Officials, Washington, D.C.

AASHTO (1998). *LRFD Bridge Design Specifications*, American Association of State Highway and Transportation Officials, Washington, D.C.

AASHTO (2000). *Guide Specifications for Seismic Isolation Design*, American Association of State Highway and Transportation Officials, Washington, D.C.

ACI (2000). ACI Committee 318, "Building Code Requirements for Structural Concrete (ACI 318-99) and Commentary (318R-99)", American Concrete Institute, Farmington Hills, MI, 2000.

AISC (1998). *Manual of Steel Construction - Load and Resistance Factor Design*, American Institute of Steel Construction, Inc., Chicago, Illinois.

AISC (2002). "Seismic Provisions for Structural Steel Buildings", ANSI/AISC 341-02, American Institute of Steel Construction, Inc., Chicago, Illinois.

Astaneh-Asl, A., Bolt, B., McMullin, K., Donikian, R., Modjtahedi, D., and Cho, S. (1994). "Seismic Performance of Steel Bridges During the 1994 Northridge Earthquake", *Report to the California Department of Transportation, Report No. UCB/CE-Steel-94/01*, College of Engineering, University at California Berkeley, April 1994.

Astaneh-Asl, A., Shen, J., and Cho, S. (1997). "Seismic Behavior and Retrofit of Steel Long Span Bridges", Proceedings of the National Seismic Conference on Bridges and Highways: Progress in Research and Practice, San Diego, CA, December 10-13, 1995.

ATC/MCEER (2003). NCHRP 12-49 *Recommended LRFD Guidelines for the Seismic Design of Highway Bridges, Part I: Specifications*, ATC/MCEER Joint Venture.

Black, C., Makris, N. and Aiken, I. (2002). "Component Testing, Stability Analysis and Characterization of Buckling-Restrained Unbonded Braces", *Report No. EERC 2002-08, Earthquake Engineering Research Center,* College of Engineering, University of California, Berkeley, September 2002.

Chopra, A. (2001). *Dynamics of Structures: Theory and Applications to Earthquake Engineering* (2nd Ed.), Prentice Hall, Englewood Cliffs, NJ.

Christopoulos, C., Filiatrault, A. and Folz, B. (2002). "Seismic response of self-centering hysteretic SDOF systems", *Earthquake Engineering and Structural Dynamics*, Vol. 31, pp. 1131-1150.

Clough, R.W. and Penzien, J. (1975). *Dynamics of Structures*, McGraw-Hill, Inc., New York.

Constantinou, M. (1996). "Experimental and Analytical Investigation of Seismic Retrofit of Structures with Supplemental Damping: Part 1, Fluid Viscous Damping Devices", *Technical Report MCEER-95-0001, Multidisciplinary Center for Earthquake Engineering Research*, State University of New York at Buffalo, Buffalo, NY.

Dietrich, A. and Itani, A. (1999). "Cyclic Behavior of Laced and Perforated Steel Members on the San Francisco-Oakland Bay Bridge", *Report No. CCEER 99-9, Center for Civil Engineering Earthquake Research,* Engineering Research and Development Center, College of Engineering, University of Nevada, Reno.

Dowdell, D. and Hamersley, B. (2001). "Lions' Gate Bridge North Approach: Seismic Retrofit", Behaviour of Steel Structures in Seismic Areas: Proceedings of the Third International Conference: STESSA 2000; Montreal, Canada, August 21-24, 2000, pp. 319-326.

FEMA (1997). *FEMA 274 NEHRP Commentary on the Guidelines for the Seismic Rehabilitation of Buildings*, Building Seismic Safety Council for the Federal Emergency Management Agency, Washington, D.C.

FEMA (2000). *FEMA 356 Prestandard and Commentary for the Seismic Rehabilitation of Buildings*, Building Seismic Safety Council for the Federal Emergency Management Agency, Washington, D.C.

Hasegawa, H., Takeuchi, T., Nakata, Y., Iwata, M., Yamada, S., and Akiyama, H. (1999). "Experimental Study on Dynamic Behavior of Unbonded Braces", *AIJ J. Technol. Des*. No. 9, pp. 103-106.

Housner, G. (1963). "The Behavior of Inverted Pendulum Structures During Earthquakes", Bulletin of the Seismological Society of America, Vol. 53, No. 2, February 1963, pp. 403-417.

Housner, G., Chairman, The Governor's Board of Inquiry on the 1989 Loma Prieta Earthquake. *Competing Against Time*. State of California, Office of Planning and Research, May 31, 1990.

Ingham, T., Rodriguez, S., Nadar, M., Taucer, F. and Seim, C. (1997). "Seismic Retrofit of the Golden Gate Bridge", Proceedings of the National Seismic Conference on Bridges and Highways: Progress in Research and Practice, December 10-13, San Diego, CA.

Iwata, M., Kato, T., Wada, A. (2000). "Buckling-restrained braces as hysteretic dampers", Behaviour of Steel Structures in Seismic Areas, STESSA 2000, pp. 33-38.

Jones, M., Holloway, L., Toan, V. and Hinman, J. (1997). "Seismic Retrofit of the 1927 Carquinez Bridge by a Displacement Capacity Approach", Proceedings of the Second National Seismic Conference on Bridges and Highways: Progress in Research and Practice, July 8-11, Sacramento, CA.

Kelley, J. and Tsztoo, D. (1977). "Earthquake Simulation Testing of a Stepping Frame with Energy-Absorbing Devices", *Report No. EERC 77-17, Earthquake Engineering Research Center*, College of Engineering, University of California, Berkeley, August 1977.

Lee, K. (2003). "Seismic Vulnerability Evaluation of Axially Loaded Steel Built-up Laced Members," Ph.D Dissertation, The State University of New York at Buffalo, Buffalo, NY.

Lee, K. and Bruneau, M. (2003). "Review of Energy Dissipation of Compression Members in Concentrically Braced Frames", *Technical Report MCEER-02-0005, Multidisciplinary Center for Earthquake Engineering Research*, The State University of New York at Buffalo, Buffalo, NY.

Makris, N. and Konstantinidis, D. (2002). "The rocking spectrum and the limitations of practical design methodologies", *Earthquake Engineering and Structural Dynamics*, Vol. 32, pp. 265-289.

Mander, J. and Cheng, C. (1997). "Seismic Resistance of Bridge Piers Based on Damage Avoidance Design", *Technical Report NCEER-97-0014, National Center for Earthquake Engineering Research*, The State University of New York at Buffalo, Buffalo, NY.

Meek, J.W. (1975). "Effects of Foundation Tipping on Dynamic Response", *Journal of the Structural Division*, ASCE, Vol. 101, No. ST7, pp. 1297-1311.

Merritt, S., Uang, C.M., and Benzoni, G. (2003a). "Subassemblage testing of Star Seismic buckling-restrained braces", *Report No. TR-2003/04*, University of California, San Diego, La Jolla, CA.

Merritt, S., Uang, C.M., and Benzoni, G. (2003b). "Subassemblage testing of CoreBrace buckling-restrained braces", *Report No. TR-2003/01*, University of California, San Diego, La Jolla, CA.

Merritt, S., Uang, C.M., and Benzoni, G. (2003c). "Uniaxial testing of Associated Bracing buckling-restrained braces", *Report No. TR-2003/05*, University of California, San Diego, La Jolla, CA.

Midorikawa, M., Azuhata, T., Ishihara, T. and Wada, A. (2003). "Shaking table tests on rocking structural systems installed yielding base plates in steel frames", Behaviour of Steel Structures in Seismic Areas, STESSA 2003, pp. 449-454.

Newmark, N., and Hall, W. (1982). *Earthquake Spectra and Design*, Earthquake Engineering Research Institute, Oakland, CA.

Pekhan, G., Mander, J.B. and Chen S.S. (1999). "Design and Retrofit Methodology for Buildings Structures with Supplemental Energy Dissipating Systems", *Technical Report MCEER-99-0021, Multidisciplinary Center for Earthquake Engineering Research*, The State University of New York at Buffalo, Buffalo, NY.

Priestley, M.J.N., Evison, R.J. and Carr, A.J. (1978). "Seismic Response of Structures Free to Rock on Their Foundations", Bulletin of the New Zealand National Society for Earthquake Engineering, Vol. 11, No. 3, Sep. 1978.

Priestley, M.J.N. and Kowalsky, M.J. (2000). "Direct displacement-based seismic design of concrete buildings", Bulletin of the New Zealand Society for Earthquake Engineering, Vol. 33, No. 4, pp. 421-444.

Priestley, M.J.N., Seible, F. and Calvi, G.M. (1996). *Seismic Design and Retrofit of Bridges*, John Wiley & Sons, New York.

Prucz, Z., Conway, W.B., Schade, J.E., and Ouyang, Y. (1997). "Seismic Retrofit Concepts and Details for Long-span Steel Bridges", Proceedings of the 2nd National Seismic Conference on Bridges and Highways: Progress in Research and Practice, Sacramento, CA, U.S.A., July 8-11, 1997.

Psycharis, I.N. (1982). "Dynamic Behavior of Rocking Structures Allowed to Uplift," Ph.D. Dissertation, California Institute of Technology, Pasadena, CA.

Ramirez, O., Constantinou, M., Kircher, C., Whittaker, A., Johnson, M. and Gomez, J. (2000). "Development and Evaluation of Simplified Procedures for Analysis and Design of Buildings with Passive Energy Dissipation Systems", *Technical Report MCEER-00-0010, Multidisciplinary Center for Earthquake Engineering Research*, The State University of New York at Buffalo, Buffalo, NY.

Ritchie, P., Kauhl, N. and Kulicki, J. (1999). "Critical Seismic Issues for Existing Steel Bridges", *Technical Report MCEER-99-0013, Multidisciplinary Center for Earthquake Engineering Research*, The State University of New York at Buffalo, Buffalo, NY.

Sadek, F., Mohraz, B. and Riley, M.A. (1999). "Linear Static and Dynamic Procedures for Structures with Velocity-Dependent Supplemental Dampers", Building and Fire Research Laboratory, National Institute of Standards and Technology, Gaithersburg, MD.

Sarraf, M. and Bruneau, M. (1998). "Ductile Seismic Retrofit of Steel Deck-Truss Bridges. II: Design Applications", J. Struct. Engrg., ASCE, Vol. 124, No. 11, pp. 1263-1271.

SEAONC-AISC (2001). *Recommended provisions for buckling-restrained braced frames*. SEAONC and AISC, 2001.

Toranzo, L.A., Carr, A.J. and Restrepo, J.I. (2001). "Displacement Based Design of Rocking Walls Incorporating Hysteretic Energy Dissipators", 7th International Seminar on Seismic Isolation, Passive Energy Dissipation and Active Control of Vibrations of Structures, Assisi, Italy, October 2-5, 2001.

Uang, Chia-Ming and Kleiser, Michael (1997). "Cyclic Performance of As-Built Latticed Members for the San Francisco-Oakland Bay Bridge," *Report No. SSRP-97/01,* June, Division of Structural Engineering, University of California, San Diego, La Jolla, California.

Wada, A., Saeki, E., Takeuch, T., and Watanabe, A. (1989). "Development of unbonded brace", Column (A Nippon Steel Publication), No. 115 1989.12.

Watanabe, A., Hitomoi, Y., Saeki, E., Wada, A., and Fujimoto, M. (1988). "Properties of brace encased in buckling-restraining concrete and steel tube", Proceedings of Ninth World Conference on Earthquake Engineering, Tokyo-Kyoto, Japan, Vol. IV, pp. 719-724.

Watanabe, A. and Nakamura, H. (1992). "Study on the behavior of buildings using steel with low yield point", Proceedings of Tenth World Conference on Earthquake Engineering, Balkema, Rotterdam, pp. 4465-4468.

Wen, Y. K. (1976). "Method for Random Vibration of Hysteretic Systems," *Journal of the Engineering Mechanics Division*, ASCE, Vol. 102, No. EM2.

Wilson, E. (2000). *Three Dimensional Static and Dynamic Analysis of Structures*. Computers and Structures, Inc., Berkeley, CA.

APPENDIX A

ANCHORAGE CONNECTION CALCULATIONS

This appendix shows pull-out capacity calculations for sample details of an existing connection. Steel and concrete properties are taken from the AASHO *Standard Specifications for Highway Bridges* (1949). Details were taken from drawings of a 4-legged pier and analyzed as such. Focus is placed solely on the anchorage connection (i.e. anchor bolts, concrete embedment). Thus, the anchorage connection is assumed to be the weak link in the lateral load path. The AISC-LRFD Manual (1998) is utilized for steel and concrete limit states. Interaction of tension and shear stresses are accounted for using an elliptical yield surface. Anchor bolt demand-capacity curves including tension-shear interaction are given and results of the global response of the representative bridge piers (Appendix D) are given in a spectral demand-capacity format (SDOF) in Figure A-1.
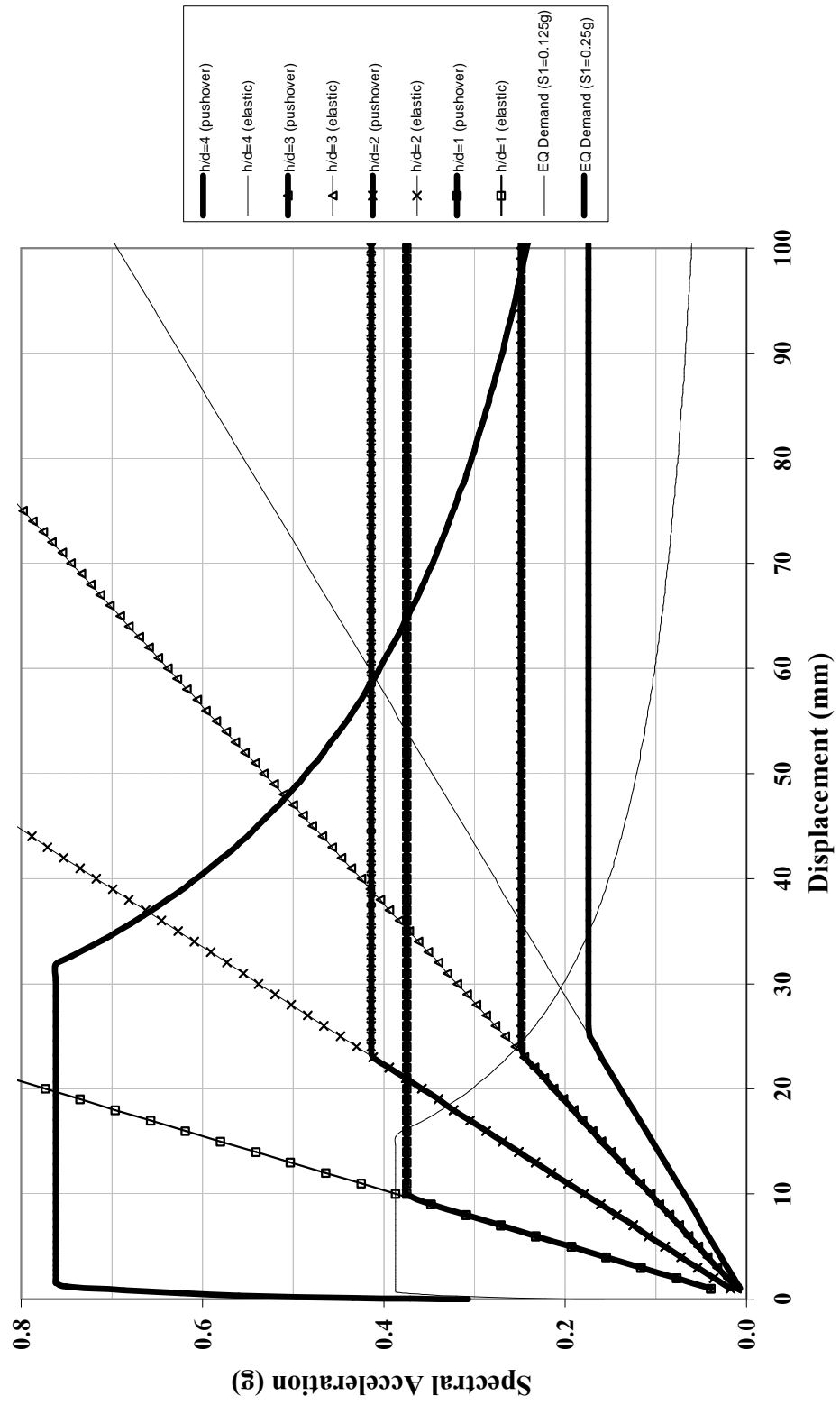
Figure A-1 Spectral Demand-Capacity of Representative Piers with Anchorage as Weak Link

Anchorage Connection Pull-out Calculations

$$g := 9.81 \, \frac{m}{sec^2}$$

Sample Details:
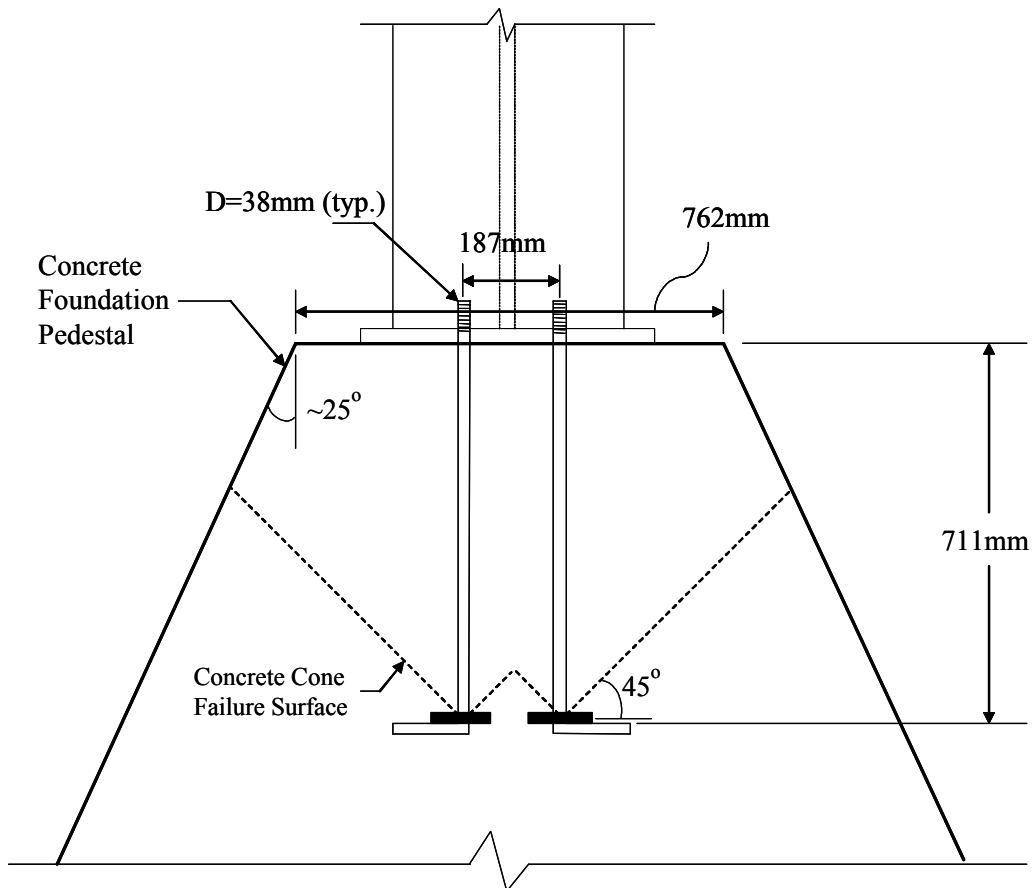
Steel and Concrete Properties from: AASHTO Standard Specifications for Highway Bridges, 5th Edition (1949)

concrete (Class B):

$f_c := 15.2 \, MPa$

steel (ASTM A7-46, replaced by A36 in 1967):

$F_t := 124 \, MPa$ (yield strength)

$F_u := 200 \, MPa$ (tensile strength, assumed)

$F_v := 0.577 \cdot F_t$

$F_v = 71.5 \, MPa$ (strength in pure shear assuming Von Mises yield criterion)

A307 Bolts:

$F_{tA307} := 310 \, MPa$

$F_{vA307} := 165 \, MPa$

$n_1 := 2$ (2 anchor bolts in single connection)

$n_2 := 2$ (details from 4-leg pier, 2 resisting connections)

<u>Tensile Strength of Single Anchor Rod per AISC LRFD Vol. II, 2nd Ed. (1995):</u>

$D_b := 38\,mm$ (nominal anchor bolt diameter)

$A_g := \dfrac{\pi \cdot D_b^2}{4}$ (gross area of single anchor bolts)

$0.75 \cdot A_g = 850.6\,mm^2$ (reduced area in threaded region)

$\phi_t := 0.75$ (resistance factor for anchor bolt in tension)

$R_n := \phi_t \cdot F_u \cdot 0.75 A_g$

$R_n = 127.6\,kN$ <mark>$n_1 \cdot n_2 \cdot R_n = 510.4\,kN$</mark>

<u>Tensile Yielding Limit State of Anchor Bolts:</u>

$\phi_t := 0.75$

$R_n := \phi_t \cdot F_t \cdot A_g$

$R_n = 105.5\,kN$ <mark>$n_1 \cdot n_2 \cdot R_n = 421.9\,kN$</mark>

<u>Concrete Cone Failure Limit State per AISC LRFD Vol. II, 2nd Ed. (1995):</u>

$\phi_t := 0.75$

$A_{cp} := \pi \cdot \left(\dfrac{187 \cdot mm}{2} - 38 \cdot mm \right)^2 + \pi \cdot (400 \cdot mm)^2$

$T_u := 4 \cdot \phi_t \cdot A_{cp1} \cdot \sqrt{f_{c1} \cdot psi}$

$T_u = 497.1\,kN$ <mark>$n_2 \cdot T_u = 994.2\,kN$</mark>

Tension Stress Limit for Combined Tension and Shear:

f_t: allowable tension stress

f_v: applied shear stress

$$f_t = \frac{F_t}{F_v} \cdot \sqrt{F_v^2 - f_v^2}$$

$$f_t \leq F_t$$

$$f_v \leq F_v$$

$$f_{ta4}(V_1) = \begin{vmatrix} 0\,\text{MPa} & \text{if } V_1 \leq \dfrac{W}{2} \cdot \dfrac{d_4}{h_4} \\[2em] \dfrac{\left(V_1 \cdot \dfrac{h_4}{d_4} - \dfrac{W}{2} \right)}{4 \cdot A_g} & \text{if } V_1 > \dfrac{W}{2} \cdot \dfrac{d_4}{h_4} \end{vmatrix}$$

$$A_4(V_1) := f_{ta4}(V_1) - f_{tc1}(V_1)$$

$\text{root}(A_4(V_1), V_1) = 336.5\,\text{kN}$

$\text{root}(A_3(V_1), V_1) = 429.0\,\text{kN}$

$\text{root}(A_2(V_1), V_1) = \blacksquare\,\text{kN}$

$\text{root}(A_1(V_1), V_1) = \blacksquare\,\text{kN}$

Tension-Shear Interaction Curves

$\dfrac{h}{d} = 4$

$\dfrac{h}{d} = 3$

$\dfrac{h}{d} = 2$

A307

$\dfrac{h}{d} = 1$

A7-46

allowable tension stress (MPa)

applied shear stress (MPa)
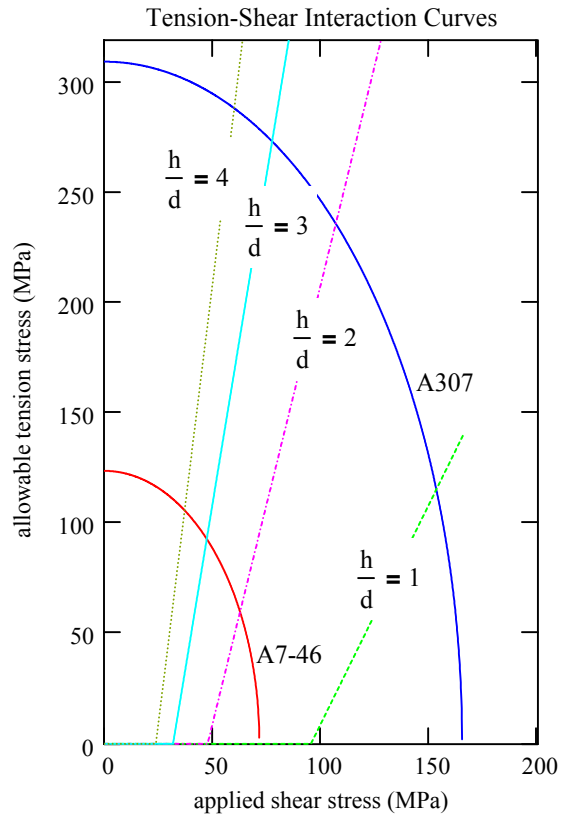
V_d: elastic base shear demand

V_c: base shear capacity based on anchorage pull-out limit

$W := 1730\,\text{kN} \qquad m := \dfrac{W}{g}$

$\dfrac{h}{d} = 4$

$T_c := 336.5\,\text{kN}$

$k_o := 12.5 \dfrac{\text{kN}}{\text{mm}}$

$T_o := 2 \cdot \pi \cdot \sqrt{\dfrac{m}{k_o}} \qquad T_o = 0.75\,\text{sec}$

$V_d = m \cdot S_a(T_o)$

$$\sum M = V_c \cdot h - W \cdot \dfrac{d}{2} - T \cdot d = 0$$
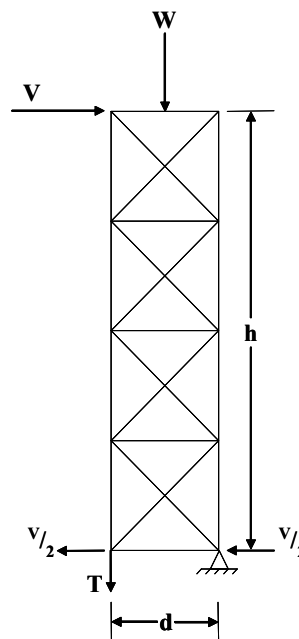
Free-body diagram of
Pier after Uplift

$$V_c := \begin{cases} \left(\dfrac{W}{2} + T_c\right)\dfrac{d}{h} & \text{if } \dfrac{h}{d} > 1 \\[2ex] (8 \cdot A_g \cdot F_v) & \text{if } \dfrac{h}{d} = 1 \end{cases}$$

$$\Delta_f := \frac{V_c}{k_o} \quad \text{(pier deformation at anchorage failure, assumes no change in stiffness after uplift)}$$

$$\Delta := 1mm, 2mm .. 300mm$$

$$V_{c1}(\Delta) := \begin{cases} (k_o \cdot \Delta) & \text{if } \Delta \le \Delta_f \\[1.5ex] V_c & \text{if } \Delta > \Delta_f \end{cases}$$

$$S_{ac}(\Delta) := \frac{V_{c1}(\Delta)}{W} \quad \text{(spectral capacity curve)}$$

NCHRP 12-49 Seismic Hazard:

$$S_1 := .25 \qquad\qquad S_S := .6125$$

For Site Class B:

$$F_a := 1.0 \qquad\qquad F_v := 1.0$$

$$S_{XS} := F_a \cdot S_S \qquad\qquad S_{X1} := F_v \cdot S_1$$
$$S_{XS} = 0.61 \qquad\qquad S_{X1} = 0.25$$

$$\zeta_{eff} := 0.02 \quad \text{(inherent structural damping)}$$

$$B_s := 0.8 \quad \text{Damping Modification Factors}$$
$$B_1 := 0.8$$

$$T_s := \frac{S_{X1}}{S_{XS}} \cdot sec \qquad\qquad T_s = 0.41 \text{ s}$$

$$T_0 := 0.2 \cdot T_s \qquad\qquad T_0 = 0.08 \text{ s}$$

$T := 0.01\sec, 0.02\sec .. 3\sec$ (period Incremented by .01 sec)

$$S_{ad}(T) := \begin{vmatrix} S_{XS} \cdot \left[\left(\dfrac{5}{B_s} - 2 \right) \dfrac{T}{T_s} + 0.4 \right] & \text{if } T \leq T_0 \\[4mm] \dfrac{S_{XS}}{B_s} & \text{if } T_0 \leq T \leq T_s \\[4mm] \dfrac{S_{X1}}{B_1 \cdot T} \cdot \sec & \text{if } T_s \leq T \end{vmatrix}$$ (spectral demand curve)

$$S_{dd}(T) := \left(\frac{T}{2 \cdot \pi} \right)^2 \cdot S_{ad}(T) \cdot g$$ (spectral displacement demand curve)

$$S_{a1}(\Delta) := \frac{4 \cdot \pi^2 \cdot \Delta}{T_o^2 \cdot g}$$ (linear spectral response curve)

$S_{ac}(\Delta)$

$S_{ad}(T)$

$S_{a1}(\Delta)$

$$\frac{\Delta}{mm}, \frac{S_{dd}(T)}{mm}, \frac{\Delta}{mm}$$

123
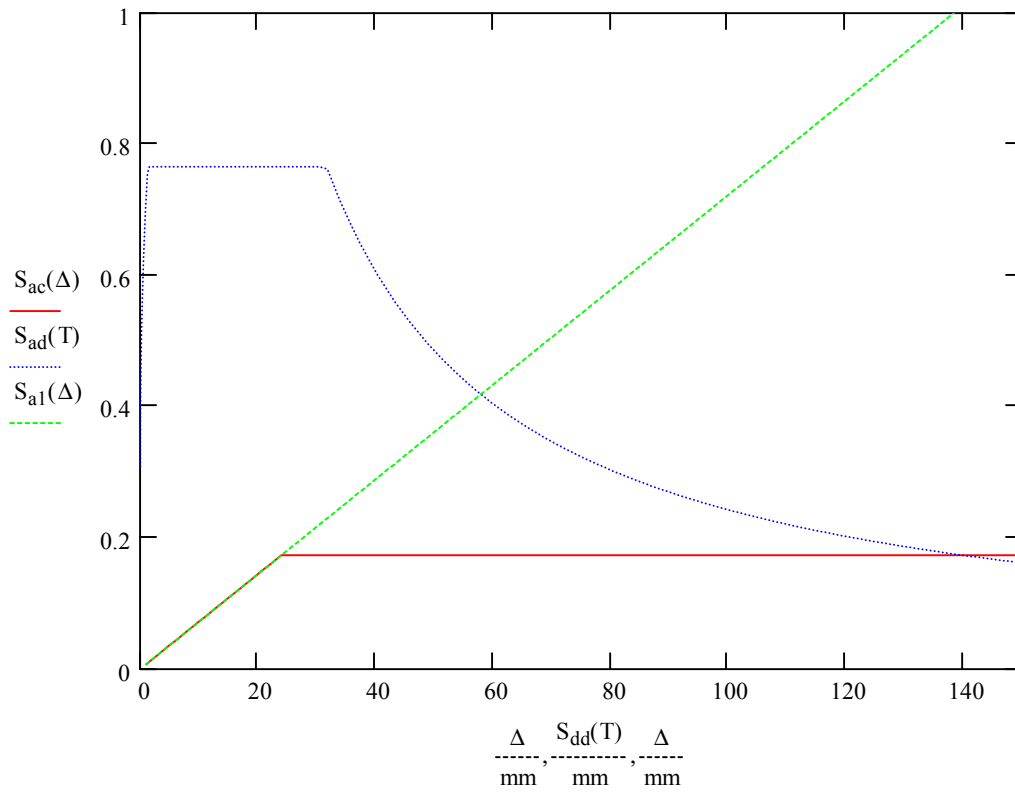
APPENDIX B
VERTICAL MODE RESPONSE CALCULATIONS

This Appendix provides sample calculations for determining the amplified response caused by dynamic loads being applied to the flexible bridge pier. As was discussed in Section 3, a series of loads are applied dynamically through the pier vertically as its axis of rotation changes from the base of one leg to another. Response to these loads is evaluated by breaking the pier into simplified, linear-elastic systems using the properties of the representative bridge piers discussed in Appendix D. The sample calculations are given for an aspect ratio of 4 to show how the amplification factors are determined for the concepts presented here. Calculations using 1st and 2nd cycle properties are given to show the decrease in dynamic amplification in the 2nd and subsequent cycles.

Vertical Mode Response Calculations

$$g := 9.81 \frac{m}{\sec^2}$$

pier properties:

earthquake demand:

$W := 1730 kN$

$$S_1 := 0.5 \cdot g$$

$$m := \frac{W}{g}$$ (effective horizontal mass)

$E := 200 GPa$

$h := 29260 mm$ (hieght of pier)

$d := 7315 mm$ (width of pier)

$$\frac{h}{d} = 4$$

$A_d := 7097 mm^2$ (cross-sectional area of diagonal)

$L_d := 10340 mm$ (length of diagonal)

$A_L := 31100 mm^2$ (cross-sectional area of tower leg)

$$I := \frac{1}{2} A_L \cdot d^2$$ (moment of inertia of pier)

$$f_p := \frac{1}{\sqrt{2}}$$ (Eq. 3.32, for X-braced pier)

$panels := 4$ (# of panels resisting vertical shearing modes)

Tower diagonal: A_d, L_d
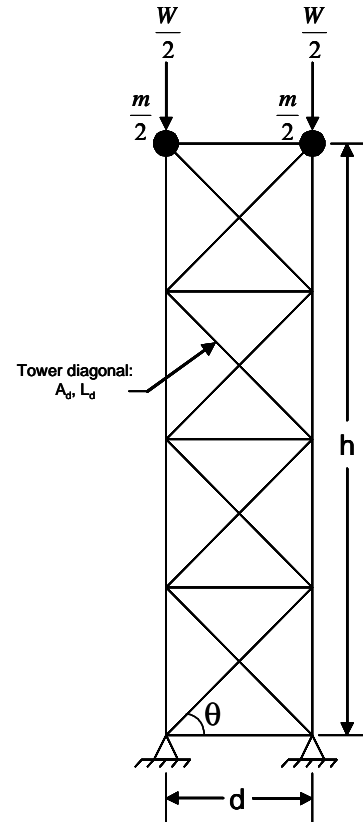
Horizontal Stiffness and Period of Vibration of "Fixed-base" Pier:

fixed base horizontal period of vibration:

$$\Delta_b := \left(P \cdot \frac{h^3}{3 \cdot E \cdot I} \right)$$ $P := 1 kN$ (virtual load)

$$\Delta_b = 0.05 \ mm$$

$$\Delta_v := \left(\frac{P \cdot L_d^3}{2 \cdot E \cdot d^2 \cdot A_d} \right)$$ $\Delta_v = 7.278 \times 10^{-3} \ mm$

$$k_o := \frac{P}{\left(\Delta_b + \frac{h}{d} \cdot \Delta_v \right)}$$ $k_o = 12.6 \frac{kN}{mm}$

$$T_o := 2 \cdot \pi \cdot \sqrt{\frac{m}{k_o}}$$ $T_o = 0.74 \ sec$
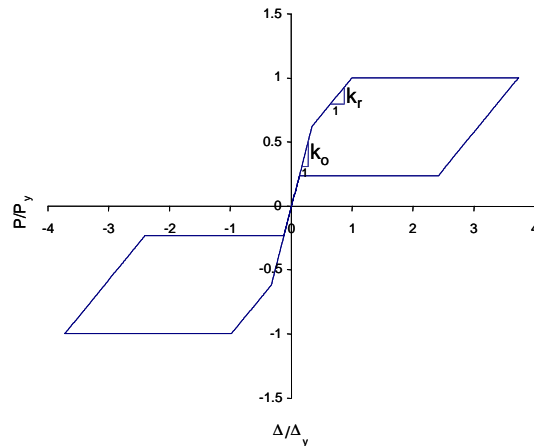
rocking period of tower (post-uplift):

unbonded brace properties:

$A_{ub} := 1850mm^2$

$L_{ub} := 3302mm$

$F_{yub} := 235MPa$

$k_r := \left[\dfrac{1}{k_o} + \dfrac{1}{\dfrac{E \cdot A_{ub}}{L_{ub}} \cdot \left(\dfrac{d}{h}\right)^2}\right]^{-1}$ $k_r = 4.5 \dfrac{kN}{mm}$

$T_r := 2 \cdot \pi \cdot \sqrt{\dfrac{m}{k_r}}$ $T_r = 1.24 \, sec$

$\eta_L := \dfrac{A_{ub} \cdot F_{yub}}{\dfrac{W}{2}}$ $\eta_L = 0.5$
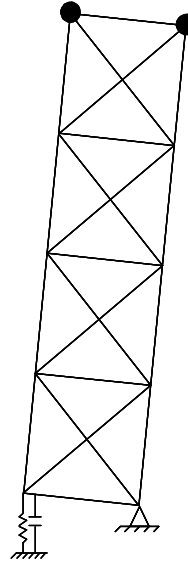
Hysteretic and Dynamic Response for 1st Cycle Properties:

$\Delta_{up1} := \dfrac{\dfrac{W}{2} \dfrac{d}{h}}{k_o}$

$\Delta_{y1} := \Delta_{up1} + \dfrac{A_{ub} \cdot F_{yub} \cdot \dfrac{d}{h}}{k_r}$

$k_{eff1} := k_o \cdot \left(\dfrac{\Delta_{up1}}{\Delta_{y1}}\right) + k_r \cdot \left(\dfrac{\Delta_{y1} - \Delta_{up1}}{\Delta_{y1}}\right)$

$T_{eff2} := 2 \cdot \pi \cdot \sqrt{\dfrac{m}{k_{eff1}}}$ $T_{eff2} = 0.94 \, sec$

$\Delta_{max} := \dfrac{S_1 \cdot T_{eff2} \cdot sec}{4 \cdot \pi^2}$ $\Delta_{max} = 116.9 \, mm$ (maximum seismic pier displacement using Method 2
from Section 3.4 and using 1st Cyle properties)
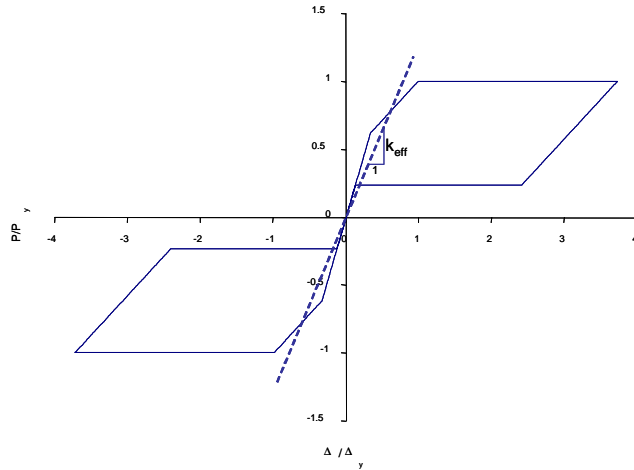
Dynamic Properties for Axial Vibration of Pier Leg:

Stiffness and Period of Vibration of Pier Leg System:

$$k_L := \frac{E \cdot A_L}{h} \qquad\qquad k_L = 213 \, \frac{kN}{mm}$$

$$T_L := 2 \cdot \pi \cdot \sqrt{\frac{\frac{m}{2}}{k_L}} \qquad T_L = 0.128 \, sec$$

Rise Time for Loading of Pier Leg System:

-Rise time approximately determined from an effective SDOF system under free vibration

SDOF Oscillator: free vibration response:

m

$$u(t) = u_{max} \cdot \sin(\omega_n \cdot t)$$

k_{eff},
T_{eff}
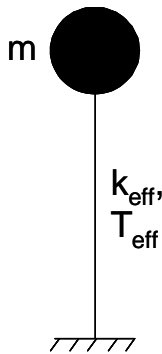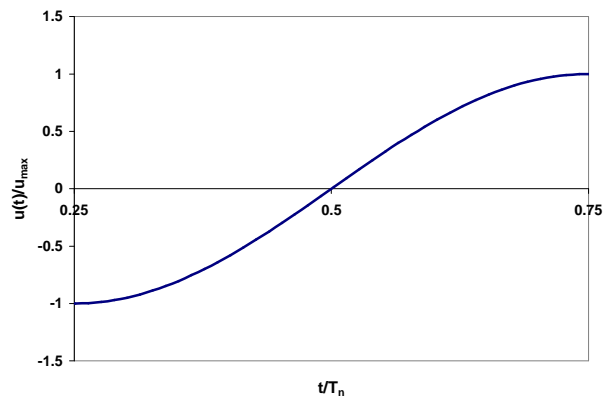
$$P_y := \left(\frac{W}{2} + A_{ub} \cdot F_{yub} \right) \frac{d}{h}$$

$$k_{sec} := \frac{P_y}{\Delta_{max}} \qquad T_{sec} := 2 \cdot \pi \cdot \sqrt{\frac{m}{k_{sec}}} \qquad T_{sec} = 1.582 \, s$$

$$t_{rL1} := asin\left(\frac{4 \cdot \pi^2 \cdot \Delta_{up1}}{S_1 \cdot T_{eff2} \cdot sec} \right) \cdot \frac{T_{sec}}{2 \cdot \pi}$$

$t_{rL1} = 0.037 \, s$ (rise time for loading applied to pier leg)

Dynamic Properties for Vertical Shearing Vibration of Pier:

Stiffness and Period of Vibration of Vertical Truss Pier System:

$$k_v := f_p \cdot \frac{E \cdot A_d}{d} \cdot panels \qquad k_v = 548.8 \frac{kN}{mm}$$

$$T_v := 2 \cdot \pi \cdot \sqrt{\frac{\frac{m}{2}}{k_v}} \qquad T_v = 0.080 \, sec$$

Rise Times for Loading of Pier Leg System:

$$t_{rv11} := asin\left(\frac{4 \cdot \pi^2 \Delta_{up1}}{S_1 \cdot T_{eff2} \cdot sec}\right) \cdot \frac{T_{sec}}{2 \cdot \pi}$$

$$t_{rv11} = 0.037 \, sec \qquad \frac{t_{rv11}}{T_v} = 0.466$$

$$t_{rv21} := asin\left(\frac{4 \cdot \pi^2 \cdot \Delta_{y1}}{S_1 \cdot T_{eff2} \cdot sec}\right) \cdot \frac{T_{sec}}{2 \cdot \pi} - t_{rv11}$$

$$t_{rv21} = 0.054 \, sec \qquad \frac{t_{rv21}}{T_v} = 0.676$$

Effective Rise Time for Both Loads during Uplift:

$$t_{rv1} := asin\left(\frac{4 \cdot \pi^2 \cdot \frac{1}{2} \Delta_{y1}}{S_1 \cdot T_{eff2} \cdot sec}\right) \cdot \frac{T_{sec}}{2 \cdot \pi}$$

$$t_{rv1} = 0.045 \, sec \qquad \frac{t_{rv1}}{T_v} = 0.562$$

_____
_____

Response Calculations for Each System Utilizing Convolution Integral Presented in Section 3.3.1.2

$i := 1..250$

$t_i := \dfrac{i}{1000} \sec$ (time increments)

_____

Axial Vibrations of Pier Legs

$\dfrac{W}{2}$

$p_{oL1} := \dfrac{W}{2}$ (magnitude of step force with finite rise time, trL, applied to pier leg)

$$p_{L1_i} := \left\| \begin{array}{l} \left[p_{oL1} \cdot \left(\dfrac{t_i}{t_{rL1}} \right) \right] \text{ if } t_i < t_{rL1} \\[2mm] p_{oL1} \text{ if } t_i \geq t_{rL1} \end{array} \right.$$ (applied force over time)

$u_{stL1_i} := \dfrac{p_{L1_i}}{k_L}$ (static displacement response)

$$u_{L1_i} := \left\| \begin{array}{l} u_{stL1_i} \cdot \left(\dfrac{t_i}{t_{rL1}} - \dfrac{\sin\left(\dfrac{2 \cdot \pi}{T_L} \cdot t_i \right)}{\dfrac{2 \cdot \pi}{T_L} \cdot t_{rL1}} \right) \text{ if } t_i \leq t_{rL1} \\[6mm] \left[u_{stL1_i} \cdot \left[1 - \dfrac{1}{\dfrac{2 \cdot \pi}{T_L} \cdot t_{rL1}} \cdot \left[\sin\left(\dfrac{2 \cdot \pi}{T_L} \cdot t_i \right) - \sin\left[\dfrac{2 \cdot \pi}{T_L} \cdot (t_i - t_{rL1}) \right] \right] \right] \right] \text{ if } t_i > t_{rL1} \end{array} \right.$$
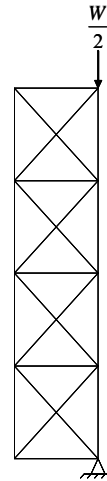
(response of system using convolution integral)
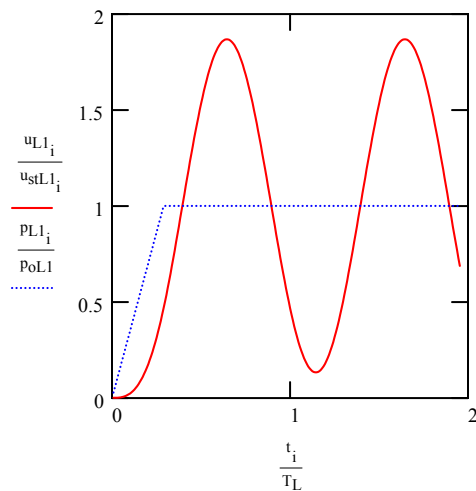
$R_{dL1_i} := \dfrac{u_{L1_i}}{u_{stL1_i}}$

$R_{dL1} := \max(R_{dL1})$

Vibrations of Vertical Truss System

p11: force from transfer of gravity to compression leg based on 1st cycle properties

$$p_{o11} := \frac{W}{2}$$

$$p_{o11} = 865 \text{ kN}$$

p21: force to yield unbonded braces based on 1st cycle properties

$$p_{o21} := A_{ub} \cdot F_{yub}$$

$$p_{o21} = 435 \text{ kN}$$
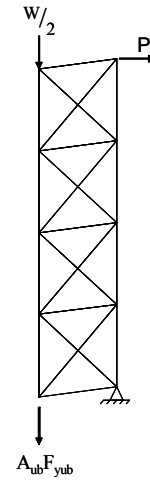
$$p_{11_i} := \left\| \begin{array}{l} \left[p_{o11} \cdot \left(\dfrac{t_i}{t_{rv11}} \right) \right] \quad \text{if} \;\; t_i < t_{rv11} \\[2mm] p_{o11} \quad \text{if} \;\; t_i \geq t_{rv11} \end{array} \right.$$

$$p_{21_i} := \left| \begin{array}{l} 0 \quad \text{if} \;\; t_i \leq t_{rv11} \\[2mm] \left[p_{o21} \cdot \left(\dfrac{t_i - t_{rv11}}{t_{rv21}} \right) \right] \quad \text{if} \;\; t_{rv11} < t_i \leq t_{rv21} + t_{rv11} \\[2mm] p_{o21} \quad \text{if} \;\; t_i > t_{rv21} + t_{rv11} \end{array} \right.$$

$\dfrac{p11_i}{\text{kips}}$ ——— (red solid)

$\dfrac{p21_i}{\text{kips}}$ ········ (blue dotted)

$\dfrac{p11_i + p21_i}{\text{kips}}$ - - - - (green dashed)

$\dfrac{t_i}{\text{sec}}$
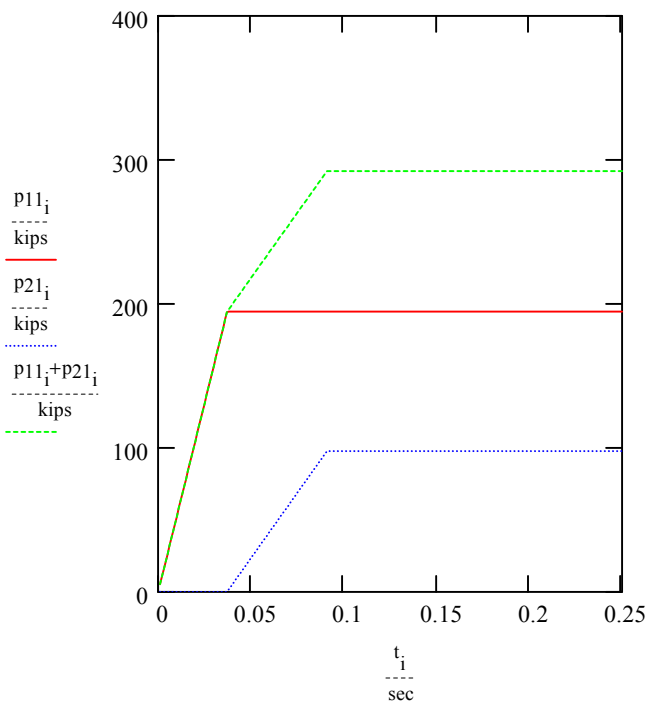
(application of vertical shearing forces over time)

$$u_{stv11_i} := \frac{p_{11_i}}{k_v}$$

$$u_{v11_i} := \left| \begin{array}{l} u_{stv11_i} \cdot \left(\dfrac{t_i}{t_{rv11}} - \dfrac{\sin\left(\dfrac{2 \cdot \pi}{T_v} \cdot t_i\right)}{\dfrac{2 \cdot \pi}{T_v} \cdot t_{rv11}} \right) \quad \text{if } t_i \le t_{rv11} \\[4ex] \left[u_{stv11_i} \cdot \left[1 - \dfrac{1}{\dfrac{2 \cdot \pi}{T_v} \cdot t_{rv11}} \cdot \left[\sin\left(\dfrac{2 \cdot \pi}{T_v} \cdot t_i\right) - \sin\left[\dfrac{2 \cdot \pi}{T_v} \cdot (t_i - t_{rv11})\right] \right] \right] \right] \quad \text{if } t_i > t_{rv11} \end{array} \right.$$

$$u_{stv21_i} := \frac{p_{21_i}}{k_v}$$

$$u_{v21_i} := \left| \begin{array}{l} 0 \quad \text{if } t_i \le t_{rv11} \\[2ex] u_{stv21_i} \cdot \left[\dfrac{t_i - t_{rv11}}{t_{rv21}} - \dfrac{\sin\left[\dfrac{2 \cdot \pi}{T_v} \cdot (t_i - t_{rv11})\right]}{\dfrac{2 \cdot \pi}{T_v} \cdot t_{rv21}} \right] \quad \text{if } t_{rv11} < t_i \le (t_{rv21} + t_{rv11}) \\[4ex] u_{stv21_i} \cdot \left[1 - \dfrac{1}{\dfrac{2 \cdot \pi}{T_v} \cdot t_{rv21}} \cdot \left[\sin\left[\dfrac{2 \cdot \pi}{T_v} \cdot (t_i - t_{rv11})\right] - \sin\left[\dfrac{2 \cdot \pi}{T_v} \cdot \left[(t_i - t_{rv11}) - t_{rv21}\right]\right] \right] \right] \quad \text{if } t_i > (t_{rv21} + t_{rv11}) \end{array} \right.$$

Normalized Response of Vertical Shearing Mode to each load and total response over time:

Normalized Total Dynamic and Static Response of Vertical Shearing Mode over time:

Legend:
$$\frac{u_{v11_i} + u_{v21_i}}{\left(\dfrac{p11_i + p21_i}{k_v}\right)}$$ (solid red line)

$$\frac{p11_i + p21_i}{P_{o11} + P_{o21}}$$ (dotted blue line)

Horizontal axis: $\dfrac{t_i}{T_v}$
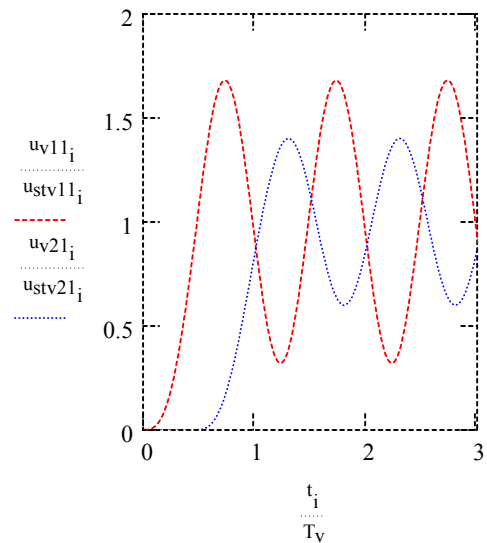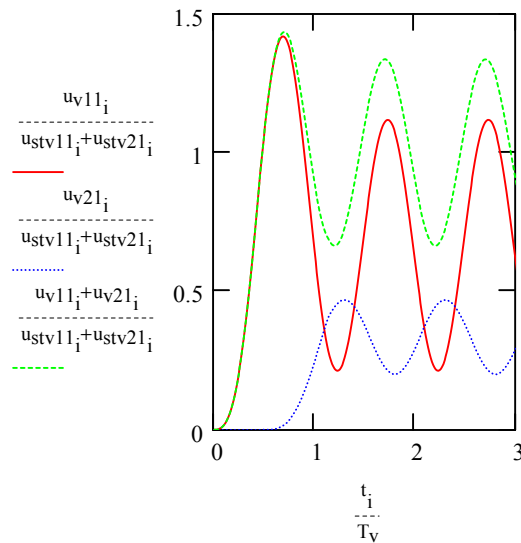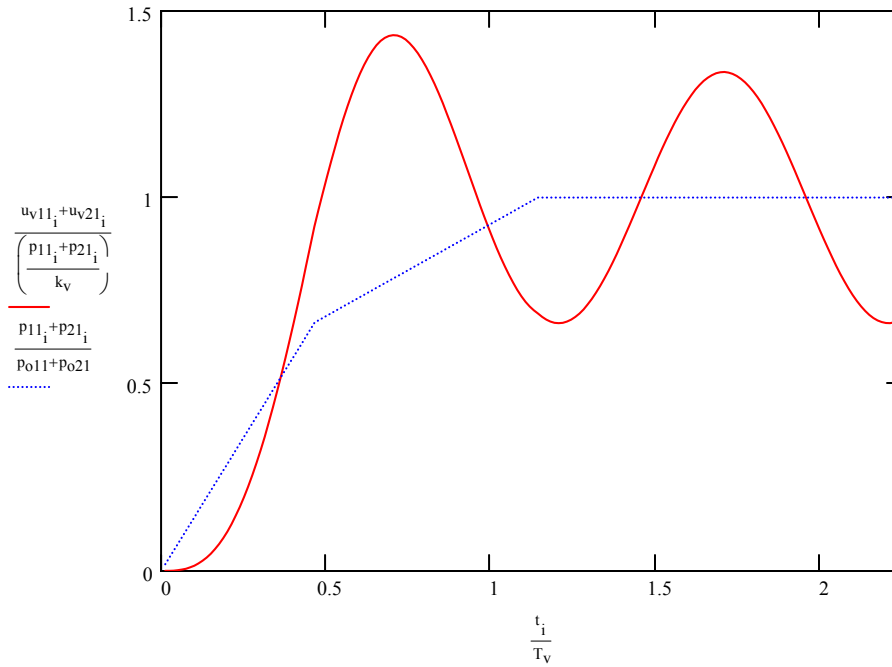
$$R_{dv11_i} := \frac{u_{v11_i} + u_{v21_i}}{u_{stv11_i} + u_{stv21_i}} \qquad\qquad R_{dv11} := \max\left(R_{dv11}\right)$$

Dynamic Amplification Factors, R_d, for Leg and Pier:

R_d: dynamic amplification factor for impulsive loads

$R_{dL1} = 1.87$ (DAF for compressed tower leg)

$R_{dv11} = 1.44$ (DAF for loads carried through vertical truss system considering phase effects)

$$R_{dv1} := 1 + \frac{\sin\left(\dfrac{\pi \cdot t_{rv1}}{T_v}\right)}{\left(\dfrac{\pi \cdot t_{rv1}}{T_v}\right)} \qquad R_{dv1} = 1.556 \qquad \text{(DAF for 2 dynamic loads during uplift using effective rise time)}$$

Hysteretic and Dynamic Response for 2nd Cycle Properties:

$$\Delta_{up2} := \frac{\left(1 - \eta_L\right)\dfrac{W}{2}\dfrac{d}{h}}{k_o}$$

$$\Delta_{y2} := \Delta_{up2} + \frac{2 \cdot A_{ub} \cdot F_{yub} \cdot \dfrac{d}{h}}{k_r}$$

$$k_{eff2} := k_o \cdot \left(\frac{\Delta_{up2}}{\Delta_{y2}}\right) + k_r \cdot \left(\frac{\Delta_{y2} - \Delta_{up2}}{\Delta_{y2}}\right)$$

$$T_{eff2} := 2 \cdot \pi \cdot \sqrt{\frac{m}{k_{eff2}}} \qquad T_{eff2} = 1.1\,sec$$

$$\Delta_{max2} := \frac{S_1 \cdot T_{eff2} \cdot sec}{4 \cdot \pi^2} \qquad \Delta_{max2} = 137.1\,mm$$
(maximum seismic pier displacement using Method 2 from Section 3.4 and using 2nd Cyle properties)
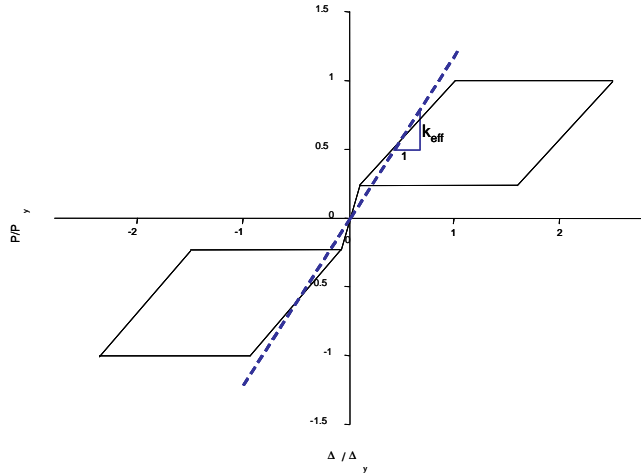
Dynamic Properties for Axial Vibration of Pier Leg:

Stiffness and Period of Vibration of Pier Leg System:

$$k_L := \frac{E \cdot A_L}{h} \qquad k_L = 213\,\frac{kN}{mm}$$

$$T_L := 2 \cdot \pi \cdot \sqrt{\frac{\dfrac{m}{2}}{k_L}} \qquad T_L = 0.128\,sec$$

Appendix B

Rise Time for Loading of Pier Leg System:

-Rise time approximately determined from an effective SDOF system under free vibration

SDOF Oscillator: free vibration response:

m

k_{eff},
T_{eff}

$$u(t) = u_{max} \cdot \sin(\omega_n \cdot t)$$
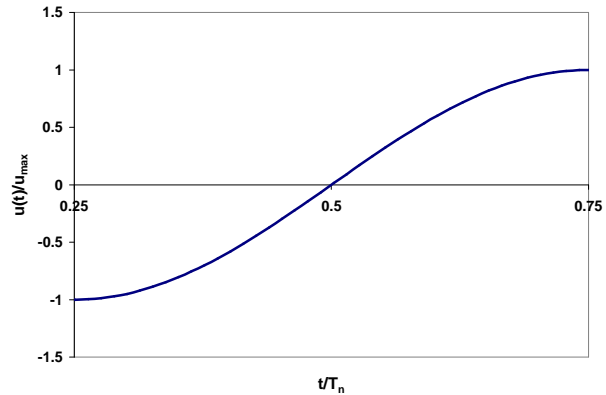
$$P_y := \left(\frac{W}{2} + A_{ub} \cdot F_{yub} \right) \cdot \frac{d}{h}$$

$$k_{sec} := \frac{P_y}{\Delta_{max2}} \quad T_{sec} := 2 \cdot \pi \cdot \sqrt{\frac{m}{k_{sec}}} \quad T_{sec} = 1.714\,s$$

$$t_{rL2} := asin\left(\frac{4 \cdot \pi^2 \cdot \Delta_{up2}}{S_1 \cdot T_{eff2} \cdot sec} \right) \cdot \frac{T_{sec}}{2 \cdot \pi}$$

$t_{rL2} = 0.017\,s$ (rise time for loading applied to pier leg)

Dynamic Properties for Vertical Shearing Vibration of Pier:

Stiffness and Period of Vibration of Vertical Truss Pier System:

$$k_v := f_p \cdot \frac{E \cdot A_d}{d} \cdot panels \quad\quad k_v = 548.8 \frac{kN}{mm}$$

$$T_v := 2 \cdot \pi \cdot \sqrt{\frac{\frac{m}{2}}{k_v}} \quad\quad T_v = 0.080\,sec$$

Rise Times for Loading of Pier Leg System:

$$t_{rv12} := asin\left(\frac{4 \cdot \pi^2 \Delta_{up2}}{S_1 \cdot T_{eff2} \cdot sec}\right) \cdot \frac{T_{sec}}{2 \cdot \pi}$$

$t_{rv12} = 0.017\,sec$ $\qquad \frac{t_{rv12}}{T_v} = 0.213$

$$t_{rv22} := asin\left(\frac{4 \cdot \pi^2 \cdot \Delta_{y2}}{S_1 \cdot T_{eff2} \cdot sec}\right) \cdot \frac{T_{sec}}{2 \cdot \pi} - t_{rv12}$$

$t_{rv22} = 0.100\,sec$ $\qquad \frac{t_{rv22}}{T_v} = 1.25$

Effective Rise Time for Both Loads during Uplift:

$$t_{rv2} := asin\left(\frac{4 \cdot \pi^2 \cdot \frac{1}{2} \Delta_{y2}}{S_1 \cdot T_{eff2} \cdot sec}\right) \cdot \frac{T_{sec}}{2 \cdot \pi}$$

$t_{rv2} = 0.057\,sec$ $\qquad \frac{t_{rv2}}{T_v} = 0.715$

Response Calculations for Each System Utilizing Convolution Integral Presented in Section 3.3.1.2

$i := 1 .. 250$

$t_i := \dfrac{i}{1000} sec$ (time increments)

Axial Vibrations of Pier Legs

$$p_{oL2} := \left(1 - \eta_L\right)\frac{W}{2} \qquad \text{(magnitude of step force with finite rise time, } t_{rL}, \text{ applied to pier leg)}$$

$$p_{L2_i} := \left\| \begin{matrix} \left[p_{oL2} \cdot \left(\dfrac{t_i}{t_{rL2}} \right) \right] & \text{if } t_i < t_{rL2} \\[2ex] p_{oL2} & \text{if } t_i \geq t_{rL2} \end{matrix} \right. \qquad \text{(applied force over time)}$$

$$u_{stL2_i} := \frac{p_{L2_i}}{k_L} \qquad \text{(static displacement response)}$$

$$u_{L2_i} := \left\| \begin{matrix} u_{stL2_i} \cdot \left(\dfrac{t_i}{t_{rL2}} - \dfrac{\sin\left(\dfrac{2\cdot\pi}{T_L}\cdot t_i\right)}{\dfrac{2\cdot\pi}{T_L}\cdot t_{rL2}} \right) & \text{if } t_i \leq t_{rL2} \\[4ex] u_{stL2_i} \cdot \left[1 - \dfrac{1}{\dfrac{2\cdot\pi}{T_L}\cdot t_{rL2}} \cdot \left[\sin\left(\dfrac{2\cdot\pi}{T_L}\cdot t_i\right) - \sin\left[\dfrac{2\cdot\pi}{T_L}\cdot\left(t_i - t_{rL2}\right)\right] \right] \right] & \text{if } t_i > t_{rL2} \end{matrix} \right.$$
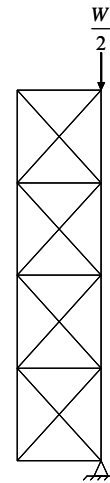
(response of system using convolution integral)
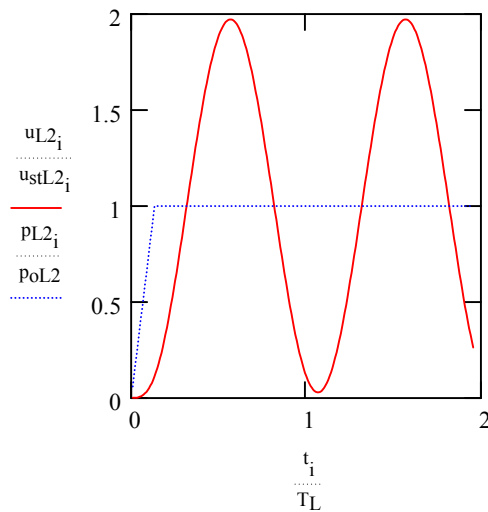
$$R_{dL2_i} := \frac{u_{L2_i}}{u_{stL2_i}}$$

$$R_{dL2} := \max\left(R_{dL2}\right)$$

137

Vibrations of Vertical Truss System

p12: force from transfer of gravity to compression leg based on 2nd cycle properties

$$p_{o12} := \left(1 - \eta_L\right)\frac{W}{2}$$

$$p_{o12} = 430 \, kN$$

p22: force to yield unbonded braces based on 2nd cycle properties

$$p_{o22} := 2 \cdot A_{ub} \cdot F_{yub}$$

$$p_{o22} = 869 \, kN$$
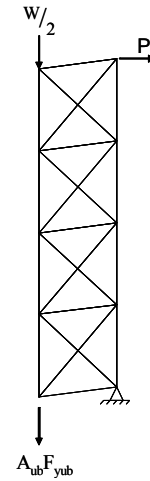
$$p12_i := \left| \begin{array}{l} \left[p_{o12} \cdot \left(\dfrac{t_i}{t_{rv12}} \right) \right] \quad \text{if} \ \ t_i < t_{rv12} \\[2ex] p_{o12} \quad \text{if} \ \ t_i \geq t_{rv12} \end{array} \right.$$

$$p22_i := \left| \begin{array}{l} 0 \quad \text{if} \ \ t_i \leq t_{rv12} \\[2ex] \left[p_{o22} \cdot \left(\dfrac{t_i - t_{rv12}}{t_{rv22}} \right) \right] \quad \text{if} \ \ t_{rv12} < t_i \leq t_{rv22} + t_{rv12} \\[2ex] p_{o22} \quad \text{if} \ \ t_i > t_{rv22} + t_{rv12} \end{array} \right.$$
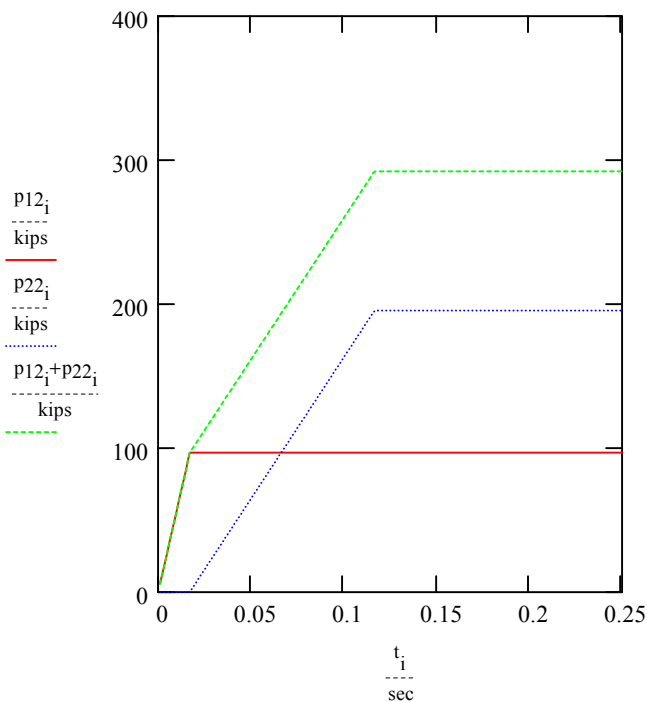
(application of vertical shearing forces over time)

$$u_{stv12_i} := \frac{p_{12_i}}{k_v}$$

$$u_{v12_i} := \left\| \begin{array}{l} u_{stv12_i} \cdot \left(\dfrac{t_i}{t_{rv12}} - \dfrac{\sin\left(\dfrac{2\cdot\pi}{T_v}\cdot t_i\right)}{\dfrac{2\cdot\pi}{T_v}\cdot t_{rv12}} \right) \quad \text{if } t_i \le t_{rv12} \\[3em] u_{stv12_i} \cdot \left[1 - \dfrac{1}{\dfrac{2\cdot\pi}{T_v}\cdot t_{rv12}} \cdot \left[\sin\left(\dfrac{2\cdot\pi}{T_v}\cdot t_i\right) - \sin\left[\dfrac{2\cdot\pi}{T_v}\cdot\left(t_i - t_{rv12}\right)\right] \right] \right] \quad \text{if } t_i > t_{rv12} \end{array} \right.$$

$$u_{stv22_i} := \frac{p_{22_i}}{k_v}$$

$$u_{v22_i} := \left\| \begin{array}{l} 0 \quad \text{if } t_i \le t_{rv12} \\[1em] u_{stv22_i} \cdot \left[\dfrac{t_i - t_{rv12}}{t_{rv22}} - \dfrac{\sin\left[\dfrac{2\cdot\pi}{T_v}\cdot\left(t_i - t_{rv12}\right)\right]}{\dfrac{2\cdot\pi}{T_v}\cdot t_{rv22}} \right] \quad \text{if } t_{rv12} < t_i \le \left(t_{rv22} + t_{rv12}\right) \\[3em] u_{stv22_i} \cdot \left[1 - \dfrac{1}{\dfrac{2\cdot\pi}{T_v}\cdot t_{rv22}} \cdot \left[\sin\left[\dfrac{2\cdot\pi}{T_v}\cdot\left(t_i - t_{rv12}\right)\right] - \sin\left[\dfrac{2\cdot\pi}{T_v}\cdot\left[\left(t_i - t_{rv12}\right) - t_{rv22}\right]\right] \right] \right] \quad \text{if } t_i > \left(t_{rv22} + t_{rv12}\right) \end{array} \right.$$

Normalized Response of Vertical Shearing Mode to each load and total response over time:
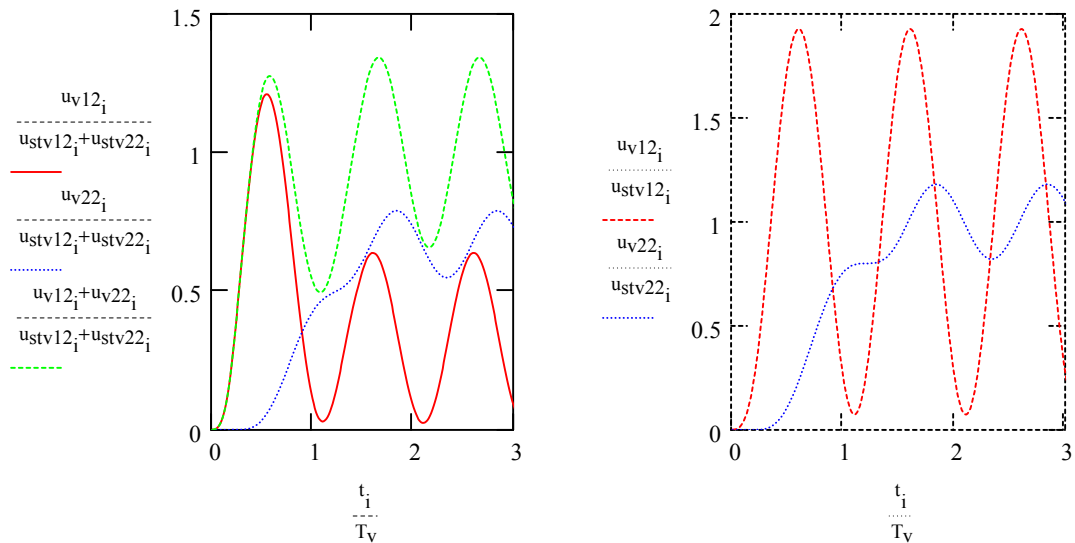
Normalized Total Dynamic and Static Response of Vertical Shearing Mode over time:
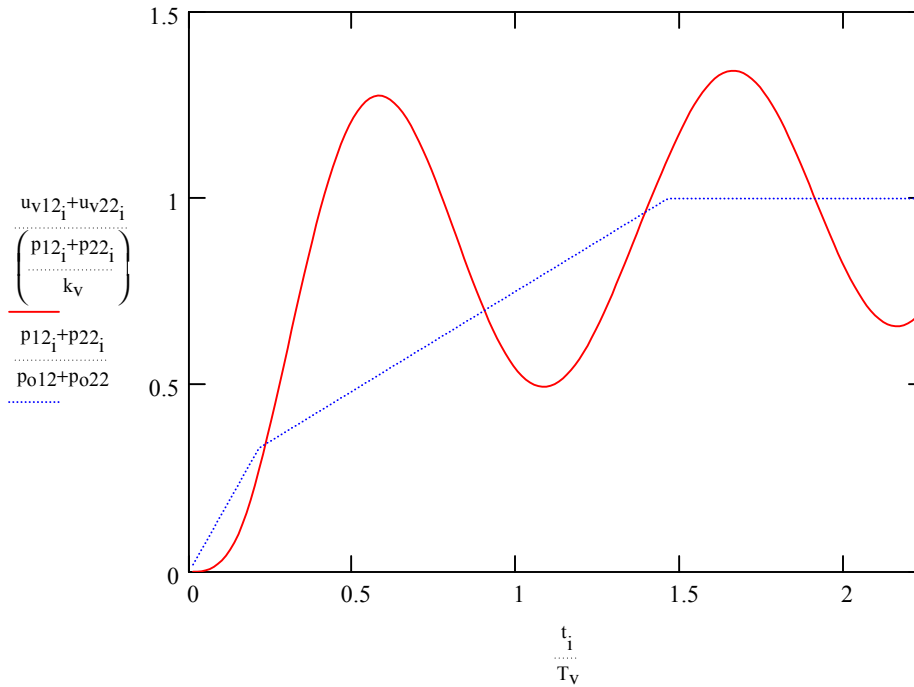
$$R_{dv2_i} := \frac{u_{v12_i} + u_{v22_i}}{u_{stv12_i} + u_{stv22_i}} \qquad\qquad R_{dv12} := \max\left(R_{dv2}\right)$$

Dynamic Amplification Factors, R_d, for Leg and Pier:

R_d: dynamic amplification factor for impulsive loads

$R_{dL2} = 1.97$ (DAF for compressed tower leg)

$R_{dv12} = 1.34$ (DAF for loads carried through vertical truss system considering phase effects)

$$R_{dv2} := 1 + \frac{\sin\left(\dfrac{\pi \cdot t_{rv2}}{T_v}\right)}{\left(\dfrac{\pi \cdot t_{rv2}}{T_v}\right)} \qquad R_{dv2} = 1.35 \quad \text{(DAF for 2 dynamic loads during uplift using effective rise time)}$$

APPENDIX C

METHODS OF ANALYSIS- EXAMPLES

C.1   General

Examples in this appendix illustrate how the methods of analysis described in Section 3.4.1 are used. The only criteria controlling the selection of unbonded brace dimensions, for the initial parametric study, was to limit the maximum strain in the unbonded brace to 1.5%. The 2nd cycle properties are used in all methods for these examples, as the displacement response is assumed to be greater during the 2nd cycle as described in Section 3.2.2.

C.2   Method 1: Coefficient Method of FEMA 356 with $k_{eff}=k_r$

This method attempts to characterize the controlled rocking system as an effective SDOF, bi-linear hysteretic system and determine its displacement response using a 2% damped response spectrum. The effective stiffness in Method 1 is characterized by the rocking stiffness defined by (3-5). Equation 3-15 of FEMA 356 (FEMA, 2000) is used to determine the ultimate horizontal deck-level displacement. Equation 3-15 of FEMA 356 is defined as: where factor C_0 is used to relate displacements in an MDOF system to the displacement of

$$\Delta_t = C_0 \, C_1 \, C_2 \, C_3 \, S_a \, \frac{T_e^{\,2}}{4\,\pi^2}\, g \qquad\qquad \text{(C-1)}$$

an equivalent SDOF system calculated by (C-1). Factor C_2 is to account for stiffness and/or strength degradation and factor C_3 is to account for dynamic P-Δ effects. Factor C_1 is used to account for the expected increase in displacement in the short period (or equal energy) range of the spectrum. C_1 is defined in the long period range ($T_e \geq T_s$) as:

$$C_1 = 1.0$$

and in the short period range, is defined as:

$$C_1 = \frac{\left[1.0 + (R-1)\dfrac{T_s}{T_e}\right]}{R}$$

T_s is the characteristic period, separating the long and short period ranges of the spectrum and is defined as:

$$T_s = \frac{S_s}{S_1}$$

where the short period spectral acceleration, S_s, and 1-second spectral acceleration, S_1, have been discussed previously. All factors, except for C_1, are set equal to 1 since the controlled rocking system is assumed to be an SDOF system without stiffness nor strength degradation and has positive post-yield stiffness. Factor C_1 is used as described above where appropriate, however this factor was not necessarily established for such a hysteretic system.

C.3 Method 2: Coefficient Method of FEMA 356 with k_{eff} defined by Equation 3-44

Method 2 is identical to Method 1 with the exception that the effective stiffness is defined by Equation 3-44 defined in Section 3.4.1.

C.4 Method 3: FEMA 274 Method for Displacement-Dependent Passive Energy Dissipation Devices

The method is based on the simple method of analysis for passive energy dissipation systems proposed in FEMA 274 (FEMA, 1997). The method uses the system's energy dissipation capabilities to reduce the demand for an equivalent amount of viscous damping. Piers are treated as SDOF systems with the pushover curves developed using the nonlinear behavior at the anchorage location. The intersection of the spectral capacity and demand curves marks the expected displacement demand.

Method 1: Conservative Estimate of Displacement Demand $k_{eff}=k_r$

$\dfrac{h}{d} = 3$ (pier aspect ratio)

$W := 1730\,\text{kN}$ (tributary bridge deck weight to pier)

$m := \dfrac{W}{g}$ $m = 1.764 \times 10^5\,\text{kg}$

$k_o := 22.2\,\dfrac{\text{kN}}{\text{mm}}$ (horizontal stiffness of pier)

$E := 200\,\text{GPa}$ (modulus of elasticity for steel in unbonded brace)

$\alpha := 0.01$ (post-elastic stiffness ratio of unbonded brace)

Following 3 parameters iterated upon to obtain desired response:

$L_{ub} := 4000\,\text{mm}$ $L_{ub} = 157\,\text{in}$ (effective length of unbonded brace)

$A_{ub} := 2650\,\text{mm}^2$ $A_{ub} = 4.1\,\text{in}^2$ (cross-sectional area of unbonded brace core)

$F_{yub} := 235\,\text{MPa}$ $F_{yub} = 34\,\text{ksi}$ (yield strength of steel within unbonded brace)

$\varepsilon_{ub} := 0.015$ (target maximum strain in unbonded brace)

$\eta_L := \dfrac{A_{ub} \cdot F_{yub}}{\dfrac{W}{2}}$ $\eta_L = 0.72$ (local strength ratio defined in Section 3.3)

$k_r := \dfrac{1}{\dfrac{1}{k_o} + \dfrac{1}{\left(\dfrac{A_{ub} \cdot E}{L_{ub}}\right) \cdot \left(\dfrac{d}{h}\right)^2}}$ (stiffness of rocking system)

$k_{eff} := k_r$

$T_{eff} := 2 \cdot \pi \cdot \sqrt{\dfrac{m}{k_{eff}}}$

$T_{eff} = 0.89 \, sec$

Yield Point of System (2nd cycle properties):

$P_{y2} := \dfrac{W}{2} \cdot \dfrac{d}{h} + A_{ub} \cdot F_{yub} \cdot \dfrac{d}{h}$ $P_{y2} = 495.9 \, kN$

$\Delta_{y2} := \dfrac{(1 - \eta_L) \cdot \dfrac{W}{2} \cdot \dfrac{d}{h}}{k_o} + \dfrac{2 \cdot A_{ub} \cdot F_{yub} \cdot \dfrac{d}{h}}{k_r}$ $\Delta_{y2} = 50.54 \, mm$

FEMA 356 Seismic Hazard (Section 1.6):

-2% damped spectrum with 2% PE in 50yr

From USGS web site:

$S_1 := .75$ $S_S := 1.8$ (2% in 50yr., MCE EQ Spectral Ordinates)

From FEMA 356 Table 1-4 and 1-5 For Site Class B:

$F_a := 1.0$ $F_v := 1.0$

$S_{XS} := F_a \cdot S_S$ $S_{X1} := F_v \cdot S_1$
$S_{XS} = 1.8$ $S_{X1} = 0.75$

$\beta_{eff} := 0.02$ (inherent structural damping)

$B_s := 0.8$ Damping Modification Factors
  (FEMA 356 Table 1-6)
$B_1 := 0.8$

$T_s := \dfrac{S_{X1}}{S_{XS}} \cdot sec$ $T_s = 0.42 \, s$

$T_0 := 0.2 \cdot T_s$ $T_0 = 0.08 \, s$

$T := 0.01\sec, 0.02\sec .. 3\sec$ (period Incremented By .01 sec)

$$S_{ad}(T) := \left| \begin{array}{l} S_{XS} \cdot \left[\left(\dfrac{5}{B_s} - 2 \right) \dfrac{T}{T_s} + 0.4 \right] \text{ if } T \le T_0 \quad \text{(general response spectrum of FEMA 356)} \\[4mm] \dfrac{S_{XS}}{B_s} \text{ if } T_0 \le T \le T_s \\[4mm] \dfrac{S_{X1}}{B_1 \cdot T} \cdot \sec \text{ if } T_s \le T \end{array} \right.$$

2% Damped Response Spectrum

$$\Delta_u = C_0 \cdot C_1 \cdot C_2 \cdot C_3 \cdot S_a \cdot \dfrac{T_{eff}^2}{4 \cdot \pi^2} \cdot g \quad \text{(Eq. 3-15, FEMA 356)}$$

C_0: modification factor to relate SDOF displacements to roof displacement of MDOF system

C_1: modification factor to relate expected inelastic displacements to those calculated for elastic response

C_2: modification factor to represent effect of pinched hysteresis

C_3: modification factor to represent increased displacement due to P-Δ effects

$C_0 = C_2 = C_3 = 1.0$

$C_m := 1.0$ (effective mass factor, entire mass assumed to participate in horizontal mode)

$$R := \frac{S_{ad}(T_{eff})}{\dfrac{P_{y2}}{W}} \cdot C_m \qquad R = 3.7$$

$$C_1 := \begin{cases} 1.0 & \text{if } T_{eff} \geq T_s \\[2ex] \dfrac{\left[1.0 + (R-1)\dfrac{T_s}{T_{eff}} \right]}{R} & \text{if } T_{eff} < T_s \end{cases}$$

$$\Delta_u := C_0 \cdot C_1 \cdot C_2 \cdot C_3 \cdot S_{ad}(T_{eff}) \cdot \frac{T_{eff}^2}{4 \cdot \pi^2} \cdot g$$

$\Delta_u = 206.6 \, mm$

$$\Delta_{ubf} := \left(\Delta_u - \frac{P_{y2}}{k_o} \right) \cdot \frac{d}{h}$$

$$\varepsilon_{ubf} := \frac{\Delta_{ubf}}{L_{ub}}$$

$\varepsilon_{ubf} = 0.015$

Method 2: Non-linear Static Procedure

$$g := 9.81 \frac{m}{sec^2}$$

-similar to FEMA 356 Section 3.3.3

Capacity (pushover) Curve:

$$\frac{h}{d} = 3 \qquad \text{(pier aspect ratio)}$$

$$W := 1730 kN \qquad \text{(tributary bridge deck weight to pier)}$$

$$m := \frac{W}{g} \qquad m = 1.764 \times 10^5 \, kg$$

$$k_o := 22.2 \frac{kN}{mm} \qquad \text{(horizontal stiffness of pier)}$$

$$E := 200 GPa \qquad \text{(modulus of elasticity for steel in unbonded brace)}$$

$$\alpha := 0.01 \qquad \text{(post-elastic stiffness ratio of unbonded brace)}$$

Following 3 parameters iterated upon to obtain desired response:

$$L_{ub} := 4000 mm \qquad L_{ub} = 157 \, in \qquad \text{(effective length of unbonded brace)}$$

$$A_{ub} := 2300 mm^2 \qquad A_{ub} = 3.6 \, in^2 \qquad \text{(cross-sectional area of unbonded brace core)}$$

$$F_{yub} := 235 MPa \qquad F_{yub} = 34 \, ksi \qquad \text{(yield strength of steel within unbonded brace)}$$

$$\varepsilon_{ub} := 0.015 \qquad \text{(target maximum strain in unbonded brace)}$$

$$\eta_L := \frac{A_{ub} \cdot F_{yub}}{\frac{W}{2}} \qquad \eta_L = 0.62 \qquad \text{(local strength ratio defined in Section 3.3)}$$

Uplift of Pier Leg, Start of Rocking:

$$P_{up2} := (1 - \eta_L) \cdot \frac{W}{2} \cdot \frac{d}{h} \qquad\qquad P_{up1} := \frac{W}{2} \cdot \frac{d}{h}$$

$$\Delta_{up2} := \frac{P_{up2}}{k_o} \qquad \Delta_{up2} = 4.87 \, mm$$

$$k_r := \cfrac{1}{\cfrac{1}{k_o} + \cfrac{1}{\left(\cfrac{A_{ub} \cdot E}{L_{ub}}\right)\left(\cfrac{d}{h}\right)^2}}$$ (stiffness of rocking system)

Yield Point of System (2nd cycle properties):

$$P_{y2} := \frac{W}{2} \cdot \frac{d}{h} + A_{ub} \cdot F_{yub} \cdot \frac{d}{h}$$ $P_{y2} = 468.5\,\text{kN}$

$$\Delta_{y2} := \frac{(1 - \eta_L) \cdot \dfrac{W}{2} \cdot \dfrac{d}{h}}{k_o} + \frac{2 \cdot A_{ub} \cdot F_{yub} \cdot \dfrac{d}{h}}{k_r}$$ $\Delta_{y2} = 49.3\,\text{mm}$

$$k_{eff} := k_o \cdot \left(\frac{\Delta_{up2}}{\Delta_{y2}}\right) + k_r \cdot \left(\frac{\Delta_{y2} - \Delta_{up2}}{\Delta_{y2}}\right)$$

$$k_{eff} = 9.50\,\frac{\text{kN}}{\text{mm}}$$

$$T_{eff} := 2 \cdot \pi \cdot \sqrt{\frac{m}{k_{eff}}}$$

$$T_{eff} = 0.86\,\text{sec}$$

$$\Delta := 0.1\text{mm}, 0.2\text{mm} .. 300\text{mm}$$

$$P(\Delta) := \begin{cases} (k_o \cdot \Delta) & \text{if } \Delta \le \Delta_{up2} \\[2mm] P_{up2} + k_r \cdot (\Delta - \Delta_{up2}) & \text{if } \Delta_{up2} < \Delta \le \Delta_{y2} \\[2mm] P_{y2} + \left[\dfrac{1}{k_o} + \cfrac{1}{\alpha \cdot \left(\dfrac{A_{ub} \cdot E}{L_{ub}}\right)\left(\dfrac{d}{h}\right)^2}\right]^{-1} \cdot (\Delta - \Delta_{y2}) & \text{if } \Delta > \Delta_{y2} \end{cases}$$

$$P_1(\Delta) := k_{eff} \cdot \Delta$$

Pushover Curve

FEMA 356 Seismic Hazard (Section 1.6):

-2% damped spectrum with 2% PE in 50yr

From USGS web site:

$S_1 := .75$ $S_S := 1.8$ (2% in 50yr., MCE EQ Spectral Ordinates)

From FEMA 356 Table 1-4 and 1-5 For Site Class B:

$F_a := 1.0$ $F_v := 1.0$

$S_{XS} := F_a \cdot S_S$ $S_{X1} := F_v \cdot S_1$

$S_{XS} = 1.8$ $S_{X1} = 0.75$

$\beta_{eff} := 0.02$ (inherent structural damping)

$B_s := 0.8$ Damping Modification Factors
(FEMA 356 Table 1-6)
$B_1 := 0.8$

$T_s := \dfrac{S_{X1}}{S_{XS}} \cdot sec$ $T_s = 0.42\ s$

$T_0 := 0.2 \cdot T_s$ $T_0 = 0.08\ s$

$T := 0.01\,\text{sec}, 0.02\,\text{sec}\,..\,3\,\text{sec}$ (period Incremented By .01 sec)

$$S_{ad}(T) := \begin{vmatrix} S_{XS}\cdot\left[\left(\dfrac{5}{B_s} - 2\right)\dfrac{T}{T_s} + 0.4\right] & \text{if } T \le T_0 \quad \text{(general response spectrum of FEMA 356)} \\[2em] \dfrac{S_{XS}}{B_s} & \text{if } T_0 \le T \le T_s \\[2em] \dfrac{S_{X1}}{B_1\cdot T}\cdot\text{sec} & \text{if } T_s \le T \end{vmatrix}$$

2% Damped Response Spectrum

$$\Delta_u = C_0 \cdot C_1 \cdot C_2 \cdot C_3 \cdot S_a \cdot \frac{T_{eff}^2}{4\cdot\pi^2}\cdot g \quad \text{(Eq. 3-15, FEMA 356)}$$

C_0: modification factor to relate SDOF displacements to roof displacement of MDOF system

C_1: modification factor to relate expected inelastic displacements to those calculated
    for elastic response

C_2: modification factor to represent effect of pinched hysteresis

C_3: modification factor to represent increased displacement due to P-Δ effects

$C_0 = C_2 = C_3 = 1.0$

$C_m := 1.0$ (effective mass factor, entire mass assumed to participate in horizontal mode)

$R := \dfrac{S_{ad}(T_{eff})}{\dfrac{P_{y2}}{W}} \cdot C_m$ $\qquad R = 4.0$

$C_1 := \begin{cases} 1.0 & \text{if } T_{eff} \geq T_s \\[2em] \dfrac{\left[1.0 + (R-1)\dfrac{T_s}{T_{eff}}\right]}{R} & \text{if } T_{eff} < T_s \end{cases}$

$\Delta_u := C_0 \cdot C_1 \cdot C_2 \cdot C_3 \cdot S_{ad}(T_{eff}) \cdot \dfrac{T_{eff}^2}{4 \cdot \pi^2} \cdot g$

$\Delta_u = 199.4 \, mm$

$\Delta_{ubf} := \left(\Delta_u - \dfrac{P_{y2}}{k_o}\right) \cdot \dfrac{d}{h}$

$\varepsilon_{ubf} := \dfrac{\Delta_{ubf}}{L_{ub}}$

$\varepsilon_{ubf} = 0.015$

Method 3: Design of Braces As Energy Dissipation Devices

*Nonlinear Static Procedure of FEMA 274 (Method 2)

Capacity (pushover) Curve:

$$g := 9.81 \frac{m}{\sec^2}$$

$$\frac{h}{d} = 3 \qquad \text{(pier aspect ratio)}$$

$$W := 1730 \text{kN} \qquad \text{(tributary bridge deck weight to pier)}$$

$$k_o := 22.2 \frac{\text{kN}}{\text{mm}} \qquad \text{(horizontal stiffness of pier)}$$

$$E := 200 \text{GPa} \qquad \text{(modulus of elasticity for steel in unbonded brace)}$$

$$\alpha := 0.01 \qquad \text{(post-elastic stiffness ratio of unbonded brace)}$$

Following 3 parameters iterated upon to obtain desired response:

$$L_{ub} := 4000 \text{mm} \qquad L_{ub} = 157 \text{in} \qquad \text{(effective length of unbonded brace)} \qquad \longleftarrow$$

$$A_{ub} := 2500 \text{mm}^2 \qquad A_{ub} = 3.9 \text{in}^2 \qquad \text{(cross-sectional area of unbonded brace core)} \qquad \longleftarrow$$

$$F_{yub} := 235 \text{MPa} \qquad F_{yub} = 34 \text{ksi} \qquad \text{(yield strength of steel within unbonded brace)} \qquad \longleftarrow$$

$$\varepsilon_{ub} := 0.015 \qquad \text{(target maximum strain in unbonded brace)} \qquad \longleftarrow$$

$$\eta_L := \frac{A_{ub} \cdot F_{yub}}{\dfrac{W}{2}} \qquad \eta_L = 0.68 \qquad \text{(local strength ratio defined in Section 3.3)}$$

Uplift of Pier Leg, Start of Rocking:

$$P_{up2} := (1 - \eta_L) \cdot \frac{W}{2} \cdot \frac{d}{h} \qquad\qquad P_{up1} := \frac{W}{2} \cdot \frac{d}{h}$$

$$\Delta_{up2} := \frac{P_{up2}}{k_o} \qquad \Delta_{up2} = 4.17 \text{mm}$$

$$k_r := \cfrac{1}{\cfrac{1}{k_o} + \cfrac{1}{\left(\cfrac{A_{ub} \cdot E}{L_{ub}}\right) \cdot \left(\cfrac{d}{h}\right)^2}}$$
(stiffness of rocking system)

Yield Point of System (2nd cycle properties):

$$P_{y2} := \frac{W}{2} \cdot \frac{d}{h} + A_{ub} \cdot F_{yub} \cdot \frac{d}{h} \qquad P_{y2} = 484.2\,kN$$

$$\Delta_{y2} := \frac{(1 - \eta_L) \cdot \dfrac{W}{2} \cdot \dfrac{d}{h}}{k_o} + \frac{2 \cdot A_{ub} \cdot F_{yub} \cdot \dfrac{d}{h}}{k_r} \qquad \Delta_{y2} = 50.01\,mm$$

System at Target Maximum Displacement:

$$\Delta_u := \varepsilon_{ub} \cdot L_{ub} \cdot \frac{h}{d} + \frac{P_{y2}}{k_o} \qquad \Delta_u = 202\,mm$$

$$\Delta := 0.1\,mm, 0.2\,mm .. 300\,mm$$

$$P(\Delta) := \begin{vmatrix} (k_o \cdot \Delta) & \text{if } \Delta \leq \Delta_{up2} \\[2mm] P_{up2} + k_r \cdot (\Delta - \Delta_{up2}) & \text{if } \Delta_{up2} < \Delta \leq \Delta_{y2} \\[2mm] P_{y2} + \left[\dfrac{1}{k_o} + \cfrac{1}{\alpha \cdot \left(\dfrac{A_{ub} \cdot E}{L_{ub}}\right) \cdot \left(\dfrac{d}{h}\right)^2} \right]^{-1} \cdot (\Delta - \Delta_{y2}) & \text{if } \Delta > \Delta_{y2} \end{vmatrix}$$

Pushover Curve

153
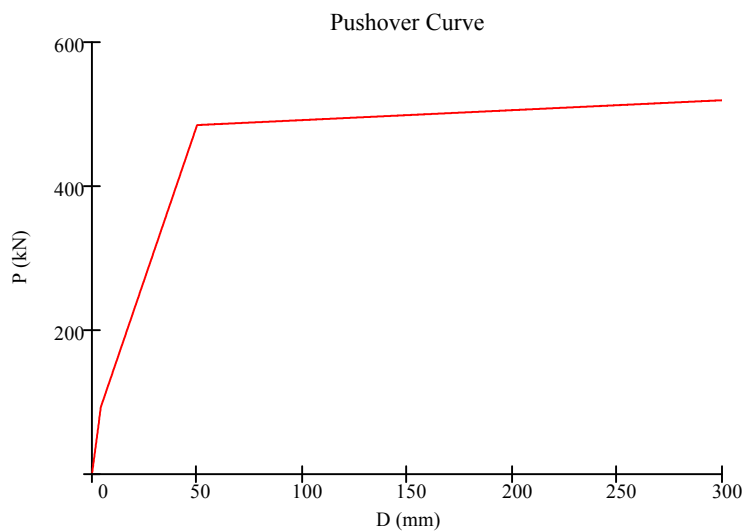
Spectral Capacity Curve:

$$S_{ac}(\Delta) := \frac{P(\Delta)}{W} \cdot \frac{g}{g} \qquad \phi := 1$$

(conversion to spectral ordinates, piers idealized as SDOF system for horizontal response)

$$\Gamma := 1$$

$$S_{dc}(\Delta) := \frac{\Delta}{\phi \cdot \Gamma}$$

Spectral Capacity Curve
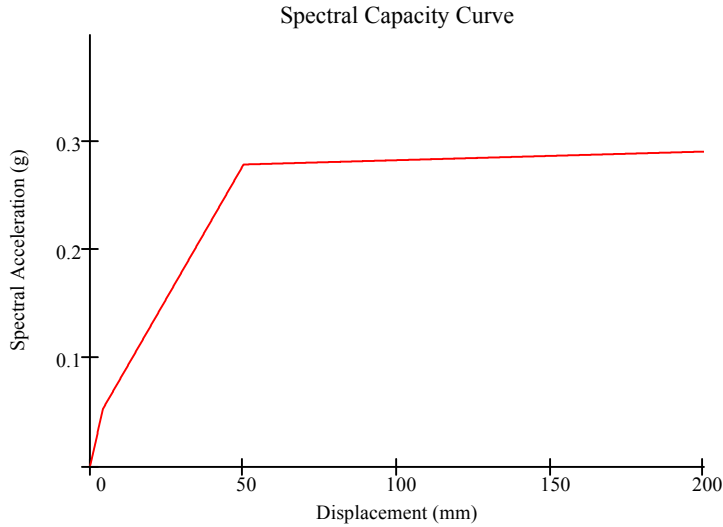
Spectral Demand Curve:

$$W_k := \frac{1}{2} \cdot P_{y2} \cdot \Delta_u \qquad \text{(stored strain energy at displacement, } \Delta_u\text{)}$$

$$W_D := 4 \cdot P_{y2} \cdot (\Delta_u - \Delta_{y2}) \qquad \text{(energy dissipation of bi-linear system at displacement, } \Delta_u\text{)}$$

$$\beta_o := 0.02 \qquad \text{(assumed inherent structural damping)}$$

$$\beta_b := \frac{W_D}{4 \cdot \pi \cdot W_k} \qquad \beta_b = 0.479$$

$$q := \frac{P_{y2} - P_{up1}}{P_{y2}} \qquad q = 0.404 \qquad \text{(factor accounting for flag-shaped hysteresis deviation from bi-linear response)}$$

$$\beta_{eff} := q \cdot \beta_b + \beta_o$$

$$\beta_{eff} = 0.21 \qquad \text{(equivalent viscous damping for inelastic system)}$$

From USGS web site:

$S_1 := .75$ $\qquad$ $S_S := 1.8$ $\qquad$ (2% in 50yr., MCE EQ Spectral Ordinates)

From FEMA 273 Table 2-13 and 2-14 For Site Class B:

$F_a := 1.0$ $\qquad\qquad$ $F_v := 1.0$

$S_{XS} := F_a \cdot S_S$ $\qquad\qquad$ $S_{X1} := F_v \cdot S_1$

$S_{XS} = 1.8$ $\qquad\qquad$ $S_{X1} = 0.75$

Damped Spectra Procedure In FEMA 273 (2.6.1.5):

$$B_s := \begin{vmatrix} 0.8 & \text{if } \beta_{eff} \leq 0.02 \\ x_1 & \text{if } 0.02 < \beta_{eff} \leq 0.05 \\ x_2 & \text{if } 0.05 < \beta_{eff} \leq 0.10 \\ x_3 & \text{if } 0.10 < \beta_{eff} \leq 0.20 \\ x_4 & \text{if } 0.20 < \beta_{eff} \leq 0.30 \\ x_5 & \text{if } 0.30 < \beta_{eff} \leq 0.40 \\ x_6 & \text{if } 0.40 < \beta_{eff} \leq 0.50 \\ 3.0 & \text{if } \beta_{eff} > 0.50 \end{vmatrix} \qquad B_1 := \begin{vmatrix} 0.8 & \text{if } \beta_{eff} \leq 0.02 \\ y_1 & \text{if } 0.02 < \beta_{eff} \leq 0.05 \\ y_2 & \text{if } 0.05 < \beta_{eff} \leq 0.10 \\ y_3 & \text{if } 0.10 < \beta_{eff} \leq 0.20 \\ y_4 & \text{if } 0.20 < \beta_{eff} \leq 0.30 \\ y_5 & \text{if } 0.30 < \beta_{eff} \leq 0.40 \\ y_6 & \text{if } 0.40 < \beta_{eff} \leq 0.50 \\ 2.0 & \text{if } \beta_{eff} > 0.50 \end{vmatrix}$$

$B_s = 1.868$ $\qquad$ Damping Modification Factors
$\qquad\qquad\qquad$ (FEMA 273 Table 2-15)
$B_1 = 1.527$

$$T_o := \frac{S_{X1} \cdot B_s}{S_{XS} \cdot B_1} \cdot \sec$$

$T_o = 0.51\,s$ $\qquad$ $0.2 \cdot T_o = 0.1\,s$

$T := 0.01\sec, 0.02\sec .. 3\sec$ $\qquad$ (period Incremented By .01 sec)

$$S_{ad}(T) := \begin{vmatrix} \left(\dfrac{S_{XS}}{B_s}\right)\left(0.4 + 3 \cdot \dfrac{T}{T_o}\right) & \text{if } T \leq 0.2 \cdot T_o \\[2ex] \dfrac{S_{XS}}{B_s} & \text{if } 0.2 \cdot T_o \leq T \leq T_o \\[2ex] \dfrac{S_{X1}}{B_1 \cdot T} \cdot \sec & \text{if } T_o \leq T \end{vmatrix} \qquad \text{(general response spectrum of FEMA 273)}$$

Demand Spectrum reduced for Eq. Damping
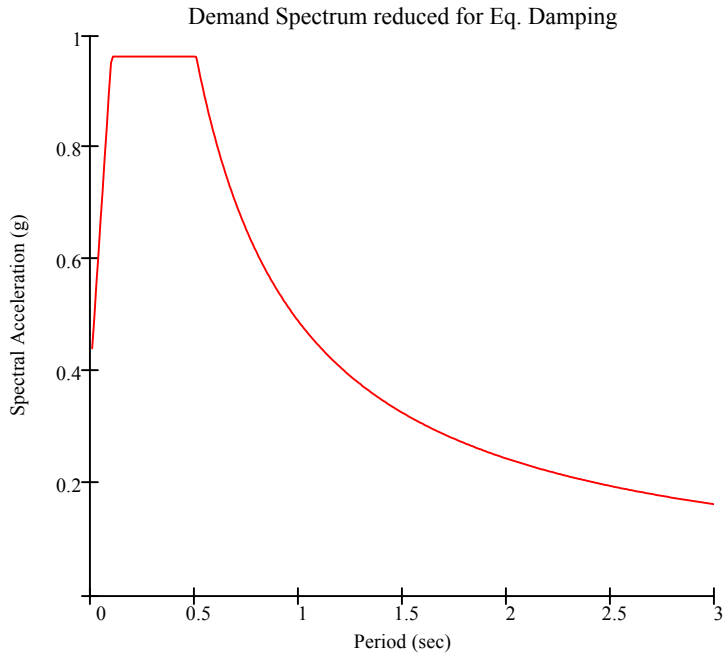
$$S_{dd}(T) := \left(\frac{T}{2 \cdot \pi}\right)^2 \cdot S_{ad}(T) \cdot g \qquad \text{(conversion to spectral displacement demand)}$$

Spectral Demand Curve

Spectral Capacity and Demand Curves

Base Shear/Weight and Spectral Acc.

Deformation and Spectral Displacement
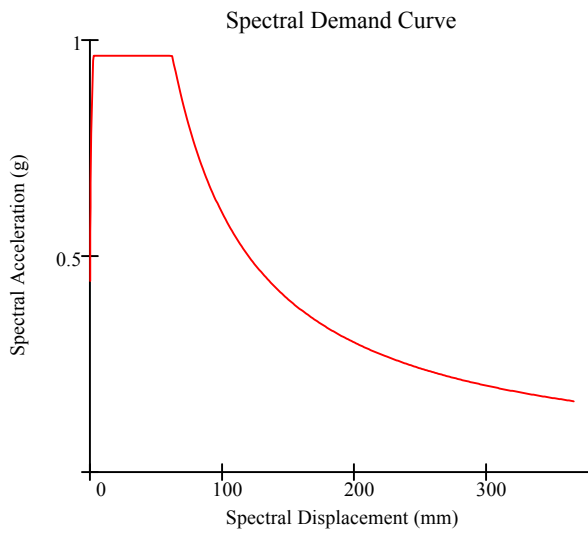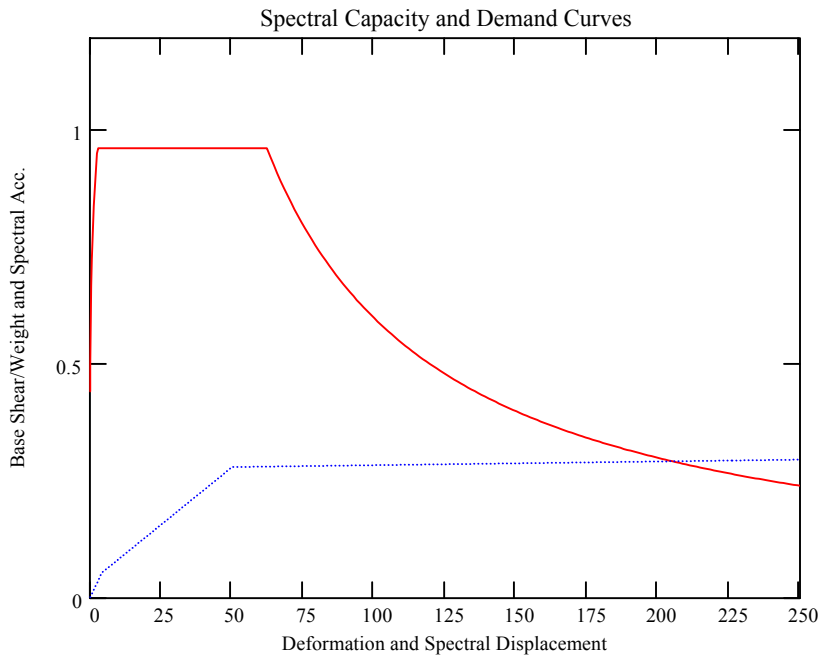
$\Delta_f := 206\text{mm}$ (displacement at intersection of spectral demand and capacity curves, iterative with initially guessed brace properties)

$$\Delta_{ubf} := \left(\Delta_f - \frac{P_{y2}}{k_o}\right)\cdot\frac{d}{h}$$

$$\varepsilon_{ubf} := \frac{\Delta_{ubf}}{L_{ub}}$$

$\varepsilon_{ubf} = 0.015$ ⟵   (final estimated strain in unbonded brace)

157

APPENDIX D
REPRESENTATIVE PIER PROPERTIES

Calculations of the "fixed-based" stiffness and period of vibration for the adopted pier properties used for the analysis procedures presented in Appendix C are shown in this appendix. The properties for four piers; having aspect ratios of 1, 2, 3 and 4, are presented.

Representative Pier Properties:

constants:

$$g := 9.81 \frac{m}{\sec^2}$$

$$E := 200\text{GPa}$$

General Pier

$P_v=1^*$ $\frac{m}{2}$ $\frac{m}{2}$

m: bridge mass tributary to pier

Tower Diagonal (A_d, L_d)

h

A_d: cross-sectional area of tower diagonals

L_d: length of tower diagonals

Tower Leg (A_L)

d

A_L: cross-sectional area of tower legs
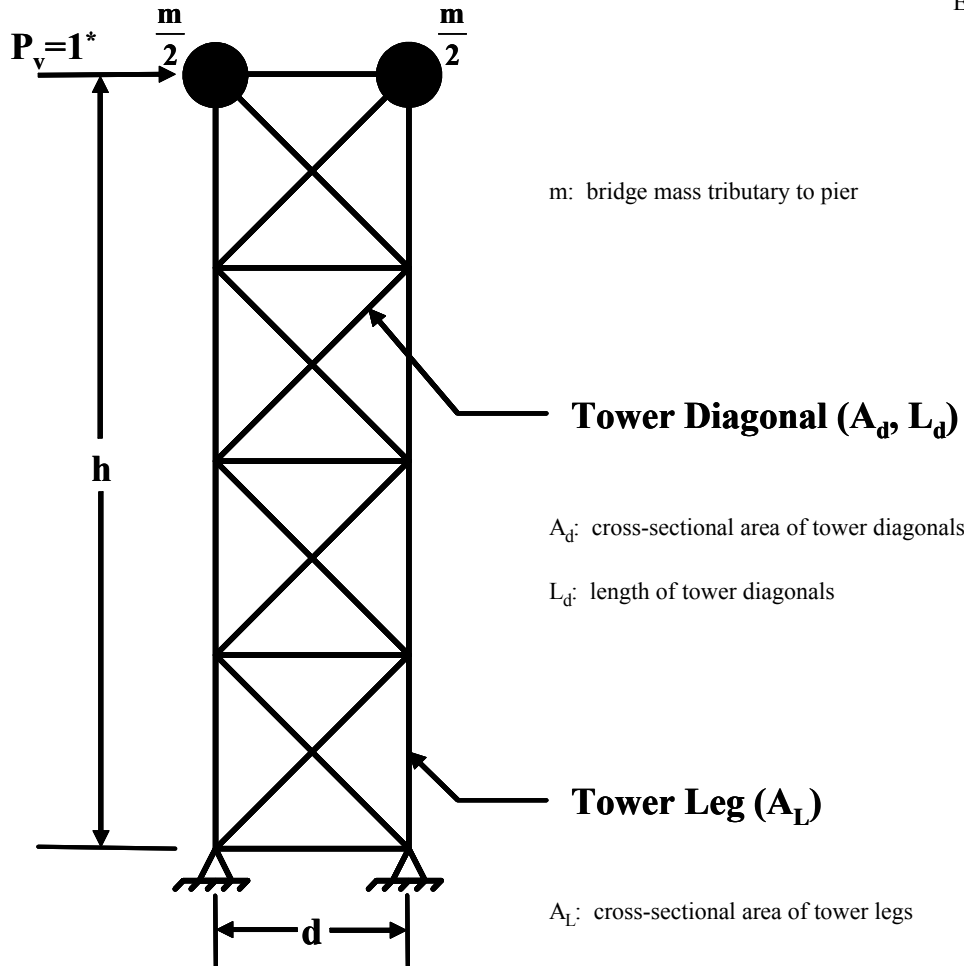
$$m := \frac{1730\text{kN}}{g}$$

$A_d := 7097\text{mm}^2$ (properties of piers assumed representative,
     as discussed in section 3.4.2)

$L_d := 10389\text{mm}$

$A_L := 31100\text{mm}^2$

-pier moment of inertia

$$I := \frac{1}{2} A_L \cdot d^2 \quad I = 0.832\,m^4$$

$\dfrac{h}{d} = 4$ $d := 7315 mm$

$h := 29260 mm$

-pier stiffness k_o:

$P_v := 1 kN$ (virtual unit load)

$n_b := 4$ (number of x-braced bays)

bending: shear:

$$\Delta_b := \frac{P_v \cdot h^3}{3 \cdot E \cdot I} \qquad\qquad \Delta_v := \frac{P_v \cdot L_d^{\,3}}{2 \cdot E \cdot d^2 \cdot A_d} \cdot n_b$$

$$k_b := \frac{P_v}{\Delta_b} \qquad\qquad k_v := \frac{P_v}{\Delta_v}$$

$$k_o := \left(\frac{1}{k_b} + \frac{1}{k_v} \right)^{-1}$$

$k_o = 12.5 \dfrac{kN}{mm}$

-natural period of vibration of fixed-base pier:

$$T_o := 2 \cdot \pi \cdot \sqrt{\frac{m}{k_o}}$$

$T_o = 0.74 \, sec$

$\dfrac{h}{d} = 3$ d := 7315mm

                          h := 21946mm

-pier stiffness k_o:

P_v := 1kN   (virtual unit load)

n_b := 3   (number of x-braced bays)

bending: shear:

$$\Delta_b := \frac{P_v \cdot h^3}{3 \cdot E \cdot I} \qquad\qquad \Delta_v := \frac{P_v \cdot L_d^{\,3}}{2 \cdot E \cdot d^2 \cdot A_d} \cdot n_b$$

$$k_b := \frac{P_v}{\Delta_b} \qquad\qquad\qquad k_v := \frac{P_v}{\Delta_v}$$

$$k_o := \left(\frac{1}{k_b} + \frac{1}{k_v} \right)^{-1}$$

$$k_o = 23.1 \, \frac{kN}{mm}$$

-natural period of vibration of fixed-base pier:

$$T_o := 2 \cdot \pi \cdot \sqrt{\frac{m}{k_o}}$$

$$T_o = 0.55 \, sec$$

$$\frac{h}{d} = 2$$

d := 7315mm

h := 14630mm

-pier stiffness k_o:

$P_v := 1kN$ (virtual unit load)

$n_b := 2$ (number of x-braced bays)

bending: shear:

$$\Delta_b := \frac{P_v \cdot h^3}{3 \cdot E \cdot I}$$ $$\Delta_v := \frac{P_v \cdot L_d^3}{2 \cdot E \cdot d^2 \cdot A_d} \cdot n_b$$

$$k_b := \frac{P_v}{\Delta_b}$$ $$k_v := \frac{P_v}{\Delta_v}$$

$$k_o := \left(\frac{1}{k_b} + \frac{1}{k_v}\right)^{-1}$$

$$k_o = 47.5 \frac{kN}{mm}$$

-natural period of vibration of fixed-base pier:

$$T_o := 2 \cdot \pi \cdot \sqrt{\frac{m}{k_o}}$$

$$T_o = 0.38 \sec$$

$$\frac{h}{d} = 1$$

$$d := 7315mm$$

$$h := 7315mm$$

-pier stiffness k_o:

$$P_v := 1kN \quad \text{(virtual unit load)}$$

$$n_b := 1 \quad \text{(number of x-braced bays)}$$

bending: shear:

$$\Delta_b := \frac{P_v \cdot h^3}{3 \cdot E \cdot I} \qquad\qquad \Delta_v := \frac{P_v \cdot L_d^3}{2 \cdot E \cdot d^2 \cdot A_d} \cdot n_b$$

$$k_b := \frac{P_v}{\Delta_b} \qquad\qquad k_v := \frac{P_v}{\Delta_v}$$

$$k_o := \left(\frac{1}{k_b} + \frac{1}{k_v} \right)^{-1}$$

$$k_o = 122.5 \frac{kN}{mm}$$

-natural period of vibration of fixed-base pier:

$$T_o := 2 \cdot \pi \cdot \sqrt{\frac{m}{k_o}}$$

$$T_o = 0.24 \, sec$$

Summary:

h/d	k_o (kN/mm)	T_o (sec.)
4	12.5	0.74
3	23.1	0.55
2	47.5	0.38
1	122.5	0.24

Appendix E
Response Spectrum of Synthetic Motions

Pseudo-acceleration response spectrum for the synthetic motions produced by the TARSCTHS code are presented in this appendix. The results are compared to the response spectrum defined by NCHRP 12-49 (ATC/MCEER 2003), which is the target spectral shape. The response spectrum for the seven motions are presented for demand levels of S_1 equal to 0.25g, 0.5g and 0.75g. The average of the seven motions are also presented for each demand level.
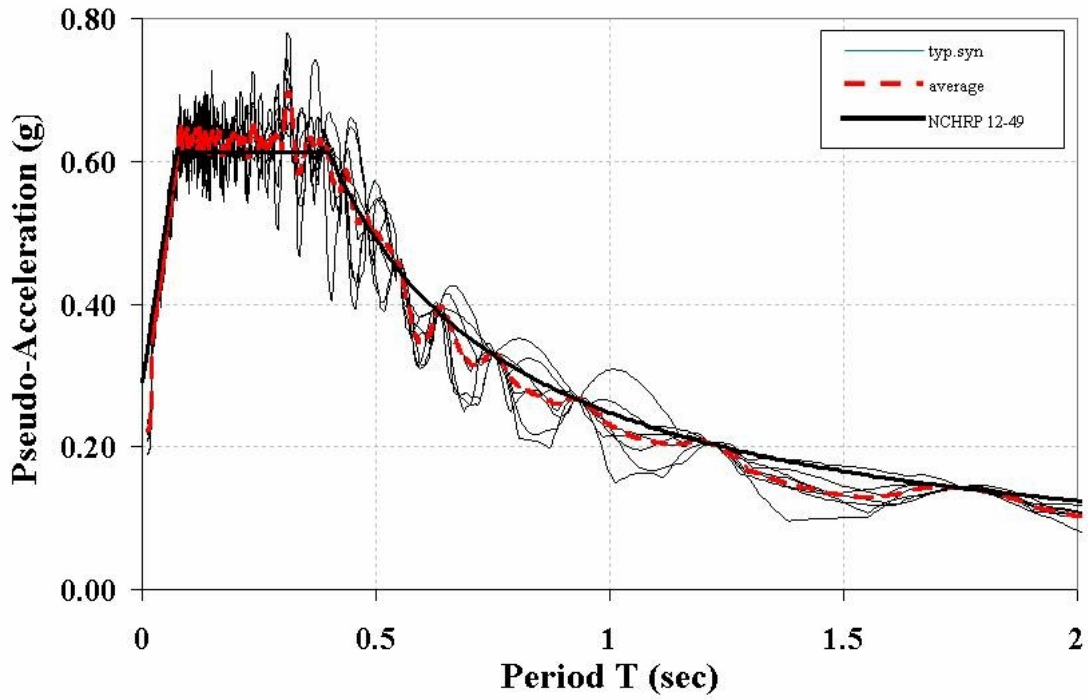
FIGURE E-1   Response Spectrum for S₁=0.25g
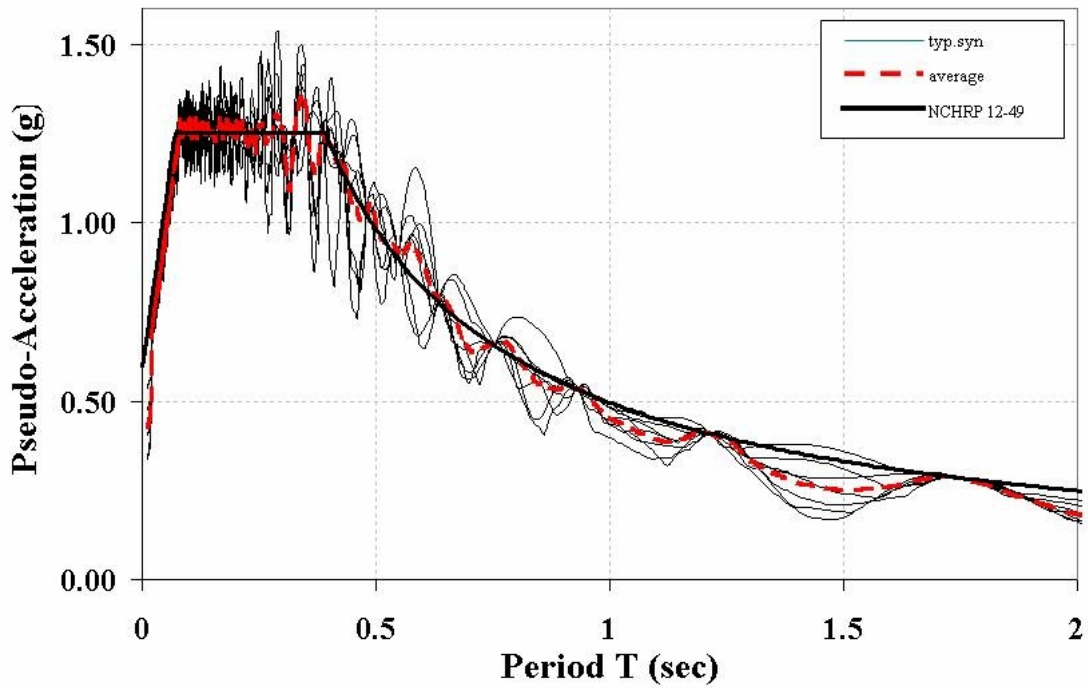
FIGURE E-2   Response Spectrum for S₁=0.5g

166
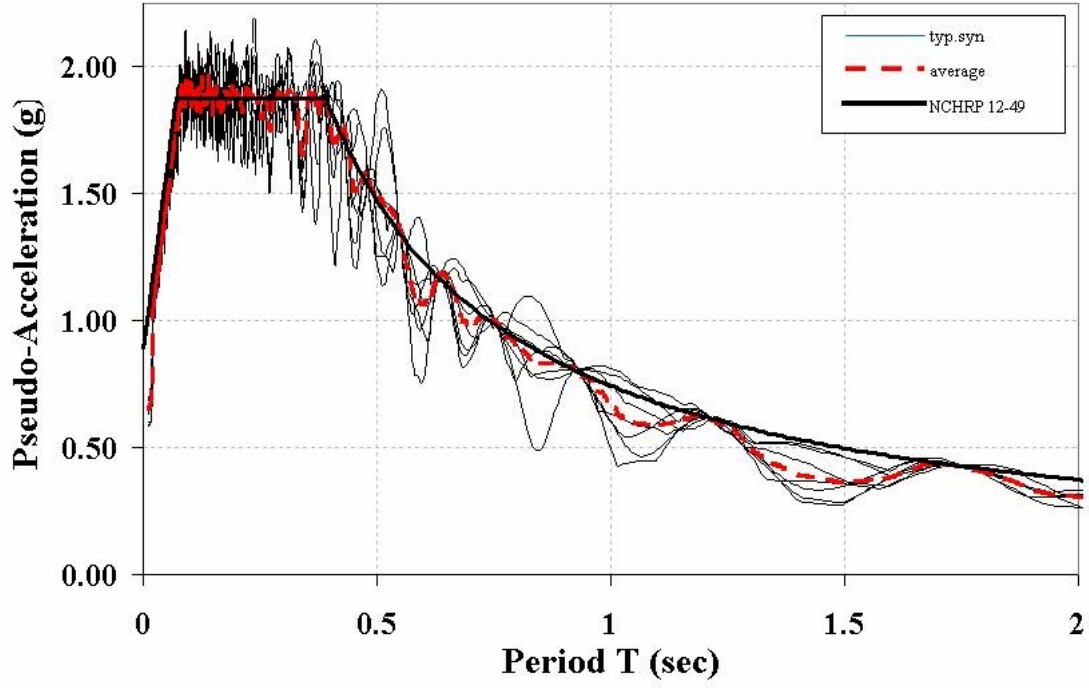
FIGURE E-3   Response Spectrum for S$_1$=0.75g

APPENDIX F
SAMPLE SAP2000 INPUT FILE

An input file for a typical analytical model is given in this appendix. A file with an extension ".$2k" can be used to generate a model. Additional files are required to supply the loading functions. These text files must be located in the same file subdirectory.

; File C:\Thesis Research\Thesis Writing\SAP Model\Input File.$2k saved 4/5/03 16:50:30
in Kip-in

SYSTEM
 DOF=UX,UZ,RY LENGTH=IN FORCE=Kip PAGE=SECTIONS

JOINT
 1 X=-144 Y=0 Z=0
 2 X=144 Y=0 Z=0
 3 X=-144 Y=0 Z=288
 4 X=144 Y=0 Z=288
 5 X=-144 Y=0 Z=576
 6 X=144 Y=0 Z=576
 7 X=-144 Y=0 Z=864
 8 X=144 Y=0 Z=864
 9 X=-144 Y=0 Z=1152
 10 X=144 Y=0 Z=1152
 11 X=-144 Y=0 Z=-120
 12 X=144 Y=0 Z=-120

RESTRAINT
 ADD=11 DOF=U1,U2,U3,R1,R2,R3
 ADD=12 DOF=U1,U2,U3,R1,R2,R3
 ADD=1 DOF=U1
 ADD=2 DOF=U1

CONSTRAINT
 NAME=EQUAL1 TYPE=EQUAL DOF=UX CSYS=0
  ADD=9
  ADD=10

PATTERN
 NAME=DEFAULT

MASS
 ADD=9 U1=.5034 U3=.5034
 ADD=10 U1=.5034 U3=.5034
 ADD=1 U3=.001
 ADD=2 U3=.001

MATERIAL
 NAME=STEEL IDES=S W=.000283
  T=0 E=29000 U=.3 A=.0000065 FY=36
 NAME=CONC IDES=C M=2.246377E-07 W=.0000868
  T=0 E=3600 U=.2 A=.0000055

170

```
   NAME=OTHER  IDES=N  M=2.246377E-07  W=.0000868
    T=0  E=3600  U=.2  A=.0000055


FRAME SECTION
    NAME=FSEC1  MAT=STEEL  SH=R  T=18,10  A=180  J=3916.671  I=4860,1500
AS=150,150
    NAME=W14X82  MAT=STEEL  A=48.2  J=5.08  I=882,148  AS=7.2981,14.435
S=123.2704,29.22014 Z=139,44.8 R=6.049588,2.47812 T=14.31,10.13,.855,.51,10.13,.855
SHN=W14X82 DSG=W
    NAME=DIAGONAL  MAT=STEEL  SH=R  T=2,5.5  A=11  J=11.31156
I=3.666667,27.72917 AS=9.166667,9.166667


NLPROP
 NAME=GAP   TYPE=Gap  M=.001
  DOF=U1  KE=50000  CE=0  K=50000  OPEN=0
 NAME=UB   TYPE=Plastic1  M=.001
  DOF=U1  KE=1120  CE=0  K=1120  YIELD=150  RATIO=.01  EXP=2


FRAME
 1  J=1,3  SEC=W14X82  NSEG=2  ANG=0
 2  J=3,5  SEC=W14X82  NSEG=2  ANG=0
 3  J=5,7  SEC=W14X82  NSEG=2  ANG=0
 4  J=7,9  SEC=W14X82  NSEG=2  ANG=0
 5  J=2,4  SEC=W14X82  NSEG=2  ANG=0
 6  J=4,6  SEC=W14X82  NSEG=2  ANG=0
 7  J=6,8  SEC=W14X82  NSEG=2  ANG=0
 8  J=8,10  SEC=W14X82  NSEG=2  ANG=0
 9  J=1,2  SEC=DIAGONAL  NSEG=4  ANG=0  IREL=R2,R3  JREL=R1,R2,R3
 10  J=3,4  SEC=DIAGONAL  NSEG=4  ANG=0  IREL=R2,R3  JREL=R1,R2,R3
 11  J=5,6  SEC=DIAGONAL  NSEG=4  ANG=0  IREL=R2,R3  JREL=R1,R2,R3
 12  J=7,8  SEC=DIAGONAL  NSEG=4  ANG=0  IREL=R2,R3  JREL=R1,R2,R3
 13  J=9,10  SEC=DIAGONAL  NSEG=4  ANG=0  IREL=R2,R3  JREL=R1,R2,R3
 14  J=1,4  SEC=DIAGONAL  NSEG=2  ANG=0  IREL=R2,R3  JREL=R1,R2,R3
 15  J=2,3  SEC=DIAGONAL  NSEG=2  ANG=0  IREL=R2,R3  JREL=R1,R2,R3
 16  J=3,6  SEC=DIAGONAL  NSEG=2  ANG=0  IREL=R2,R3  JREL=R1,R2,R3
 17  J=4,5  SEC=DIAGONAL  NSEG=2  ANG=0  IREL=R2,R3  JREL=R1,R2,R3
 18  J=5,8  SEC=DIAGONAL  NSEG=2  ANG=0  IREL=R2,R3  JREL=R1,R2,R3
 19  J=6,7  SEC=DIAGONAL  NSEG=2  ANG=0  IREL=R2,R3  JREL=R1,R2,R3
 20  J=7,10  SEC=DIAGONAL  NSEG=2  ANG=0  IREL=R2,R3  JREL=R1,R2,R3
 21  J=8,9  SEC=DIAGONAL  NSEG=2  ANG=0  IREL=R2,R3  JREL=R1,R2,R3


NLLINK
 1  J=1  NLP=GAP  ANG=0  AXDIR=+Z
 2  J=2  NLP=GAP  ANG=0  AXDIR=+Z
 3  J=11,1  NLP=UB  ANG=0
 4  J=12,2  NLP=UB  ANG=0
```

```
LOAD
 NAME=GRAVITY CSYS=0
  TYPE=FORCE
    ADD=9 UZ=-194.5
    ADD=10 UZ=-194.5
 NAME=VIRTUALX CSYS=0
  TYPE=FORCE
    ADD=9 UX=.5
    ADD=10 UX=.5
 NAME=LOAD1 CSYS=0
  TYPE=FORCE
    ADD=9 UZ=1
 NAME=LOAD2 CSYS=0
  TYPE=FORCE
    ADD=10 UZ=1
 NAME=LOAD3 CSYS=0
  TYPE=FORCE
    ADD=9 UZ=-1
 NAME=LOAD4 CSYS=0
  TYPE=FORCE
    ADD=10 UZ=-1

MODE
 TYPE=RITZ N=16
  ACC=UX
  ACC=UZ
  LOAD=GRAVITY
  LOAD=VIRTUALX
  LOAD=LOAD1
  LOAD=LOAD2
  LOAD=LOAD3
  LOAD=LOAD4
  NLLINK=*

FUNCTION
 NAME=RAMP1 DT=1 NPL=1 PRINT=Y FILE=ramp1.txt
 NAME=SYN1 DT=.005 NPL=1 PRINT=Y FILE=syn1.txt

HISTORY
 NAME=GRAV TYPE=NON NSTEP=40 DT=1 DAMP=.99 DTMAX=.5 DTMIN=.000001
   LOAD=GRAVITY FUNC=RAMP1 SF=1 AT=0
    NAME=SYN1  TYPE=NON  NSTEP=3000  DT=.005  DAMP=.02  PREV=GRAV
DTMIN=.000001
   ACC=U1  ANG=0 FUNC=SYN1 SF=1 AT=0

OUTPUT
```

; No Output Requested

END

; The following data is used for graphics, design and pushover analysis.
; If changes are made to the analysis data above, then the following data
; should be checked for consistency.
SAP2000 V7.40 SUPPLEMENTAL DATA
  GRID GLOBAL X "1" -120
  GRID GLOBAL X "2" -72
  GRID GLOBAL X "3" -24
  GRID GLOBAL X "4" 24
  GRID GLOBAL X "5" 72
  GRID GLOBAL X "6" 120
  GRID GLOBAL Y "7" -120
  GRID GLOBAL Y "8" -72
  GRID GLOBAL Y "9" -24
  GRID GLOBAL Y "10" 24
  GRID GLOBAL Y "11" 72
  GRID GLOBAL Y "12" 120
  GRID GLOBAL Z "13" 0
  GRID GLOBAL Z "14" 48
  GRID GLOBAL Z "15" 96
  GRID GLOBAL Z "16" 144
  MATERIAL STEEL FY 36
  MATERIAL CONC FYREBAR 60 FYSHEAR 40 FC 4 FCSHEAR 4
  FRAMESECTION W14X82 A 24.1 MFA 2
  STATICLOAD GRAVITY TYPE DEAD
  STATICLOAD VIRTUALX TYPE DEAD
  STATICLOAD LOAD1 TYPE DEAD
  STATICLOAD LOAD2 TYPE DEAD
  STATICLOAD LOAD3 TYPE DEAD
  STATICLOAD LOAD4 TYPE DEAD
END SUPPLEMENTAL DATA

Appendix G

CAPACITY OF ARBITRARY CONCRETE FOUNDATION PEDESTAL

The constraints key to capacity protection of existing elements, established in Section 4.2 (constraints (iii) and (ii)), are dependent on existing pier properties and may be limited by the foundation capacity. For example, a foundation limit state based on the compressive capacity of a concrete foundation pedestal could define this value in a specific application. To illustrate this situation, the capacity of a concrete pedestal is determined utilizing ACI 318 (ACI, 2000). The limiting foundation strength is used in the design example shown in Section 4 and design procedure results shown in Section 5.

Appendix G

Capacity of Arbitrary Concrete Pedestal

$$g := 386.4 \frac{in}{sec^2}$$

Pedestal Dimensions:

$h_p := 120in$

$B_p := 126in$

$b_p := 22in$

Concrete Material Properties:

$f_c := 2000$

$$E_c := \frac{57000}{1000} \cdot \sqrt{f_c} \frac{kips}{in^2}$$

$E_c = 18\,GPa$

Compressive Capacity of Pedestal (ACI 22.5.5):

$\phi \cdot B_n \geq P_u$

$\phi := 0.70$ (ACI 9.3.2.2)

$A_1 := b_p^2$

$A_2 := B_p^2$

$$\eta := \begin{vmatrix} \sqrt{\dfrac{A_2}{A_1}} & if & \sqrt{\dfrac{A_2}{A_1}} \leq 2 \\ 2 & otherwise \end{vmatrix}$$

$B_n := 0.85 \cdot f_c \cdot A_1 \cdot \eta$

$\phi B_n = 5124\,kN$

176

APPENDIX H

GRAPHICAL DESIGN PROCEDURE CALCULATIONS

This appendix provides a sample set of calculations for the proposed design procedure, automated so that many designs could be evaluated quickly. Calculations are based on a 2-dimensional pier with identical unbonded braces added to each leg of a pier. The cross-sectional area and effective length of the unbonded brace, A_{ub} and L_{ub} respectively, are variables, while other important properties are held constant. A_{ub} and L_{ub} are varied using the range variables i and j. The unbonded brace length, L_{ub}, is varied from zero to approximately 7.1 meters. A_{ub} is varied from zero to its limit to allow self-centering capability.

The graphical procedure is given for 2 of the methods of analysis discussed in Section 3. The first presented is Method 2, which is similar to the NSP of FEMA 356 with k_{eff} defined using (3-44). The second is Method 3, similar to the FEMA 274 procedure for systems with passive energy dissipation devices. The second one presented uses the parameters established for the design example shown in Section 4. Both use the modified displacement ductility ratio method for determining the maximum velocity demand.

Appendix H

Method 2: NSP Procedure of FEMA 356 with k_{eff} defined by Equation 3.39

Design Constraints:

(1) $A_{ub1} = A_{ub1}(L_{ub1}, \Delta_{all})$ $\Delta < \Delta_{all}$ (code mandated max displacement)

(2) $A_{ub2} = A_{ub2}(L_{ub2}, \mu_{all})$ $\mu_L < \mu_{all}$ (limit local displacement ductility)

(3) $A_{ub3} = A_{ub3}(L_{ub3}, P_{max})$ $P_y < P_{all}$ (fuse concept to protect vulnerable elements)

(4) $A_{ub4} = A_{ub4}(L_{ub4}, V_{cr})$ $V_{inelastic} < V_{cr}$ (limit impact velocity on foundation)

(5) $A_{ub5} = A_{ub5}(\eta_L)$ $\eta_L < 1$ (inherent re-centering capability)

$d := 7.315m$

$h := 29.261m$ (pier dimensions)

$g := 981 \dfrac{cm}{sec^2}$

Pier Properties: Unbonded Brace:

$\dfrac{h}{d} = 4$ $E := 200GPa$

$W := 1730kN$ $F_{yub} := 235MPa$

$k_o := 12.6 \dfrac{kN}{mm}$ $m_1 := \dfrac{W}{386.4 \dfrac{in}{sec^2}}$

$T_o = 0.74 \, s$ $T_o := 2\pi \cdot \sqrt{\dfrac{m_1}{k_o}}$

Seismic Demand (FEMA 356, Sec. 1.6):

$S_1 := 0.5 \cdot g$ $F_a = F_v = 1.0$ (assumed site class B)

$S_s := 1.25 \cdot g$

$B_s := 0.8$ $B_1 := 0.8$ (2% damping)

$T_s := \dfrac{S_1 \cdot B_s}{S_s \cdot B_1} \cdot sec$ $T_O := 0.2 \cdot T_s$

$T_s = 0.4 \, s$ $T_O = 0.08 \, s$

$i := 0, 1 .. 300$

$T_i := \dfrac{i}{100} \sec$

$S_{a_i} := \begin{vmatrix} \left[S_s \cdot \left[\left(\dfrac{5}{B_s} - 2 \right) \cdot \dfrac{T_i}{T_s} + 0.4 \right] \right] & \text{if } T_i \leq T_O \\[2em] \dfrac{S_s}{B_s} & \text{if } T_O \leq T_i \leq T_s \\[2em] \dfrac{S_1 \cdot \sec}{B_1 \cdot T_i} & \text{if } T_s \leq T_i \end{vmatrix}$

Spectral Demand Curve

(1) $\Delta < \Delta_{all}$ (A_{ub}, L_{ub}, k_o)

$FS := 5$

$\Delta_{all1} := \dfrac{d}{2 \cdot FS}$ (overturning stability limit) $\Delta_{all1} = 732 \text{ mm}$

$\Delta_{all2} := 0.25 \cdot \dfrac{P_{y1}}{W} \cdot H$ (NCHRP 12-49 limit to prevent P-Δ effects from significantly affecting the seismic behavior)

$H := h$ $A_{ub11} := 0.1 \text{mm}^2$

$P_{y1} := \dfrac{W}{2} \cdot \dfrac{d}{h} + A_{ub11} \cdot F_{yub} \cdot \dfrac{d}{h}$

$\Delta_{all2} = 930.4 \text{ mm}$ (P_{y1} is dependent on A_{ub} however assume very small or no A_{ub} to determine yield displacement of system, conservative)

$\Delta_{cr} := \begin{pmatrix} \Delta_{all1} \\ \Delta_{all2} \end{pmatrix}$

$n_1 := 400$ $n_2 := 74$

$i := 1, 2 .. n_1$ $j := 1, 2 .. n_2$ (range of unbonded brace cross-sectional area and effective length)

$f_2 := 25.4$ $f_1 := 50$

$L_{ub_i} := i \cdot f_2 \text{ mm}$ $A_{ub_j} := j \cdot f_1 \text{ mm}^2$

$\eta_{L_j} := \dfrac{2 \cdot A_{ub_j} \cdot F_{yub}}{W}$

$\Delta_{up2_j} := \dfrac{\dfrac{W}{2} \cdot \left(1 - \eta_{L_j}\right) \cdot \dfrac{d}{h}}{k_o}$

$k_{r_{i,j}} := \dfrac{1}{\dfrac{1}{k_o} + \dfrac{1}{\left(\dfrac{E \cdot A_{ub_j}}{L_{ub_i}}\right) \cdot \left(\dfrac{d}{h}\right)^2}}$

$P_{y_j} := \left(\dfrac{W}{2} + A_{ub_j} \cdot F_{yub}\right) \cdot \dfrac{d}{h}$

$\Delta_{y2_{i,j}} := \Delta_{up2_j} + \dfrac{2 \cdot A_{ub_j} \cdot F_{yub} \cdot \dfrac{d}{h}}{k_{r_{i,j}}}$

$$k_{eff_{i,j}} := \left[k_o \cdot \left(\frac{\Delta up2_j}{\Delta y2_{i,j}} \right) + k_{r_{i,j}} \cdot \left(\frac{\Delta y2_{i,j} - \Delta up2_j}{\Delta y2_{i,j}} \right) \right]$$

$$T_{eff_{i,j}} := 2 \cdot \pi \cdot \sqrt{\frac{m_1}{k_{eff_{i,j}}}}$$

$C_m := 1.0$ (effective mass factor)

$$R_j := \frac{\frac{S_s}{B_s \cdot g}}{\frac{P_{y_j}}{W}} \cdot C_m$$

$$C_{1_{i,j}} := \begin{cases} 1.5 & \text{if } T_{eff_{i,j}} < T_O \\[2mm] \dfrac{\left[1.0 + \dfrac{(R_j - 1) \cdot T_s}{T_{eff_{i,j}}} \right]}{R_j} & \text{if } T_O \le T_{eff_{i,j}} \le T_s \\[2mm] 1.0 & \text{if } T_{eff_{i,j}} > T_s \end{cases}$$

(factor from FEMA 356 to account for increased displacements in equal energy range of spectrum)

$$\Delta_{G_{i,j}} := \begin{cases} \dfrac{m_1 \cdot \dfrac{S_1}{B_1} \cdot \sec}{T_{eff_{i,j}} \cdot k_{eff_{i,j}}} & \text{if } C_{1_{i,j}} = 1.0 \\[4mm] \left(C_{1_{i,j}} \cdot \dfrac{m_1 \cdot \dfrac{S_s}{B_s}}{k_{eff_{i,j}}} \right) & \text{if } C_{1_{i,j}} \ne 1.0 \end{cases}$$

(sorts through array to find values of A_{ub} for a given L_{ub} that satisfy the constraint and gives the "solution vector")

$$A_{ub1} := \begin{array}{|l} r \leftarrow 0 \\ \text{for } i \in 1, 2 .. n_1 \\ \quad \begin{array}{|l} c \leftarrow 0 \\ \text{for } j \in 1, 2 .. n_2 \\ \quad \begin{array}{|l} A_i \leftarrow j \cdot f_1 \text{ in}^2 \text{ if } \left(\min(\Delta_{cr}) - 0.01 \text{in} \right) \le \Delta_{G_{i,j}} \le \left(\min(\Delta_{cr}) + 0.01 \text{in} \right) \\ c \leftarrow c + 1 \end{array} \\ r \leftarrow r + 1 \end{array} \\ A \end{array}$$
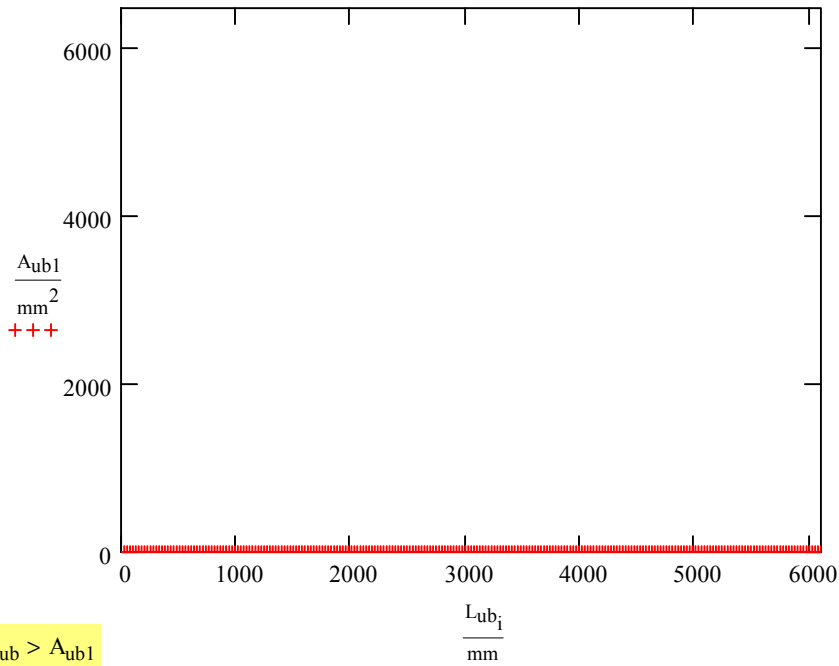
$$\frac{A_{ub1}}{mm^2}$$
$$+\;+\;+$$

6000

4000

2000

0

0   1000   2000   3000   4000   5000   6000

$$\frac{L_{ub_i}}{mm}$$

$A_{ub} > A_{ub1}$

end constraint 1

(2) $\mu_L < \mu_{all}$ $(A_{ub}, L_{ub}, k_o, F_y)$

1.5% strain:

$$\mu_{all} := \frac{0.015 \cdot E}{F_{yub}}$$

$\mu_{all} = 12.8$ (allowable local displacement ductility ratio)

$$\mu_{L_{i,j}} := \frac{\left[\Delta_{G_{i,j}} - \frac{\left(A_{ub_j} \cdot F_{yub} + \frac{W}{2} \right) \cdot \frac{d}{h}}{k_o} \right] \cdot \frac{d}{h}}{\left(\frac{F_{yub} \cdot L_{ub_i}}{E} \right)}$$

$A_{ub2} :=$
$r \leftarrow 0$
for $i \in 1, 2 .. n_1$
$\quad c \leftarrow 0$
$\quad$ for $j \in 1, 2 .. n_2$
$\qquad A_i \leftarrow j \cdot f_1 \, mm^2 \quad$ if $\left(\mu_{all} - 0.1\right) \leq \mu_{L_{i, j}} \leq \left(\mu_{all} + 0.1\right)$
$\qquad c \leftarrow c + 1$
$\quad r \leftarrow r + 1$
A
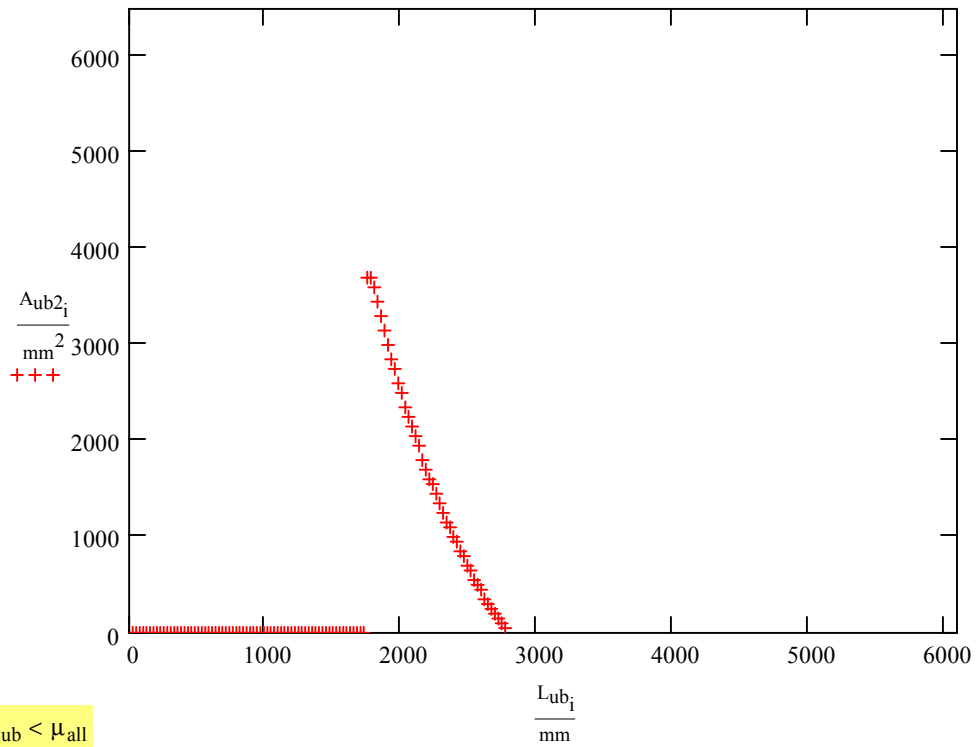
$\mu_{ub} < \mu_{all}$

$A_{ub} > A_{ub2}$

end constraint 2

(3) $P_y < P_{all}$ $\quad$ (A$_{ub}$, F$_y$)

$P_{all} := 0.5 \cdot W$ $\qquad$ (allowable base shear) $\qquad\qquad$ $R_d := 1.56$ $\qquad$ (factor to account for vertical modes of vibration)

$$P_y = \left(\frac{W}{2} + A_{ub} \cdot F_{yub} \right) \frac{d}{h}$$

$$A_{ub3} := \frac{P_{all}}{1.5 R_d \cdot F_{yub}} \cdot \frac{h}{d} - \frac{W}{2 \cdot F_{yub}}$$

$A_{ub3} = 2611 \, mm^2$ $\qquad\qquad$ $\left(A_{ub} < A_{ub3} \right)$

---

end constraint 3

(4) $V_{inelastic} < V_{cr}$ $\quad$ (A$_{ub}$, L$_{ub}$, k$_o$, F$_y$)

$$\beta_j := \begin{vmatrix} \dfrac{2\,\eta_{L_j}}{1 + \eta_{L_j}} & \text{if } T_{eff_{i,j}} \geq T_s \\[4mm] \dfrac{\eta_{L_j}}{1 + \eta_{L_j}} & \text{if } T_{eff_{i,j}} < T_s \end{vmatrix}$$

$$\mu_m = \beta \cdot \mu_G = \beta \cdot \frac{\Delta_G}{\Delta_{y2}}$$

$$\mu_{m_{i,j}} := \begin{vmatrix} 1.0 & \text{if } \beta_j \cdot \dfrac{\Delta_{G_{i,j}}}{\Delta_{y2_{i,j}}} < 1.0 \\[4mm] \beta_j \cdot \dfrac{\Delta_{G_{i,j}}}{\Delta_{y2_{i,j}}} & \text{otherwise} \end{vmatrix}$$ $\qquad$ (modified displacement ductility ratio)

$V_{cr} := 75 \dfrac{cm}{sec}$ $\qquad$ (critical deck-level velocity to control impact to foundation)

$$V_{e_{i,j}} := \begin{vmatrix} \left(\dfrac{\frac{S_1}{B_1}}{2 \cdot \pi} \cdot sec \right) & \text{if } C_{1_{i,j}} = 1.0 \\[6mm] \left(\dfrac{\frac{S_s}{B_s}}{2 \cdot \pi} \cdot T_{eff_{i,j}} \right) & \text{if } C_{1_{i,j}} \neq 1.0 \end{vmatrix}$$ $\qquad$ (elastic pseudo velocity)

$$V_{cr} = \begin{vmatrix} \dfrac{V_{e_{i,j}}}{\mu_m} & \text{if } C_{1_{i,j}} = 1.0 \\[5mm] \dfrac{V_{e_{i,j}}}{\sqrt{2 \cdot \mu_m - 1}} & \text{if } C_{1_{i,j}} \neq 1.0 \end{vmatrix}$$ $\qquad\qquad$ $\mu_m > \dfrac{V_e}{V_{cr}}$

Modified Displacement Ductility Ratio

μ_m
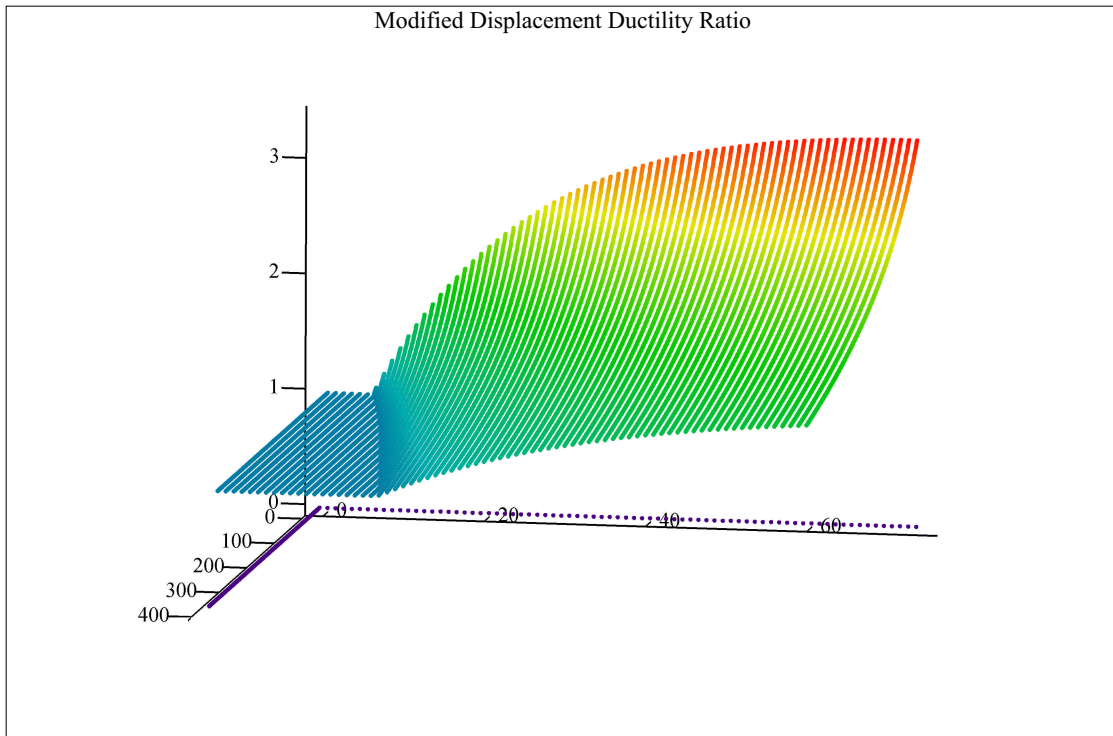
$$\mu_{mcr_{i,j}} := \begin{vmatrix} \dfrac{V_{e_{i,j}}}{V_{cr}} & \text{if } C_{1_{i,j}} = 1.0 \\ \\ \dfrac{\left(V_{e_{i,j}}\right)^2}{2 \cdot V_{cr}^2} + \dfrac{1}{2} & \text{if } C_{1_{i,j}} \neq 1.0 \end{vmatrix}$$

$(\mu_m > \mu_{mcr},$ critical displacement ductility ratio)

$$A_{ub4} := \begin{vmatrix} r \leftarrow 0 \\ \text{for } i \in 1, 2 .. n_1 \\ \quad \begin{vmatrix} c \leftarrow 0 \\ \text{for } j \in 1, 2 .. n_2 \\ \quad \begin{vmatrix} A_i \leftarrow j \cdot f_1 \cdot mm^2 & \text{if } \left(\mu_{mcr_{i,j}} - 0.02\right) \leq \mu_{m_{i,j}} \leq \left(\mu_{mcr_{i,j}} + 0.02\right) \\ c \leftarrow c + 1 \end{vmatrix} \\ r \leftarrow r + 1 \end{vmatrix} \\ A \end{vmatrix}$$

$$\frac{A_{ub4_i}}{mm^2}$$
$+++$
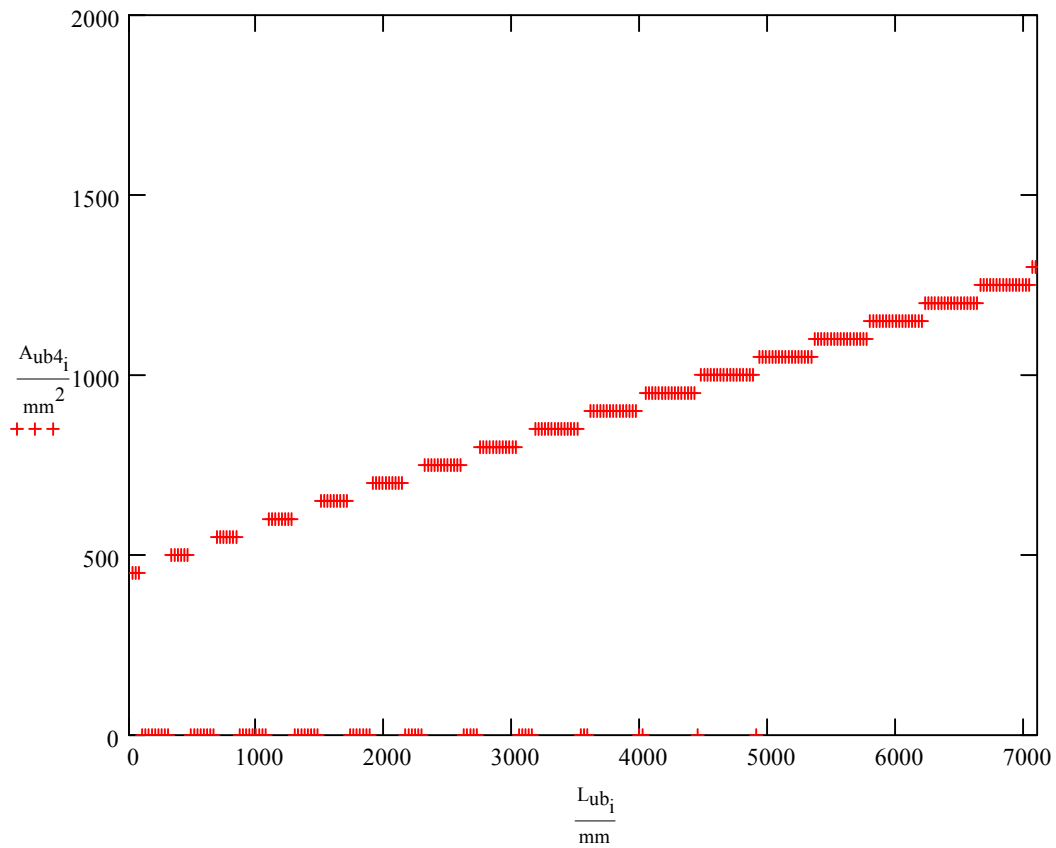
end constraint 4

(5) h_L <1, Inherent Recentering (A_{ub}, F_y)

$$\eta_L = \frac{A_{ub} \cdot F_{yub}}{\frac{W}{2}}$$

$\eta_L < 1.0$

$$A_{ub5} := \frac{W}{2 \cdot F_{yub}}$$

$A_{ub5} = 3681 \, mm^2$ $A_{ub} < A_{ub5}$

end constraint 5

Design Chart:
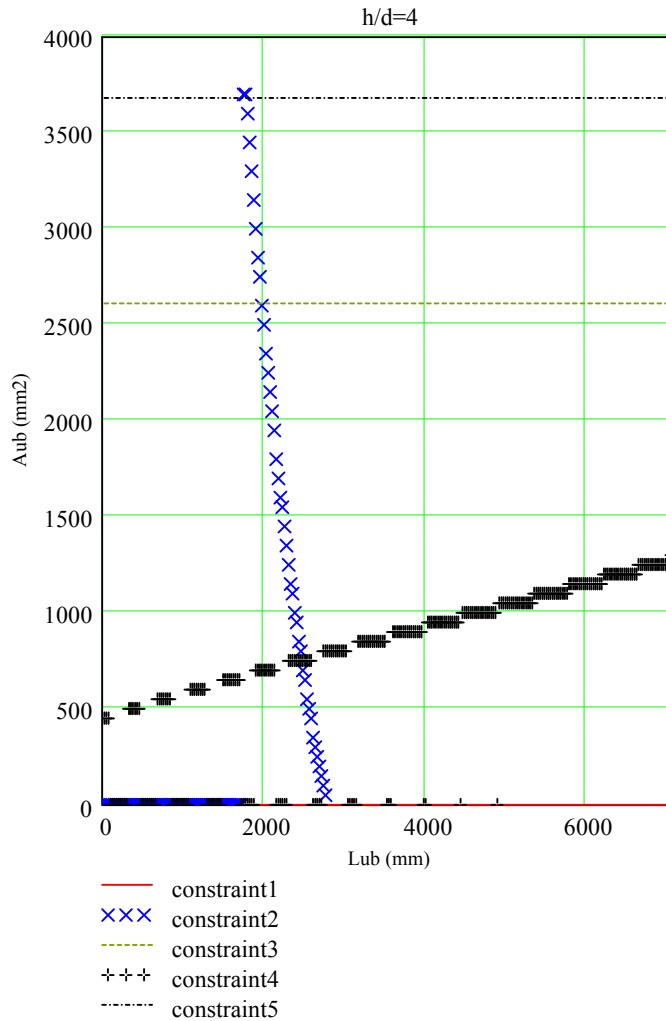
$R_d = 1.56$

$P_{all} := 0.5 \cdot W$

$P_o := 0.5 \cdot W$

h/d=4

Strength Retrofit Coefficient:

$$\eta_o := \frac{P_o}{W} \qquad \eta := \frac{P_{all}}{W}$$

$\eta_o = 0.5 \qquad \eta = 0.5$

$$R_E := \frac{\eta}{\eta_o} \qquad \boxed{R_E = 1}$$

Stiffness Retrofit Coefficient:

$$k_p = 12.6 \frac{kN}{mm} \qquad k_o = 12.6 \frac{kN}{mm}$$

$$R_E := \frac{k_o}{k_p} \qquad \boxed{R_E = 1}$$

$$\boxed{A_{ub_m} = 1800 \, mm^2}$$

$$\boxed{L_{ub_k} = 2489 \, mm}$$

$$k_{ubf} := \frac{E \cdot A_{ub_m}}{L_{ub_k}}$$

$$k_{ubf} = 144.6 \frac{kN}{mm}$$

Design Constraints:

(1) $A_{ub1} = A_{ub1}\left(L_{ub1}, \Delta_{all}\right)$ $\qquad \Delta < \Delta_{all}$ $\qquad \boxed{\dfrac{\Delta_{G_{k,m}}}{\min\left(\Delta_{cr}\right)} = 0.22}$

(2) $A_{ub2} = A_{ub2}\left(L_{ub2}, \mu_{all}\right)$ $\qquad \mu_L < \mu_{all}$ $\qquad \boxed{\dfrac{\mu_{L_{k,m}}}{\mu_{all}} = 0.9}$

(3) $A_{ub3} = A_{ub3}\left(L_{ub3}, P_{max}\right)$ $\qquad P_y < P_{all}$ $\qquad \boxed{\dfrac{P_{y_m} \cdot R_d}{P_{all}} = 0.58}$

(4) $A_{ub4} = A_{ub4}\left(L_{ub4}, V_{cr}\right)$ $\qquad PS_{in} < V_{cr}$ $\qquad \boxed{\dfrac{V_{e_{k,m}}}{\mu_{m_{k,m}} \cdot V_{cr}} = 0.6}$

(5) $A_{ub5} = A_{ub5}\left(\eta_L\right)$ $\qquad \eta_L < 1$ $\qquad \boxed{\eta_{L_m} = 0.49}$

Method 3: Simplified Method of Analysis for Passive Energy Dissipation Systems

Design Constraints:

(1) $A_{ub1} = A_{ub1}(L_{ub1}, \Delta_{all})$ $\Delta < \Delta_{all}$ (code mandated max displacement)

(2) $A_{ub2} = A_{ub2}(L_{ub2}, \mu_{all})$ $\mu_L < \mu_{all}$ (limit local displacement ductility)

(3) $A_{ub3} = A_{ub3}(L_{ub3}, P_{max})$ $P_y < P_{all}$ (fuse concept to protect vulnerable elements)

(4) $A_{ub4} = A_{ub4}(L_{ub4}, V_{cr})$ $V_{inelastic} < V_{cr}$ (limit impact velocity on foundation)

(5) $A_{ub5} = A_{ub5}(\eta_L)$ $\eta_L < 1$ (inherent re-centering capability)

$d := 7.315 m$

$h := 29.26 m$

$g := 981 \dfrac{cm}{sec^2}$

Pier Properties: Unbonded Brace:

$\dfrac{h}{d} = 4$ $E := 200 GPa$

$W := 1730 kN$ $F_{yub} := 235 MPa$ $m_1 := \dfrac{W}{g}$

$k_o := 12.6 \dfrac{kN}{mm}$

$T_o = 0.74 s$ $T_o := 2\pi \cdot \sqrt{\dfrac{m_1}{k_o}}$

$R_{dv} := 1.56$

Seismic Demand (FEMA 356, Sec. 1.6):

$S_1 := 0.5 \cdot g$ $F_a = F_v = 1.0$ (assumed site class B)

$S_s := 1.25 \cdot g$

$B_s := 0.8$ $B_1 := 0.8$ (2% damping)

$T_s := \dfrac{S_1 \cdot B_s}{S_s \cdot B_1} \cdot sec$ $T_O := 0.2 \cdot T_s$

$T_s = 0.4 s$ $T_O = 0.08 s$

$$i := 0, 1 .. 300$$

$$T_i := \frac{i}{100} \sec$$

$$S_{a_i} := \left| \begin{array}{ll} \left[S_s \cdot \left[\left(\frac{5}{B_s} - 2 \right) \cdot \frac{T_i}{T_s} + 0.4 \right] \right] & \text{if } T_i \leq T_O \\[4ex] \dfrac{S_s}{B_s} & \text{if } T_O \leq T_i \leq T_s \\[4ex] \dfrac{S_1 \cdot \sec}{B_1 \cdot T_i} & \text{if } T_s \leq T_i \end{array} \right.$$

Spectral Demand Curve

Determination of Global Displacement Demand based on Passive Energy Dissipation System

-range of variables A_{ub} and L_{ub}

$$n_1 := 200 \qquad f_1 := \frac{1}{10}$$

$$k := 1, 2 .. n_1$$

$$n_2 := \frac{W}{2 \cdot F_{yub} \cdot f_1 \cdot in^2} - 1$$

$$L_{ub_k} := k \cdot 3 \cdot in$$

$$m := 1, 2 .. n_2$$

$$A_{ub_m} := m \cdot f_1 \, in^2$$

$\alpha := 0.01$ (assumed post-yield stiffness of unbonded brace)

$$\eta_{L_m} := \frac{A_{ub_m} \cdot F_{yub}}{\frac{W}{2}}$$

$$k_{ub_{k,m}} := \frac{E \cdot A_{ub_m}}{L_{ub_k}}$$

$$P_{up_m} := \left(1 - \eta_{L_m}\right) \cdot \frac{W}{2} \cdot \frac{d}{h}$$

$$P_{up1} := \frac{W}{2} \cdot \frac{d}{h}$$

$$\Delta_{up_m} := \frac{P_{up_m}}{k_o}$$

$$k_{r_{k,m}} := \frac{1}{\dfrac{1}{k_o} + \dfrac{1}{\left(\dfrac{A_{ub_m} \cdot E}{L_{ub_k}}\right)\left(\dfrac{d}{h}\right)^2}}$$

$$P_{y_m} := \frac{W}{2} \cdot \frac{d}{h} + A_{ub_m} \cdot F_{yub} \cdot \frac{d}{h}$$

$$\Delta_{y_{k,m}} := \frac{\left(1 - \eta_{L_m}\right) \cdot \dfrac{W}{2} \cdot \dfrac{d}{h}}{k_o} + \frac{2 \cdot A_{ub_m} \cdot F_{yub} \cdot \dfrac{d}{h}}{k_{r_{k,m}}}$$

$\beta_o := 0.028$ (assumed inherent structural damping)

Deck-level Displacement Demand

$$\frac{\Delta_G}{in}$$

(1) $\Delta < \Delta_{all}$ $\quad\quad (A_{ub}, L_{ub}, k_o)$

$FS := 5$

$\Delta_{all1} := \dfrac{d}{2 \cdot FS}$ (overturning stability limit) $\quad\quad \Delta_{all1} = 732 \text{ mm}$

$\Delta_{all2} := 0.25 \cdot \dfrac{P_{y1}}{W} \cdot H$ $\quad\quad$ (NCHRP 12-49 limit to prevent P-Δ effects from significantly affecting the seismic behavior)

$H := h \quad\quad A_{ub11} := 0.1 \text{mm}^2$

$P_{y1} := \dfrac{W}{2} \cdot \dfrac{d}{h} + A_{ub11} \cdot F_{yub} \cdot \dfrac{d}{h}$

$\Delta_{all2} = 930.4 \text{ mm}$ (P_{y1} is dependent on A_{ub} however assume very small or no A_{ub} to determine yield displacement of system, conservative) $\quad \Delta_{cr} := \begin{pmatrix} \Delta_{all1} \\ \Delta_{all2} \end{pmatrix}$

$A_{ub1} := \begin{vmatrix} r \leftarrow 0 \\ \text{for } k \in 1, 2 .. n_1 \\ \quad \begin{vmatrix} c \leftarrow 0 \\ \text{for } m \in 1, 2 .. n_2 \\ \quad \begin{vmatrix} A_{k,m} \leftarrow m \cdot f_1 \text{ in}^2 \text{ if } \left(\min(\Delta_{cr}) - 1\text{mm}\right) \leq \Delta_{G_{k,m}} \leq \left(\min(\Delta_{cr}) + 1\text{mm}\right) \\ c \leftarrow c + 1 \end{vmatrix} \\ r \leftarrow r + 1 \end{vmatrix} \\ A \end{vmatrix}$

:s through array finds values within stated range that are he critical value e)
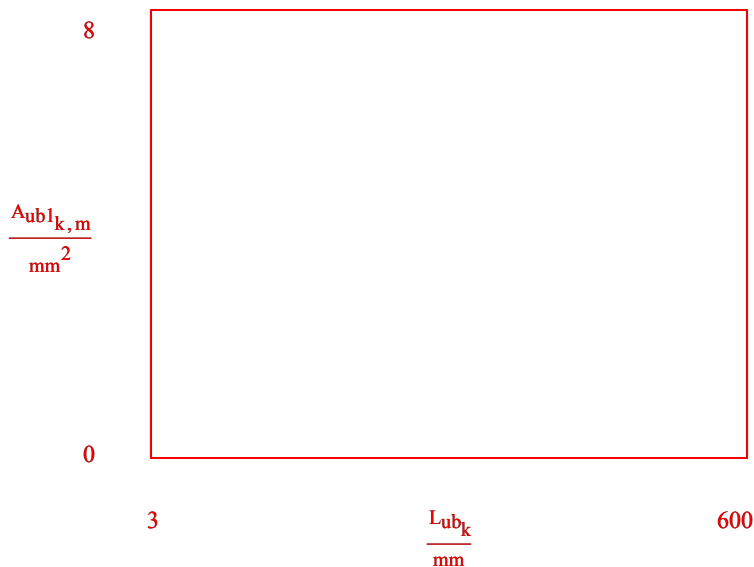
(no boundary, thus all unbonded brace dimensions and the pure rocking case satisfies the displacement constraint)

$A_{ub} > A_{ub1}$

---

end constraint 1

(2) $\mu_L < \mu_{all}$ $(A_{ub}, L_{ub}, k_o, F_y)$ 1.5% strain:

$$\mu_{all} := \frac{0.015 \cdot E}{F_{yub}}$$

$\mu_{all} = 12.8$ (allowable local displacement ductility ratio)

$$\mu_{L_{k,m}} := \frac{\left(\Delta_{G_{k,m}} - \dfrac{P_{y_m}}{k_o}\right) \cdot \dfrac{d}{h}}{\left(\dfrac{F_{yub} \cdot L_{ub_k}}{E}\right)}$$

$A_{ub2} :=$ | $r \leftarrow 0$
| for $k \in 1, 2 .. n_1$
| | $c \leftarrow 0$
| | for $m \in 1, 2 .. n_2$
| | | $A_k \leftarrow m \cdot f_1 \text{ in}^2$ if $(\mu_{all} - 0.5) \leq \mu_{L_{k,m}} \leq (\mu_{all} + 0.5)$
| | | $c \leftarrow c + 1$
| | $r \leftarrow r + 1$
| A

$\mu_{ub} < \mu_{all}$

$A_{ub} > A_{ub2}$

---
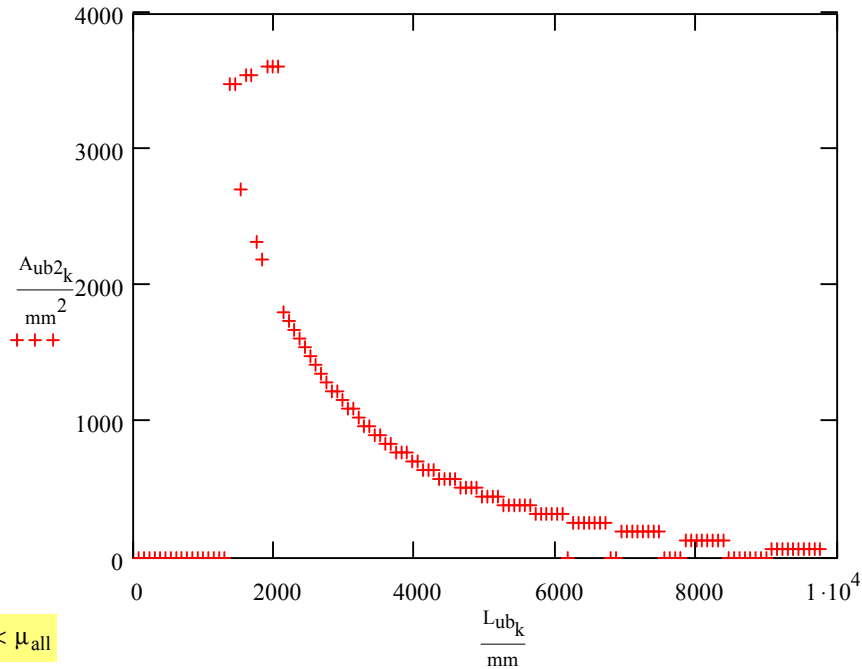
end constraint 2

(3) $P_y < P_{all}$ (A_{ub}, F_y)

$P_{all} := 0.5 \cdot W$ (allowable base shear)

R_d: (factor to account for vertical modes of vibration and factor of safety)

$P_y = \dfrac{W}{2} \cdot \dfrac{d}{h} + A_{ub3} \cdot F_y \cdot \dfrac{d}{h}$

$A_{ub3} := \dfrac{P_{all}}{1.5 R_{dv} \cdot F_{yub}} \cdot \dfrac{h}{d} - \dfrac{W}{2 \cdot F_{yub}}$

$A_{ub3} = 2611 \, mm^2$ $\left(A_{ub} < A_{ub3} \right)$

---

end constraint 3

(4) $V_{inelastic} < V_{cr}$ $(A_{ub}, L_{ub}, k_{o,} F_y)$

-Using the modified displacement ductility approach for prediction of velocity

$T_{eff_{k,m}} := 2 \cdot \pi \cdot \sqrt{\dfrac{m_1 \cdot \Delta_{G_{k,m}}}{P_{y_m}}}$

$\beta_m := \begin{cases} \dfrac{2\,\eta_{L_m}}{1 + \eta_{L_m}} & \text{if } T_{eff_{k,m}} \geq T_s \\[3mm] \dfrac{\eta_{L_m}}{1 + \eta_{L_m}} & \text{if } T_{eff_{k,m}} < T_s \end{cases}$

$\mu_m = \beta \cdot \mu_G = \beta \cdot \dfrac{\Delta_G}{\Delta_y}$

$\mu_{m_{k,m}} := \begin{cases} 1.0 & \text{if } \beta_m \cdot \dfrac{\Delta_{G_{k,m}}}{\Delta_{y_{k,m}}} < 1.0 \\[3mm] \beta_m \cdot \dfrac{\Delta_{G_{k,m}}}{\Delta_{y_{k,m}}} & \text{otherwise} \end{cases}$

$PS_{v_{k,m}} := \begin{cases} \dfrac{S_s \cdot T_{eff_{k,m}}}{B_s \cdot 2 \cdot \pi \cdot \sqrt{2 \cdot \mu_{m_{k,m}} - 1}} & \text{if } T_{eff_{k,m}} < T_s \\[3mm] \dfrac{S_1 \cdot \sec}{2 \cdot \pi \cdot B_1 \cdot \mu_{m_{k,m}}} & \text{if } T_{eff_{k,m}} \geq T_s \end{cases}$

$V_{cr} := 75 \dfrac{cm}{sec}$ (critical deck-level velocity to control impact to foundation)

$A_{ub4} :=$
$r \leftarrow 0$
for $k \in 1, 2 .. n_1$
$\quad c \leftarrow 0$
$\quad$ for $m \in 1, 2 .. n_2$
$\qquad A_{k,m} \leftarrow m \cdot f_1 \cdot in^2$ if $\left(V_{cr} - 0.2\dfrac{cm}{sec}\right) \le PS_{v_{k,m}} \le \left(V_{cr} + 0.2\dfrac{cm}{sec}\right)$
$\qquad c \leftarrow c + 1$
$\quad r \leftarrow r + 1$
A
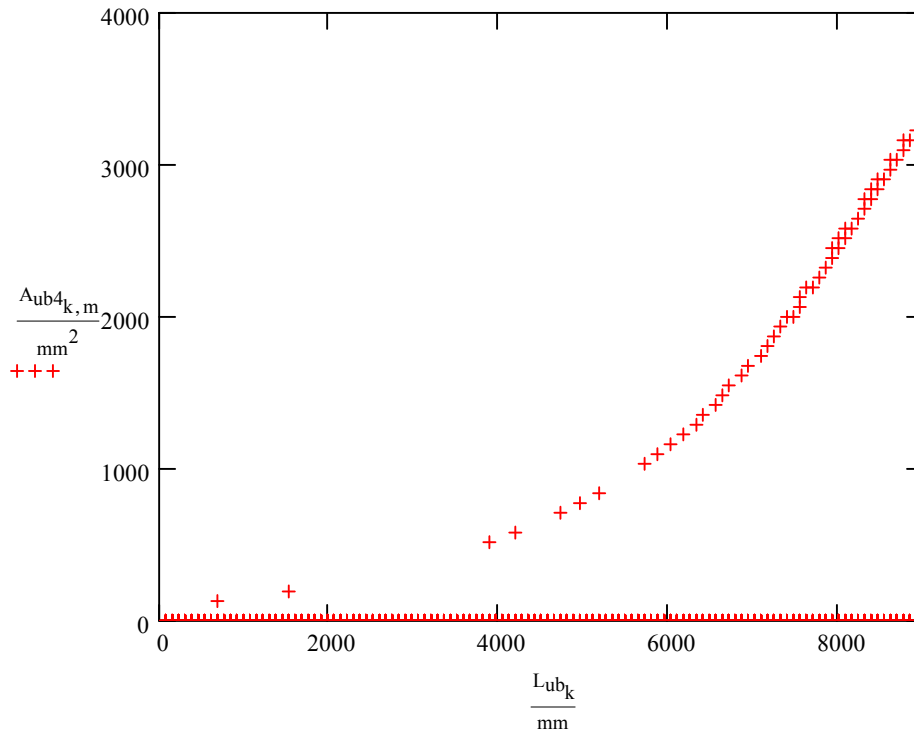
end constraint 4

(5) $\eta_L < 1$, Inherent Recentering (A_{ub}, F_y)

$$\eta_{L1} = \frac{4 \cdot A_{ub5} \cdot F_{yub}}{W + 2 \cdot A_{ub5} \cdot F_{yub}}$$

if $\eta_L = 1$, critical recentering area

$$1 = \frac{4 \cdot A_{ub} \cdot F_y}{W_1 + 2 \cdot A_{ub} \cdot F_y}$$

$$\eta_{L1} := 1$$

$$W_1 + 2 \cdot A_{ub} \cdot F_y = 4 \cdot A_{ub} \cdot F_y$$

$$A_{ub5} := \frac{-\eta_{L1} \cdot W}{2 \cdot \eta_{L1} \cdot F_{yub} - 4 \cdot F_{yub}}$$

$$W_1 = 2 \cdot A_{ub} \cdot F_y$$

$$\frac{W_1}{2} = A_{ub} \cdot F_y$$
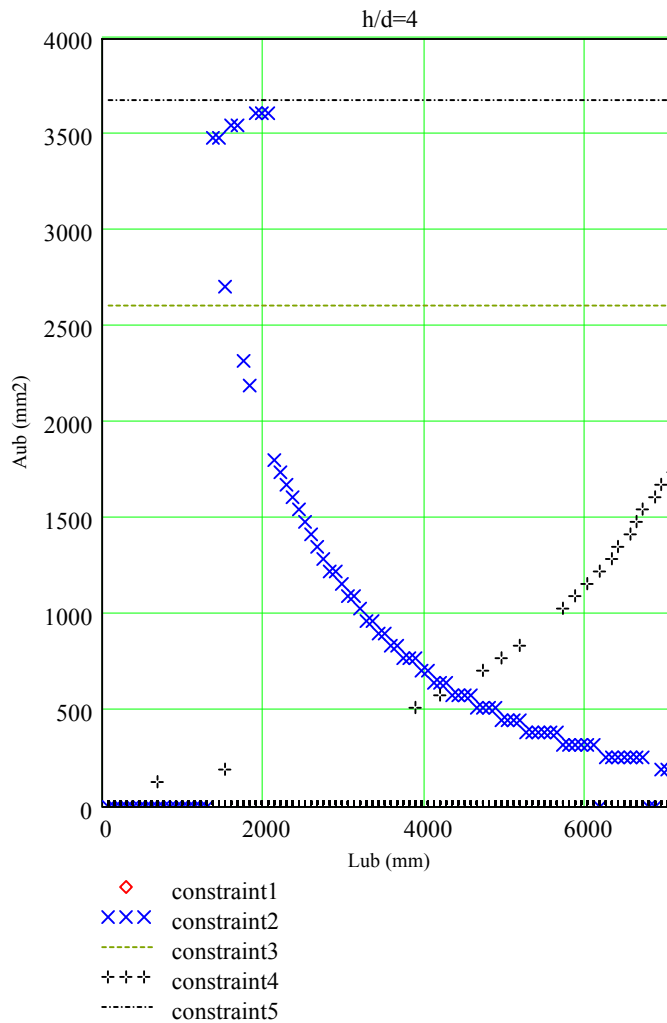
$$A_{ub5} = 3681 \text{ mm}^2 \qquad A_{ub} < A_{ub5}$$

---

end constraint 5

Design Chart:

$R_{dv} = 1.56$ $P_{all} = 865 \text{ kN}$

$P_o := 0.5 \cdot W$

h/d=4

Aub (mm2)

Lub (mm)

◇   constraint1
××× constraint2
– – –   constraint3
+ + +   constraint4
– · – · –   constraint5

Strength Retrofit Coefficient:

$$\eta_o := \frac{P_o}{W} \qquad \eta := \frac{P_{all}}{W}$$

$$\eta_o = 0.5 \qquad \eta = 0.5$$

$$R_E := \frac{\eta}{\eta_o} \qquad \boxed{R_E = 1}$$

Stiffness Retrofit Coefficient:

$$k_p = 12.6 \frac{kN}{mm} \qquad k_o = 12.6 \frac{kN}{mm}$$

$$R_E := \frac{k_o}{k_p} \qquad \boxed{R_E = 1}$$

Final Unbonded Brace Dimensions:

$$\boxed{A_{ub_j} = 1226 \text{ mm}^2}$$

$$\boxed{L_{ub_i} = 2743 \text{ mm}}$$

$$k_{ubf} := \frac{E \cdot A_{ub_j}}{L_{ub_i}}$$

$$k_{ubf} = 89.4 \frac{kN}{mm}$$

<u>Design Constraints:</u>

(1) $A_{ub1} = A_{ub1}\left(L_{ub1}, \Delta_{all}\right)$ $\Delta < \Delta_{all}$ $\boxed{\dfrac{\Delta_{G_{i,j}}}{\min\left(\Delta_{cr}\right)} = 0.26}$

(2) $A_{ub2} = A_{ub2}\left(L_{ub2}, \mu_{all}\right)$ $\mu_L < \mu_{all}$ $\boxed{\dfrac{\mu_{L_{i,j}}}{\mu_{all}} = 1}$

(3) $A_{ub3} = A_{ub3}\left(L_{ub3}, P_{max}\right)$ $P_y < P_{max}$ $\boxed{\dfrac{P_{y_j} \cdot R_{dv}}{P_{all}} = 0.52}$

(4) $A_{ub4} = A_{ub4}\left(L_{ub4}, V_{cr}\right)$ $PS_{in} < V_{cr}$ $\boxed{\dfrac{PS_{v_{i,j}}}{V_{cr}} = 0.67}$

(5) $A_{ub5} = A_{ub5}\left(\eta_L\right)$ $\eta_L < 1$ $\boxed{\eta_{L_j} = 0.333}$

Multidisciplinary Center for Earthquake Engineering Research
List of Technical Reports

The Multidisciplinary Center for Earthquake Engineering Research (MCEER) publishes technical reports on a variety of subjects related to earthquake engineering written by authors funded through MCEER. These reports are available from both MCEER Publications and the National Technical Information Service (NTIS). Requests for reports should be directed to MCEER Publications, Multidisciplinary Center for Earthquake Engineering Research, State University of New York at Buffalo, Red Jacket Quadrangle, Buffalo, New York 14261. Reports can also be requested through NTIS, 5285 Port Royal Road, Springfield, Virginia 22161. NTIS accession numbers are shown in parenthesis, if available.

NCEER-87-0001　"First-Year Program in Research, Education and Technology Transfer," 3/5/87, (PB88-134275, A04, MF-A01).

NCEER-87-0002　"Experimental Evaluation of Instantaneous Optimal Algorithms for Structural Control," by R.C. Lin, T.T. Soong and A.M. Reinhorn, 4/20/87, (PB88-134341, A04, MF-A01).

NCEER-87-0003　"Experimentation Using the Earthquake Simulation Facilities at University at Buffalo," by A.M. Reinhorn and R.L. Ketter, to be published.

NCEER-87-0004　"The System Characteristics and Performance of a Shaking Table," by J.S. Hwang, K.C. Chang and G.C. Lee, 6/1/87, (PB88-134259, A03, MF-A01). This report is available only through NTIS (see address given above).

NCEER-87-0005　"A Finite Element Formulation for Nonlinear Viscoplastic Material Using a Q Model," by O. Gyebi and G. Dasgupta, 11/2/87, (PB88-213764, A08, MF-A01).

NCEER-87-0006　"Symbolic Manipulation Program (SMP) - Algebraic Codes for Two and Three Dimensional Finite Element Formulations," by X. Lee and G. Dasgupta, 11/9/87, (PB88-218522, A05, MF-A01).

NCEER-87-0007　"Instantaneous Optimal Control Laws for Tall Buildings Under Seismic Excitations," by J.N. Yang, A. Akbarpour and P. Ghaemmaghami, 6/10/87, (PB88-134333, A06, MF-A01). This report is only available through NTIS (see address given above).

NCEER-87-0008　"IDARC: Inelastic Damage Analysis of Reinforced Concrete Frame - Shear-Wall Structures," by Y.J. Park, A.M. Reinhorn and S.K. Kunnath, 7/20/87, (PB88-134325, A09, MF-A01). This report is only available through NTIS (see address given above).

NCEER-87-0009　"Liquefaction Potential for New York State: A Preliminary Report on Sites in Manhattan and Buffalo," by M. Budhu, V. Vijayakumar, R.F. Giese and L. Baumgras, 8/31/87, (PB88-163704, A03, MF-A01). This report is available only through NTIS (see address given above).

NCEER-87-0010　"Vertical and Torsional Vibration of Foundations in Inhomogeneous Media," by A.S. Veletsos and K.W. Dotson, 6/1/87, (PB88-134291, A03, MF-A01). This report is only available through NTIS (see address given above).

NCEER-87-0011　"Seismic Probabilistic Risk Assessment and Seismic Margins Studies for Nuclear Power Plants," by Howard H.M. Hwang, 6/15/87, (PB88-134267, A03, MF-A01). This report is only available through NTIS (see address given above).

NCEER-87-0012　"Parametric Studies of Frequency Response of Secondary Systems Under Ground-Acceleration Excitations," by Y. Yong and Y.K. Lin, 6/10/87, (PB88-134309, A03, MF-A01). This report is only available through NTIS (see address given above).

NCEER-87-0013　"Frequency Response of Secondary Systems Under Seismic Excitation," by J.A. HoLung, J. Cai and Y.K. Lin, 7/31/87, (PB88-134317, A05, MF-A01). This report is only available through NTIS (see address given above).

NCEER-87-0014　"Modelling Earthquake Ground Motions in Seismically Active Regions Using Parametric Time Series Methods," by G.W. Ellis and A.S. Cakmak, 8/25/87, (PB88-134283, A08, MF-A01). This report is only available through NTIS (see address given above).

NCEER-87-0015   "Detection and Assessment of Seismic Structural Damage," by E. DiPasquale and A.S. Cakmak, 8/25/87, (PB88-163712, A05, MF-A01). This report is only available through NTIS (see address given above).

NCEER-87-0016   "Pipeline Experiment at Parkfield, California," by J. Isenberg and E. Richardson, 9/15/87, (PB88-163720, A03, MF-A01). This report is available only through NTIS (see address given above).

NCEER-87-0017   "Digital Simulation of Seismic Ground Motion," by M. Shinozuka, G. Deodatis and T. Harada, 8/31/87, (PB88-155197, A04, MF-A01). This report is available only through NTIS (see address given above).

NCEER-87-0018   "Practical Considerations for Structural Control: System Uncertainty, System Time Delay and Truncation of Small Control Forces," J.N. Yang and A. Akbarpour, 8/10/87, (PB88-163738, A08, MF-A01). This report is only available through NTIS (see address given above).

NCEER-87-0019   "Modal Analysis of Nonclassically Damped Structural Systems Using Canonical Transformation," by J.N. Yang, S. Sarkani and F.X. Long, 9/27/87, (PB88-187851, A04, MF-A01).

NCEER-87-0020   "A Nonstationary Solution in Random Vibration Theory," by J.R. Red-Horse and P.D. Spanos, 11/3/87, (PB88-163746, A03, MF-A01).

NCEER-87-0021   "Horizontal Impedances for Radially Inhomogeneous Viscoelastic Soil Layers," by A.S. Veletsos and K.W. Dotson, 10/15/87, (PB88-150859, A04, MF-A01).

NCEER-87-0022   "Seismic Damage Assessment of Reinforced Concrete Members," by Y.S. Chung, C. Meyer and M. Shinozuka, 10/9/87, (PB88-150867, A05, MF-A01). This report is available only through NTIS (see address given above).

NCEER-87-0023   "Active Structural Control in Civil Engineering," by T.T. Soong, 11/11/87, (PB88-187778, A03, MF-A01).

NCEER-87-0024   "Vertical and Torsional Impedances for Radially Inhomogeneous Viscoelastic Soil Layers," by K.W. Dotson and A.S. Veletsos, 12/87, (PB88-187786, A03, MF-A01).

NCEER-87-0025   "Proceedings from the Symposium on Seismic Hazards, Ground Motions, Soil-Liquefaction and Engineering Practice in Eastern North America," October 20-22, 1987, edited by K.H. Jacob, 12/87, (PB88-188115, A23, MF-A01). This report is available only through NTIS (see address given above).

NCEER-87-0026   "Report on the Whittier-Narrows, California, Earthquake of October 1, 1987," by J. Pantelic and A. Reinhorn, 11/87, (PB88-187752, A03, MF-A01). This report is available only through NTIS (see address given above).

NCEER-87-0027   "Design of a Modular Program for Transient Nonlinear Analysis of Large 3-D Building Structures," by S. Srivastav and J.F. Abel, 12/30/87, (PB88-187950, A05, MF-A01). This report is only available through NTIS (see address given above).

NCEER-87-0028   "Second-Year Program in Research, Education and Technology Transfer," 3/8/88, (PB88-219480, A04, MF-A01).

NCEER-88-0001   "Workshop on Seismic Computer Analysis and Design of Buildings With Interactive Graphics," by W. McGuire, J.F. Abel and C.H. Conley, 1/18/88, (PB88-187760, A03, MF-A01). This report is only available through NTIS (see address given above).

NCEER-88-0002   "Optimal Control of Nonlinear Flexible Structures," by J.N. Yang, F.X. Long and D. Wong, 1/22/88, (PB88-213772, A06, MF-A01).

NCEER-88-0003   "Substructuring Techniques in the Time Domain for Primary-Secondary Structural Systems," by G.D. Manolis and G. Juhn, 2/10/88, (PB88-213780, A04, MF-A01).

NCEER-88-0004   "Iterative Seismic Analysis of Primary-Secondary Systems," by A. Singhal, L.D. Lutes and P.D. Spanos, 2/23/88, (PB88-213798, A04, MF-A01).

NCEER-88-0005   "Stochastic Finite Element Expansion for Random Media," by P.D. Spanos and R. Ghanem, 3/14/88, (PB88-213806, A03, MF-A01).

NCEER-88-0006   "Combining Structural Optimization and Structural Control," by F.Y. Cheng and C.P. Pantelides, 1/10/88, (PB88-213814, A05, MF-A01).

NCEER-88-0007   "Seismic Performance Assessment of Code-Designed Structures," by H.H-M. Hwang, J-W. Jaw and H-J. Shau, 3/20/88, (PB88-219423, A04, MF-A01). This report is only available through NTIS (see address given above).

NCEER-88-0008   "Reliability Analysis of Code-Designed Structures Under Natural Hazards," by H.H-M. Hwang, H. Ushiba and M. Shinozuka, 2/29/88, (PB88-229471, A07, MF-A01). This report is only available through NTIS (see address given above).

NCEER-88-0009   "Seismic Fragility Analysis of Shear Wall Structures," by J-W Jaw and H.H-M. Hwang, 4/30/88, (PB89-102867, A04, MF-A01).

NCEER-88-0010   "Base Isolation of a Multi-Story Building Under a Harmonic Ground Motion - A Comparison of Performances of Various Systems," by F-G Fan, G. Ahmadi and I.G. Tadjbakhsh, 5/18/88, (PB89-122238, A06, MF-A01). This report is only available through NTIS (see address given above).

NCEER-88-0011   "Seismic Floor Response Spectra for a Combined System by Green's Functions," by F.M. Lavelle, L.A. Bergman and P.D. Spanos, 5/1/88, (PB89-102875, A03, MF-A01).

NCEER-88-0012   "A New Solution Technique for Randomly Excited Hysteretic Structures," by G.Q. Cai and Y.K. Lin, 5/16/88, (PB89-102883, A03, MF-A01).

NCEER-88-0013   "A Study of Radiation Damping and Soil-Structure Interaction Effects in the Centrifuge," by K. Weissman, supervised by J.H. Prevost, 5/24/88, (PB89-144703, A06, MF-A01).

NCEER-88-0014   "Parameter Identification and Implementation of a Kinematic Plasticity Model for Frictional Soils," by J.H. Prevost and D.V. Griffiths, to be published.

NCEER-88-0015   "Two- and Three- Dimensional Dynamic Finite Element Analyses of the Long Valley Dam," by D.V. Griffiths and J.H. Prevost, 6/17/88, (PB89-144711, A04, MF-A01).

NCEER-88-0016   "Damage Assessment of Reinforced Concrete Structures in Eastern United States," by A.M. Reinhorn, M.J. Seidel, S.K. Kunnath and Y.J. Park, 6/15/88, (PB89-122220, A04, MF-A01). This report is only available through NTIS (see address given above).

NCEER-88-0017   "Dynamic Compliance of Vertically Loaded Strip Foundations in Multilayered Viscoelastic Soils," by S. Ahmad and A.S.M. Israil, 6/17/88, (PB89-102891, A04, MF-A01).

NCEER-88-0018   "An Experimental Study of Seismic Structural Response With Added Viscoelastic Dampers," by R.C. Lin, Z. Liang, T.T. Soong and R.H. Zhang, 6/30/88, (PB89-122212, A05, MF-A01). This report is available only through NTIS (see address given above).

NCEER-88-0019   "Experimental Investigation of Primary - Secondary System Interaction," by G.D. Manolis, G. Juhn and A.M. Reinhorn, 5/27/88, (PB89-122204, A04, MF-A01).

NCEER-88-0020   "A Response Spectrum Approach For Analysis of Nonclassically Damped Structures," by J.N. Yang, S. Sarkani and F.X. Long, 4/22/88, (PB89-102909, A04, MF-A01).

NCEER-88-0021   "Seismic Interaction of Structures and Soils: Stochastic Approach," by A.S. Veletsos and A.M. Prasad, 7/21/88, (PB89-122196, A04, MF-A01). This report is only available through NTIS (see address given above).

NCEER-88-0022   "Identification of the Serviceability Limit State and Detection of Seismic Structural Damage," by E. DiPasquale and A.S. Cakmak, 6/15/88, (PB89-122188, A05, MF-A01). This report is available only through NTIS (see address given above).

NCEER-88-0023   "Multi-Hazard Risk Analysis: Case of a Simple Offshore Structure," by B.K. Bhartia and E.H. Vanmarcke, 7/21/88, (PB89-145213, A05, MF-A01).

NCEER-88-0024   "Automated Seismic Design of Reinforced Concrete Buildings," by Y.S. Chung, C. Meyer and M. Shinozuka, 7/5/88, (PB89-122170, A06, MF-A01). This report is available only through NTIS (see address given above).

NCEER-88-0025   "Experimental Study of Active Control of MDOF Structures Under Seismic Excitations," by L.L. Chung, R.C. Lin, T.T. Soong and A.M. Reinhorn, 7/10/88, (PB89-122600, A04, MF-A01).

NCEER-88-0026   "Earthquake Simulation Tests of a Low-Rise Metal Structure," by J.S. Hwang, K.C. Chang, G.C. Lee and R.L. Ketter, 8/1/88, (PB89-102917, A04, MF-A01).

NCEER-88-0027   "Systems Study of Urban Response and Reconstruction Due to Catastrophic Earthquakes," by F. Kozin and H.K. Zhou, 9/22/88, (PB90-162348, A04, MF-A01).

NCEER-88-0028   "Seismic Fragility Analysis of Plane Frame Structures," by H.H-M. Hwang and Y.K. Low, 7/31/88, (PB89-131445, A06, MF-A01).

NCEER-88-0029   "Response Analysis of Stochastic Structures," by A. Kardara, C. Bucher and M. Shinozuka, 9/22/88, (PB89-174429, A04, MF-A01).

NCEER-88-0030   "Nonnormal Accelerations Due to Yielding in a Primary Structure," by D.C.K. Chen and L.D. Lutes, 9/19/88, (PB89-131437, A04, MF-A01).

NCEER-88-0031   "Design Approaches for Soil-Structure Interaction," by A.S. Veletsos, A.M. Prasad and Y. Tang, 12/30/88, (PB89-174437, A03, MF-A01). This report is available only through NTIS (see address given above).

NCEER-88-0032   "A Re-evaluation of Design Spectra for Seismic Damage Control," by C.J. Turkstra and A.G. Tallin, 11/7/88, (PB89-145221, A05, MF-A01).

NCEER-88-0033   "The Behavior and Design of Noncontact Lap Splices Subjected to Repeated Inelastic Tensile Loading," by V.E. Sagan, P. Gergely and R.N. White, 12/8/88, (PB89-163737, A08, MF-A01).

NCEER-88-0034   "Seismic Response of Pile Foundations," by S.M. Mamoon, P.K. Banerjee and S. Ahmad, 11/1/88, (PB89-145239, A04, MF-A01).

NCEER-88-0035   "Modeling of R/C Building Structures With Flexible Floor Diaphragms (IDARC2)," by A.M. Reinhorn, S.K. Kunnath and N. Panahshahi, 9/7/88, (PB89-207153, A07, MF-A01).

NCEER-88-0036   "Solution of the Dam-Reservoir Interaction Problem Using a Combination of FEM, BEM with Particular Integrals, Modal Analysis, and Substructuring," by C-S. Tsai, G.C. Lee and R.L. Ketter, 12/31/88, (PB89-207146, A04, MF-A01).

NCEER-88-0037   "Optimal Placement of Actuators for Structural Control," by F.Y. Cheng and C.P. Pantelides, 8/15/88, (PB89-162846, A05, MF-A01).

NCEER-88-0038   "Teflon Bearings in Aseismic Base Isolation: Experimental Studies and Mathematical Modeling," by A. Mokha, M.C. Constantinou and A.M. Reinhorn, 12/5/88, (PB89-218457, A10, MF-A01). This report is available only through NTIS (see address given above).

NCEER-88-0039   "Seismic Behavior of Flat Slab High-Rise Buildings in the New York City Area," by P. Weidlinger and M. Ettouney, 10/15/88, (PB90-145681, A04, MF-A01).

NCEER-88-0040   "Evaluation of the Earthquake Resistance of Existing Buildings in New York City," by P. Weidlinger and M. Ettouney, 10/15/88, to be published.

NCEER-88-0041   "Small-Scale Modeling Techniques for Reinforced Concrete Structures Subjected to Seismic Loads," by W. Kim, A. El-Attar and R.N. White, 11/22/88, (PB89-189625, A05, MF-A01).

NCEER-88-0042   "Modeling Strong Ground Motion from Multiple Event Earthquakes," by G.W. Ellis and A.S. Cakmak, 10/15/88, (PB89-174445, A03, MF-A01).

NCEER-88-0043   "Nonstationary Models of Seismic Ground Acceleration," by M. Grigoriu, S.E. Ruiz and E. Rosenblueth, 7/15/88, (PB89-189617, A04, MF-A01).

NCEER-88-0044   "SARCF User's Guide: Seismic Analysis of Reinforced Concrete Frames," by Y.S. Chung, C. Meyer and M. Shinozuka, 11/9/88, (PB89-174452, A08, MF-A01).

NCEER-88-0045   "First Expert Panel Meeting on Disaster Research and Planning," edited by J. Pantelic and J. Stoyle, 9/15/88, (PB89-174460, A05, MF-A01).

NCEER-88-0046   "Preliminary Studies of the Effect of Degrading Infill Walls on the Nonlinear Seismic Response of Steel Frames," by C.Z. Chrysostomou, P. Gergely and J.F. Abel, 12/19/88, (PB89-208383, A05, MF-A01).

NCEER-88-0047   "Reinforced Concrete Frame Component Testing Facility - Design, Construction, Instrumentation and Operation," by S.P. Pessiki, C. Conley, T. Bond, P. Gergely and R.N. White, 12/16/88, (PB89-174478, A04, MF-A01).

NCEER-89-0001   "Effects of Protective Cushion and Soil Compliancy on the Response of Equipment Within a Seismically Excited Building," by J.A. HoLung, 2/16/89, (PB89-207179, A04, MF-A01).

NCEER-89-0002   "Statistical Evaluation of Response Modification Factors for Reinforced Concrete Structures," by H.H-M. Hwang and J-W. Jaw, 2/17/89, (PB89-207187, A05, MF-A01).

NCEER-89-0003   "Hysteretic Columns Under Random Excitation," by G-Q. Cai and Y.K. Lin, 1/9/89, (PB89-196513, A03, MF-A01).

NCEER-89-0004   "Experimental Study of `Elephant Foot Bulge' Instability of Thin-Walled Metal Tanks," by Z-H. Jia and R.L. Ketter, 2/22/89, (PB89-207195, A03, MF-A01).

NCEER-89-0005   "Experiment on Performance of Buried Pipelines Across San Andreas Fault," by J. Isenberg, E. Richardson and T.D. O'Rourke, 3/10/89, (PB89-218440, A04, MF-A01). This report is available only through NTIS (see address given above).

NCEER-89-0006   "A Knowledge-Based Approach to Structural Design of Earthquake-Resistant Buildings," by M. Subramani, P. Gergely, C.H. Conley, J.F. Abel and A.H. Zaghw, 1/15/89, (PB89-218465, A06, MF-A01).

NCEER-89-0007   "Liquefaction Hazards and Their Effects on Buried Pipelines," by T.D. O'Rourke and P.A. Lane, 2/1/89, (PB89-218481, A09, MF-A01).

NCEER-89-0008   "Fundamentals of System Identification in Structural Dynamics," by H. Imai, C-B. Yun, O. Maruyama and M. Shinozuka, 1/26/89, (PB89-207211, A04, MF-A01).

NCEER-89-0009   "Effects of the 1985 Michoacan Earthquake on Water Systems and Other Buried Lifelines in Mexico," by A.G. Ayala and M.J. O'Rourke, 3/8/89, (PB89-207229, A06, MF-A01).

NCEER-89-R010   "NCEER Bibliography of Earthquake Education Materials," by K.E.K. Ross, Second Revision, 9/1/89, (PB90-125352, A05, MF-A01). This report is replaced by NCEER-92-0018.

NCEER-89-0011   "Inelastic Three-Dimensional Response Analysis of Reinforced Concrete Building Structures (IDARC-3D), Part I - Modeling," by S.K. Kunnath and A.M. Reinhorn, 4/17/89, (PB90-114612, A07, MF-A01). This report is available only through NTIS (see address given above).

NCEER-89-0012   "Recommended Modifications to ATC-14," by C.D. Poland and J.O. Malley, 4/12/89, (PB90-108648, A15, MF-A01).

NCEER-89-0013   "Repair and Strengthening of Beam-to-Column Connections Subjected to Earthquake Loading," by M. Corazao and A.J. Durrani, 2/28/89, (PB90-109885, A06, MF-A01).

NCEER-89-0014   "Program EXKAL2 for Identification of Structural Dynamic Systems," by O. Maruyama, C-B. Yun, M. Hoshiya and M. Shinozuka, 5/19/89, (PB90-109877, A09, MF-A01).

NCEER-89-0015   "Response of Frames With Bolted Semi-Rigid Connections, Part I - Experimental Study and Analytical Predictions," by P.J. DiCorso, A.M. Reinhorn, J.R. Dickerson, J.B. Radziminski and W.L. Harper, 6/1/89, to be published.

NCEER-89-0016   "ARMA Monte Carlo Simulation in Probabilistic Structural Analysis," by P.D. Spanos and M.P. Mignolet, 7/10/89, (PB90-109893, A03, MF-A01).

NCEER-89-P017   "Preliminary Proceedings from the Conference on Disaster Preparedness - The Place of Earthquake Education in Our Schools," Edited by K.E.K. Ross, 6/23/89, (PB90-108606, A03, MF-A01).

NCEER-89-0017   "Proceedings from the Conference on Disaster Preparedness - The Place of Earthquake Education in Our Schools," Edited by K.E.K. Ross, 12/31/89, (PB90-207895, A012, MF-A02). This report is available only through NTIS (see address given above).

NCEER-89-0018   "Multidimensional Models of Hysteretic Material Behavior for Vibration Analysis of Shape Memory Energy Absorbing Devices, by E.J. Graesser and F.A. Cozzarelli, 6/7/89, (PB90-164146, A04, MF-A01).

NCEER-89-0019   "Nonlinear Dynamic Analysis of Three-Dimensional Base Isolated Structures (3D-BASIS)," by S. Nagarajaiah, A.M. Reinhorn and M.C. Constantinou, 8/3/89, (PB90-161936, A06, MF-A01). This report has been replaced by NCEER-93-0011.

NCEER-89-0020   "Structural Control Considering Time-Rate of Control Forces and Control Rate Constraints," by F.Y. Cheng and C.P. Pantelides, 8/3/89, (PB90-120445, A04, MF-A01).

NCEER-89-0021   "Subsurface Conditions of Memphis and Shelby County," by K.W. Ng, T-S. Chang and H-H.M. Hwang, 7/26/89, (PB90-120437, A03, MF-A01).

NCEER-89-0022   "Seismic Wave Propagation Effects on Straight Jointed Buried Pipelines," by K. Elhmadi and M.J. O'Rourke, 8/24/89, (PB90-162322, A10, MF-A02).

NCEER-89-0023   "Workshop on Serviceability Analysis of Water Delivery Systems," edited by M. Grigoriu, 3/6/89, (PB90-127424, A03, MF-A01).

NCEER-89-0024   "Shaking Table Study of a 1/5 Scale Steel Frame Composed of Tapered Members," by K.C. Chang, J.S. Hwang and G.C. Lee, 9/18/89, (PB90-160169, A04, MF-A01).

NCEER-89-0025   "DYNA1D: A Computer Program for Nonlinear Seismic Site Response Analysis - Technical Documentation," by Jean H. Prevost, 9/14/89, (PB90-161944, A07, MF-A01). This report is available only through NTIS (see address given above).

NCEER-89-0026   "1:4 Scale Model Studies of Active Tendon Systems and Active Mass Dampers for Aseismic Protection," by A.M. Reinhorn, T.T. Soong, R.C. Lin, Y.P. Yang, Y. Fukao, H. Abe and M. Nakai, 9/15/89, (PB90-173246, A10, MF-A02). This report is available only through NTIS (see address given above).

NCEER-89-0027   "Scattering of Waves by Inclusions in a Nonhomogeneous Elastic Half Space Solved by Boundary Element Methods," by P.K. Hadley, A. Askar and A.S. Cakmak, 6/15/89, (PB90-145699, A07, MF-A01).

NCEER-89-0028   "Statistical Evaluation of Deflection Amplification Factors for Reinforced Concrete Structures," by H.H.M. Hwang, J-W. Jaw and A.L. Ch'ng, 8/31/89, (PB90-164633, A05, MF-A01).

NCEER-89-0029   "Bedrock Accelerations in Memphis Area Due to Large New Madrid Earthquakes," by H.H.M. Hwang, C.H.S. Chen and G. Yu, 11/7/89, (PB90-162330, A04, MF-A01).

NCEER-89-0030   "Seismic Behavior and Response Sensitivity of Secondary Structural Systems," by Y.Q. Chen and T.T. Soong, 10/23/89, (PB90-164658, A08, MF-A01).

NCEER-89-0031   "Random Vibration and Reliability Analysis of Primary-Secondary Structural Systems," by Y. Ibrahim, M. Grigoriu and T.T. Soong, 11/10/89, (PB90-161951, A04, MF-A01).

NCEER-89-0032   "Proceedings from the Second U.S. - Japan Workshop on Liquefaction, Large Ground Deformation and Their Effects on Lifelines, September 26-29, 1989," Edited by T.D. O'Rourke and M. Hamada, 12/1/89, (PB90-209388, A22, MF-A03).

NCEER-89-0033   "Deterministic Model for Seismic Damage Evaluation of Reinforced Concrete Structures," by J.M. Bracci, A.M. Reinhorn, J.B. Mander and S.K. Kunnath, 9/27/89, (PB91-108803, A06, MF-A01).

NCEER-89-0034   "On the Relation Between Local and Global Damage Indices," by E. DiPasquale and A.S. Cakmak, 8/15/89, (PB90-173865, A05, MF-A01).

NCEER-89-0035   "Cyclic Undrained Behavior of Nonplastic and Low Plasticity Silts," by A.J. Walker and H.E. Stewart, 7/26/89, (PB90-183518, A10, MF-A01).

NCEER-89-0036   "Liquefaction Potential of Surficial Deposits in the City of Buffalo, New York," by M. Budhu, R. Giese and L. Baumgrass, 1/17/89, (PB90-208455, A04, MF-A01).

NCEER-89-0037   "A Deterministic Assessment of Effects of Ground Motion Incoherence," by A.S. Veletsos and Y. Tang, 7/15/89, (PB90-164294, A03, MF-A01).

NCEER-89-0038   "Workshop on Ground Motion Parameters for Seismic Hazard Mapping," July 17-18, 1989, edited by R.V. Whitman, 12/1/89, (PB90-173923, A04, MF-A01).

NCEER-89-0039   "Seismic Effects on Elevated Transit Lines of the New York City Transit Authority," by C.J. Costantino, C.A. Miller and E. Heymsfield, 12/26/89, (PB90-207887, A06, MF-A01).

NCEER-89-0040   "Centrifugal Modeling of Dynamic Soil-Structure Interaction," by K. Weissman, Supervised by J.H. Prevost, 5/10/89, (PB90-207879, A07, MF-A01).

NCEER-89-0041   "Linearized Identification of Buildings With Cores for Seismic Vulnerability Assessment," by I-K. Ho and A.E. Aktan, 11/1/89, (PB90-251943, A07, MF-A01).

NCEER-90-0001   "Geotechnical and Lifeline Aspects of the October 17, 1989 Loma Prieta Earthquake in San Francisco," by T.D. O'Rourke, H.E. Stewart, F.T. Blackburn and T.S. Dickerman, 1/90, (PB90-208596, A05, MF-A01).

NCEER-90-0002   "Nonnormal Secondary Response Due to Yielding in a Primary Structure," by D.C.K. Chen and L.D. Lutes, 2/28/90, (PB90-251976, A07, MF-A01).

NCEER-90-0003   "Earthquake Education Materials for Grades K-12," by K.E.K. Ross, 4/16/90, (PB91-251984, A05, MF-A05). This report has been replaced by NCEER-92-0018.

NCEER-90-0004   "Catalog of Strong Motion Stations in Eastern North America," by R.W. Busby, 4/3/90, (PB90-251984, A05, MF-A01).

NCEER-90-0005   "NCEER Strong-Motion Data Base: A User Manual for the GeoBase Release (Version 1.0 for the Sun3)," by P. Friberg and K. Jacob, 3/31/90 (PB90-258062, A04, MF-A01).

NCEER-90-0006   "Seismic Hazard Along a Crude Oil Pipeline in the Event of an 1811-1812 Type New Madrid Earthquake," by H.H.M. Hwang and C-H.S. Chen, 4/16/90, (PB90-258054, A04, MF-A01).

NCEER-90-0007   "Site-Specific Response Spectra for Memphis Sheahan Pumping Station," by H.H.M. Hwang and C.S. Lee, 5/15/90, (PB91-108811, A05, MF-A01).

NCEER-90-0008   "Pilot Study on Seismic Vulnerability of Crude Oil Transmission Systems," by T. Ariman, R. Dobry, M. Grigoriu, F. Kozin, M. O'Rourke, T. O'Rourke and M. Shinozuka, 5/25/90, (PB91-108837, A06, MF-A01).

NCEER-90-0009   "A Program to Generate Site Dependent Time Histories: EQGEN," by G.W. Ellis, M. Srinivasan and A.S. Cakmak, 1/30/90, (PB91-108829, A04, MF-A01).

NCEER-90-0010   "Active Isolation for Seismic Protection of Operating Rooms," by M.E. Talbott, Supervised by M. Shinozuka, 6/8/9, (PB91-110205, A05, MF-A01).

NCEER-90-0011   "Program LINEARID for Identification of Linear Structural Dynamic Systems," by C-B. Yun and M. Shinozuka, 6/25/90, (PB91-110312, A08, MF-A01).

NCEER-90-0012   "Two-Dimensional Two-Phase Elasto-Plastic Seismic Response of Earth Dams," by A.N. Yiagos, Supervised by J.H. Prevost, 6/20/90, (PB91-110197, A13, MF-A02).

NCEER-90-0013   "Secondary Systems in Base-Isolated Structures: Experimental Investigation, Stochastic Response and Stochastic Sensitivity," by G.D. Manolis, G. Juhn, M.C. Constantinou and A.M. Reinhorn, 7/1/90, (PB91-110320, A08, MF-A01).

NCEER-90-0014   "Seismic Behavior of Lightly-Reinforced Concrete Column and Beam-Column Joint Details," by S.P. Pessiki, C.H. Conley, P. Gergely and R.N. White, 8/22/90, (PB91-108795, A11, MF-A02).

NCEER-90-0015   "Two Hybrid Control Systems for Building Structures Under Strong Earthquakes," by J.N. Yang and A. Danielians, 6/29/90, (PB91-125393, A04, MF-A01).

NCEER-90-0016   "Instantaneous Optimal Control with Acceleration and Velocity Feedback," by J.N. Yang and Z. Li, 6/29/90, (PB91-125401, A03, MF-A01).

NCEER-90-0017   "Reconnaissance Report on the Northern Iran Earthquake of June 21, 1990," by M. Mehrain, 10/4/90, (PB91-125377, A03, MF-A01).

NCEER-90-0018   "Evaluation of Liquefaction Potential in Memphis and Shelby County," by T.S. Chang, P.S. Tang, C.S. Lee and H. Hwang, 8/10/90, (PB91-125427, A09, MF-A01).

NCEER-90-0019   "Experimental and Analytical Study of a Combined Sliding Disc Bearing and Helical Steel Spring Isolation System," by M.C. Constantinou, A.S. Mokha and A.M. Reinhorn, 10/4/90, (PB91-125385, A06, MF-A01). This report is available only through NTIS (see address given above).

NCEER-90-0020   "Experimental Study and Analytical Prediction of Earthquake Response of a Sliding Isolation System with a Spherical Surface," by A.S. Mokha, M.C. Constantinou and A.M. Reinhorn, 10/11/90, (PB91-125419, A05, MF-A01).

NCEER-90-0021   "Dynamic Interaction Factors for Floating Pile Groups," by G. Gazetas, K. Fan, A. Kaynia and E. Kausel, 9/10/90, (PB91-170381, A05, MF-A01).

NCEER-90-0022   "Evaluation of Seismic Damage Indices for Reinforced Concrete Structures," by S. Rodriguez-Gomez and A.S. Cakmak, 9/30/90, PB91-171322, A06, MF-A01).

NCEER-90-0023   "Study of Site Response at a Selected Memphis Site," by H. Desai, S. Ahmad, E.S. Gazetas and M.R. Oh, 10/11/90, (PB91-196857, A03, MF-A01).

NCEER-90-0024   "A User's Guide to Strongmo: Version 1.0 of NCEER's Strong-Motion Data Access Tool for PCs and Terminals," by P.A. Friberg and C.A.T. Susch, 11/15/90, (PB91-171272, A03, MF-A01).

NCEER-90-0025   "A Three-Dimensional Analytical Study of Spatial Variability of Seismic Ground Motions," by L-L. Hong and A.H.-S. Ang, 10/30/90, (PB91-170399, A09, MF-A01).

NCEER-90-0026   "MUMOID User's Guide - A Program for the Identification of Modal Parameters," by S. Rodriguez-Gomez and E. DiPasquale, 9/30/90, (PB91-171298, A04, MF-A01).

NCEER-90-0027   "SARCF-II User's Guide - Seismic Analysis of Reinforced Concrete Frames," by S. Rodriguez-Gomez, Y.S. Chung and C. Meyer, 9/30/90, (PB91-171280, A05, MF-A01).

NCEER-90-0028   "Viscous Dampers: Testing, Modeling and Application in Vibration and Seismic Isolation," by N. Makris and M.C. Constantinou, 12/20/90 (PB91-190561, A06, MF-A01).

NCEER-90-0029   "Soil Effects on Earthquake Ground Motions in the Memphis Area," by H. Hwang, C.S. Lee, K.W. Ng and T.S. Chang, 8/2/90, (PB91-190751, A05, MF-A01).

NCEER-91-0001   "Proceedings from the Third Japan-U.S. Workshop on Earthquake Resistant Design of Lifeline Facilities and Countermeasures for Soil Liquefaction, December 17-19, 1990," edited by T.D. O'Rourke and M. Hamada, 2/1/91, (PB91-179259, A99, MF-A04).

NCEER-91-0002   "Physical Space Solutions of Non-Proportionally Damped Systems," by M. Tong, Z. Liang and G.C. Lee, 1/15/91, (PB91-179242, A04, MF-A01).

NCEER-91-0003   "Seismic Response of Single Piles and Pile Groups," by K. Fan and G. Gazetas, 1/10/91, (PB92-174994, A04, MF-A01).

NCEER-91-0004   "Damping of Structures: Part 1 - Theory of Complex Damping," by Z. Liang and G. Lee, 10/10/91, (PB92-197235, A12, MF-A03).

NCEER-91-0005   "3D-BASIS - Nonlinear Dynamic Analysis of Three Dimensional Base Isolated Structures: Part II," by S. Nagarajaiah, A.M. Reinhorn and M.C. Constantinou, 2/28/91, (PB91-190553, A07, MF-A01). This report has been replaced by NCEER-93-0011.

NCEER-91-0006   "A Multidimensional Hysteretic Model for Plasticity Deforming Metals in Energy Absorbing Devices," by E.J. Graesser and F.A. Cozzarelli, 4/9/91, (PB92-108364, A04, MF-A01).

NCEER-91-0007   "A Framework for Customizable Knowledge-Based Expert Systems with an Application to a KBES for Evaluating the Seismic Resistance of Existing Buildings," by E.G. Ibarra-Anaya and S.J. Fenves, 4/9/91, (PB91-210930, A08, MF-A01).

NCEER-91-0008   "Nonlinear Analysis of Steel Frames with Semi-Rigid Connections Using the Capacity Spectrum Method," by G.G. Deierlein, S-H. Hsieh, Y-J. Shen and J.F. Abel, 7/2/91, (PB92-113828, A05, MF-A01).

NCEER-91-0009   "Earthquake Education Materials for Grades K-12," by K.E.K. Ross, 4/30/91, (PB91-212142, A06, MF-A01). This report has been replaced by NCEER-92-0018.

NCEER-91-0010   "Phase Wave Velocities and Displacement Phase Differences in a Harmonically Oscillating Pile," by N. Makris and G. Gazetas, 7/8/91, (PB92-108356, A04, MF-A01).

NCEER-91-0011   "Dynamic Characteristics of a Full-Size Five-Story Steel Structure and a 2/5 Scale Model," by K.C. Chang, G.C. Yao, G.C. Lee, D.S. Hao and Y.C. Yeh," 7/2/91, (PB93-116648, A06, MF-A02).

NCEER-91-0012   "Seismic Response of a 2/5 Scale Steel Structure with Added Viscoelastic Dampers," by K.C. Chang, T.T. Soong, S-T. Oh and M.L. Lai, 5/17/91, (PB92-110816, A05, MF-A01).

NCEER-91-0013   "Earthquake Response of Retaining Walls; Full-Scale Testing and Computational Modeling," by S. Alampalli and A-W.M. Elgamal, 6/20/91, to be published.

NCEER-91-0014   "3D-BASIS-M: Nonlinear Dynamic Analysis of Multiple Building Base Isolated Structures," by P.C. Tsopelas, S. Nagarajaiah, M.C. Constantinou and A.M. Reinhorn, 5/28/91, (PB92-113885, A09, MF-A02).

NCEER-91-0015   "Evaluation of SEAOC Design Requirements for Sliding Isolated Structures," by D. Theodossiou and M.C. Constantinou, 6/10/91, (PB92-114602, A11, MF-A03).

NCEER-91-0016   "Closed-Loop Modal Testing of a 27-Story Reinforced Concrete Flat Plate-Core Building," by H.R. Somaprasad, T. Toksoy, H. Yoshiyuki and A.E. Aktan, 7/15/91, (PB92-129980, A07, MF-A02).

NCEER-91-0017   "Shake Table Test of a 1/6 Scale Two-Story Lightly Reinforced Concrete Building," by A.G. El-Attar, R.N. White and P. Gergely, 2/28/91, (PB92-222447, A06, MF-A02).

NCEER-91-0018   "Shake Table Test of a 1/8 Scale Three-Story Lightly Reinforced Concrete Building," by A.G. El-Attar, R.N. White and P. Gergely, 2/28/91, (PB93-116630, A08, MF-A02).

NCEER-91-0019   "Transfer Functions for Rigid Rectangular Foundations," by A.S. Veletsos, A.M. Prasad and W.H. Wu, 7/31/91, to be published.

NCEER-91-0020   "Hybrid Control of Seismic-Excited Nonlinear and Inelastic Structural Systems," by J.N. Yang, Z. Li and A. Danielians, 8/1/91, (PB92-143171, A06, MF-A02).

NCEER-91-0021   "The NCEER-91 Earthquake Catalog: Improved Intensity-Based Magnitudes and Recurrence Relations for U.S. Earthquakes East of New Madrid," by L. Seeber and J.G. Armbruster, 8/28/91, (PB92-176742, A06, MF-A02).

NCEER-91-0022   "Proceedings from the Implementation of Earthquake Planning and Education in Schools: The Need for Change - The Roles of the Changemakers," by K.E.K. Ross and F. Winslow, 7/23/91, (PB92-129998, A12, MF-A03).

NCEER-91-0023   "A Study of Reliability-Based Criteria for Seismic Design of Reinforced Concrete Frame Buildings," by H.H.M. Hwang and H-M. Hsu, 8/10/91, (PB92-140235, A09, MF-A02).

NCEER-91-0024   "Experimental Verification of a Number of Structural System Identification Algorithms," by R.G. Ghanem, H. Gavin and M. Shinozuka, 9/18/91, (PB92-176577, A18, MF-A04).

NCEER-91-0025   "Probabilistic Evaluation of Liquefaction Potential," by H.H.M. Hwang and C.S. Lee," 11/25/91, (PB92-143429, A05, MF-A01).

NCEER-91-0026   "Instantaneous Optimal Control for Linear, Nonlinear and Hysteretic Structures - Stable Controllers," by J.N. Yang and Z. Li, 11/15/91, (PB92-163807, A04, MF-A01).

NCEER-91-0027   "Experimental and Theoretical Study of a Sliding Isolation System for Bridges," by M.C. Constantinou, A. Kartoum, A.M. Reinhorn and P. Bradford, 11/15/91, (PB92-176973, A10, MF-A03).

NCEER-92-0001   "Case Studies of Liquefaction and Lifeline Performance During Past Earthquakes, Volume 1: Japanese Case Studies," Edited by M. Hamada and T. O'Rourke, 2/17/92, (PB92-197243, A18, MF-A04).

NCEER-92-0002   "Case Studies of Liquefaction and Lifeline Performance During Past Earthquakes, Volume 2: United States Case Studies," Edited by T. O'Rourke and M. Hamada, 2/17/92, (PB92-197250, A20, MF-A04).

NCEER-92-0003   "Issues in Earthquake Education," Edited by K. Ross, 2/3/92, (PB92-222389, A07, MF-A02).

NCEER-92-0004   "Proceedings from the First U.S. - Japan Workshop on Earthquake Protective Systems for Bridges," Edited by I.G. Buckle, 2/4/92, (PB94-142239, A99, MF-A06).

NCEER-92-0005   "Seismic Ground Motion from a Haskell-Type Source in a Multiple-Layered Half-Space," A.P. Theoharis, G. Deodatis and M. Shinozuka, 1/2/92, to be published.

NCEER-92-0006   "Proceedings from the Site Effects Workshop," Edited by R. Whitman, 2/29/92, (PB92-197201, A04, MF-A01).

NCEER-92-0007   "Engineering Evaluation of Permanent Ground Deformations Due to Seismically-Induced Liquefaction," by M.H. Baziar, R. Dobry and A-W.M. Elgamal, 3/24/92, (PB92-222421, A13, MF-A03).

NCEER-92-0008   "A Procedure for the Seismic Evaluation of Buildings in the Central and Eastern United States," by C.D. Poland and J.O. Malley, 4/2/92, (PB92-222439, A20, MF-A04).

NCEER-92-0009   "Experimental and Analytical Study of a Hybrid Isolation System Using Friction Controllable Sliding Bearings," by M.Q. Feng, S. Fujii and M. Shinozuka, 5/15/92, (PB93-150282, A06, MF-A02).

NCEER-92-0010   "Seismic Resistance of Slab-Column Connections in Existing Non-Ductile Flat-Plate Buildings," by A.J. Durrani and Y. Du, 5/18/92, (PB93-116812, A06, MF-A02).

NCEER-92-0011   "The Hysteretic and Dynamic Behavior of Brick Masonry Walls Upgraded by Ferrocement Coatings Under Cyclic Loading and Strong Simulated Ground Motion," by H. Lee and S.P. Prawel, 5/11/92, to be published.

NCEER-92-0012   "Study of Wire Rope Systems for Seismic Protection of Equipment in Buildings," by G.F. Demetriades, M.C. Constantinou and A.M. Reinhorn, 5/20/92, (PB93-116655, A08, MF-A02).

NCEER-92-0013   "Shape Memory Structural Dampers: Material Properties, Design and Seismic Testing," by P.R. Witting and F.A. Cozzarelli, 5/26/92, (PB93-116663, A05, MF-A01).

NCEER-92-0014   "Longitudinal Permanent Ground Deformation Effects on Buried Continuous Pipelines," by M.J. O'Rourke, and C. Nordberg, 6/15/92, (PB93-116671, A08, MF-A02).

NCEER-92-0015   "A Simulation Method for Stationary Gaussian Random Functions Based on the Sampling Theorem," by M. Grigoriu and S. Balopoulou, 6/11/92, (PB93-127496, A05, MF-A01).

NCEER-92-0016   "Gravity-Load-Designed Reinforced Concrete Buildings: Seismic Evaluation of Existing Construction and Detailing Strategies for Improved Seismic Resistance," by G.W. Hoffmann, S.K. Kunnath, A.M. Reinhorn and J.B. Mander, 7/15/92, (PB94-142007, A08, MF-A02).

NCEER-92-0017   "Observations on Water System and Pipeline Performance in the Limón Area of Costa Rica Due to the April 22, 1991 Earthquake," by M. O'Rourke and D. Ballantyne, 6/30/92, (PB93-126811, A06, MF-A02).

NCEER-92-0018   "Fourth Edition of Earthquake Education Materials for Grades K-12," Edited by K.E.K. Ross, 8/10/92, (PB93-114023, A07, MF-A02).

NCEER-92-0019   "Proceedings from the Fourth Japan-U.S. Workshop on Earthquake Resistant Design of Lifeline Facilities and Countermeasures for Soil Liquefaction," Edited by M. Hamada and T.D. O'Rourke, 8/12/92, (PB93-163939, A99, MF-E11).

NCEER-92-0020   "Active Bracing System: A Full Scale Implementation of Active Control," by A.M. Reinhorn, T.T. Soong, R.C. Lin, M.A. Riley, Y.P. Wang, S. Aizawa and M. Higashino, 8/14/92, (PB93-127512, A06, MF-A02).

NCEER-92-0021   "Empirical Analysis of Horizontal Ground Displacement Generated by Liquefaction-Induced Lateral Spreads," by S.F. Bartlett and T.L. Youd, 8/17/92, (PB93-188241, A06, MF-A02).

NCEER-92-0022   "IDARC Version 3.0: Inelastic Damage Analysis of Reinforced Concrete Structures," by S.K. Kunnath, A.M. Reinhorn and R.F. Lobo, 8/31/92, (PB93-227502, A07, MF-A02).

NCEER-92-0023   "A Semi-Empirical Analysis of Strong-Motion Peaks in Terms of Seismic Source, Propagation Path and Local Site Conditions, by M. Kamiyama, M.J. O'Rourke and R. Flores-Berrones, 9/9/92, (PB93-150266, A08, MF-A02).

NCEER-92-0024   "Seismic Behavior of Reinforced Concrete Frame Structures with Nonductile Details, Part I: Summary of Experimental Findings of Full Scale Beam-Column Joint Tests," by A. Beres, R.N. White and P. Gergely, 9/30/92, (PB93-227783, A05, MF-A01).

NCEER-92-0025   "Experimental Results of Repaired and Retrofitted Beam-Column Joint Tests in Lightly Reinforced Concrete Frame Buildings," by A. Beres, S. El-Borgi, R.N. White and P. Gergely, 10/29/92, (PB93-227791, A05, MF-A01).

NCEER-92-0026   "A Generalization of Optimal Control Theory: Linear and Nonlinear Structures," by J.N. Yang, Z. Li and S. Vongchavalitkul, 11/2/92, (PB93-188621, A05, MF-A01).

NCEER-92-0027   "Seismic Resistance of Reinforced Concrete Frame Structures Designed Only for Gravity Loads: Part I - Design and Properties of a One-Third Scale Model Structure," by J.M. Bracci, A.M. Reinhorn and J.B. Mander, 12/1/92, (PB94-104502, A08, MF-A02).

NCEER-92-0028   "Seismic Resistance of Reinforced Concrete Frame Structures Designed Only for Gravity Loads: Part II - Experimental Performance of Subassemblages," by L.E. Aycardi, J.B. Mander and A.M. Reinhorn, 12/1/92, (PB94-104510, A08, MF-A02).

NCEER-92-0029   "Seismic Resistance of Reinforced Concrete Frame Structures Designed Only for Gravity Loads: Part III - Experimental Performance and Analytical Study of a Structural Model," by J.M. Bracci, A.M. Reinhorn and J.B. Mander, 12/1/92, (PB93-227528, A09, MF-A01).

NCEER-92-0030   "Evaluation of Seismic Retrofit of Reinforced Concrete Frame Structures: Part I - Experimental Performance of Retrofitted Subassemblages," by D. Choudhuri, J.B. Mander and A.M. Reinhorn, 12/8/92, (PB93-198307, A07, MF-A02).

NCEER-92-0031   "Evaluation of Seismic Retrofit of Reinforced Concrete Frame Structures: Part II - Experimental Performance and Analytical Study of a Retrofitted Structural Model," by J.M. Bracci, A.M. Reinhorn and J.B. Mander, 12/8/92, (PB93-198315, A09, MF-A03).

NCEER-92-0032   "Experimental and Analytical Investigation of Seismic Response of Structures with Supplemental Fluid Viscous Dampers," by M.C. Constantinou and M.D. Symans, 12/21/92, (PB93-191435, A10, MF-A03). This report is available only through NTIS (see address given above).

NCEER-92-0033   "Reconnaissance Report on the Cairo, Egypt Earthquake of October 12, 1992," by M. Khater, 12/23/92, (PB93-188621, A03, MF-A01).

NCEER-92-0034   "Low-Level Dynamic Characteristics of Four Tall Flat-Plate Buildings in New York City," by H. Gavin, S. Yuan, J. Grossman, E. Pekelis and K. Jacob, 12/28/92, (PB93-188217, A07, MF-A02).

NCEER-93-0001   "An Experimental Study on the Seismic Performance of Brick-Infilled Steel Frames With and Without Retrofit," by J.B. Mander, B. Nair, K. Wojtkowski and J. Ma, 1/29/93, (PB93-227510, A07, MF-A02).

NCEER-93-0002   "Social Accounting for Disaster Preparedness and Recovery Planning," by S. Cole, E. Pantoja and V. Razak, 2/22/93, (PB94-142114, A12, MF-A03).

NCEER-93-0003   "Assessment of 1991 NEHRP Provisions for Nonstructural Components and Recommended Revisions," by T.T. Soong, G. Chen, Z. Wu, R-H. Zhang and M. Grigoriu, 3/1/93, (PB93-188639, A06, MF-A02).

NCEER-93-0004   "Evaluation of Static and Response Spectrum Analysis Procedures of SEAOC/UBC for Seismic Isolated Structures," by C.W. Winters and M.C. Constantinou, 3/23/93, (PB93-198299, A10, MF-A03).

NCEER-93-0005   "Earthquakes in the Northeast - Are We Ignoring the Hazard? A Workshop on Earthquake Science and Safety for Educators," edited by K.E.K. Ross, 4/2/93, (PB94-103066, A09, MF-A02).

NCEER-93-0006   "Inelastic Response of Reinforced Concrete Structures with Viscoelastic Braces," by R.F. Lobo, J.M. Bracci, K.L. Shen, A.M. Reinhorn and T.T. Soong, 4/5/93, (PB93-227486, A05, MF-A02).

NCEER-93-0007   "Seismic Testing of Installation Methods for Computers and Data Processing Equipment," by K. Kosar, T.T. Soong, K.L. Shen, J.A. HoLung and Y.K. Lin, 4/12/93, (PB93-198299, A07, MF-A02).

NCEER-93-0008   "Retrofit of Reinforced Concrete Frames Using Added Dampers," by A. Reinhorn, M. Constantinou and C. Li, to be published.

NCEER-93-0009   "Seismic Behavior and Design Guidelines for Steel Frame Structures with Added Viscoelastic Dampers," by K.C. Chang, M.L. Lai, T.T. Soong, D.S. Hao and Y.C. Yeh, 5/1/93, (PB94-141959, A07, MF-A02).

NCEER-93-0010   "Seismic Performance of Shear-Critical Reinforced Concrete Bridge Piers," by J.B. Mander, S.M. Waheed, M.T.A. Chaudhary and S.S. Chen, 5/12/93, (PB93-227494, A08, MF-A02).

NCEER-93-0011   "3D-BASIS-TABS: Computer Program for Nonlinear Dynamic Analysis of Three Dimensional Base Isolated Structures," by S. Nagarajaiah, C. Li, A.M. Reinhorn and M.C. Constantinou, 8/2/93, (PB94-141819, A09, MF-A02).

NCEER-93-0012   "Effects of Hydrocarbon Spills from an Oil Pipeline Break on Ground Water," by O.J. Helweg and H.H.M. Hwang, 8/3/93, (PB94-141942, A06, MF-A02).

NCEER-93-0013   "Simplified Procedures for Seismic Design of Nonstructural Components and Assessment of Current Code Provisions," by M.P. Singh, L.E. Suarez, E.E. Matheu and G.O. Maldonado, 8/4/93, (PB94-141827, A09, MF-A02).

NCEER-93-0014   "An Energy Approach to Seismic Analysis and Design of Secondary Systems," by G. Chen and T.T. Soong, 8/6/93, (PB94-142767, A11, MF-A03).

NCEER-93-0015   "Proceedings from School Sites: Becoming Prepared for Earthquakes - Commemorating the Third Anniversary of the Loma Prieta Earthquake," Edited by F.E. Winslow and K.E.K. Ross, 8/16/93, (PB94-154275, A16, MF-A02).

NCEER-93-0016   "Reconnaissance Report of Damage to Historic Monuments in Cairo, Egypt Following the October 12, 1992 Dahshur Earthquake," by D. Sykora, D. Look, G. Croci, E. Karaesmen and E. Karaesmen, 8/19/93, (PB94-142221, A08, MF-A02).

NCEER-93-0017   "The Island of Guam Earthquake of August 8, 1993," by S.W. Swan and S.K. Harris, 9/30/93, (PB94-141843, A04, MF-A01).

NCEER-93-0018   "Engineering Aspects of the October 12, 1992 Egyptian Earthquake," by A.W. Elgamal, M. Amer, K. Adalier and A. Abul-Fadl, 10/7/93, (PB94-141983, A05, MF-A01).

NCEER-93-0019   "Development of an Earthquake Motion Simulator and its Application in Dynamic Centrifuge Testing," by I. Krstelj, Supervised by J.H. Prevost, 10/23/93, (PB94-181773, A-10, MF-A03).

NCEER-93-0020   "NCEER-Taisei Corporation Research Program on Sliding Seismic Isolation Systems for Bridges: Experimental and Analytical Study of a Friction Pendulum System (FPS)," by M.C. Constantinou, P. Tsopelas, Y-S. Kim and S. Okamoto, 11/1/93, (PB94-142775, A08, MF-A02).

NCEER-93-0021   "Finite Element Modeling of Elastomeric Seismic Isolation Bearings," by L.J. Billings, Supervised by R. Shepherd, 11/8/93, to be published.

NCEER-93-0022   "Seismic Vulnerability of Equipment in Critical Facilities: Life-Safety and Operational Consequences," by K. Porter, G.S. Johnson, M.M. Zadeh, C. Scawthorn and S. Eder, 11/24/93, (PB94-181765, A16, MF-A03).

NCEER-93-0023   "Hokkaido Nansei-oki, Japan Earthquake of July 12, 1993, by P.I. Yanev and C.R. Scawthorn, 12/23/93, (PB94-181500, A07, MF-A01).

NCEER-94-0001   "An Evaluation of Seismic Serviceability of Water Supply Networks with Application to the San Francisco Auxiliary Water Supply System," by I. Markov, Supervised by M. Grigoriu and T. O'Rourke, 1/21/94, (PB94-204013, A07, MF-A02).

NCEER-94-0002   "NCEER-Taisei Corporation Research Program on Sliding Seismic Isolation Systems for Bridges: Experimental and Analytical Study of Systems Consisting of Sliding Bearings, Rubber Restoring Force Devices and Fluid Dampers," Volumes I and II, by P. Tsopelas, S. Okamoto, M.C. Constantinou, D. Ozaki and S. Fujii, 2/4/94, (PB94-181740, A09, MF-A02 and PB94-181757, A12, MF-A03).

NCEER-94-0003   "A Markov Model for Local and Global Damage Indices in Seismic Analysis," by S. Rahman and M. Grigoriu, 2/18/94, (PB94-206000, A12, MF-A03).

NCEER-94-0004   "Proceedings from the NCEER Workshop on Seismic Response of Masonry Infills," edited by D.P. Abrams, 3/1/94, (PB94-180783, A07, MF-A02).

NCEER-94-0005   "The Northridge, California Earthquake of January 17, 1994: General Reconnaissance Report," edited by J.D. Goltz, 3/11/94, (PB94-193943, A10, MF-A03).

NCEER-94-0006   "Seismic Energy Based Fatigue Damage Analysis of Bridge Columns: Part I - Evaluation of Seismic Capacity," by G.A. Chang and J.B. Mander, 3/14/94, (PB94-219185, A11, MF-A03).

NCEER-94-0007   "Seismic Isolation of Multi-Story Frame Structures Using Spherical Sliding Isolation Systems," by T.M. Al-Hussaini, V.A. Zayas and M.C. Constantinou, 3/17/94, (PB94-193745, A09, MF-A02).

NCEER-94-0008   "The Northridge, California Earthquake of January 17, 1994: Performance of Highway Bridges," edited by I.G. Buckle, 3/24/94, (PB94-193851, A06, MF-A02).

NCEER-94-0009   "Proceedings of the Third U.S.-Japan Workshop on Earthquake Protective Systems for Bridges," edited by I.G. Buckle and I. Friedland, 3/31/94, (PB94-195815, A99, MF-A06).

NCEER-94-0010   "3D-BASIS-ME: Computer Program for Nonlinear Dynamic Analysis of Seismically Isolated Single and Multiple Structures and Liquid Storage Tanks," by P.C. Tsopelas, M.C. Constantinou and A.M. Reinhorn, 4/12/94, (PB94-204922, A09, MF-A02).

NCEER-94-0011   "The Northridge, California Earthquake of January 17, 1994: Performance of Gas Transmission Pipelines," by T.D. O'Rourke and M.C. Palmer, 5/16/94, (PB94-204989, A05, MF-A01).

NCEER-94-0012   "Feasibility Study of Replacement Procedures and Earthquake Performance Related to Gas Transmission Pipelines," by T.D. O'Rourke and M.C. Palmer, 5/25/94, (PB94-206638, A09, MF-A02).

NCEER-94-0013   "Seismic Energy Based Fatigue Damage Analysis of Bridge Columns: Part II - Evaluation of Seismic Demand," by G.A. Chang and J.B. Mander, 6/1/94, (PB95-18106, A08, MF-A02).

NCEER-94-0014   "NCEER-Taisei Corporation Research Program on Sliding Seismic Isolation Systems for Bridges: Experimental and Analytical Study of a System Consisting of Sliding Bearings and Fluid Restoring Force/Damping Devices," by P. Tsopelas and M.C. Constantinou, 6/13/94, (PB94-219144, A10, MF-A03).

NCEER-94-0015   "Generation of Hazard-Consistent Fragility Curves for Seismic Loss Estimation Studies," by H. Hwang and J-R. Huo, 6/14/94, (PB95-181996, A09, MF-A02).

NCEER-94-0016   "Seismic Study of Building Frames with Added Energy-Absorbing Devices," by W.S. Pong, C.S. Tsai and G.C. Lee, 6/20/94, (PB94-219136, A10, A03).

NCEER-94-0017   "Sliding Mode Control for Seismic-Excited Linear and Nonlinear Civil Engineering Structures," by J. Yang, J. Wu, A. Agrawal and Z. Li, 6/21/94, (PB95-138483, A06, MF-A02).

NCEER-94-0018   "3D-BASIS-TABS Version 2.0: Computer Program for Nonlinear Dynamic Analysis of Three Dimensional Base Isolated Structures," by A.M. Reinhorn, S. Nagarajaiah, M.C. Constantinou, P. Tsopelas and R. Li, 6/22/94, (PB95-182176, A08, MF-A02).

NCEER-94-0019   "Proceedings of the International Workshop on Civil Infrastructure Systems: Application of Intelligent Systems and Advanced Materials on Bridge Systems," Edited by G.C. Lee and K.C. Chang, 7/18/94, (PB95-252474, A20, MF-A04).

NCEER-94-0020   "Study of Seismic Isolation Systems for Computer Floors," by V. Lambrou and M.C. Constantinou, 7/19/94, (PB95-138533, A10, MF-A03).

NCEER-94-0021   "Proceedings of the U.S.-Italian Workshop on Guidelines for Seismic Evaluation and Rehabilitation of Unreinforced Masonry Buildings," Edited by D.P. Abrams and G.M. Calvi, 7/20/94, (PB95-138749, A13, MF-A03).

NCEER-94-0022   "NCEER-Taisei Corporation Research Program on Sliding Seismic Isolation Systems for Bridges: Experimental and Analytical Study of a System Consisting of Lubricated PTFE Sliding Bearings and Mild Steel Dampers," by P. Tsopelas and M.C. Constantinou, 7/22/94, (PB95-182184, A08, MF-A02).

NCEER-94-0023   "Development of Reliability-Based Design Criteria for Buildings Under Seismic Load," by Y.K. Wen, H. Hwang and M. Shinozuka, 8/1/94, (PB95-211934, A08, MF-A02).

NCEER-94-0024   "Experimental Verification of Acceleration Feedback Control Strategies for an Active Tendon System," by S.J. Dyke, B.F. Spencer, Jr., P. Quast, M.K. Sain, D.C. Kaspari, Jr. and T.T. Soong, 8/29/94, (PB95-212320, A05, MF-A01).

NCEER-94-0025   "Seismic Retrofitting Manual for Highway Bridges," Edited by I.G. Buckle and I.F. Friedland, published by the Federal Highway Administration (PB95-212676, A15, MF-A03).

NCEER-94-0026   "Proceedings from the Fifth U.S.-Japan Workshop on Earthquake Resistant Design of Lifeline Facilities and Countermeasures Against Soil Liquefaction," Edited by T.D. O'Rourke and M. Hamada, 11/7/94, (PB95-220802, A99, MF-E08).

NCEER-95-0001   "Experimental and Analytical Investigation of Seismic Retrofit of Structures with Supplemental Damping: Part 1 - Fluid Viscous Damping Devices," by A.M. Reinhorn, C. Li and M.C. Constantinou, 1/3/95, (PB95-266599, A09, MF-A02).

NCEER-95-0002   "Experimental and Analytical Study of Low-Cycle Fatigue Behavior of Semi-Rigid Top-And-Seat Angle Connections," by G. Pekcan, J.B. Mander and S.S. Chen, 1/5/95, (PB95-220042, A07, MF-A02).

NCEER-95-0003   "NCEER-ATC Joint Study on Fragility of Buildings," by T. Anagnos, C. Rojahn and A.S. Kiremidjian, 1/20/95, (PB95-220026, A06, MF-A02).

NCEER-95-0004   "Nonlinear Control Algorithms for Peak Response Reduction," by Z. Wu, T.T. Soong, V. Gattulli and R.C. Lin, 2/16/95, (PB95-220349, A05, MF-A01).

NCEER-95-0005   "Pipeline Replacement Feasibility Study: A Methodology for Minimizing Seismic and Corrosion Risks to Underground Natural Gas Pipelines," by R.T. Eguchi, H.A. Seligson and D.G. Honegger, 3/2/95, (PB95-252326, A06, MF-A02).

NCEER-95-0006   "Evaluation of Seismic Performance of an 11-Story Frame Building During the 1994 Northridge Earthquake," by F. Naeim, R. DiSulio, K. Benuska, A. Reinhorn and C. Li, to be published.

NCEER-95-0007   "Prioritization of Bridges for Seismic Retrofitting," by N. Basöz and A.S. Kiremidjian, 4/24/95, (PB95-252300, A08, MF-A02).

NCEER-95-0008   "Method for Developing Motion Damage Relationships for Reinforced Concrete Frames," by A. Singhal and A.S. Kiremidjian, 5/11/95, (PB95-266607, A06, MF-A02).

NCEER-95-0009   "Experimental and Analytical Investigation of Seismic Retrofit of Structures with Supplemental Damping: Part II - Friction Devices," by C. Li and A.M. Reinhorn, 7/6/95, (PB96-128087, A11, MF-A03).

NCEER-95-0010   "Experimental Performance and Analytical Study of a Non-Ductile Reinforced Concrete Frame Structure Retrofitted with Elastomeric Spring Dampers," by G. Pekcan, J.B. Mander and S.S. Chen, 7/14/95, (PB96-137161, A08, MF-A02).

NCEER-95-0011   "Development and Experimental Study of Semi-Active Fluid Damping Devices for Seismic Protection of Structures," by M.D. Symans and M.C. Constantinou, 8/3/95, (PB96-136940, A23, MF-A04).

NCEER-95-0012   "Real-Time Structural Parameter Modification (RSPM): Development of Innervated Structures," by Z. Liang, M. Tong and G.C. Lee, 4/11/95, (PB96-137153, A06, MF-A01).

NCEER-95-0013   "Experimental and Analytical Investigation of Seismic Retrofit of Structures with Supplemental Damping: Part III - Viscous Damping Walls," by A.M. Reinhorn and C. Li, 10/1/95, (PB96-176409, A11, MF-A03).

NCEER-95-0014   "Seismic Fragility Analysis of Equipment and Structures in a Memphis Electric Substation," by J-R. Huo and H.H.M. Hwang, 8/10/95, (PB96-128087, A09, MF-A02).

NCEER-95-0015   "The Hanshin-Awaji Earthquake of January 17, 1995: Performance of Lifelines," Edited by M. Shinozuka, 11/3/95, (PB96-176383, A15, MF-A03).

NCEER-95-0016   "Highway Culvert Performance During Earthquakes," by T.L. Youd and C.J. Beckman, available as NCEER-96-0015.

NCEER-95-0017   "The Hanshin-Awaji Earthquake of January 17, 1995: Performance of Highway Bridges," Edited by I.G. Buckle, 12/1/95, to be published.

NCEER-95-0018   "Modeling of Masonry Infill Panels for Structural Analysis," by A.M. Reinhorn, A. Madan, R.E. Valles, Y. Reichmann and J.B. Mander, 12/8/95, (PB97-110886, MF-A01, A06).

NCEER-95-0019   "Optimal Polynomial Control for Linear and Nonlinear Structures," by A.K. Agrawal and J.N. Yang, 12/11/95, (PB96-168737, A07, MF-A02).

NCEER-95-0020   "Retrofit of Non-Ductile Reinforced Concrete Frames Using Friction Dampers," by R.S. Rao, P. Gergely and R.N. White, 12/22/95, (PB97-133508, A10, MF-A02).

NCEER-95-0021   "Parametric Results for Seismic Response of Pile-Supported Bridge Bents," by G. Mylonakis, A. Nikolaou and G. Gazetas, 12/22/95, (PB97-100242, A12, MF-A03).

NCEER-95-0022   "Kinematic Bending Moments in Seismically Stressed Piles," by A. Nikolaou, G. Mylonakis and G. Gazetas, 12/23/95, (PB97-113914, MF-A03, A13).

NCEER-96-0001   "Dynamic Response of Unreinforced Masonry Buildings with Flexible Diaphragms," by A.C. Costley and D.P. Abrams," 10/10/96, (PB97-133573, MF-A03, A15).

NCEER-96-0002   "State of the Art Review: Foundations and Retaining Structures," by I. Po Lam, to be published.

NCEER-96-0003   "Ductility of Rectangular Reinforced Concrete Bridge Columns with Moderate Confinement," by N. Wehbe, M. Saiidi, D. Sanders and B. Douglas, 11/7/96, (PB97-133557, A06, MF-A02).

NCEER-96-0004   "Proceedings of the Long-Span Bridge Seismic Research Workshop," edited by I.G. Buckle and I.M. Friedland, to be published.

NCEER-96-0005   "Establish Representative Pier Types for Comprehensive Study: Eastern United States," by J. Kulicki and Z. Prucz, 5/28/96, (PB98-119217, A07, MF-A02).

NCEER-96-0006   "Establish Representative Pier Types for Comprehensive Study: Western United States," by R. Imbsen, R.A. Schamber and T.A. Osterkamp, 5/28/96, (PB98-118607, A07, MF-A02).

NCEER-96-0007   "Nonlinear Control Techniques for Dynamical Systems with Uncertain Parameters," by R.G. Ghanem and M.I. Bujakov, 5/27/96, (PB97-100259, A17, MF-A03).

NCEER-96-0008   "Seismic Evaluation of a 30-Year Old Non-Ductile Highway Bridge Pier and Its Retrofit," by J.B. Mander, B. Mahmoodzadegan, S. Bhadra and S.S. Chen, 5/31/96, (PB97-110902, MF-A03, A10).

NCEER-96-0009   "Seismic Performance of a Model Reinforced Concrete Bridge Pier Before and After Retrofit," by J.B. Mander, J.H. Kim and C.A. Ligozio, 5/31/96, (PB97-110910, MF-A02, A10).

NCEER-96-0010   "IDARC2D Version 4.0: A Computer Program for the Inelastic Damage Analysis of Buildings," by R.E. Valles, A.M. Reinhorn, S.K. Kunnath, C. Li and A. Madan, 6/3/96, (PB97-100234, A17, MF-A03).

NCEER-96-0011   "Estimation of the Economic Impact of Multiple Lifeline Disruption: Memphis Light, Gas and Water Division Case Study," by S.E. Chang, H.A. Seligson and R.T. Eguchi, 8/16/96, (PB97-133490, A11, MF-A03).

NCEER-96-0012   "Proceedings from the Sixth Japan-U.S. Workshop on Earthquake Resistant Design of Lifeline Facilities and Countermeasures Against Soil Liquefaction, Edited by M. Hamada and T. O'Rourke, 9/11/96, (PB97-133581, A99, MF-A06).

NCEER-96-0013   "Chemical Hazards, Mitigation and Preparedness in Areas of High Seismic Risk: A Methodology for Estimating the Risk of Post-Earthquake Hazardous Materials Release," by H.A. Seligson, R.T. Eguchi, K.J. Tierney and K. Richmond, 11/7/96, (PB97-133565, MF-A02, A08).

NCEER-96-0014   "Response of Steel Bridge Bearings to Reversed Cyclic Loading," by J.B. Mander, D-K. Kim, S.S. Chen and G.J. Premus, 11/13/96, (PB97-140735, A12, MF-A03).

NCEER-96-0015   "Highway Culvert Performance During Past Earthquakes," by T.L. Youd and C.J. Beckman, 11/25/96, (PB97-133532, A06, MF-A01).

NCEER-97-0001   "Evaluation, Prevention and Mitigation of Pounding Effects in Building Structures," by R.E. Valles and A.M. Reinhorn, 2/20/97, (PB97-159552, A14, MF-A03).

NCEER-97-0002   "Seismic Design Criteria for Bridges and Other Highway Structures," by C. Rojahn, R. Mayes, D.G. Anderson, J. Clark, J.H. Hom, R.V. Nutt and M.J. O'Rourke, 4/30/97, (PB97-194658, A06, MF-A03).

NCEER-97-0003   "Proceedings of the U.S.-Italian Workshop on Seismic Evaluation and Retrofit," Edited by D.P. Abrams and G.M. Calvi, 3/19/97, (PB97-194666, A13, MF-A03).

NCEER-97-0004   "Investigation of Seismic Response of Buildings with Linear and Nonlinear Fluid Viscous Dampers," by A.A. Seleemah and M.C. Constantinou, 5/21/97, (PB98-109002, A15, MF-A03).

NCEER-97-0005   "Proceedings of the Workshop on Earthquake Engineering Frontiers in Transportation Facilities," edited by G.C. Lee and I.M. Friedland, 8/29/97, (PB98-128911, A25, MR-A04).

NCEER-97-0006   "Cumulative Seismic Damage of Reinforced Concrete Bridge Piers," by S.K. Kunnath, A. El-Bahy, A. Taylor and W. Stone, 9/2/97, (PB98-108814, A11, MF-A03).

NCEER-97-0007   "Structural Details to Accommodate Seismic Movements of Highway Bridges and Retaining Walls," by R.A. Imbsen, R.A. Schamber, E. Thorkildsen, A. Kartoum, B.T. Martin, T.N. Rosser and J.M. Kulicki, 9/3/97, (PB98-108996, A09, MF-A02).

NCEER-97-0008   "A Method for Earthquake Motion-Damage Relationships with Application to Reinforced Concrete Frames," by A. Singhal and A.S. Kiremidjian, 9/10/97, (PB98-108988, A13, MF-A03).

NCEER-97-0009   "Seismic Analysis and Design of Bridge Abutments Considering Sliding and Rotation," by K. Fishman and R. Richards, Jr., 9/15/97, (PB98-108897, A06, MF-A02).

NCEER-97-0010   "Proceedings of the FHWA/NCEER Workshop on the National Representation of Seismic Ground Motion for New and Existing Highway Facilities," edited by I.M. Friedland, M.S. Power and R.L. Mayes, 9/22/97, (PB98-128903, A21, MF-A04).

NCEER-97-0011   "Seismic Analysis for Design or Retrofit of Gravity Bridge Abutments," by K.L. Fishman, R. Richards, Jr. and R.C. Divito, 10/2/97, (PB98-128937, A08, MF-A02).

NCEER-97-0012   "Evaluation of Simplified Methods of Analysis for Yielding Structures," by P. Tsopelas, M.C. Constantinou, C.A. Kircher and A.S. Whittaker, 10/31/97, (PB98-128929, A10, MF-A03).

NCEER-97-0013   "Seismic Design of Bridge Columns Based on Control and Repairability of Damage," by C-T. Cheng and J.B. Mander, 12/8/97, (PB98-144249, A11, MF-A03).

NCEER-97-0014   "Seismic Resistance of Bridge Piers Based on Damage Avoidance Design," by J.B. Mander and C-T. Cheng, 12/10/97, (PB98-144223, A09, MF-A02).

NCEER-97-0015   "Seismic Response of Nominally Symmetric Systems with Strength Uncertainty," by S. Balopoulou and M. Grigoriu, 12/23/97, (PB98-153422, A11, MF-A03).

NCEER-97-0016   "Evaluation of Seismic Retrofit Methods for Reinforced Concrete Bridge Columns," by T.J. Wipf, F.W. Klaiber and F.M. Russo, 12/28/97, (PB98-144215, A12, MF-A03).

NCEER-97-0017   "Seismic Fragility of Existing Conventional Reinforced Concrete Highway Bridges," by C.L. Mullen and A.S. Cakmak, 12/30/97, (PB98-153406, A08, MF-A02).

NCEER-97-0018   "Loss Asssessment of Memphis Buildings," edited by D.P. Abrams and M. Shinozuka, 12/31/97, (PB98-144231, A13, MF-A03).

NCEER-97-0019   "Seismic Evaluation of Frames with Infill Walls Using Quasi-static Experiments," by K.M. Mosalam, R.N. White and P. Gergely, 12/31/97, (PB98-153455, A07, MF-A02).

NCEER-97-0020   "Seismic Evaluation of Frames with Infill Walls Using Pseudo-dynamic Experiments," by K.M. Mosalam, R.N. White and P. Gergely, 12/31/97, (PB98-153430, A07, MF-A02).

NCEER-97-0021   "Computational Strategies for Frames with Infill Walls: Discrete and Smeared Crack Analyses and Seismic Fragility," by K.M. Mosalam, R.N. White and P. Gergely, 12/31/97, (PB98-153414, A10, MF-A02).

NCEER-97-0022   "Proceedings of the NCEER Workshop on Evaluation of Liquefaction Resistance of Soils," edited by T.L. Youd and I.M. Idriss, 12/31/97, (PB98-155617, A15, MF-A03).

MCEER-98-0001   "Extraction of Nonlinear Hysteretic Properties of Seismically Isolated Bridges from Quick-Release Field Tests," by Q. Chen, B.M. Douglas, E.M. Maragakis and I.G. Buckle, 5/26/98, (PB99-118838, A06, MF-A01).

MCEER-98-0002   "Methodologies for Evaluating the Importance of Highway Bridges," by A. Thomas, S. Eshenaur and J. Kulicki, 5/29/98, (PB99-118846, A10, MF-A02).

MCEER-98-0003   "Capacity Design of Bridge Piers and the Analysis of Overstrength," by J.B. Mander, A. Dutta and P. Goel, 6/1/98, (PB99-118853, A09, MF-A02).

MCEER-98-0004   "Evaluation of Bridge Damage Data from the Loma Prieta and Northridge, California Earthquakes," by N. Basoz and A. Kiremidjian, 6/2/98, (PB99-118861, A15, MF-A03).

MCEER-98-0005   "Screening Guide for Rapid Assessment of Liquefaction Hazard at Highway Bridge Sites," by T. L. Youd, 6/16/98, (PB99-118879, A06, not available on microfiche).

MCEER-98-0006   "Structural Steel and Steel/Concrete Interface Details for Bridges," by P. Ritchie, N. Kauhl and J. Kulicki, 7/13/98, (PB99-118945, A06, MF-A01).

MCEER-98-0007   "Capacity Design and Fatigue Analysis of Confined Concrete Columns," by A. Dutta and J.B. Mander, 7/14/98, (PB99-118960, A14, MF-A03).

MCEER-98-0008   "Proceedings of the Workshop on Performance Criteria for Telecommunication Services Under Earthquake Conditions," edited by A.J. Schiff, 7/15/98, (PB99-118952, A08, MF-A02).

MCEER-98-0009   "Fatigue Analysis of Unconfined Concrete Columns," by J.B. Mander, A. Dutta and J.H. Kim, 9/12/98, (PB99-123655, A10, MF-A02).

MCEER-98-0010   "Centrifuge Modeling of Cyclic Lateral Response of Pile-Cap Systems and Seat-Type Abutments in Dry Sands," by A.D. Gadre and R. Dobry, 10/2/98, (PB99-123606, A13, MF-A03).

MCEER-98-0011   "IDARC-BRIDGE: A Computational Platform for Seismic Damage Assessment of Bridge Structures," by A.M. Reinhorn, V. Simeonov, G. Mylonakis and Y. Reichman, 10/2/98, (PB99-162919, A15, MF-A03).

MCEER-98-0012   "Experimental Investigation of the Dynamic Response of Two Bridges Before and After Retrofitting with Elastomeric Bearings," by D.A. Wendichansky, S.S. Chen and J.B. Mander, 10/2/98, (PB99-162927, A15, MF-A03).

MCEER-98-0013   "Design Procedures for Hinge Restrainers and Hinge Sear Width for Multiple-Frame Bridges," by R. Des Roches and G.L. Fenves, 11/3/98, (PB99-140477, A13, MF-A03).

MCEER-98-0014   "Response Modification Factors for Seismically Isolated Bridges," by M.C. Constantinou and J.K. Quarshie, 11/3/98, (PB99-140485, A14, MF-A03).

MCEER-98-0015   "Proceedings of the U.S.-Italy Workshop on Seismic Protective Systems for Bridges," edited by I.M. Friedland and M.C. Constantinou, 11/3/98, (PB2000-101711, A22, MF-A04).

MCEER-98-0016   "Appropriate Seismic Reliability for Critical Equipment Systems: Recommendations Based on Regional Analysis of Financial and Life Loss," by K. Porter, C. Scawthorn, C. Taylor and N. Blais, 11/10/98, (PB99-157265, A08, MF-A02).

MCEER-98-0017   "Proceedings of the U.S. Japan Joint Seminar on Civil Infrastructure Systems Research," edited by M. Shinozuka and A. Rose, 11/12/98, (PB99-156713, A16, MF-A03).

MCEER-98-0018   "Modeling of Pile Footings and Drilled Shafts for Seismic Design," by I. PoLam, M. Kapuskar and D. Chaudhuri, 12/21/98, (PB99-157257, A09, MF-A02).

MCEER-99-0001   "Seismic Evaluation of a Masonry Infilled Reinforced Concrete Frame by Pseudodynamic Testing," by S.G. Buonopane and R.N. White, 2/16/99, (PB99-162851, A09, MF-A02).

MCEER-99-0002   "Response History Analysis of Structures with Seismic Isolation and Energy Dissipation Systems: Verification Examples for Program SAP2000," by J. Scheller and M.C. Constantinou, 2/22/99, (PB99-162869, A08, MF-A02).

MCEER-99-0003   "Experimental Study on the Seismic Design and Retrofit of Bridge Columns Including Axial Load Effects," by A. Dutta, T. Kokorina and J.B. Mander, 2/22/99, (PB99-162877, A09, MF-A02).

MCEER-99-0004   "Experimental Study of Bridge Elastomeric and Other Isolation and Energy Dissipation Systems with Emphasis on Uplift Prevention and High Velocity Near-source Seismic Excitation," by A. Kasalanati and M. C. Constantinou, 2/26/99, (PB99-162885, A12, MF-A03).

MCEER-99-0005   "Truss Modeling of Reinforced Concrete Shear-flexure Behavior," by J.H. Kim and J.B. Mander, 3/8/99, (PB99-163693, A12, MF-A03).

MCEER-99-0006   "Experimental Investigation and Computational Modeling of Seismic Response of a 1:4 Scale Model Steel Structure with a Load Balancing Supplemental Damping System," by G. Pekcan, J.B. Mander and S.S. Chen, 4/2/99, (PB99-162893, A11, MF-A03).

MCEER-99-0007   "Effect of Vertical Ground Motions on the Structural Response of Highway Bridges," by M.R. Button, C.J. Cronin and R.L. Mayes, 4/10/99, (PB2000-101411, A10, MF-A03).

MCEER-99-0008   "Seismic Reliability Assessment of Critical Facilities: A Handbook, Supporting Documentation, and Model Code Provisions," by G.S. Johnson, R.E. Sheppard, M.D. Quilici, S.J. Eder and C.R. Scawthorn, 4/12/99, (PB2000-101701, A18, MF-A04).

MCEER-99-0009   "Impact Assessment of Selected MCEER Highway Project Research on the Seismic Design of Highway Structures," by C. Rojahn, R. Mayes, D.G. Anderson, J.H. Clark, D'Appolonia Engineering, S. Gloyd and R.V. Nutt, 4/14/99, (PB99-162901, A10, MF-A02).

MCEER-99-0010   "Site Factors and Site Categories in Seismic Codes," by R. Dobry, R. Ramos and M.S. Power, 7/19/99, (PB2000-101705, A08, MF-A02).

MCEER-99-0011   "Restrainer Design Procedures for Multi-Span Simply-Supported Bridges," by M.J. Randall, M. Saiidi, E. Maragakis and T. Isakovic, 7/20/99, (PB2000-101702, A10, MF-A02).

MCEER-99-0012   "Property Modification Factors for Seismic Isolation Bearings," by M.C. Constantinou, P. Tsopelas, A. Kasalanati and E. Wolff, 7/20/99, (PB2000-103387, A11, MF-A03).

MCEER-99-0013   "Critical Seismic Issues for Existing Steel Bridges," by P. Ritchie, N. Kauhl and J. Kulicki, 7/20/99, (PB2000-101697, A09, MF-A02).

MCEER-99-0014   "Nonstructural Damage Database," by A. Kao, T.T. Soong and A. Vender, 7/24/99, (PB2000-101407, A06, MF-A01).

MCEER-99-0015   "Guide to Remedial Measures for Liquefaction Mitigation at Existing Highway Bridge Sites," by H.G. Cooke and J. K. Mitchell, 7/26/99, (PB2000-101703, A11, MF-A03).

MCEER-99-0016   "Proceedings of the MCEER Workshop on Ground Motion Methodologies for the Eastern United States," edited by N. Abrahamson and A. Becker, 8/11/99, (PB2000-103385, A07, MF-A02).

MCEER-99-0017   "Quindío, Colombia Earthquake of January 25, 1999: Reconnaissance Report," by A.P. Asfura and P.J. Flores, 10/4/99, (PB2000-106893, A06, MF-A01).

MCEER-99-0018   "Hysteretic Models for Cyclic Behavior of Deteriorating Inelastic Structures," by M.V. Sivaselvan and A.M. Reinhorn, 11/5/99, (PB2000-103386, A08, MF-A02).

MCEER-99-0019 "Proceedings of the 7th U.S.- Japan Workshop on Earthquake Resistant Design of Lifeline Facilities and Countermeasures Against Soil Liquefaction," edited by T.D. O'Rourke, J.P. Bardet and M. Hamada, 11/19/99, (PB2000-103354, A99, MF-A06).

MCEER-99-0020 "Development of Measurement Capability for Micro-Vibration Evaluations with Application to Chip Fabrication Facilities," by G.C. Lee, Z. Liang, J.W. Song, J.D. Shen and W.C. Liu, 12/1/99, (PB2000-105993, A08, MF-A02).

MCEER-99-0021 "Design and Retrofit Methodology for Building Structures with Supplemental Energy Dissipating Systems," by G. Pekcan, J.B. Mander and S.S. Chen, 12/31/99, (PB2000-105994, A11, MF-A03).

MCEER-00-0001 "The Marmara, Turkey Earthquake of August 17, 1999: Reconnaissance Report," edited by C. Scawthorn; with major contributions by M. Bruneau, R. Eguchi, T. Holzer, G. Johnson, J. Mander, J. Mitchell, W. Mitchell, A. Papageorgiou, C. Scaethorn, and G. Webb, 3/23/00, (PB2000-106200, A11, MF-A03).

MCEER-00-0002 "Proceedings of the MCEER Workshop for Seismic Hazard Mitigation of Health Care Facilities," edited by G.C. Lee, M. Ettouney, M. Grigoriu, J. Hauer and J. Nigg, 3/29/00, (PB2000-106892, A08, MF-A02).

MCEER-00-0003 "The Chi-Chi, Taiwan Earthquake of September 21, 1999: Reconnaissance Report," edited by G.C. Lee and C.H. Loh, with major contributions by G.C. Lee, M. Bruneau, I.G. Buckle, S.E. Chang, P.J. Flores, T.D. O'Rourke, M. Shinozuka, T.T. Soong, C-H. Loh, K-C. Chang, Z-J. Chen, J-S. Hwang, M-L. Lin, G-Y. Liu, K-C. Tsai, G.C. Yao and C-L. Yen, 4/30/00, (PB2001-100980, A10, MF-A02).

MCEER-00-0004 "Seismic Retrofit of End-Sway Frames of Steel Deck-Truss Bridges with a Supplemental Tendon System: Experimental and Analytical Investigation," by G. Pekcan, J.B. Mander and S.S. Chen, 7/1/00, (PB2001-100982, A10, MF-A02).

MCEER-00-0005 "Sliding Fragility of Unrestrained Equipment in Critical Facilities," by W.H. Chong and T.T. Soong, 7/5/00, (PB2001-100983, A08, MF-A02).

MCEER-00-0006 "Seismic Response of Reinforced Concrete Bridge Pier Walls in the Weak Direction," by N. Abo-Shadi, M. Saiidi and D. Sanders, 7/17/00, (PB2001-100981, A17, MF-A03).

MCEER-00-0007 "Low-Cycle Fatigue Behavior of Longitudinal Reinforcement in Reinforced Concrete Bridge Columns," by J. Brown and S.K. Kunnath, 7/23/00, (PB2001-104392, A08, MF-A02).

MCEER-00-0008 "Soil Structure Interaction of Bridges for Seismic Analysis," I. PoLam and H. Law, 9/25/00, (PB2001-105397, A08, MF-A02).

MCEER-00-0009 "Proceedings of the First MCEER Workshop on Mitigation of Earthquake Disaster by Advanced Technologies (MEDAT-1), edited by M. Shinozuka, D.J. Inman and T.D. O'Rourke, 11/10/00, (PB2001-105399, A14, MF-A03).

MCEER-00-0010 "Development and Evaluation of Simplified Procedures for Analysis and Design of Buildings with Passive Energy Dissipation Systems," by O.M. Ramirez, M.C. Constantinou, C.A. Kircher, A.S. Whittaker, M.W. Johnson, J.D. Gomez and C. Chrysostomou, 11/16/01, (PB2001-105523, A23, MF-A04).

MCEER-00-0011 "Dynamic Soil-Foundation-Structure Interaction Analyses of Large Caissons," by C-Y. Chang, C-M. Mok, Z-L. Wang, R. Settgast, F. Waggoner, M.A. Ketchum, H.M. Gonnermann and C-C. Chin, 12/30/00, (PB2001-104373, A07, MF-A02).

MCEER-00-0012 "Experimental Evaluation of Seismic Performance of Bridge Restrainers," by A.G. Vlassis, E.M. Maragakis and M. Saiid Saiidi, 12/30/00, (PB2001-104354, A09, MF-A02).

MCEER-00-0013 "Effect of Spatial Variation of Ground Motion on Highway Structures," by M. Shinozuka, V. Saxena and G. Deodatis, 12/31/00, (PB2001-108755, A13, MF-A03).

MCEER-00-0014 "A Risk-Based Methodology for Assessing the Seismic Performance of Highway Systems," by S.D. Werner, C.E. Taylor, J.E. Moore, II, J.S. Walton and S. Cho, 12/31/00, (PB2001-108756, A14, MF-A03).

MCEER-01-0001 "Experimental Investigation of P-Delta Effects to Collapse During Earthquakes," by D. Vian and M. Bruneau, 6/25/01, (PB2002-100534, A17, MF-A03).

MCEER-01-0002 "Proceedings of the Second MCEER Workshop on Mitigation of Earthquake Disaster by Advanced Technologies (MEDAT-2)," edited by M. Bruneau and D.J. Inman, 7/23/01, (PB2002-100434, A16, MF-A03).

MCEER-01-0003 "Sensitivity Analysis of Dynamic Systems Subjected to Seismic Loads," by C. Roth and M. Grigoriu, 9/18/01, (PB2003-100884, A12, MF-A03).

MCEER-01-0004 "Overcoming Obstacles to Implementing Earthquake Hazard Mitigation Policies: Stage 1 Report," by D.J. Alesch and W.J. Petak, 12/17/01, (PB2002-107949, A07, MF-A02).

MCEER-01-0005 "Updating Real-Time Earthquake Loss Estimates: Methods, Problems and Insights," by C.E. Taylor, S.E. Chang and R.T. Eguchi, 12/17/01, (PB2002-107948, A05, MF-A01).

MCEER-01-0006 "Experimental Investigation and Retrofit of Steel Pile Foundations and Pile Bents Under Cyclic Lateral Loadings," by A. Shama, J. Mander, B. Blabac and S. Chen, 12/31/01, (PB2002-107950, A13, MF-A03).

MCEER-02-0001 "Assessment of Performance of Bolu Viaduct in the 1999 Duzce Earthquake in Turkey" by P.C. Roussis, M.C. Constantinou, M. Erdik, E. Durukal and M. Dicleli, 5/8/02, (PB2003-100883, A08, MF-A02).

MCEER-02-0002 "Seismic Behavior of Rail Counterweight Systems of Elevators in Buildings," by M.P. Singh, Rildova and L.E. Suarez, 5/27/02. (PB2003-100882, A11, MF-A03).

MCEER-02-0003 "Development of Analysis and Design Procedures for Spread Footings," by G. Mylonakis, G. Gazetas, S. Nikolaou and A. Chauncey, 10/02/02, (PB2004-101636, A13, MF-A03, CD-A13).

MCEER-02-0004 "Bare-Earth Algorithms for Use with SAR and LIDAR Digital Elevation Models," by C.K. Huyck, R.T. Eguchi and B. Houshmand, 10/16/02, (PB2004-101637, A07, CD-A07).

MCEER-02-0005 "Review of Energy Dissipation of Compression Members in Concentrically Braced Frames," by K.Lee and M. Bruneau, 10/18/02, (PB2004-101638, A10, CD-A10).

MCEER-03-0001 "Experimental Investigation of Light-Gauge Steel Plate Shear Walls for the Seismic Retrofit of Buildings" by J. Berman and M. Bruneau, 5/2/03, (PB2004-101622, A10, MF-A03, CD-A10).

MCEER-03-0002 "Statistical Analysis of Fragility Curves," by M. Shinozuka, M.Q. Feng, H. Kim, T. Uzawa and T. Ueda, 6/16/03, (PB2004-101849, A09, CD-A09).

MCEER-03-0003 "Proceedings of the Eighth U.S.-Japan Workshop on Earthquake Resistant Design f Lifeline Facilities and Countermeasures Against Liquefaction," edited by M. Hamada, J.P. Bardet and T.D. O'Rourke, 6/30/03, (PB2004-104386, A99, CD-A99).

MCEER-03-0004 "Proceedings of the PRC-US Workshop on Seismic Analysis and Design of Special Bridges," edited by L.C. Fan and G.C. Lee, 7/15/03, (PB2004-104387, A14, CD-A14).

MCEER-03-0005 "Urban Disaster Recovery: A Framework and Simulation Model," by S.B. Miles and S.E. Chang, 7/25/03, (PB2004-104388, A07, CD-A07).

MCEER-03-0006 "Behavior of Underground Piping Joints Due to Static and Dynamic Loading," by R.D. Meis, M. Maragakis and R. Siddharthan, 11/17/03.

MCEER-03-0007 "Seismic Vulnerability of Timber Bridges and Timber Substructures," by A.A. Shama, J.B. Mander, I.M. Friedland and D.R. Allicock, 12/15/03.

MCEER-04-0001 "Experimental Study of Seismic Isolation Systems with Emphasis on Secondary System Response and Verification of Accuracy of Dynamic Response History Analysis Methods," by E. Wolff and M. Constantinou, 1/16/04.

MCEER-04-0002   "Tension, Compression and Cyclic Testing of Engineered Cementitious Composite Materials," by K. Kesner and S.L. Billington, 3/1/04.

MCEER-04-0003   "Cyclic Testing of Braces Laterally Restrained by Steel Studs to Enhance Performance During Earthquakes," by O.C. Celik, J.W. Berman and M. Bruneau, 3/16/04.

MCEER-04-0004   "Methodologies for Post Earthquake Building Damage Detection Using SAR and Optical Remote Sensing: Application to the August 17, 1999 Marmara, Turkey Earthquake," by C.K. Huyck, B.J. Adams, S. Cho, R.T. Eguchi, B. Mansouri and B. Houshmand, 6/15/04.

MCEER-04-0005   "Nonlinear Structural Analysis Towards Collapse Simulation: A Dynamical Systems Approach," by M.V. Sivaselvan and A.M. Reinhorn, 6/16/04.

MCEER-04-0006   "Proceedings of the Second PRC-US Workshop on Seismic Analysis and Design of Special Bridges," edited by G.C. Lee and L.C. Fan, 6/25/04.

MCEER-04-0007   "Seismic Vulnerability Evaluation of Axially Loaded Steel Built-up Laced Members," by K. Lee and M. Bruneau, 6/30/04.

MCEER-04-0008   "Evaluation of Accuracy of Simplified Methods of Analysis and Design of Buildings with Damping Systems for Near-Fault and for Soft-Soil Seismic Motions," by E.A. Pavlou and M.C. Constantinou, 8/16/04.

MCEER-04-0009   "Assessment of Geotechnical Issues in Acute Care Facilities in California," by M. Lew, T.D. O'Rourke, R. Dobry and M. Koch, 9/15/04.

MCEER-04-0010   "Scissor-Jack-Damper Energy Dissipation System," by A.N. Sigaher-Boyle and M.C. Constantinou, 12/1/04.

MCEER-04-0011   "Seismic Retrofit of Bridge Steel Truss Piers Using a Controlled Rocking Approach," by M. Pollino and M. Bruneau, 12/20/04.